White Paper: Probabilistic Projections of the Total Fertility Rate for All Countries for the 2010 World Population Prospects

Adrian E. Raftery, Leontine Alkema, Patrick Gerland,
Samuel J. Clark, François Pelletier, Thomas Buettner,
Gerhard Heilig, Nan Li, Hana Ševčíková [1]

November 12, 2009

[1]Adrian E. Raftery, Departments of Statistics and Sociology, University of Washington, Seattle, WA 98195-4322; Email: raftery@u.washington.edu. Leontine Alkema, Department of Statistics and Applied Probability, National University of Singapore, Singapore 117546; Email: alkema@nus.edu.sg. Patrick Gerland, Policy Section, United Nations Population Division, New York, NY 10017; Email:gerland@un.org. Samuel J. Clark, Department of Sociology, University of Washington, Seattle, WA 98195-3340; MRC/Wits University Rural Public Health and Health Transitions Research Unit (Agincourt), School of Public Health, University of the Witwatersrand, South Africa and INDEPTH Network; Email: work@samclark.net. François Pelletier, Mortality Section, United Nations Population Division, New York, NY 10017; Email: pelletierf@un.org. Thomas Buettner, United Nations Population Division, New York, NY 10017; Email: buettner@un.org. Gerhard Heilig and Nan Li, Population Estimates and Projections Section, United Nations Population Division, New York, NY 10017; Email: heilig@un.org, li32@un.org. Hana Ševčíková, Department of Computer Science and Engineering, University of Washington, Seattle, WA 98195-2350; Email: hana@cs.washington.edu. The project described was partially supported by grants numbered HD054511 (Adrian E. Raftery, Principal Investigator) and HD057246 (Samuel J. Clark, Principal Investigator) from the National Institute of Child Health and Human Development. Its contents are solely the responsibility of the authors and do not necessarily represent the official views of the National Institute of Child Health and Human Development or those of the United Nations. Its contents have not been formally edited and cleared by the United Nations. The authors are grateful to John Bongaarts, Taeke Gjaltema and Vladimíra Kantorová for helpful comments.

Abstract

We describe a methodology for producing probabilistic projections of the total fertility rate (TFR) for all the countries of the world, as a first step towards the production of fully probabilistic population projections. The methodology is built on the current deterministic UN methodology for producing the World Population Prospects. It models the evolution of TFR in three phases: pre-transition high fertility, the fertility transition, and post-transition low fertility. It uses a Bayesian hierarchical model that borrows strength from all countries when projecting TFR for a single country. The fertility transition is modeled using the double logistic function currently used in WPP, but allowing a more flexible range of possible parameterizations. The post-transition low fertility phase is modeled using an autoregressive model that varies around replacement level.

The model is estimated from UN estimates of past TFR in all countries using a Markov chain Monte Carlo algorithm. We assess the method using out-of-sample predictions for the period since 1980 and the period since 1995. We compare the results to those from WPP 2008. We also show partially probabilistic projections of total population, that take account of uncertainty about fertility level. We describe a software package for implementing the method in the R statistical language. Finally we provide probabilistic projections of TFR until 2100 for all the countries of the world.

Contents

List of Tables

List of Figures

1 Introduction

Population forecasts predict the future size and composition of populations, based on predictions of fertility, mortality and migration. They are used for many purposes, including for predicting the demand for food, water, education, medical services, labor markets, pension systems, and predicting future impact on the environment. It is important for decision makers to not only have a point forecast that states the most likely scenario of a future population, but also to know the uncertainty around it, that is, the possible future values of an outcome, and how likely each set of possible future values is.

Fertility is a key driver of the size and composition of the population. Fertility decline has been a primary determinant of population ageing and projected levels of fertility have important implications on the age structure of future populations, including on the pace of population ageing. The total fertility rate (TFR) is one of the key components in population projections; it is the average number of children a woman would bear if she survived through the end of the reproductive age span, and experienced at each age the age-specific fertility rates of that period. The UN Population Division produces projections of the total fertility rate for 196 countries that are revised every two years and published in the World Population Prospects (United Nations, Department of Economic and Social Affairs, Population Division 2009). For countries with above-replacement fertility, a demographic transition model is used to project the decline in the total fertility rate and assumes that fertility will eventually fall below replacement level. Three sets of parameter values describe three different trajectories of future declines, from which the UN analyst chooses one which seems most appropriate for the country of interest. The UN projections for countries that are currently experiencing below-replacement fertility are constructed based on the assumption that fertility will increase again towards replacement level, to stabilize at 1.85 children. Fertility is assumed to increase linearly at a maximum rate of 0.05 children per woman per quinquennium.

While using the cohort-component method, the TFR projection, together with projections of mortality and international migration, provide the so-called *Medium* variant of the official United Nations population projections. The effect of lower or higher fertility when projecting populations is illustrated with the *Low* and *High* variants of the projections. In the high variant, half a child is added to the medium variant in order to examine the influence of a slower fertility decline on the population projections. Similarly, for the low variant, half a child is subtracted from the medium variant.

Though useful to highlight the sensitivity of demographic outcomes to a difference of one child in TFR, the drawback of the variants is that they do not assess the uncertainty in future fertility levels (Bongaarts and Bulatao 2000), and to what extent the low or high fertility variants are more likely. Future levels of fertility will be more uncertain in countries where the fertility transition has only just started than in countries where fertility is close to replacement level. A shortcoming of the current projection methodology is that the rate of change used in the projections is not sufficiently country-specific; only three options for modeling the future rate of change as a function of the fertility level are considered, from which one is chosen for each country. This means that the current approach works well for capturing the average experience of groups of countries which experience a similar pace of decline at the same fertility level, but it is less adequate to depict much slower or faster declines deviating from the typical group average experiences.

In this paper we develop methodology to construct probabilistic projections of the TFR for all countries in the world. Our methodology builds on the one currently used by the

United Nations Population Division for projecting the TFR. For countries that are going through the fertility transition from high fertility towards replacement fertility, the pace of the fertility decline is decomposed into a systematic decline, with distortion terms added to it. The pace of the systematic decline in TFR is modeled as a function of its level, based on the UN methodology. We propose a Bayesian hierarchical model to estimate the parameters of the decline function. A time series model is used for projecting trends in fertility after reaching replacement level, assuming that in long-term projections the TFR will fluctuate around replacement level fertility. The results are country-specific projections that are reproducible and take into account past trends.

This new approach provides valuable insights about future fertility trends worldwide. The prediction intervals for future fertility levels vary by country. The intervals are wider in most high-fertility countries than those currently inferred with the low and high variants of the official UN population projections. The projected TFRs and the corresponding prediction intervals will shed new light on future population dynamics, including on dependency ratios and on the pace of population ageing.

Several other methods have been used for making probabilistic projections. Early methods were based on the errors in past forecasts (Keyfitz 1981; Stoto 1983). Time series methods were developed for aggregate population quantities by Cohen (1986) and, for fertility by Lee and Tuljapurkar (1994), particularly for developed countries. Methods based on expert judgement have been developed and applied by Lutz, Sanderson, and Scherbov (2001). We draw on this previous work, particularly the time series methods, but our methodology is based more closely on UN experience and existing methods, and aims to be applicable to countries at all stages of demographic evolution.

In this paper UN estimates and projections of the TFR are taken from the 2008 revision of the UN World Population Prospects (United Nations, Department of Economic and Social Affairs, Population Division 2009).

This white paper is organized as follows. Section 2 describes the current UN methodology for projecting fertility, and Section 3 describes our Bayesian projection model. Results from our method are summarized in Section 4, and compared with the current UN results from the 2008 World Population Prospects in Section 5. Initial results from the application of the methodology to probabilistic population projections are described in Section 6. Finally, software implementing the approach is described in Section 7. Two appendices give more detail on the methodology, and detailed results for all countries.

2 UN Methodology for Projecting Fertility

The UN Population Division estimates and projects the TFR for five-year time periods from 1950 until 2050 (in the most recent revision). Five year intervals are chosen such that the estimates and projections can be used as input to the cohort-component projections, which are based on 5-year age groups.

A demographic transition model is used to project a fertility decline for countries in which the TFR is above 2.1 children for each woman (which is equal to replacement level fertility for countries with low mortality rates). In this model, the TFR is predicted to decline because of decreasing child mortality and economic development. The UN projects that total fertility will decline toward 1.85 children per woman. This assumption is based on what has been observed in countries that have gone through their fertility transition. The pace of the future fertility decline is modeled as a function of the level of the TFR, also based on what has been observed in countries that have gone through (most of) their fertility transition.

This is illustrated for Thailand and India in Figure 1. The plot on the left shows the 5-year UN estimates for Thailand and India over time, where $f_{c,t}$ is the TFR for country c, 5-year period t. Thailand went through its fertility transition relatively fast compared to other countries. The fertility transition in India has not been completed yet; its TFR has decreased from around 6 to 3 children and is still declining. The pace of the fertility decline during the transition is modeled as a function of its level in terms of 5-year decrements, which are the decreases in TFR in a 5-year period. The 5-year decrements as observed in Thailand and India are plotted against TFR in Figure 1(b). The TFR decreases along the horizontal axis from left to right, and the 5-year decrements at each level of TFR are plotted on the vertical axis. The decline curves in Thailand and India show the typical pattern of a fertility decline that starts slowly at high TFR values. The pace increases and is at its maximum around a TFR of 5 children per woman, and then slows down again towards the end of the transition.

The UN uses a parametric function to project the next 5-year decrement given a certain TFR value, whose shape is similar to the curves observed in Thailand and India (United Nations, Department of Economic and Social Affairs, Population Division 2006). The UN projection model is

$$f_{c,t+1} \;=\; f_{c,t} - d(\boldsymbol{\theta}, f_{c,t}), \tag{1}$$

where $d(\cdot,\cdot)$ is the parametric decline function to model the fertility transition. This function specifies a 5-year decrement (decrease) as a function of the current level of the TFR and parameter vector $\boldsymbol{\theta}$. The decline function itself is given by the sum of two logistic functions, a double logistic function (Meyer 1994). The first logistic function describes a high pace of decline at high total fertility rates decreasing towards a slower pace for lower fertility. The second function describes the opposite effect to slow down the pace of fertility decline at the beginning of the transition. The sum of the two is a parametric function with 6 parameters that describes a decline in fertility that starts with a slow pace at high TFR values, peaks around a TFR of 5 and slows down again at lower TFR values.

In the UN projections, the parameter vector is chosen from a set of 3 different vectors, with each parameter vector describing a different overall pace for the fertility decline: $\boldsymbol{\theta} \in \{\boldsymbol{\theta}_{SS}, \boldsymbol{\theta}_{FS}, \boldsymbol{\theta}_{FF}\}$. These parameter vectors have been estimated based on fertility declines in countries that have completed the fertility transition (United Nations, Department of

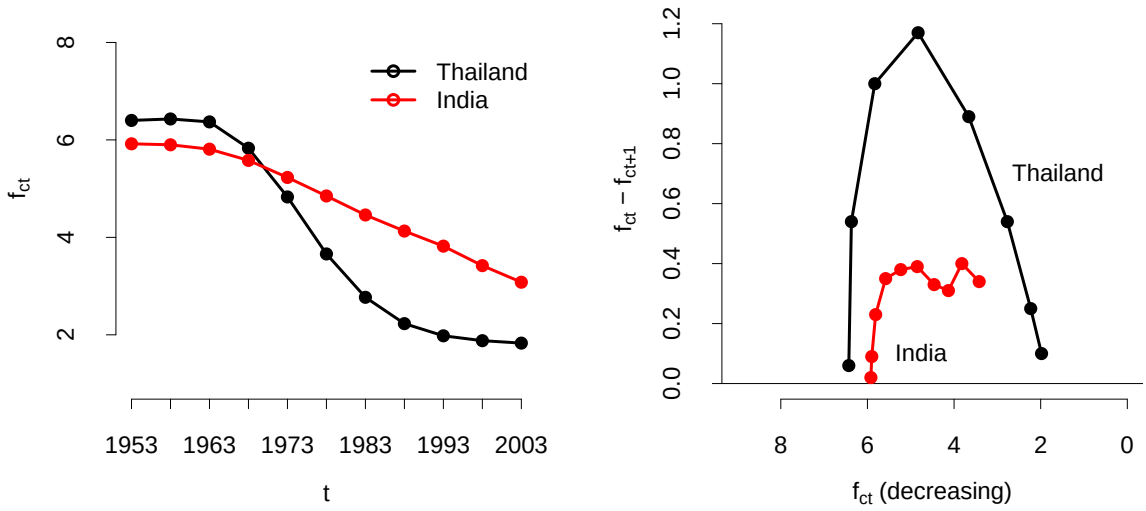

Figure 1: UN estimates of the fertility transition in Thailand and India: (a) Total fertility rate $f_{c,t}$ versus 5-year period t, (b) 5-year decrements $f_{c,t} - f_{c,t+1}$ versus total fertility rate $f_{c,t}$.

Economic and Social Affairs, Population Division 2006). The subscripts of $\boldsymbol{\theta}$ refer to the pace at the start and the end of the fertility decline, with "S" meaning slow, and "F" meaning fast. The decline functions corresponding to these three parameter vectors are shown in Figure 2. The Fast/Slow decline curve is given by the solid line. Compared to the Fast/Slow decline curve, the Slow/Slow decline curve gives a slower-paced decline at the start of the transition, the Fast/Fast trajectory a faster pace at the end. For all three projected declines, the TFR is kept constant after it reaches 1.85 children.

For each country, the UN analyst chooses the decline curve that seems most reasonable for the future fertility decline in that country, based on what has been observed in that country or region so far, or based on expert knowledge about the country. Generally, the resulting projected path of future fertility is checked against recent trends in fertility for each country. When a country's recent fertility trends deviate considerably from the standard decline curves, fertility is projected over an initial period of 5 or 10 years in such a way that it follows recent experience, and the model projection takes over after that initial transition period. For instance, in countries where fertility has stalled or where there is no evidence of fertility decline, fertility is projected to remain constant for several more years before a declining path sets in.

Note that the double logistic model does not predict the onset of the fertility transition; it gives the pace of the decline after its onset. In order to predict future fertility levels in countries for which a decline has not yet been observed, additional assumptions are needed about the timing of the onset of the decline, e.g. the decline takes off in the next five or ten years.

Several countries, mainly in Europe and Asia, are currently experiencing below-replacement fertility. The UN projections for these countries are based on the assumption that fertility will increase again and will stabilize at 1.85 children. For these countries it is assumed that over the first 5 or 10 years of the projection period fertility will follow the recently observed

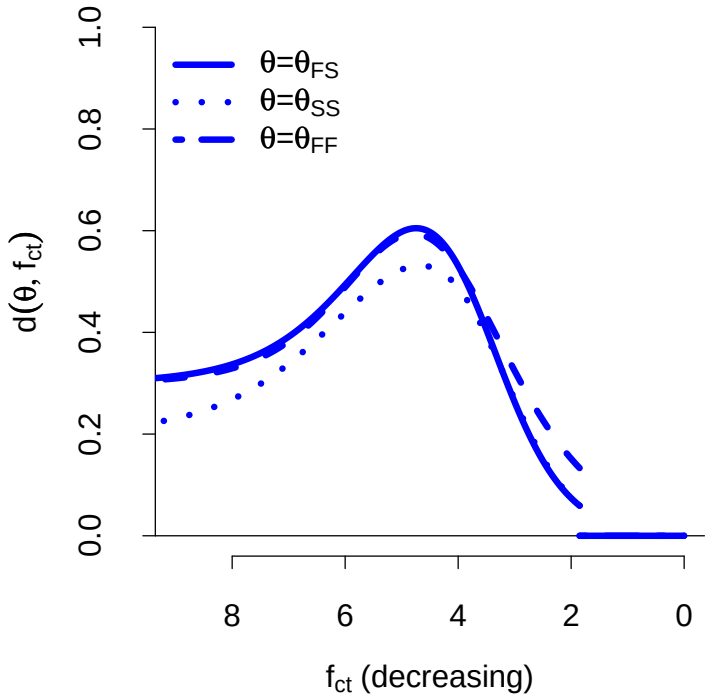

Figure 2: The UN decline curves that underlie the fertility projections for countries with above-replacement fertility. Each curve is given by the double logistic decline function with one choice of the parameter vector $\boldsymbol{\theta}$.

trends. After that transition period, fertility is assumed to increase linearly at a rate of 0.05 children per woman per quinquennium until it reaches 1.85 children per woman. For countries with very low fertility, replacement does not need to be reached by 2050.

There are some drawbacks of the UN projection model. It is a deterministic model, and so there is no uncertainty assessment of the projections. Secondly, the projections for the high fertility countries are based on choosing the parameter vector $\boldsymbol{\theta}$ of the decline function from a set of three vectors. This results in projections that are not country-specific. Moreover, the three sets of parameter values do not capture the variation in the past. This is illustrated in Figure 3. This figure shows the decrement curves as observed in Thailand and India, with the outcomes of the UN decline function for the three parameter vectors. The UN decline curves do not differ much at all compared to the observed decrements in Thailand and India.

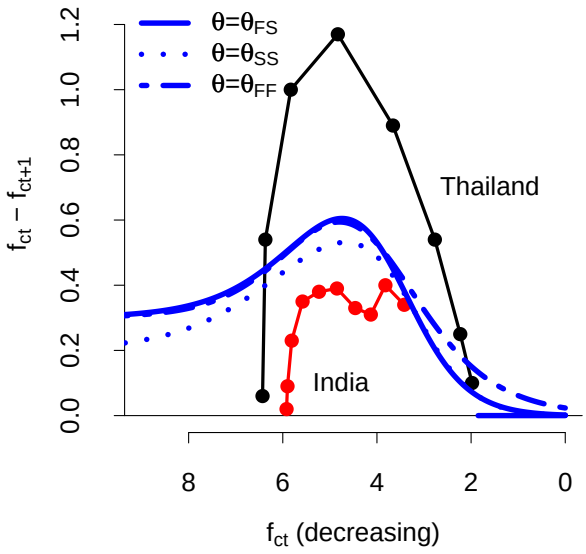

Figure 3: Comparison of the UN decline curves with the observed decrements in Thailand and India.

3 Bayesian Projection Model

Our objective is to construct country-specific probabilistic projections of the TFR. Building on the existing fertility modeling framework used by the UN, trends in TFR over time are described by a 3-phase model:

1. Stable pre-transition high fertility: The fertility transition has not started yet and fertility fluctuates around high TFR levels. In some countries, an increase has occurred before it started to decline. This first phase is not of interest for projections, and it is left out of the Bayesian projection model.

2. Fertility transition from high fertility to replacement level fertility or below

3. Post-transition low fertility: Recovery from below-replacement fertility towards replacement fertility and oscillations around replacement level fertility.

The next sections discuss the modeling of phases 2 and 3. Earlier versions of the model were described by Alkema (2008) and Alkema, Raftery, Gerland, Clark and Pelletier (2008, 2009).

3.1 Phase 2: Fertility transition

The projection model for the fertility transition is based on the UN model, with modifications to overcome its drawbacks. The UN model is modified as follows: (i) instead of having only 3 options for parameter vector $\boldsymbol{\theta}$ of the decline function, this vector is estimated for each country separately, and (ii) an uncertainty assessment is included by allowing for random distortions from the parametric decline curve, and by assessing the uncertainty in $\boldsymbol{\theta}$ for each country.

For countries that are currently going through the fertility transition, the 5-year decrements are decomposed into a systematic decline, with a distortion term added to it. More formally, the TFR for 5-year periods is modeled by a random walk model with drift:

$$f_{c,t+1} = f_{c,t} - d_{c,t} + \varepsilon_{c,t}, \text{ for } \tau_c \leq t < \lambda_c, \quad (2)$$

$$\varepsilon_{c,t} \sim N(0, \sigma^2_{c,t}), \text{ for } t \neq \tau_c, \quad (3)$$

where $d_{c,t}$ is the drift term that models the systematic decline during the fertility transition, $\varepsilon_{c,t}$ are the random distortions and model the deviations from the systematic decline, τ_c is the start period of the fertility decline, and λ_c is the start period of the post-transition phase. The distortions in the start year will be discussed below.

The expression for the standard deviation $\sigma_{c,t}$ of the distortions after the start period is based on examination of the absolute distortions as a function of the TFR level, which showed a higher variance around a TFR of 4-5, and over time, which showed a higher variance before 1975. Since 1975 fertility transitions have become more predictable, possibly a result of improvement in family planning programs. The standard deviation function is given in the Methodology Appendix.

The drift term $d_{c,t}$ gives the 5-year decrement during the fertility transition. A slightly modified version of the same double logistic function used by the UN, is chosen as the decline function to model the decrements. The decrements are given by $d_{c,t} = d(\boldsymbol{\theta}_c, \lambda_c, \tau_c, f_{c,t})$, where

$$d(\boldsymbol{\theta}_c, \lambda_c, \tau_c, f_{c,t}) = \begin{cases} g(\boldsymbol{\theta}_c, f_{c,t}) & \text{for } \tau_c \leq t < \lambda_c \text{ and } f_{c,t} \geq 1; \\ 0 & \text{otherwise,} \end{cases} \quad (4)$$

where τ_c is the start period of the fertility transition, $\lambda_c - 1$ is its end period and $g(\boldsymbol{\theta}_c, f_{c,t})$ is the double logistic function with country-specific parameter vector $\boldsymbol{\theta}_c = (\triangle_{c1}, \triangle_{c2}, \triangle_{c3}, \triangle_{c4}, d_c)$, given by

$$\frac{-d_c}{1 + \exp\left(-\frac{2\ln(9)}{\triangle_{c1}}(f_{c,t} - \sum_i \triangle_{ci} + 0.5\triangle_{c1})\right)} + \frac{d_c}{1 + \exp\left(-\frac{2\ln(9)}{\triangle_{c3}}(f_{c,t} - \triangle_{c4} - 0.5\triangle_{c3})\right)}.$$

Figure 4 illustrates the parametrization of the double logistic function. The 5-year decrements as given by the decline function are plotted against TFR. The maximum pace of the decline (the maximum 5-year decrement) is given by d_c. Note that the actual attained maximum pace tends to be slightly smaller than d_c; it depends on the four $\triangle_{ci}$'s, which describe the TFR ranges in which the pace of the fertility decline changes. The decline takes off at TFR level $U_c = \sum_{i=1}^{4} \triangle_i$, where the decrement is between 0 and 10% of its maximum pace. Between TFR levels U_c and $U_c - \triangle_{c1}$, the pace of the decline increases from around $0.1d_c$ to over $0.8d_c$. During the TFR range denoted by $\triangle_{c2}$, the TFR is declining at a higher pace than during the rest of the transition; its 5-year decrements range between $0.8d_c$ and d_c. In $\triangle_{c3}$ the pace of the fertility decline decreases further to $0.1d_c$ at TFR level $\triangle_{c4}$. The decline is set to zero if the TFR is smaller than one.

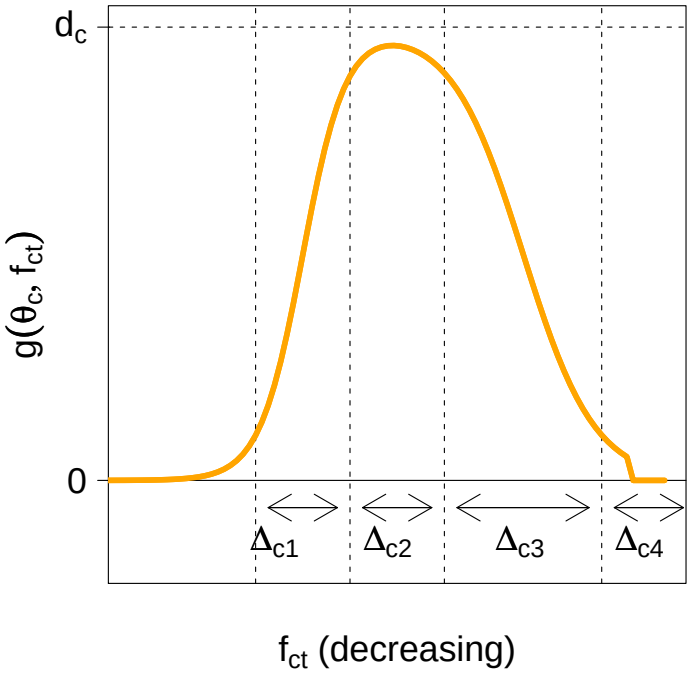

Figure 4: 5-year decrements as given by the double logistic function plotted against the TFR. The horizontal TFR axis is negatively oriented (i.e. decreasing).

The double logistic function is chosen to project the pace of the fertility decline (i) because of the straightforward interpretation of its parameters, (ii) to be consistent with the current UN methodology, and (iii) because of its ability to represent various declines by varying the maximum decrement and the $\triangle_{ci}$'s. This is illustrated in Figure 5, which shows

the observed decrements in Thailand and India, as discussed earlier. The orange line gives the least-squares fit of the parameters of the decline function as described above to these decrements to illustrate the flexibility of the model to describe various declines.

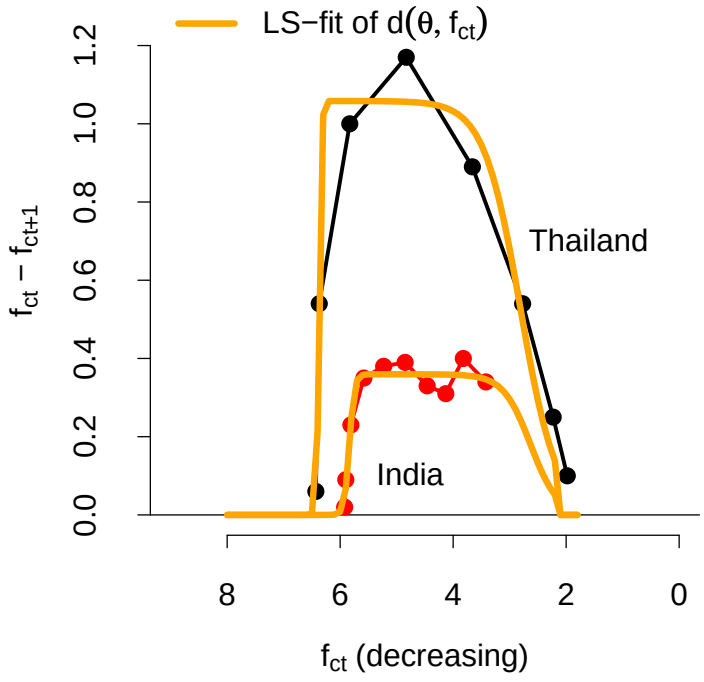

Figure 5: Observed 5-year decrements in Thailand and India, with least-squares fits of the double logistic decline function that is used in the time series projection model.

The parameters of the decline function are estimated for each country. The start period of the transition, τ_c, is given by the period in which the TFR starts declining. For countries in which the fertility decline started after 1950, the start period τ_c is within the observation period. We fix the start level in that period at U_c such that the systematic decline in that period is between 0 and 10% of the maximum decline, with a "start year" distortion term ε_{c,τ_c} added to it to allow a bigger decrease in that specific period:

$$\begin{aligned} U_c &= f_{c,\tau_c} \text{ for } \tau_c \geq 1950. \\ \varepsilon_{c,\tau_c} &\sim N(m_{\tau_c}, s_\tau^2), \end{aligned}$$

where m_τ is the mean and s_τ the standard deviation of the distortion in the start period. For countries in which the decline started before 1950, the start level U_c is added as a parameter to the model. (for details on τ_c, U_c and ε_{c,τ_c}, see the Methodology Appendix).

The 5 parameters in the double logistic function that determine the pace of the fertility decline and the total time that the transition takes, are given by $\triangle_{c4}$, $\frac{\triangle_{ci}}{U_c - \triangle_{c4}}$ for $i = 1, 2, 3$, and d_c. To estimate these parameters and assess their uncertainty in high-fertility countries, especially in countries where the decline has barely started, we assume that these parameters are exchangeable between countries and use a Bayesian hierarchical model to derive the country-specific distributions (Gelman et al. 2004). This means that the predicted systematic part of the fertility decline in a country is based on its observed decline so far, as well

as observed declines in all other countries. The Bayesian hierarchical model is described in detail in the Methodology Appendix.

3.2 Phase 3: Post-transition low fertility

After the fertility transition has been completed we assume that in long-term projections the TFR will fluctuate around replacement level fertility (around 2.1 children per woman). As proposed by Lee and Tuljapurkar (1994), this is modeled with a first order autoregressive time series model, an AR(1) model, with its mean fixed at the approximate replacement fertility level, $\mu = 2.1$. This model is

$$f_{c,t} \sim N(\mu + \rho(f_{c,t-1} - \mu), s^2) \text{ for } t > \lambda_c. \tag{5}$$

It can also be written as:

$$\begin{aligned} f_{c,t} &= f_{c,t-1} + (1-\rho)(\mu - f_{c,t-1}) + e_{c,t}, \\ e_{c,t} &\sim N(0, s^2), \end{aligned}$$

where ρ is the autoregressive parameter with $|\rho| < 1$ and s^2 is the variance of the random errors. In this model the expected increase or decrease towards 2.1 is larger if the current TFR is further away from 2.1, and depends on ρ. For example, at a TFR of 1.5, the expected next TFR is $2.1 - 0.6\rho$; a smaller ρ will give a larger expected increase. The smaller ρ, the more quickly the TFR will increase towards replacement level fertility.

In the AR(1) model, the asymptotic $100(1-\alpha)\%$ prediction interval is

$$\left(2.1 - z_\alpha \frac{s}{\sqrt{1-\rho^2}}, 2.1 + z_\alpha \frac{s}{\sqrt{1-\rho^2}}\right), \tag{6}$$

where z_α is the $(1 - \frac{\alpha}{2})$ quantile of the standard normal distribution. For example, for an 80% prediction interval, $z_\alpha = 1.28$ and for a 95% prediction interval, $z_\alpha = 1.96$. Equation (6) is the prediction interval for the TFR in the distant future.

This paper is concerned with projecting period TFR, which is what the UN uses as a basis for its population projections. Bongaarts and Feeney (1998) have pointed out that current below-replacement period TFRs may be lower than the cohort TFRs for the currently fertile cohorts, reflecting a tempo rather than a quantum effect. Our AR(1) model for the low fertility Phase 3 predicts a recovery from below-replacement period TFR, as does the Bongaarts-Feeney work, and so it may to some extent capture this phenomenon.

3.3 Estimation of model parameters

Ideally, empirical data from censuses, surveys and vital registration records would be used directly to estimate the parameters of the models in phases 2 and 3. However, empirical data of this kind are not available in a standard format for most countries. Also, for most developing countries, issues with data quantity and quality require extra attention. To overcome this problem, the 5-year UN estimates are used as the data set of TFR observations. Using the UN estimates allows us to construct prediction intervals for all countries, based on the declines and trends that have been observed so far in all countries.

We assume that the UN estimates for period t, denoted by $u_{c,t}$, are equal to the TFR:

$$u_{c,t} = f_{c,t}, \text{ for } t = 1, \ldots, T_c, \tag{7}$$

where T_c is the number of observation periods for country c. In reality the UN estimates are measured or estimated with error. No sampling model for the estimates is included here, because the error variance of the UN estimates cannot be estimated based on single 5-year estimates for each country. This means that the prediction intervals as constructed by this method are expected to be narrower than intervals for which the additional error variance has been taken into account.

To estimate the parameters of fertility transition model, as well as the AR(1) process, we separate the observation period into the different phases. Countries in which recovery has started are defined as countries in which 2 subsequent periods of increase below a TFR of 2 have been observed; the start period, λ_c, of Phase 3 for country c is defined as the earliest period t for which:

$$\begin{cases} f_{c,t} > f_{c,t-1}, \\ f_{c,t+1} > f_{c,t}, \\ f_{c,p} < 2 \text{ for } p = t-1, t, t+1. \end{cases}$$

With observations for phases 2 and 3, the parameters of both models can be estimated. A Markov Chain Monte Carlo (MCMC) algorithm is used to get samples of the posterior distributions of each of the parameters of the fertility transition model (Gelfand and Smith 1990). This algorithm is a combination of Gibbs sampling, Metropolis-Hastings and slice sampling steps (Neal 2003).

The AR(1) parameters ρ and s are estimated using maximum-likelihood estimation based on all the data points after period λ_c. A turnaround point has been observed in 20 countries (Singapore, Bulgaria, Czech Republic, Russian Federation, Channel Islands, Denmark, Estonia, Finland, Latvia, Norway, Sweden, United Kingdom, Italy, Spain, Belgium, France, Germany, Luxembourg, Netherlands, United States of America), giving 52 post-transition outcomes $(f_{c,t-1}, f_{c,t})$ to estimate the parameters of the AR(1) process. The maximum-likelihood estimate for ρ is 0.906. The post-transition outcomes and fitted regression line are shown in Figure 6. The fitted regression line fits the data well, and the estimated value of ρ gives expected increases that are similar to those from the current UN methodology.

The estimated standard deviation of the residuals is 0.09, illustrated with the dashed red lines in the same figure. This standard deviation is used for projecting 4 periods after the turnaround, based on having observed at least 4 periods after the turnaround for 8 countries.

After four projection periods, we change the standard deviation of the AR(1) distortions to its asymptotic value, $s^{(a)}$, based on an estimate of the marginal standard deviation of Phase 3 TFR values. This is the conditional standard deviation of the TFRs identified as belonging to Phase 3, estimated conditionally on their mean being equal to 2.1. The resulting estimate of the AR(1) distortion standard deviation is 0.203. Based on $\mu = 2.1$, $\rho = 0.906$ and $s^{(a)} = 0.203$, the asymptotic predictive distribution has standard deviation 0.48. Thus the asymptotic 95% prediction interval is [1.16, 3.04] and the asymptotic 80% prediction interval is [1.49, 2.72]. Our model for Phase 3 differs from that of Lee and Tuljapurkar (1994) in this respect.

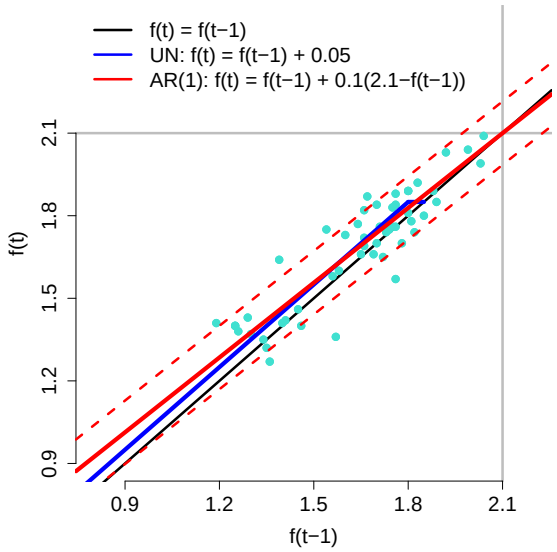

Figure 6: Observed UN estimates after turnaround point, with fitted regression (through the origin) line for AR(1) model. The dashed red lines show the limits of the 95% prediction intervals.

3.4 TFR projections

TFR projections during the fertility transition are based on the model as described earlier, using the posterior sample of estimates of the parameters of the decline curve and of the parameters of the variance of the distortion terms. This results in a set of country-specific future TFR trajectories.

For countries that have not yet completed the fertility transition, Phase 3 will not start until after the TFR has decreased below $\triangle_{c4}$ (the TFR level at which the expected decrements are smaller than 10% of the maximum decrements). Once the TFR has decreased below that level, Phase 3 starts after an increase in the TFR has been observed. The projected start period of the recovery process λ_c is defined as the earliest period $t > T_c$ for which:

$$\begin{cases} f_{c,t} > f_{c,t-1}, \\ f_{c,t-1} < \triangle_{c4}. \end{cases}$$

The period between reaching $\triangle_{c4}$ and starting to recover is still part of the fertility transition (Phase 2). The duration of this period depends on the random draws of the distortion terms, as well as on the expected decrements as given by the double-logistic function.

After the fertility transition has ended at period $\lambda_c - 1$, and for projecting post-transition countries, the AR(1) model is used to project future TFR outcomes. The estimated standard deviation s of the distortions in the AR(1) model is used for a limited number of periods, equal to 4 minus the number of post-transition periods observed so far (or zero if this is negative). Afterwards, the standard deviation of the distortions is increased to the asymptotic standard deviation $s^{(a)} = 0.203$.

The result is a set of future TFR trajectories for each country. The "best" TFR projection is given by the median outcome of the TFR trajectories in each period, and the bounds of

the 80% and 95% prediction intervals are given by the 10th and 90th percentiles, and the 2.5-th and 97.5-th percentiles, respectively.

4 Results

4.1 Projections

Macao and Hong Kong were left out when estimating the parameters of the BHM and in the results below (these are the only two countries with current TFR below 1), as it is questionable whether the experiences in these countries are comparable with other countries. (They can be included again if there is consensus to do so). Plots for all countries are given in the Results Appendix and the tables below give a summary of the results for selected countries and by region.

Figures 7 and 8 show the widths and the asymmetry of the prediction intervals in 2045-2050 and 2095-2100. The figures show (i) increasing uncertainty with current TFR level, (ii) more uncertainty towards higher values for the high fertility countries, and more uncertainty towards lower outcomes for lower TFR countries.

Table 1: Projection results for 2045-2050 and 2095-2100 for selected countries, ordered by increasing TFR in 2005-2010.

Country	UN 2005-10	UN 2045-50	BHM 2045-50			BHM 2095-2100		
			Low	Median	High	Low	Median	High
Singapore	1.27	1.64	1.48	1.73	1.97	1.69	1.96	2.23
Poland	1.27	1.64	1.45	1.71	1.97	1.67	1.95	2.23
Italy	1.38	1.74	1.53	1.77	2.02	1.70	1.98	2.26
Canada	1.57	1.85	1.36	1.80	2.08	1.65	1.97	2.26
Netherlands	1.74	1.85	1.69	1.94	2.19	1.76	2.04	2.31
Chile	1.94	1.85	1.19	1.67	2.07	1.44	1.87	2.20
India	2.76	1.85	1.42	1.85	2.31	1.30	1.77	2.15
Zimbabwe	3.47	2.05	1.38	1.83	2.30	1.16	1.71	2.11
Bolivia	3.50	1.85	1.69	2.19	2.73	1.28	1.77	2.21
Mozambique	5.11	2.41	1.93	2.67	3.43	1.36	1.86	2.45
Malawi	5.59	2.56	2.43	3.18	3.93	1.49	2.06	2.81
Zambia	5.87	2.55	2.85	3.67	4.41	1.69	2.41	3.24
Burkina Faso	5.95	2.72	2.47	3.37	4.18	1.51	2.12	2.92
Uganda	6.38	2.62	2.15	3.18	4.16	1.37	1.95	2.73
Niger	7.15	3.77	2.69	4.00	5.05	1.49	2.25	3.31

Table 2: Mean projection results by region for period 2045-2050; UN projection and median projection with Bayesian projection model (BHM), and the mean widths of the 80% and 95% prediction intervals (PI).

Region	UN 2008	Projection		Mean width	
		UN	BHM	95% PI	80% PI
Eastern Africa	4.65	2.32	2.61	2.04	1.33
Middle Africa	4.95	2.39	2.51	2.16	1.43
Northern Africa	2.74	1.91	1.68	1.42	0.97
Southern Africa	3.16	1.98	1.85	1.42	0.92
Western Africa	5.10	2.54	2.84	2.26	1.48
Eastern Asia	1.44	1.64	1.63	1.30	0.85
South-Central Asia	2.91	1.97	1.80	1.49	1.00
South-Eastern Asia	2.77	1.95	1.78	1.47	0.99
Western Asia	2.77	1.92	1.81	1.44	0.96
Eastern Europe	1.35	1.76	1.74	0.86	0.55
Northern Europe	1.74	1.83	1.87	0.87	0.57
Southern Europe	1.45	1.78	1.67	1.10	0.70
Western Europe	1.60	1.81	1.85	0.86	0.54
Caribbean	2.09	1.85	1.69	1.34	0.90
Central America	2.78	1.85	1.79	1.44	0.96
South America	2.54	1.86	1.82	1.39	0.92
Northern America	1.83	1.85	1.95	0.99	0.61
Australia/New Zealand	1.92	1.85	1.78	1.34	0.90
Melanesia	3.37	2.05	2.19	1.59	1.04
Micronesia	3.08	1.85	2.00	1.46	0.94
Polynesia	3.42	2.06	2.31	1.61	1.07

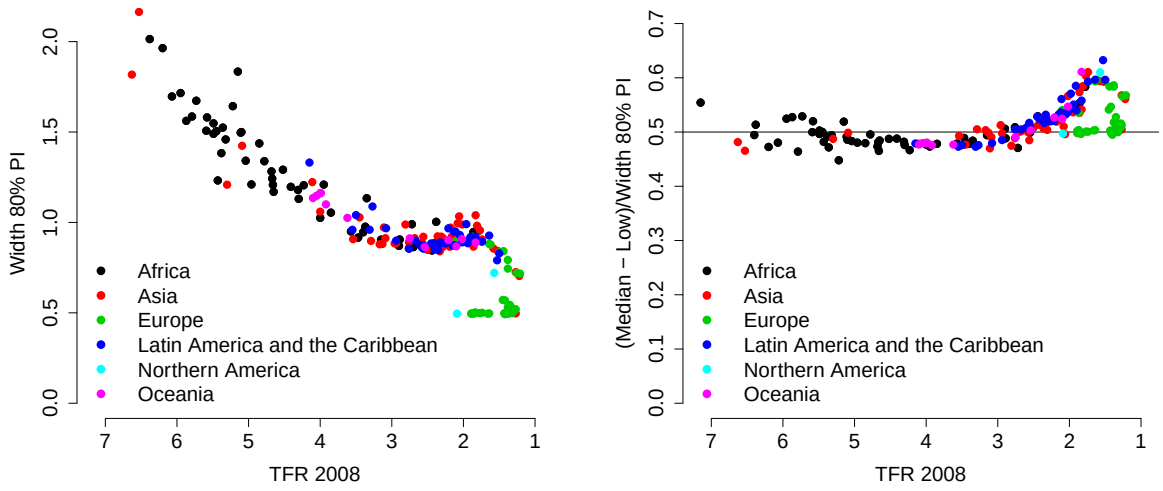

Figure 7: (a) Widths of 80% prediction intervals for 2045-2050, plotted against TFR in 2005-2010 (decreasing). The width is largest at high TFR, and at its minimum for countries with a TFR between 2 and 3. (b) Ratios of the width of the lower half of the 80% prediction interval, over its total width.

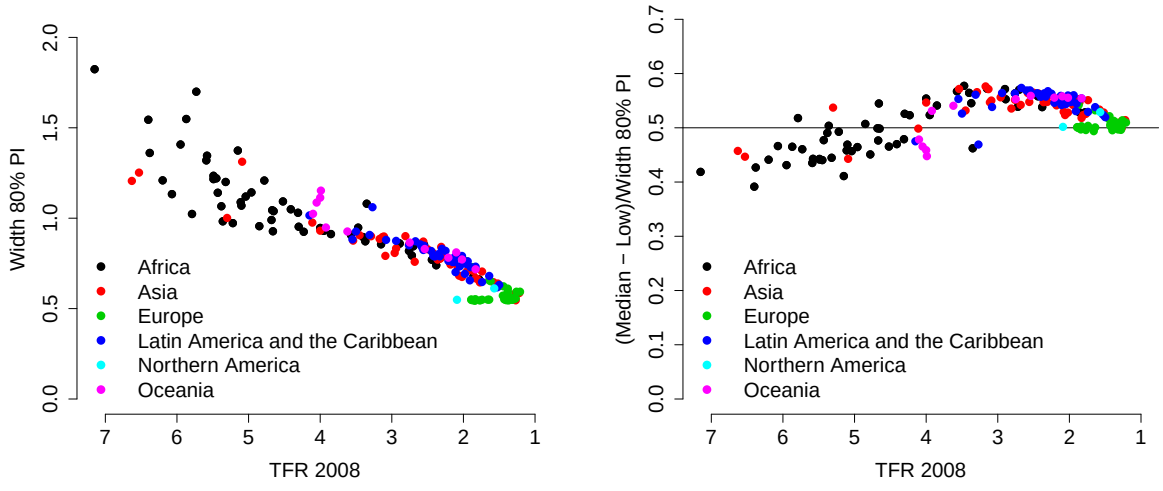

Figure 8: (a) Widths of 80% prediction intervals for 2095-2100, plotted against TFR in 2005-2010 (decreasing). The width is largest at high TFR, and at its minimum for countries with a TFR between 2 and 3. The few countries with narrow PIs are the countries in which a turnaround has been observed. (b) Ratios of the width of the lower half of the 80% prediction interval, over its total width. Note the asymmetry: more uncertainty towards higher values at high TFR, while more uncertainty towards lower outcomes for low TFR countries.

4.2 Model validation

Modeling assumptions are validated using out-of-sample projections. In the first set of out-of-sample projections, the BHM is used to construct projections for 1980–2010 based on the UN estimates up to and including the five-year period 1975–1980. In the second set of out-of-sample projections, the BHM is used to construct projections for 1995–2010 based on the UN estimates up to and including the 5-year period 1990–1995. The first set of projections is compared to the UN estimates for the six five-year periods from 1980–1985 up to 2005-2010, and the second set of projections is compared to the UN estimates for the three five-year periods 1995–2000, 2000–2005 and 2005–2010. The calibration of the prediction intervals is evaluated by calculating the proportion of left-out UN estimates that fall outside their prediction intervals. If the modeling assumptions hold, we expect 10%/2.5% of the estimates to fall above/below the 80%/95% intervals.

The results are shown in Tables 3 and 4 and Figures 9 and 10. The prediction intervals were reasonably well calibrated, although in more recent periods, the TFR was slightly overpredicted.

Table 3: Model validation results: Mean squared error (MSE) and proportion of left-out UN estimates that falls above the median projected TFR, and above or below their 80% and 95% prediction intervals in future periods, when projecting from 1975-1980. We expect 10%/2.5% of the estimates to fall above/below the 80%/95% intervals.

Periods ahead	MSE	Above Median	Proportion of obs.			
			Above 95%PI	Below 95%PI	Above 80%PI	Below 80%PI
1980-85	0.11	0.49	0.05	0.01	0.11	0.11
1985-90	0.22	0.51	0.03	0.05	0.11	0.10
1990-95	0.38	0.45	0.04	0.07	0.08	0.14
1995-2000	0.59	0.38	0.03	0.10	0.07	0.21
2000-05	0.63	0.38	0.02	0.07	0.07	0.21
2005 - 2010	0.59	0.39	0.02	0.04	0.07	0.15

Table 4: Model validation results: Mean squared error (MSE) and proportion of left-out UN estimates that falls above the median projected TFR,and above or below their 80% and 95% prediction intervals in future periods, when projecting from 1990–1995. We expect 10%/2.5% of the estimates to fall above/below the 80%/95% intervals.

Periods ahead	MSE	Above Median	Proportion of obs.			
			Above 95%PI	Below 95%PI	Above 80%PI	Below 80%PI
1995-2000	0.07	0.33	0.02	0.08	0.04	0.19
2000-05	0.17	0.37	0.02	0.05	0.06	0.19
2005 - 2010	0.21	0.39	0.02	0.03	0.05	0.11

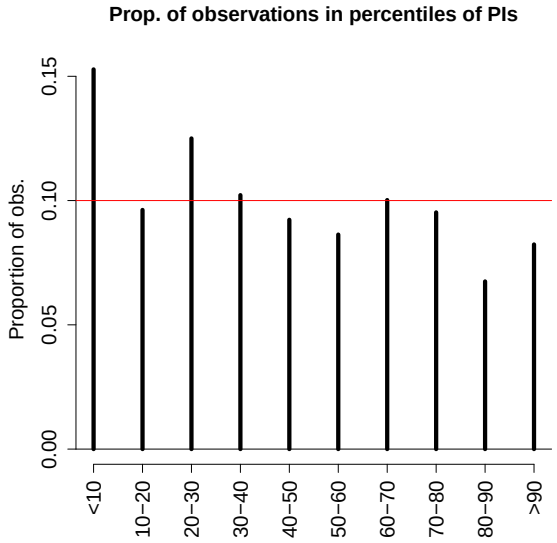

Figure 9: Proportion of observations that fell in the ten deciles of the predictive distribution (0–10%, 10–20%, etc.), when projecting from 1975–1980. We expect 10% of the observations to fall within each 10% interval, as shown by the red horizontal line.

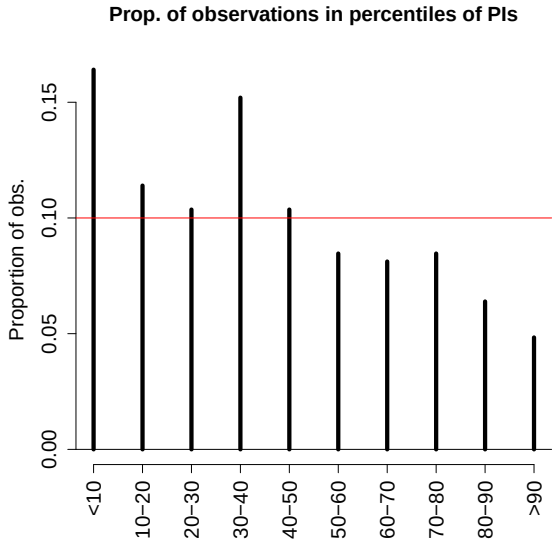

Figure 10: Proportion of observations that fell in the ten deciles of the predictive distribution (0–10%, 10–20%, etc.), when projecting from 1990–1995. We expect 10% of the observations to fall within each 10% interval, as shown by the red horizontal line.

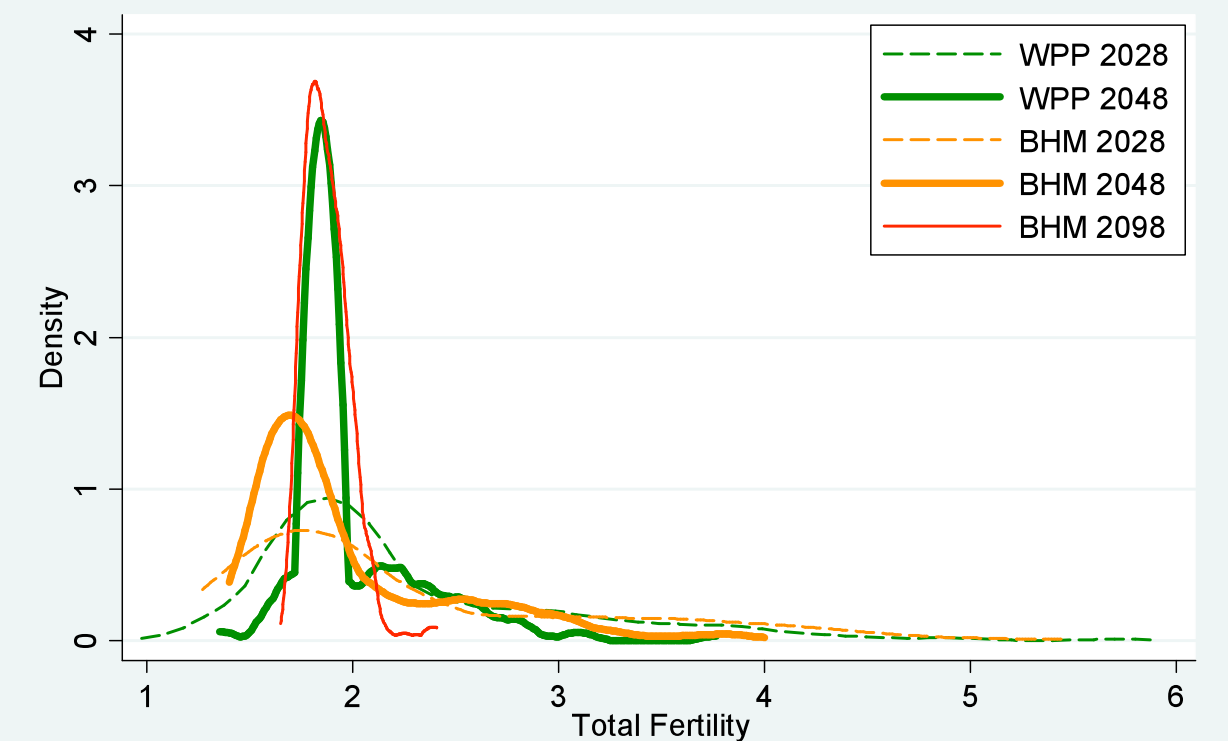

Figure 11: Density distribution of countries by Total Fertility

5 Comparison between Bayesian Hierarchical Model and WPP 2008 Projections of TFR

5.1 Comparison of WPP Medium TFR Projection with BHM Median Projection

Overall the BHM median TFR projections by country provide results similar to WPP, and the overall distributions of countries by TFR are similar. But the BHM approach preserves a much greater variance between countries than WPP by 2048 as seen in Figure 11 and Table 5; the BHM median TFR prediction ranges for 90% of the countries between 1.5–3.1 in 2048 compared to 1.7–2.6 for the 2008 revision of the World Population Prospects. In addition, the BHM projection allows many more countries to go below replacement (up to around 1.5) by 2048 and to return toward sub-replacement level (around 1.85) by 2098, closely matching the overall distribution assumed by WPP for 2048.

Magnitude of the differences: The BHM prediction is within ±10% of the WPP projection between 2008 and 2048 for the majority of countries (about 60%); see Table 6. Yet noticeable differences between BHM and WPP projections start in 2018 and by 2033 only about one third of the countries have differences of less than 5%. Differences are more often negative with BHM projections lower than WPP, but for about one quarter of the countries BHM gives higher TFR projections than WPP. For a small number of countries (fewer than 25), BHM TFR exceeds WPP by 15% or more, and is lower by more than 15% in 20+ countries.

Table 5: Percentile distribution of countries by Total Fertility

Total Fertility		WPP Medium		BHM Median		
Percentile	2008	2028	2048	2028	2048	2098
5	1.28	1.48	1.67	1.46	1.51	1.73
10	1.38	1.58	1.76	1.54	1.56	1.75
25	1.83	1.85	1.85	1.64	1.66	1.79
50	2.38	1.96	1.85	1.93	1.77	1.86
75	3.90	2.63	2.12	2.78	2.18	1.95
90	5.33	3.39	2.45	3.78	2.84	2.01
95	5.80	3.83	2.64	4.22	3.06	2.06

Table 6: Percentage distribution of countries by % Diff. (BHM - WPP) / WPP

% Diff.	2013	2018	2023	2028	2033	2038	2043	2048	Total
< -15	0.0	0.5	3.6	6.7	9.3	10.3	10.8	11.9	6.6
-15/-10	0.0	5.7	11.9	10.8	10.8	13.9	13.4	12.4	9.9
-10/-5	9.3	20.1	15.0	16.0	17.5	15.0	17.0	21.7	16.4
-5/+5	87.1	58.8	43.8	37.6	34.0	32.0	32.5	28.9	44.3
+5/+10	3.6	13.4	17.5	12.4	10.3	10.8	8.8	7.2	10.5
+10/+15	0.0	1.6	6.7	9.8	8.8	5.2	4.1	5.2	5.2
+15/+20	0.0	0.0	1.6	5.7	5.7	6.7	6.2	4.1	3.7
+20/+30	0.0	0.0	0.0	1.0	3.1	5.7	6.2	7.7	3.0
> +30	0.0	0.0	0.0	0.0	0.5	0.5	1.0	1.0	0.4
Total	100.0	100.0	100.0	100.0	100.0	100.0	100.0	100.0	100.0

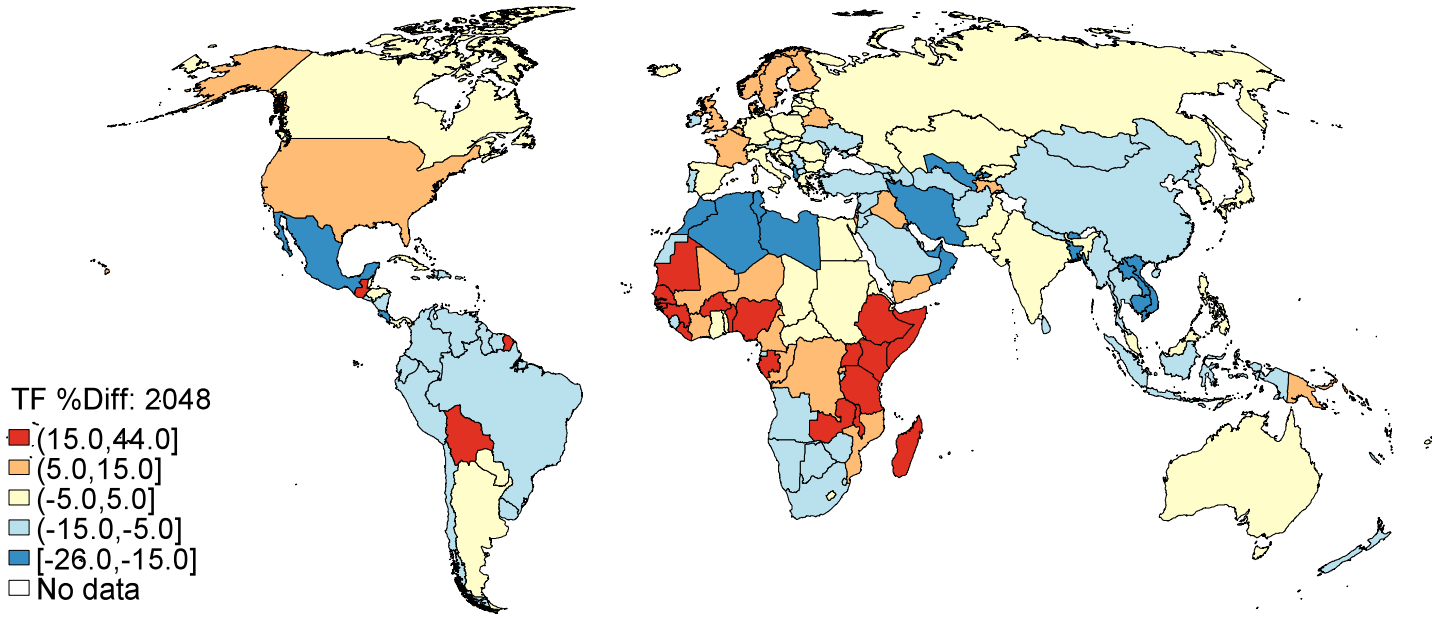

Figure 12: Countries with largest TFR percentage differences (BHM-WPP)/WPP in 2048

Breakdown of the differences by subgroups: As seen in Table 7 (Panel A), for medium-high fertility countries (TFR above 3), BHM gives on average higher TFR than WPP (except for the next 20 years for countries with TFR above 6). Overall, BHM is more conservative than WPP about the speed of decline for most medium-high fertility countries. For countries with medium-low fertility (TFR between 1.4 and 3.0), BHM gives slightly smaller average TFR than WPP. For very low fertility countries (TFR < 1.4), BHM median provides results similar to WPP 2008 about the speed of recovery from very low fertility.

Overall, the average differences for more developed regions and other less developed regions are very small, and most of the differences with WPP are for the Least Developed Countries with BHM higher than WPP (Table 7, Panel B). In term of regional patterns, the largest average positive differences with BHM higher than WPP are in several regions of Oceania and Africa (Western, Eastern, and Middle Africa), and to a lesser extent in North America. BHM projects much faster declines than WPP in Northern and Southern Africa, and in all Asian regions (especially South-East and South-Central Asia), the Caribbean and Southern Europe (Table 7, Panel C).

Countries with the largest differences: We first consider the countries with BHM>WPP, colored in red in the map in Figure 12. The list of countries in Table 8 focuses on the countries with the largest relative positive difference ($\geq 15\%$) between BHM and WPP TFR projections in 2048. Most of these cases involve developing countries with medium-high fertility in 2008 for which recent levels and trends in TFR suggest much *slower* fertility declines as projected by BHM compared to WPP.

The countries listed in Table 9, colored in blue on the map in Figure 12, are those for which recent levels and trends in TFR suggest much *faster* fertility declines as projected by BHM compared to WPP's more conservative projected declines. These Asian and African countries have experienced some of the fastest TFR declines in recent decades. It is also worth noting that BHM allows countries to continue their decline below sub-replacement

Table 7: Unweighted average absolute difference TFR (BHM - WPP)

Panel A. by level of total fertility in 2008:

TF2008	2013	2018	2023	2028	2033	2038	2043	2048
6+	-0.08	-0.12	-0.09	-0.02	0.07	0.15	0.21	0.24
5.0-6.0	0.02	0.13	0.25	0.35	0.41	0.43	0.43	0.41
4.0-5.0	0.07	0.16	0.22	0.25	0.26	0.25	0.24	0.22
3.0-4.0	0.03	0.06	0.08	0.09	0.09	0.09	0.06	0.03
2.1-3.0	-0.02	-0.05	-0.06	-0.08	-0.11	-0.13	-0.16	-0.17
1.85-2.1	-0.03	-0.06	-0.10	-0.13	-0.16	-0.17	-0.17	-0.16
1.6-1.85	-0.06	-0.11	-0.14	-0.15	-0.15	-0.13	-0.10	-0.08
1.4-1.6	-0.04	-0.07	-0.09	-0.10	-0.10	-0.11	-0.11	-0.10
1.2-1.4	-0.01	-0.02	-0.01	-0.01	0.00	-0.01	-0.01	-0.02

Panel B. by development groups

DevGroup	2013	2018	2023	2028	2033	2038	2043	2048
LDC	0.00	0.04	0.09	0.13	0.16	0.18	0.18	0.18
Other LDR	-0.01	-0.01	-0.02	-0.03	-0.04	-0.06	-0.07	-0.08
MDR	-0.02	-0.02	-0.03	-0.02	-0.02	-0.02	-0.02	-0.02

Panel C. by regions

Area	Region	2013	2018	2023	2028	2033	2038	2043	2048
Africa	Eastern Africa	0.02	0.10	0.18	0.24	0.28	0.30	0.30	0.29
	Middle Africa	0.00	0.02	0.06	0.09	0.11	0.12	0.12	0.11
	Northern Africa	-0.05	-0.10	-0.14	-0.17	-0.19	-0.21	-0.22	-0.23
	Southern Africa	-0.03	-0.06	-0.08	-0.10	-0.11	-0.12	-0.13	-0.13
	Western Africa	0.01	0.11	0.19	0.26	0.30	0.31	0.31	0.30
Asia	Eastern Asia	-0.08	-0.14	-0.17	-0.17	-0.17	-0.15	-0.14	-0.12
	South-Central Asia	-0.05	-0.08	-0.11	-0.12	-0.13	-0.15	-0.16	-0.17
	South-Eastern Asia	-0.03	-0.07	-0.11	-0.13	-0.15	-0.16	-0.17	-0.18
	Western Asia	-0.03	-0.05	-0.05	-0.06	-0.07	-0.09	-0.11	-0.12
Europe	Eastern Europe	-0.01	-0.01	-0.01	0.00	-0.01	-0.01	-0.02	-0.03
	Northern Europe	0.00	0.01	0.02	0.03	0.03	0.03	0.04	0.04
	Southern Europe	-0.05	-0.09	-0.11	-0.12	-0.12	-0.12	-0.11	-0.11
	Western Europe	0.01	0.00	0.00	0.01	0.02	0.03	0.04	0.04
Latin America and the Caribbean	Caribbean	-0.04	-0.08	-0.12	-0.14	-0.16	-0.17	-0.17	-0.16
	Central America	0.00	0.01	0.00	-0.01	-0.01	-0.02	-0.04	-0.06
	South America	0.03	0.05	0.05	0.04	0.03	0.01	-0.02	-0.05
Northern America	Northern America	0.03	0.05	0.08	0.08	0.08	0.08	0.09	0.10
Oceania	Australia/New Zealand	-0.04	-0.04	-0.04	-0.05	-0.07	-0.07	-0.07	-0.07
	Melanesia	0.06	0.13	0.16	0.18	0.17	0.16	0.15	0.14
	Micronesia	0.06	0.10	0.13	0.15	0.17	0.19	0.20	0.15
	Polynesia	0.11	0.20	0.25	0.28	0.29	0.28	0.26	0.25

Table 8: Countries with BHM median TFR greater than WPP medium TFR in 2048 by more than 15%

			2028				2048			
Country	**Region**	**2008**	**BHM**	**WPP**	**Diff**	**%Diff**	**BHM**	**WPP**	**Diff**	**%Diff**
Zambia	Eastern Africa	5.87	4.62	3.65	0.97	26.4	3.67	2.55	1.12	43.9
Occupied Palestinian Territory	Western Asia	5.09	3.88	3.12	0.76	24.6	3.08	2.35	0.73	31.1
Guatemala	Central America	4.15	3.01	2.61	0.40	15.5	2.39	1.85	0.54	29.2
Guinea-Bissau	Western Africa	5.73	4.66	4.07	0.59	14.6	3.70	2.87	0.83	28.8
United Republic of Tanzania	Eastern Africa	5.58	4.28	3.80	0.48	12.6	3.29	2.62	0.67	25.7
Madagascar	Eastern Africa	4.78	3.63	3.06	0.57	18.8	2.91	2.32	0.59	25.3
Samoa	Polynesia	3.99	3.21	2.69	0.52	19.3	2.70	2.16	0.54	25.2
Somalia	Eastern Africa	6.40	5.22	4.78	0.44	9.1	3.83	3.06	0.77	25.1
Malawi	Eastern Africa	5.59	4.15	3.64	0.51	13.9	3.18	2.56	0.62	24.4
Burkina Faso	Western Africa	5.94	4.47	4.05	0.42	10.3	3.37	2.72	0.65	24.0
Vanuatu	Melanesia	4.00	3.18	2.72	0.46	17.0	2.64	2.17	0.47	21.7
Tonga	Polynesia	4.05	3.18	2.72	0.46	16.9	2.64	2.17	0.47	21.6
Nigeria	Western Africa	5.32	3.85	3.27	0.58	17.6	2.93	2.41	0.52	21.4
Uganda	Eastern Africa	6.38	4.53	4.22	0.31	7.5	3.18	2.62	0.56	21.3
French Guiana	South America	3.27	2.78	2.41	0.37	15.3	2.43	2.01	0.42	20.8
Ethiopia	Eastern Africa	5.38	3.59	3.25	0.34	10.3	2.64	2.19	0.45	20.5
Kenya	Eastern Africa	4.96	3.65	3.22	0.43	13.4	2.87	2.39	0.48	20.1
Gabon	Middle Africa	3.35	2.81	2.44	0.37	15.1	2.43	2.03	0.40	19.8
Benin	Western Africa	5.48	4.02	3.62	0.40	11.0	3.05	2.55	0.50	19.7
Liberia	Western Africa	5.14	3.81	3.32	0.49	14.9	2.90	2.43	0.47	19.4
Bolivia	South America	3.50	2.65	2.26	0.39	17.3	2.19	1.85	0.34	18.4
Senegal	Western Africa	5.04	3.60	3.12	0.48	15.5	2.77	2.35	0.42	17.8
Guinea	Western Africa	5.45	3.92	3.56	0.36	10.2	2.95	2.52	0.43	17.0
Micronesia (Fed. States of)	Micronesia	3.62	2.65	2.36	0.29	12.3	2.14	1.85	0.29	15.7
Mauritania	Western Africa	4.52	3.32	2.95	0.37	12.6	2.62	2.28	0.34	15.1

Table 9: Countries with BHM median TFR lower than WPP medium TFR in 2048 by more than 15%

			2028				2048			
Country	**Region**	**2008**	**BHM**	**WPP**	**Diff**	**%Diff**	**BHM**	**WPP**	**Diff**	**%Diff**
Oman	Western Asia	3.09	1.83	2.34	-0.51	-21.9	1.47	1.97	-0.50	-25.5
Maldives	South-Central Asia	2.06	1.38	1.85	-0.47	-25.4	1.40	1.85	-0.45	-24.3
Libyan Arab Jamahiriya	Northern Africa	2.72	1.77	1.93	-0.16	-8.3	1.43	1.85	-0.42	-22.7
Viet Nam	South-Eastern Asia	2.08	1.55	1.85	-0.30	-16.2	1.46	1.85	-0.39	-21.1
Bhutan	South-Central Asia	2.68	1.73	1.89	-0.16	-8.4	1.48	1.85	-0.37	-20.0
Bangladesh	South-Central Asia	2.36	1.70	1.95	-0.25	-12.8	1.49	1.85	-0.36	-19.5
Iran (Islamic Republic of)	South-Central Asia	1.83	1.35	1.85	-0.50	-27.0	1.49	1.85	-0.36	-19.5
Kuwait	Western Asia	2.18	1.62	1.88	-0.26	-13.7	1.49	1.85	-0.36	-19.5
Algeria	Northern Africa	2.38	1.67	2.00	-0.33	-16.3	1.50	1.85	-0.35	-18.9
United Arab Emirates	Western Asia	1.95	1.54	1.85	-0.31	-16.8	1.52	1.85	-0.33	-17.8
Mexico	Central America	2.21	1.68	1.85	-0.17	-9.2	1.53	1.85	-0.32	-17.3
Saint Lucia	Caribbean	2.05	1.61	1.85	-0.24	-13.0	1.53	1.85	-0.32	-17.3
Cambodia	South-Eastern Asia	2.96	1.93	2.27	-0.34	-14.9	1.60	1.93	-0.33	-17.0
Brunei Darussalam	South-Eastern Asia	2.11	1.69	1.85	-0.16	-8.6	1.55	1.85	-0.30	-16.2
Saint Vincent and the Grenadines	Caribbean	2.13	1.67	1.86	-0.19	-10.0	1.55	1.85	-0.30	-16.2
Lao People's Democratic Republic	South-Eastern Asia	3.54	2.22	2.52	-0.30	-11.8	1.74	2.07	-0.33	-15.9
Albania	Southern Europe	1.87	1.57	1.85	-0.28	-15.1	1.56	1.85	-0.29	-15.7
Bahrain	Western Asia	2.29	1.77	1.85	-0.08	-4.3	1.56	1.85	-0.29	-15.7
Costa Rica	Central America	1.96	1.59	1.85	-0.26	-14.1	1.56	1.85	-0.29	-15.7
Tunisia	Northern Africa	1.86	1.50	1.85	-0.35	-18.9	1.56	1.85	-0.29	-15.7
Lebanon	Western Asia	1.86	1.58	1.85	-0.27	-14.6	1.57	1.85	-0.28	-15.1
Morocco	Northern Africa	2.38	1.78	1.99	-0.21	-10.6	1.57	1.85	-0.28	-15.1
Uzbekistan	South-Central Asia	2.29	1.76	1.94	-0.18	-9.4	1.57	1.85	-0.28	-15.1

level and to edge back toward replacement level once they reach very low fertility (instead of keeping them at 1.85 once they reach this floor value, as in WPP).

5.2 Comparison between WPP High and Low Variants and the BHM 95% Prediction Intervals

While WPP assumes for its high and low variants a constant ±0.5 child difference from the Medium variant (equivalent to a High-Low range of 1 child), the average width of the BHM 95% prediction interval increases over time, with greater uncertainty about the more distant future. The BHM prediction interval is wider for the Least Developed Countries and other Less Developed Regions, and narrower for More Developed Regions than WPP (Table 10 and Figure 13). The BHM interval for the LDCs increases up to 2048 and decreases back afterward with countries converging toward replacement level (Figure 13A). The BHM interval for other LDRs keeps increasing over time but becomes more concentrated once countries reach replacement level (Figure 13B). Overall the interval is wider than the ±0.5 child used by WPP. Finally the BHM interval for MDR keeps increasing over time and becomes more concentrated (less than ± 0.5 child) once countries reach replacement level (Figure 13C).

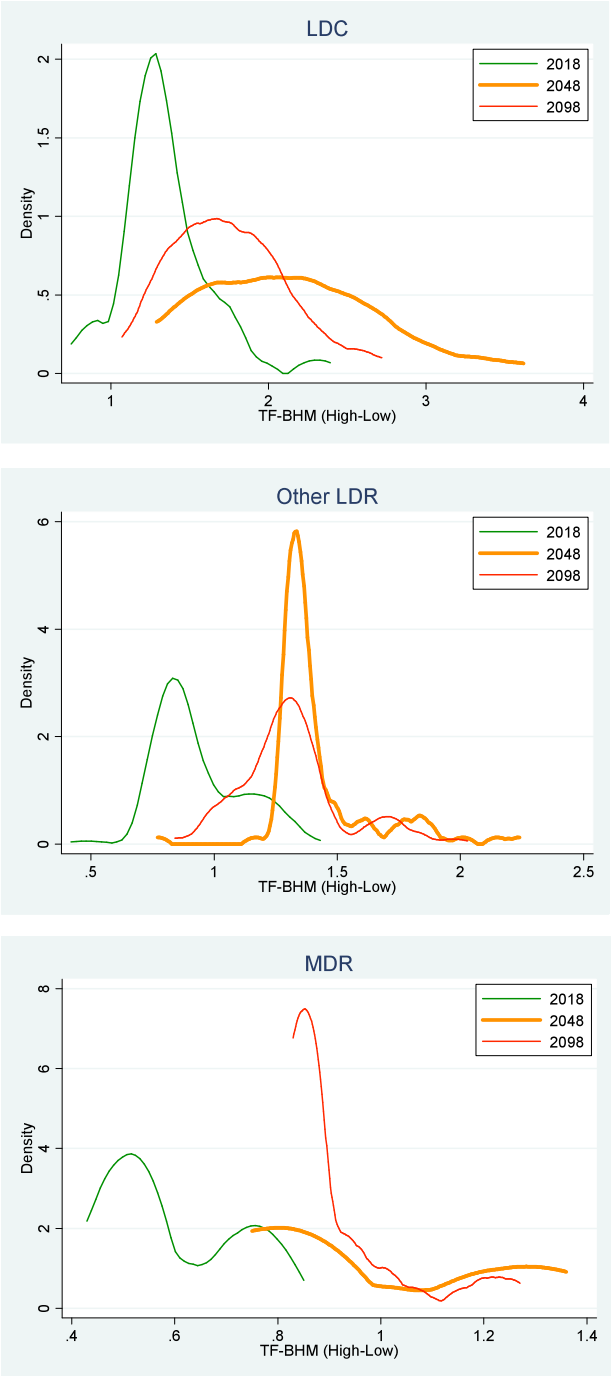

Figure 13: Densities of the width of the BHM prediction intervals for TFR, by development groups

Table 10: Unweighted average width of the BHM prediction interval by development groups

Development Group	2013	2018	2023	2028	2033	2038	2043	2048	2073	2098
Least-Developed Countries	0.89	1.34	1.66	1.88	2.02	2.09	2.12	2.12	1.97	1.74
Other Less Developed Regions	0.69	0.93	1.09	1.20	1.28	1.34	1.39	1.42	1.43	1.31
More Developed Regions	0.42	0.59	0.71	0.80	0.87	0.92	0.95	0.96	0.96	0.92

5.3 2010-2100 Trends and Potential Crossovers

As seen in Figure 14, the Medium TFR projection between 2010-2050 by the 2008 Revision of the World Population Prospects contains very few crossovers between countries within each region. But the WPP assumption that all countries above replacement will stabilize at 1.85, or will converge almost linearly toward 1.85 if they are currently below replacement leads many countries to evolve in parallel toward the same goal.

By relaxing this artificial WPP constraint that all countries stabilize at 1.85 once they reach this level, the new BHM approach introduces much more variability between countries within each region, and between regions (Figure 15). The faster/slower pace of decline (or recovery) for various countries (especially in Eastern Asia, Northern and Southern Europe, Caribbean, Australia and New Zealand) leads to some crossovers which overall remain plausible since in most cases they are based on recent fertility trends and the experience of other countries at similar levels. But between 2050-2100 most of these crossovers are resolved and most countries are converging toward replacement level (Figures 16, 17, 18, 19, 20).

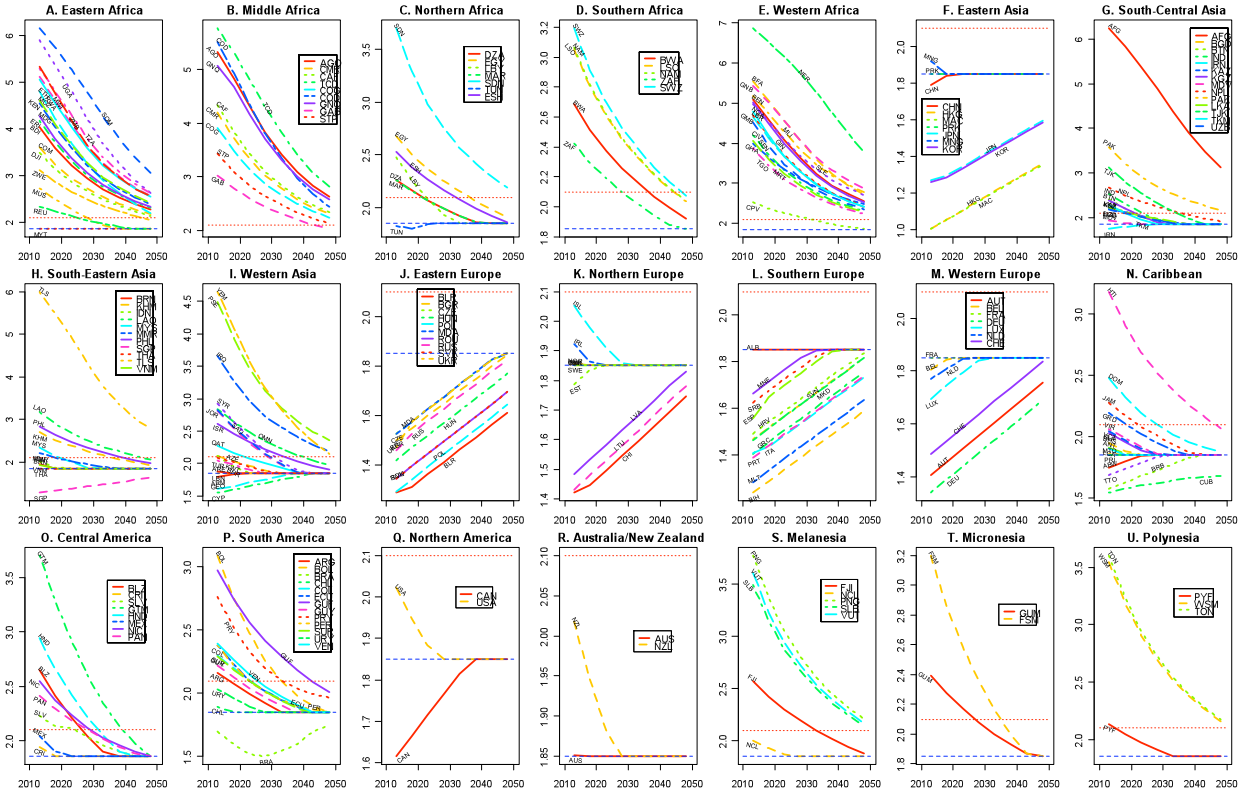

Figure 14: WPP 2008 Revision: Medium TFR projection 2010-2050 by Regions

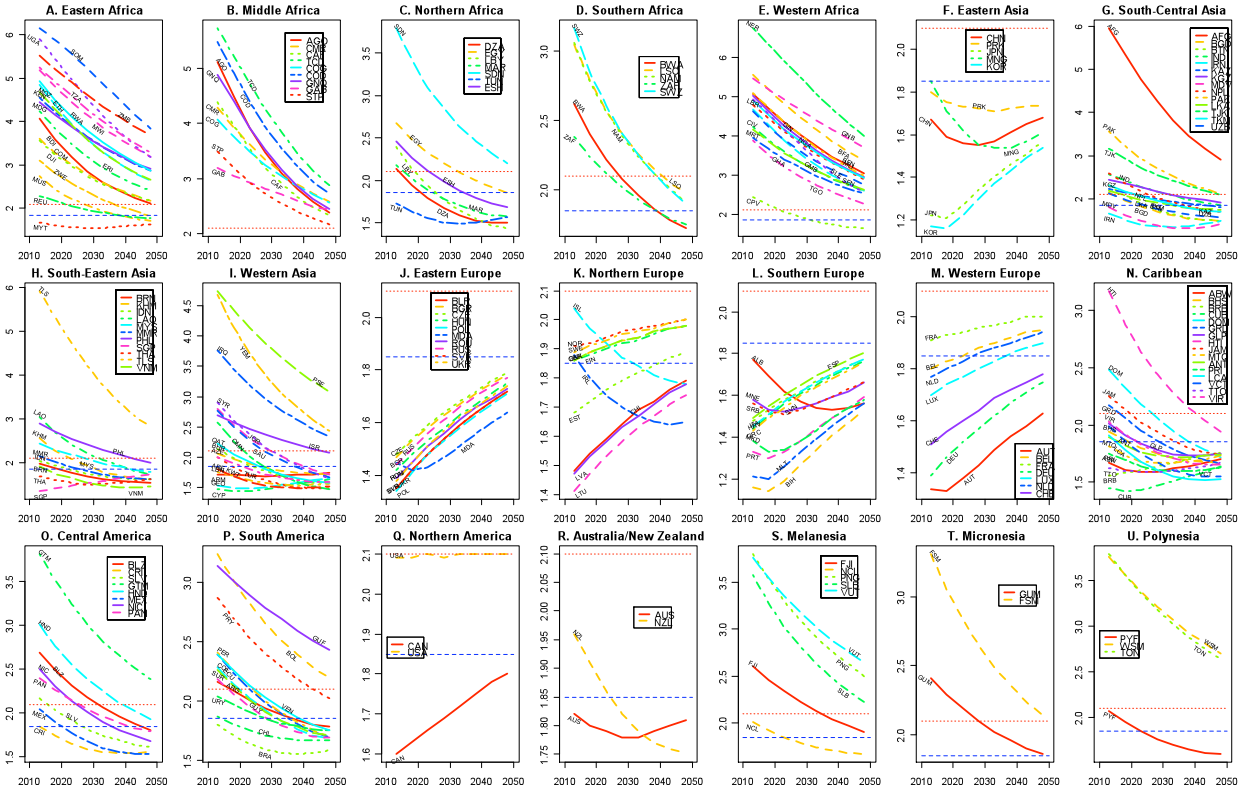

Figure 15: BHM Median TFR projection 2010-2050 by Regions

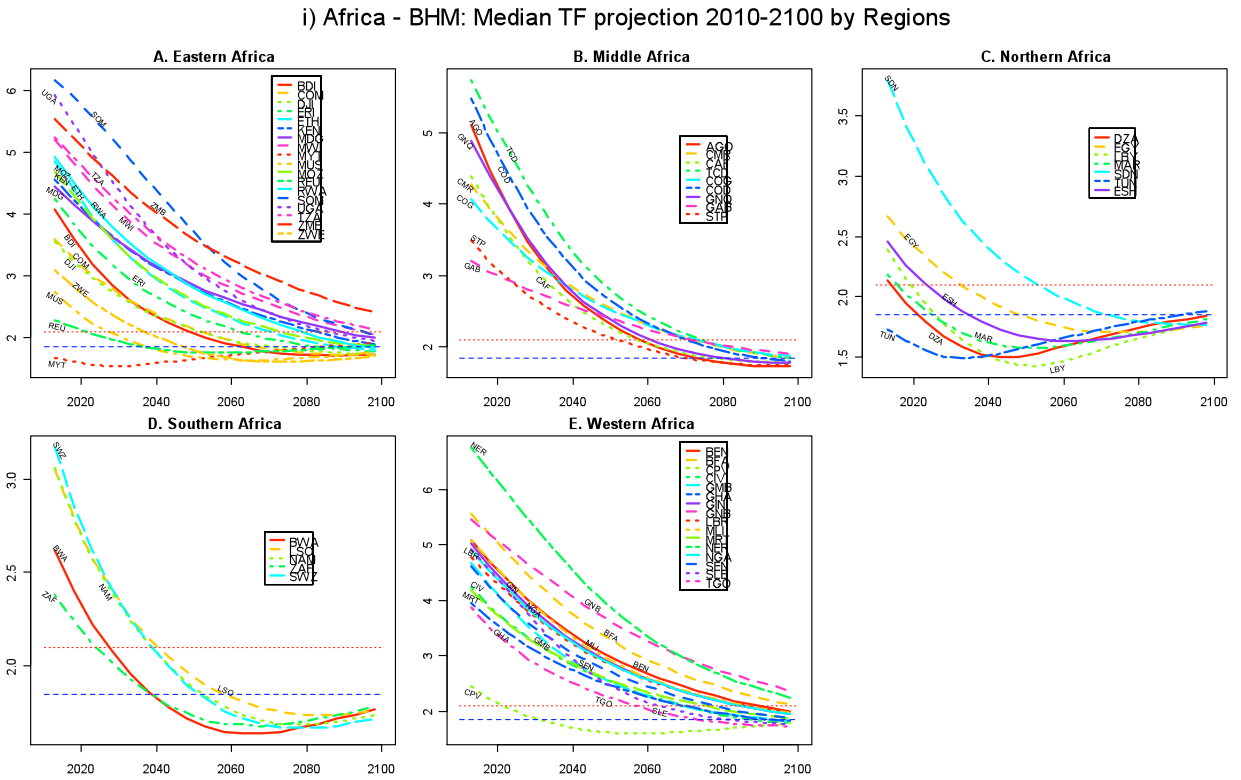

Figure 16: BHM Median TFR Projection 2010–2100 by Regions for Africa

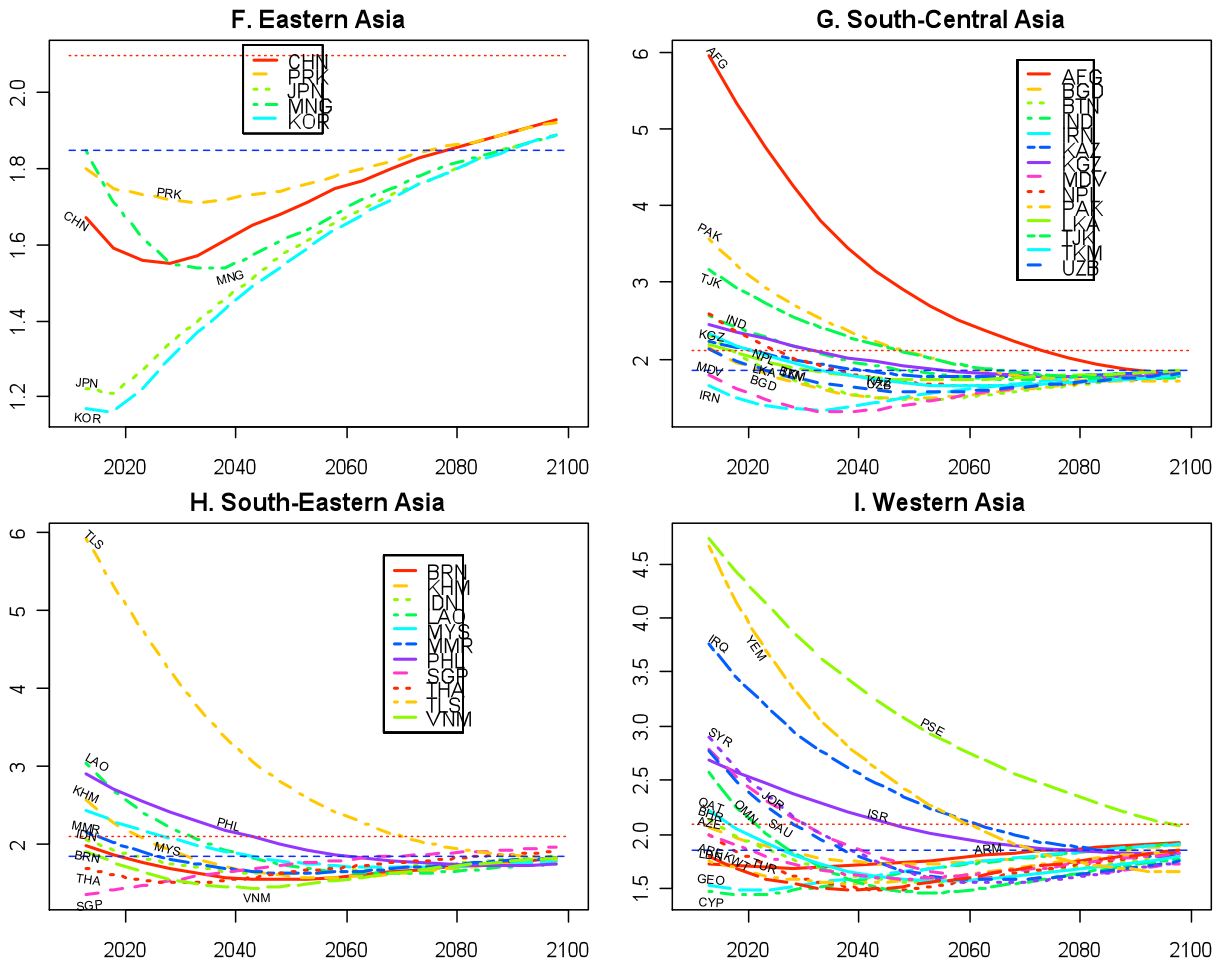

Figure 17: BHM Median TFR Projection 2010–2100 by Regions for Asia

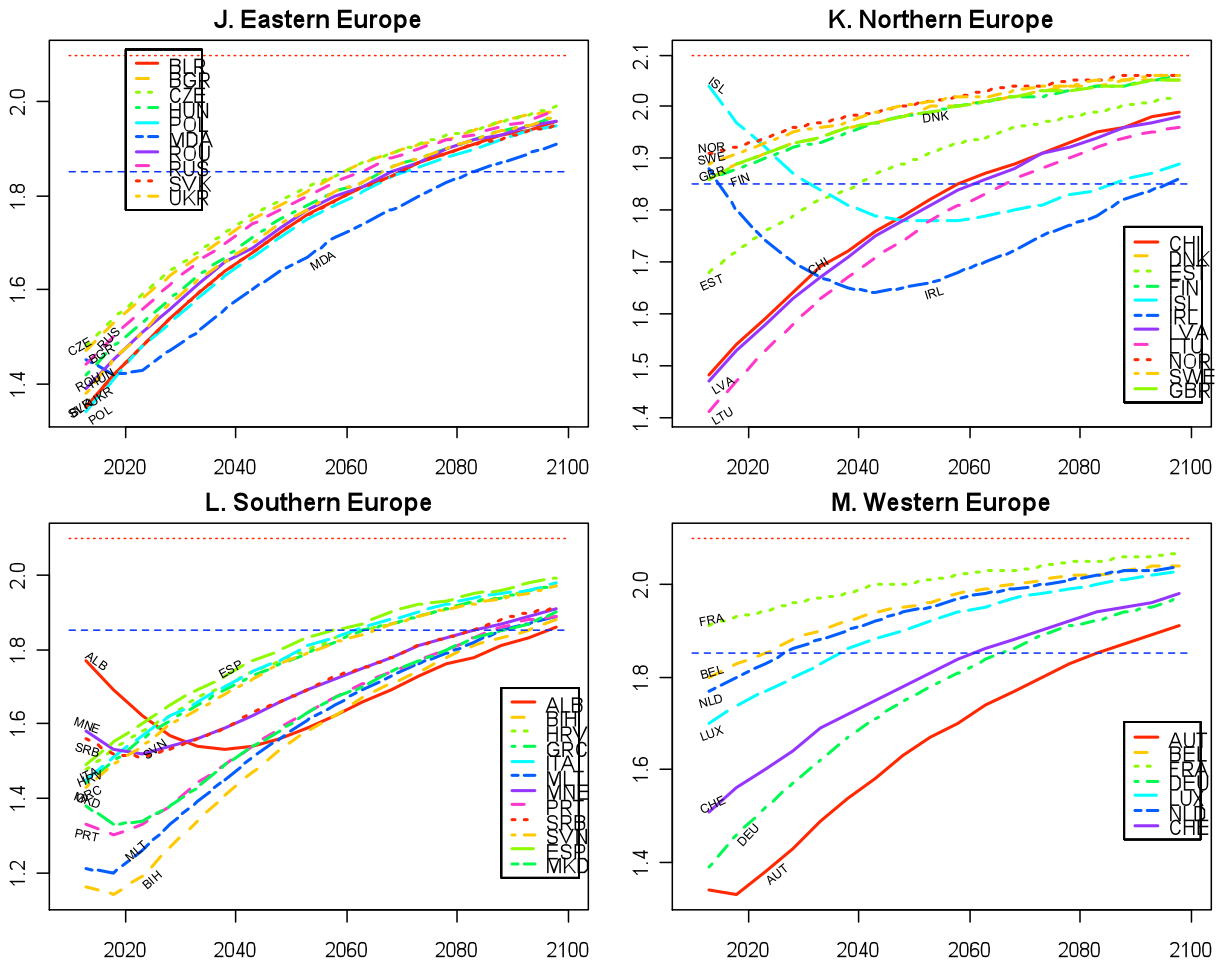

Figure 18: BHM Median TFR Projection 2010–2100 by Regions for Europe

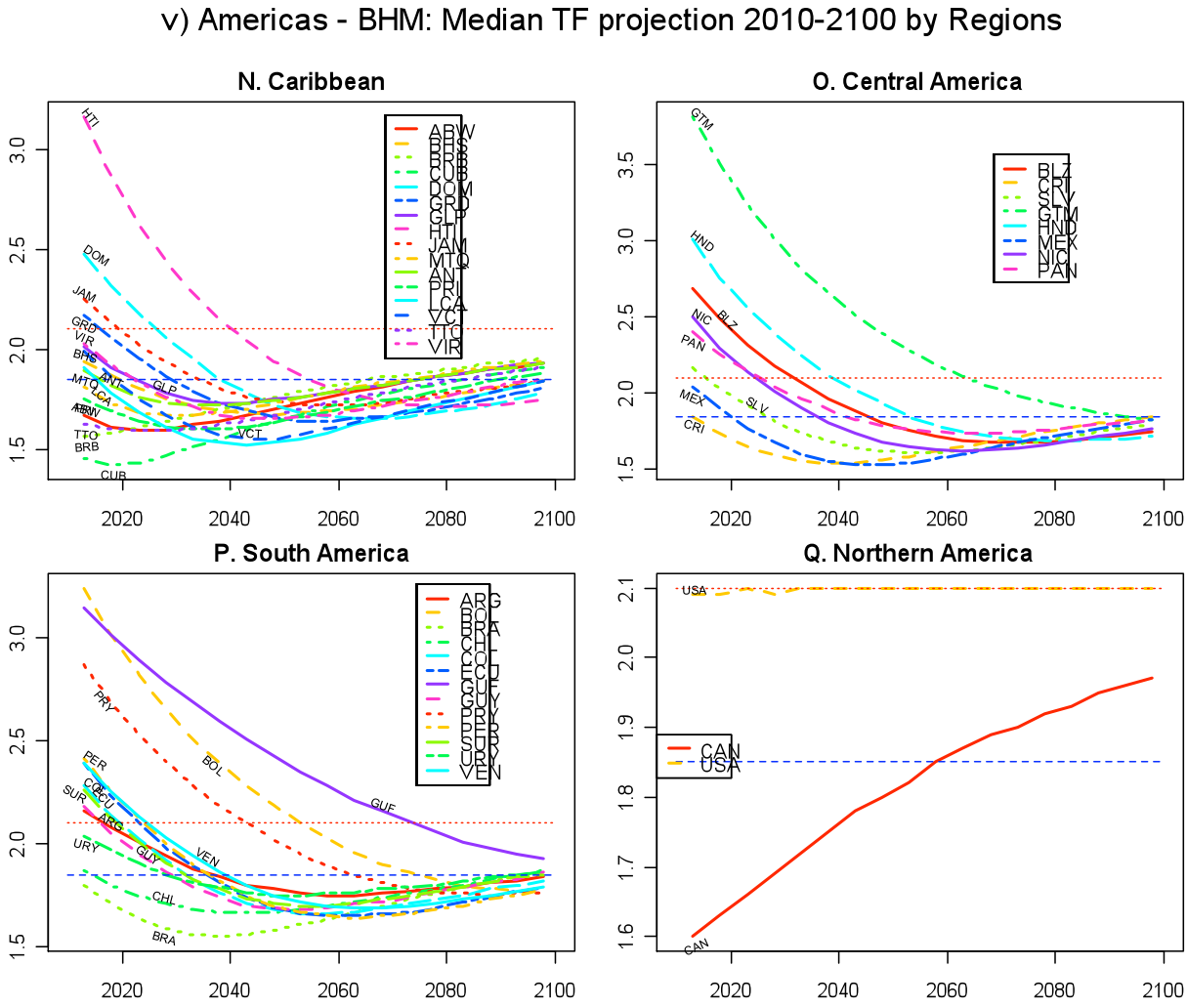

Figure 19: BHM Median TFR Projection 2010–2100 by Regions for the Americas

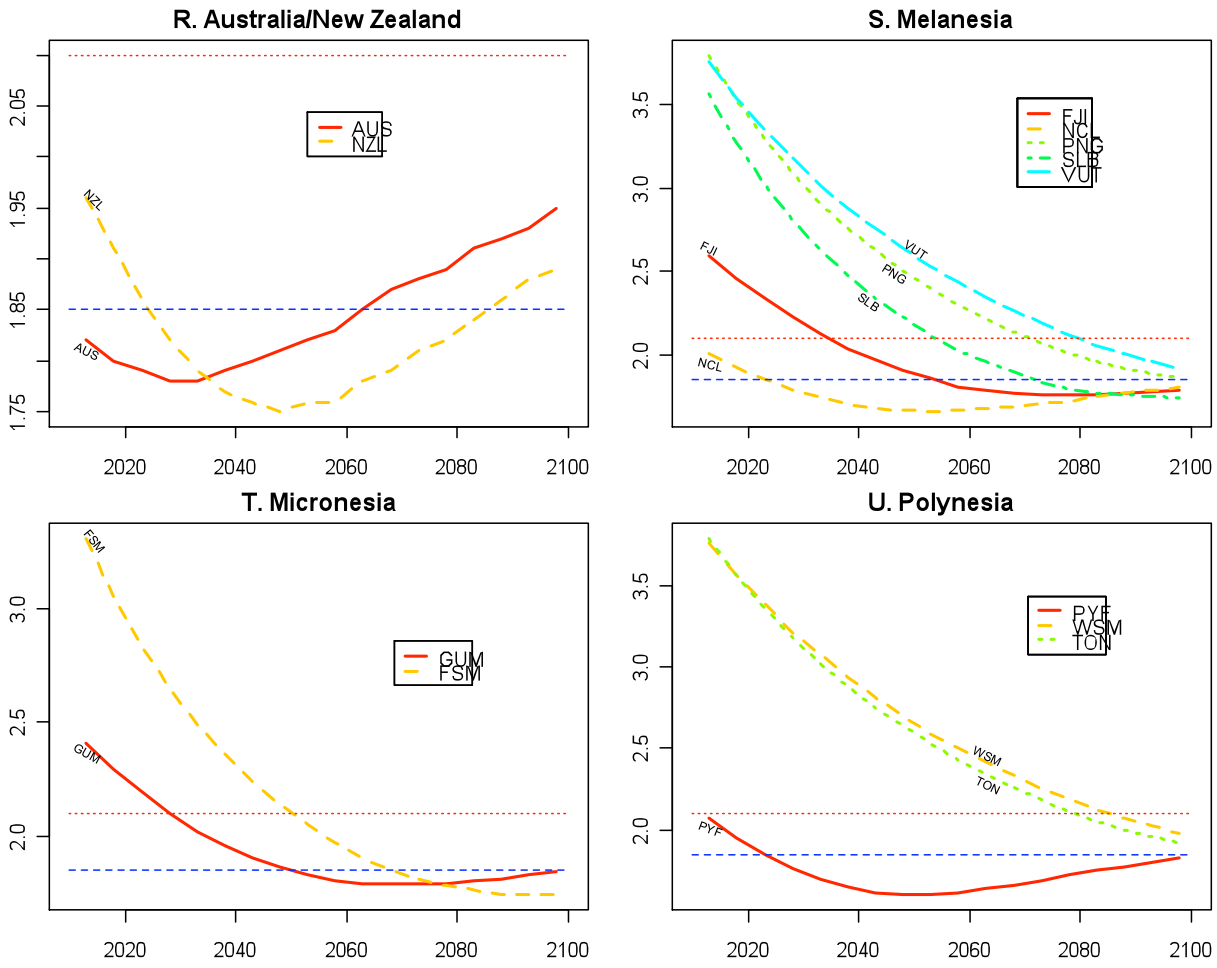

Figure 20: BHM Median TFR Projection 2010–2100 by Regions for Oceania

6 Application to Probabilistic Population Projections

In the 2008 WPP and previous versions, the UN Population Division has issued high, medium and low variants of their population projections for many age- and sex-specific quantities. The quantities projected by the Population Division include age- and sex-specific population counts, fertility, mortality and migration rates, by country and aggregated across regions and development groups. The high and low variants differ from the median variant only in that the TFR is allowed to vary by plus or minus half a child.

As a first step toward fully probabilistic population projections for all quantities of interest, we produced probabilistic projections that take account of uncertainty about the future TFR. Our simulation started the projections from the year 2005 and used data on the initial populations, survival ratios, migrations, PASFRs, and SRBs for years later than 2005 from WPP 2008, and 1000 TFR trajectories for each of the 196 normal countries. The 1,000 TFR trajectories were sampled from the original 33,000 MCMC BHM trajectories by taking every 33rd; this essentially eliminates the autocorrelation in the MCMC output. We used a program written in Visual Basic for Applications (VBA) that produces projections identical to those produced by Abacus, the program used by the Population Division to produce the WPP projections.

The simulation ran 1000 projections of the population by age and sex for each of the 196 countries. Here we give results for projecting the total population of China as an example; see Figure 21. We see that the WPP 2008 medium projection is very close to the BHM median projection. We also see that the BHM 95% prediction interval is slightly wider than the WPP 2008 High-Low range.

Figure 21 also shows the results of projections with the BHM median TFR and year-specific 95% upper and lower bounds as scenarios. The resulting intervals are somewhat wider than the probabilistic bounds. This is because the 95% upper and lower bounds are more extreme than would actually be seen in practice: few stochastic trajectories stay consistently at the extreme values, although many do go beyond the 95% bounds at some point.

We plan to make these projections fully probabilistic by taking account of all major sources of uncertainty, notably the overall level of mortality. We plan to take account of this using the Bayesian hierarchical model of Chunn, Raftery, and Gerland (2009) to project life expectancy; this is similar to the BHM used here for fertility. We also plan to investigate whether the contributions of uncertainty about migration and the future age-structure of fertility and mortality are large, and if so to take account of these sources of uncertainty also.

The method can also be used to obtain probabilistic projections of quantities that are aggregated across countries, under the assumptions that underly the Bayesian hierarchical model. Summing up the n^{th} MCMC trajectories of the total population of the 196 countries, the n^{th} trajectory of the world's total population is obtained. The resulting distributions are shown in Figure 22.

The BHM median projection of the total world population is very close to the WPP 2008 medium projection. However, the BHM 95% interval is much narrower than the WPP 2008 high-low range, and also than the range from taking the high and low variants as the BHM 95% upper and lower bounds for all countries. This is because these other two high-low scenarios assume that all countries have high fertility simultaneously, or that all have low fertility, which seems unlikely; it is more likely that some countries will be above expectation

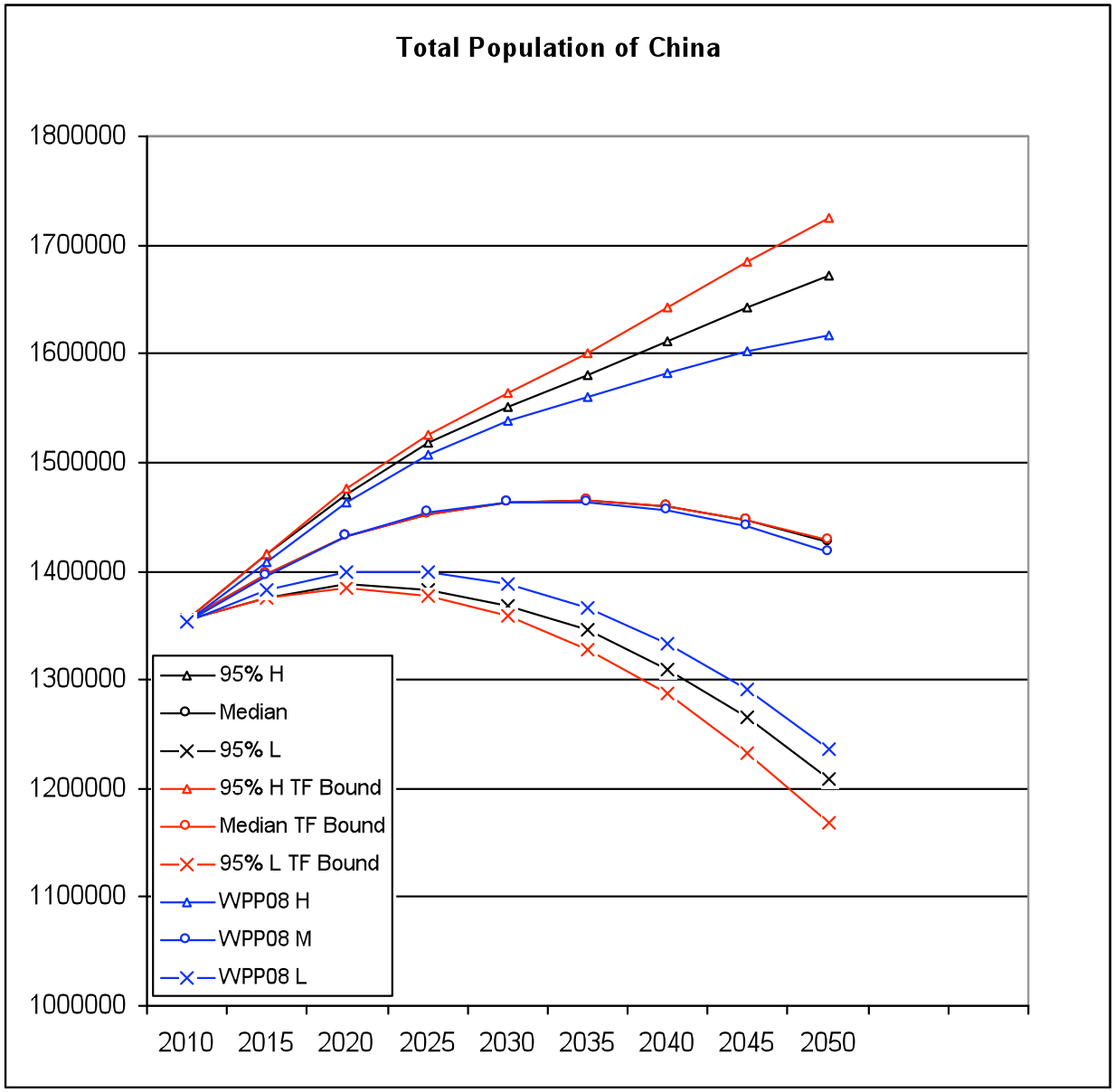

Figure 21: Probabilistic Projections of the Total Population of China, taking account of uncertainty about TFR. The blue curves show the High, Medium and Low variants from the 2008 World Population Prospects. The black curves show the results of the Bayesian hierarchical model projection described in the text. The red curves show projections using the median and bounds of the Bayesian 95% prediction intervals as scenarios.

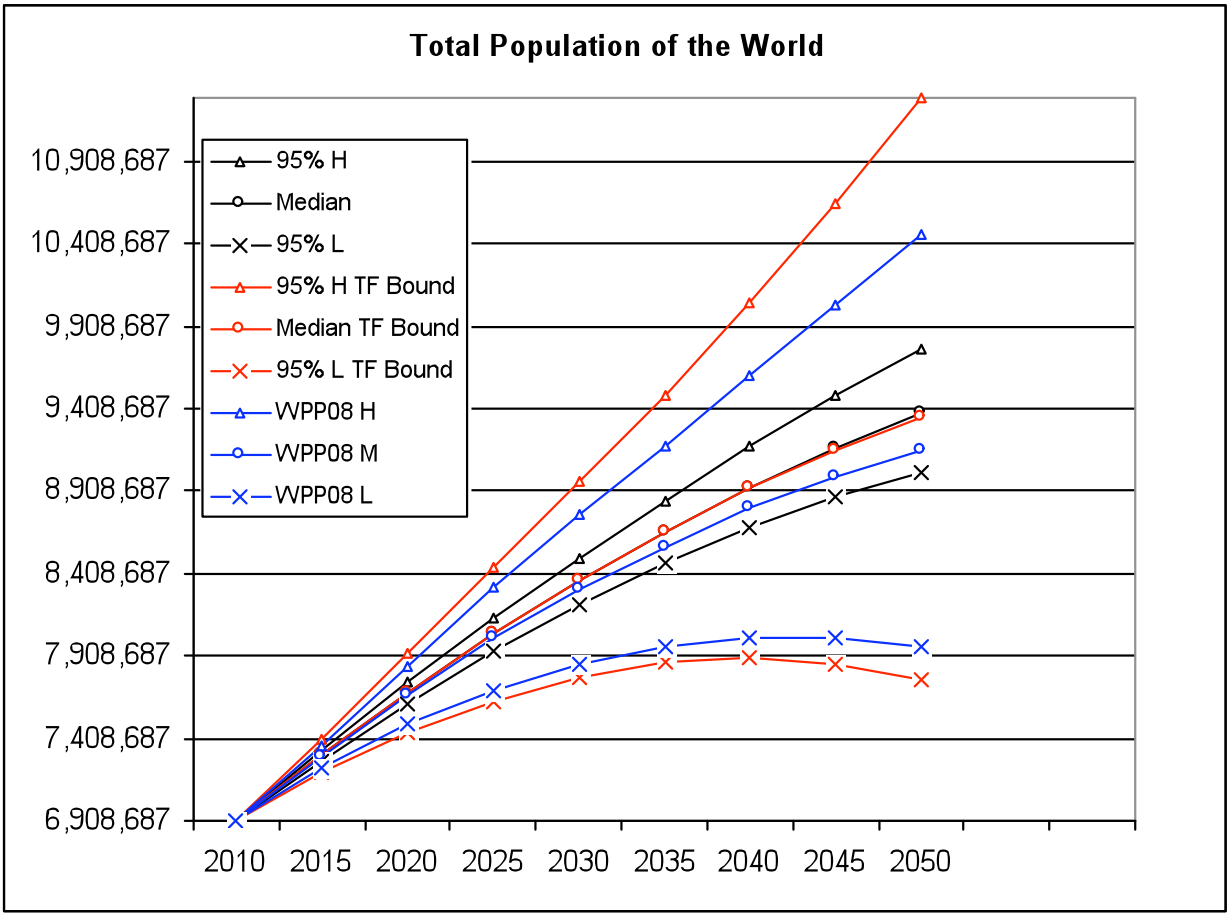

Figure 22: Probabilistic Projections of the Total Population of the World, taking account of uncertainty about TFR. The blue curves show the High, Medium and Low variants from the 2008 World Population Prospects. The black curves show the results of the Bayesian hierarchical model projection described in the text. The red curves show projections using the median and bounds of the Bayesian 95% prediction intervals as scenarios.

and some below. The BHM reflects this more realistic scenario.

However, it should be noted that the validity of the predictive distribution of aggregated quantities depends on the validity of the conditional independence assumptions in the Bayesian hierarchical model. The BHM does not assume that changes in TFR in all countries are statistically independent; instead, it models the pattern of fertility decline that is common to all countries, and this introduces dependence between countries. It does not, however, model additional local or regional correlations, for example between the extent to which fertility changes in neighboring countries differ from expected patterns. If such correlations are present, uncertainty may be underestimated.

This has been discussed by Lutz, Sanderson, and Scherbov (2001), who used judgement-based assessments of correlations, and by Keilman and Pham (2004) and Alho (2008), who used empirical correlations for aggregated stochastic population forecasts for the European Union. We will assess the validity of the aggregated probabilistic projections using the same kind of out-of-sample validation assessment as we used for the TFR. If necessary, we will take account of additional between-country correlation in the error term beyond that allowed by the BHM, using methods such as those cited.

7 Software Implementation

The method described in the previous sections is implemented as a stand-alone package of the statistical programming language **R** (Ihaka and Gentleman 1996; r-project.org). R is widely used among data analysts, because it provides a wide variety of statistical and graphical techniques, it is easy to use, it is open source and it is highly extensible through user-defined packages.

The R package that implements the Bayesian hierarchical model for predicting the total fertility rate is called **bayesTFR**. It is a collection of functions that can be used in the interactive R environment. It has the advantage of having all the capabilities of R and its many packages available for analyzing results. Furthermore, it allows the user to create batch files and run especially time-intensive tasks as batch processes.

For users who prefer a windows-based environment there is a graphical user interface (GUI) for the package available, itself implemented as an R package. It is called **bayesDem** and it reduces the complexity of the task of generating probabilistic TFR predictions to a button click.

Working with bayesTFR either directly or through bayesDem is easy and straightforward. In a standard case, the analyst would follow four basic steps of which one is optional:

1. **Running Markov Chain Monte Carlo (MCMC) chains.** The user can set among other inputs a location on the hard disk (i.e. a directory name) for storing results, the number of chains that should be run, the number of iterations for each chain, which time series of the historical data to use and the parameters of the prior distributions. Furthermore, if the user wishes, multiple chains can be run in parallel which can speed up the computation considerably. The result of this step is a sample from the posterior distribution of the model parameters stored on the hard disk.

2. (optional) **Continuing MCMC chains.** If at a later time point the user decides to continue an existing MCMC run, the package provides functions to do so without having to start again from the beginning. This may be useful, for example, if MCMC diagnostics show that some parameters have not converged, or if a simulation was interrupted due to a hardware or software failure. The function updates the posterior distribution generated in step 1.

3. **Generating predictions.** Using the result from step 1 or step 2, posterior trajectories of TFR for all countries can be generated. Again, the user can enter a location on disk for storing the predictions, the end year of the prediction or the number of burn-in iterations in the MCMC. The package stores the generated trajectories on disk, one file per country, as well as an ASCII summary file, containing the median, the lower and upper bounds of the 80 and 95% confidence intervals. Furthermore, it generates a sample of trajectories in a UN-specific table format, i.e. the column names match those in the UN database, so that it can be immediately used within the UN framework.

4. **Analyzing results.** The package offers a set of functions for summarizing, plotting and diagnosing the results of the steps above. For example one can create a graph of the trajectories for each country including user-defined confidence intervals, or view the same results as a table. One can plot the posterior distribution of the double logistic function for each country, including the historical values. The package also offers

functionality to diagnose the MCMC convergence, using either graphical outputs, such as viewing the MCMC traces of all parameters, or using standard MCMC diagnostic functions available in R and modified for the TFR purposes.

In Figures 23 and 24, screenshots of the bayesDem package are shown. The main window contains four tabs that correspond to the four steps above. Figure 23 shows the interface for completing step one. All input parameters have reasonable default values which allow the user to just click the 'Run MCMC' button in order to start the simulation. Parameters of the prior distributions of the model are hidden behind the 'Advanced Settings' button. The 'Generate Script' button provides the user with an R command that can be used in an interactive mode and produces exactly the same results as the 'Run MCMC' button.

Figure 24 shows the interface available to proceed with step 4. The user can explore TFR trajectories, double logistic curves or the MCMC traces of model parameters. These tasks are again implemented as tab widgets. In the figure, TFR trajectories were generated for China in graphical and numerical form, respectively, using the buttons 'Graph' and 'Table'. The interface also allows the user to create such trajectories for all countries with one button click. The user can control the displayed confidence intervals, or the number of trajectories plotted in the graph.

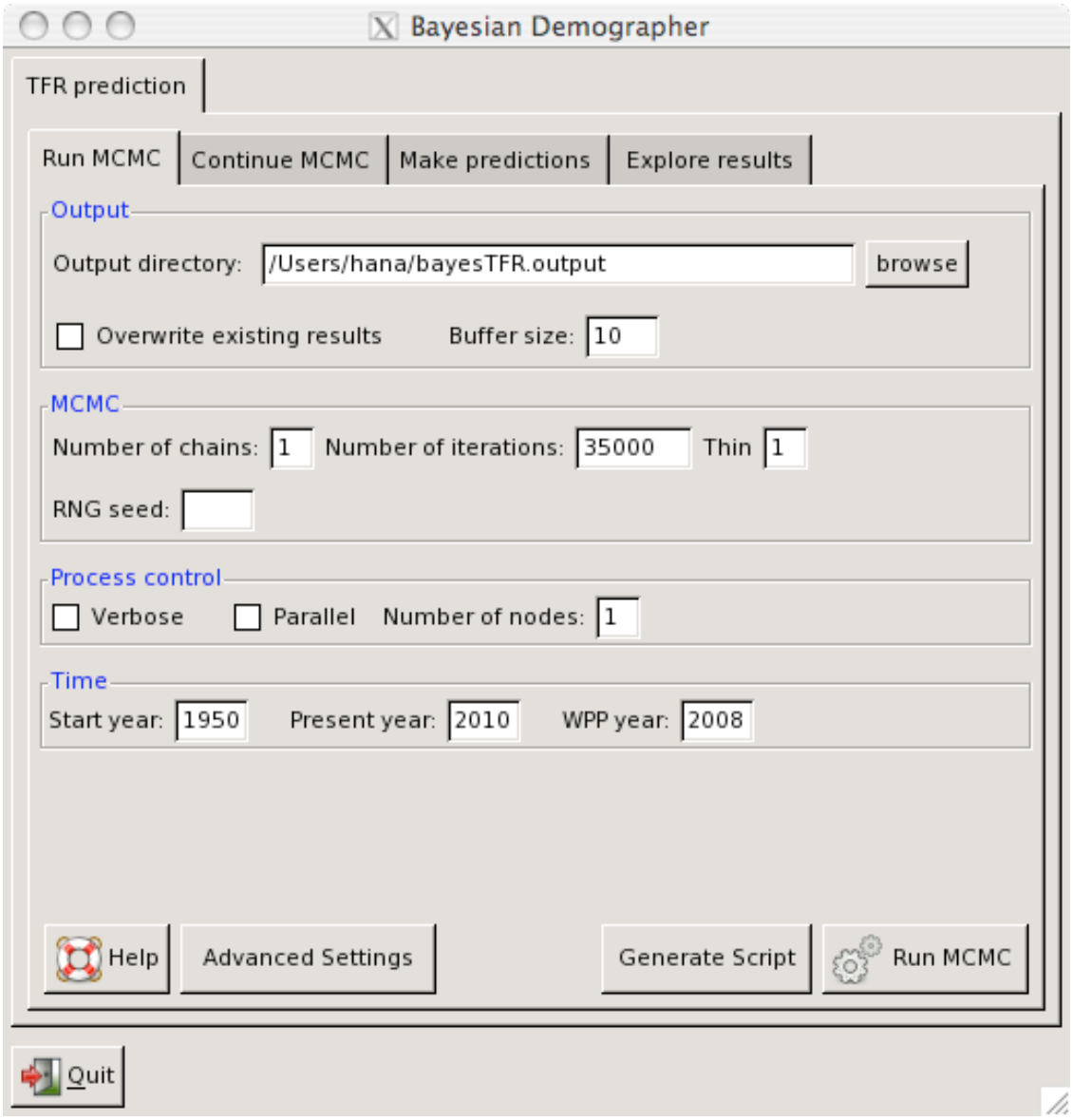

Figure 23: bayesDem: Graphical User Interface for Probabilistic Projection of the Total Fertility Rate. It supports a four-step workflow: Running MCMC, continuing MCMC, making predictions, analyzing results. Each step is supported by a separate tab widget. In the figure, the first step, running MCMC, is shown.

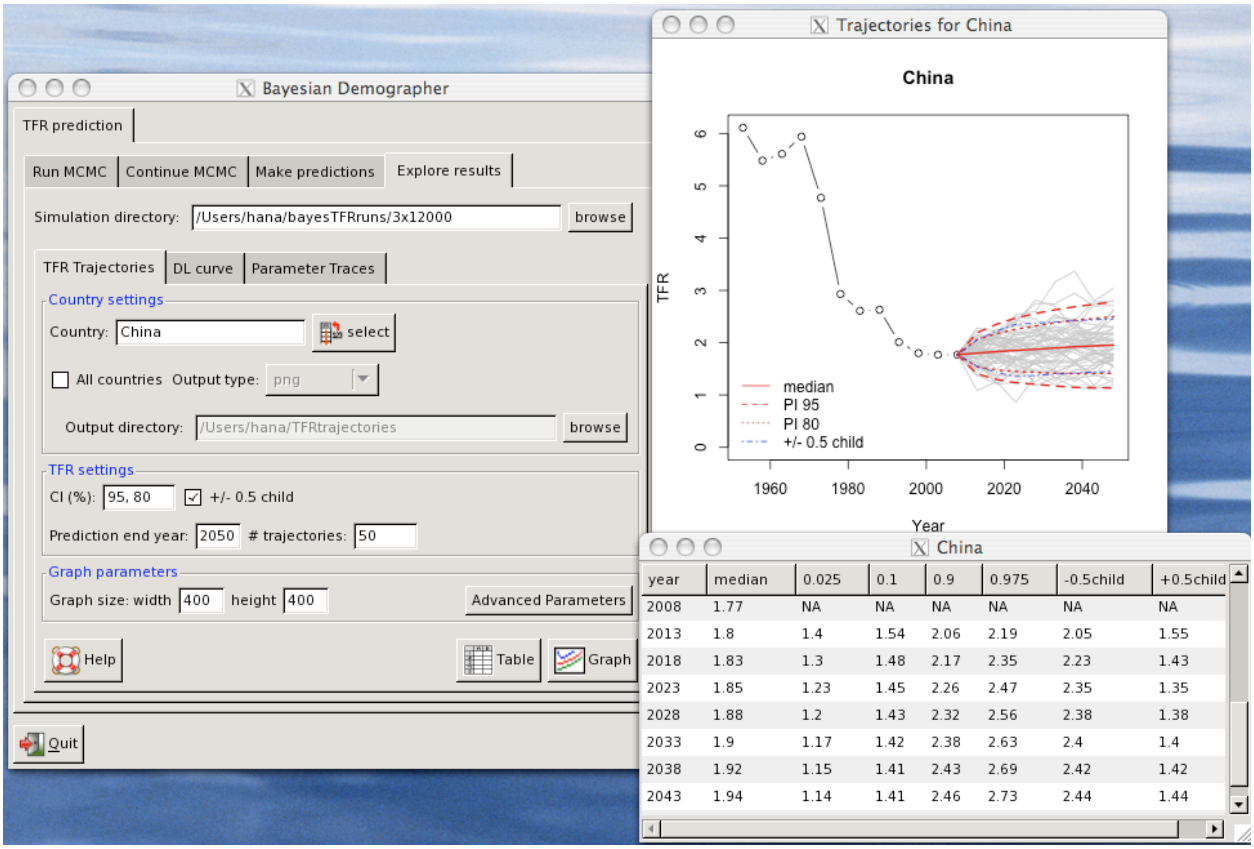

Figure 24: Interface of bayesDem for Analyzing Results. In particular, a tab for displaying TFR trajectories in both graphical and tabular forms is shown.

8 Methodology appendix

8.1 Start period and start level

The start period of the fertility transition is denoted by τ_c for country c. For a number of countries the fertility transition has started (well) before 1950, which means the start of the decline was not observed in the observation period. These countries are identified by a maximum TFR smaller than 5.5 children in the observation period. The cut-off of 5.5 children was chosen after visual inspection of the start periods for all countries, based on different cut-off values. Using 5.5 children best identified the countries in which the decline had possibly already started before 1950. For these countries, the start level $U_c = \sum \triangle_{ci}$ of the fertility decline is added as a parameter to the model, with prior distribution:

$$U_c \;=\; U(\min\{5.5, \max_t f_{c,t}\}, 8.8) \text{ for } \tau_c \geq 1950, \tag{8}$$

The upper bound of the prior distribution is based on the observed maximum in the UN estimates (8.7). Its lower bound is the maximum of the minimum observed TFR value and 5.5 children (5.5 children is based on examining decline curves, the minimum level at which the decline starts is slightly under 6).

For countries in which the fertility decline started after 1950, the start period τ_c is within the observation period. For these countries, the start period of the fertility decline is defined as the most recent period with a local maximum that is within 0.5 children of the global maximum of the TFR. This definition is used instead of simply taking the global maximum to exclude the Phase (1) period, in which the TFR fluctuates around high values.

The start level in τ_c for these countries is fixed at U_c such that the systematic decline in that period is at 10% of the maximum decline, with a "start year" distortion term ε_{c,τ_c} added to it, to allow a bigger decrease in that specific period:

$$\begin{aligned} U_c &= f_{c,\tau_c} \text{ for } \tau_c \geq 1950. \\ \varepsilon_{c,\tau_c} &\sim N(m_{\tau_c}, s_\tau^2) \end{aligned}$$

with m_τ the mean, and s_τ the standard deviation of the distortion in the start period. The different distribution for ε_{c,τ_c} compared to the other distortions is based on the observed starts in the data set; the decrements in the start period tend to be larger than decrements in subsequent years (after taking into account the decline as given by the double-logistic curve).

With these definitions, the start period is defined by:

$$\tau_c \;=\; \max\{t : (M_c - L_{c,t}) < 0.5\}, \text{ if } L_{c,t} > 5.5, \tag{9}$$

$$<\; 1950 \text{ otherwise.} \tag{10}$$

with global maximum $M_c = \max_t f_{c,t}$, and local maxima denoted by $L_{c,t}$.

8.2 Bayesian hierarchical model

A Bayesian hierarchical model is used to estimate the decline parameters $(\triangle_{c1}, \triangle_{c2}, \triangle_{c3}, \triangle_{c4}, d_c)$ for each country.

A logit transform is used to restrict the maximum decrement d_c to be between 0.25 and 2.5 children decrease per time period. The upper bound of 2.5 reflects the maximum pace of fertility decline observed in the past of around 2 children per 5 year period, in China. The hierarchical model for the log-transformed d_c is: by:

$$\phi_c \sim N(\chi, \psi^2), \tag{11}$$

with ϕ_c the logit-transform of $d_c/5$:

$$\phi_c = \log\left(\frac{d_c/5 - l_d}{u_d - d_c/5}\right), \tag{12}$$

and $[l_d, u_d] = [0.05, 0.5]$, χ the hierarchical mean of the logit-transformed maximum decline for all countries in which (part of) the fertility transition has been observed and ψ^2 the error variance. (The model is implemented in terms of $d_c/5$ because it was originally fitted to 1-year decrement data).

A logit transform is used to restrict $\triangle_{c4}$, the TFR level at which the decrements are at 10% of the maximum pace, to be between 1 and 2.5 children. Its hierarchical model is given by:

$$\triangle'_{c4} \sim N(\triangle_4, \delta_4^2), \tag{13}$$

with $\triangle'_{c4}$ the logit-transform of $\triangle_{c4}$:

$$\triangle'_{c4} = \log\left(\frac{\triangle_{c4} - 1}{2.5 - \triangle_{c4}}\right), \tag{14}$$

Given $\triangle_{c4}$ and the start level $U_c = \sum_i \triangle_{ci}$, the other three TFR ranges $(\triangle_{c1}, \triangle_{c2}, \triangle_{c3})$ can be expressed as proportions of $U_c - \triangle_{c4}$. Define:

$$p_{ci} = \frac{\triangle_{ci}}{U_c - \triangle_{c4}} \text{ for } i = 1, 2, 3, \tag{15}$$

such that $\sum_{i=1}^{3} p_{ci} = 1$. We assume that the proportions are exchangeable between countries. For the purpose of computation, a new set of parameters $\gamma_{ci}, i = 1, 2, 3$ are introduced, with the p_{ci}'s defined as a function of these parameters (Gelman et al. 1996):

$$p_{ci} = \frac{\exp(\gamma_{ci})}{\sum_j \exp(\gamma_{cj})}. \tag{16}$$

The hierarchical model for the γ_{ci}'s is given by:

$$\gamma_{ci} \sim N(\alpha_i, \delta_i^2), \tag{17}$$

with α_i the hierarchical mean of the γ_{ci}'s and δ_i^2 their variance.

8.3 Standard deviation of the random distortions

The standard deviation $\sigma_{c,t}$ of the random distortions, $\varepsilon_{c,t}$, is

$$\sigma_{c,t} \quad = \quad c_{1975}(t)\left(\sigma_0 + (f_{c,t} - S)\left(-aI_{f_{c,t}>S} + bI_{f_{c,t}<S}\right)\right), \tag{18}$$

where $\sigma_0$is the maximum standard deviation of the distortions, attained at TFR $f_{c,t} = S$, and a and b are multipliers of the standard deviation, to model the linear decrease for larger and smaller outcomes of the TFR. The constant $c_{1975}(t)$ is added to model the higher error variance of the distortions before 1975, and is given by:

$$c_{1975}(t) \quad = \quad \begin{cases} c, & t \in [1950 - 1955, 1970 - 1975]; \\ 1, & t \in [1975 - 1980, \infty) \end{cases} \tag{19}$$

The variance function is illustrated in Figure 25.

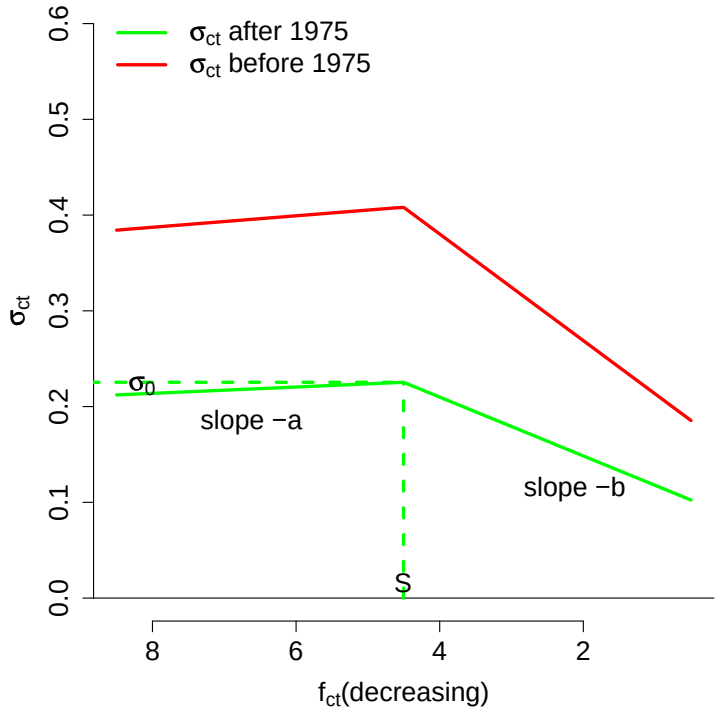

Figure 25: Standard deviation of the distortion terms

8.4 Parameters in TFR projection model

Table 11: Parameters in the TFR projection model

Symbol	Definition
$f_{c,t}$	TFR in country c, year $t = 1, \ldots, T_c$.
T_c	Last observation period (currently $T_c = 2005 - 2010 \forall c$)
$u_{c,t}$	UN estimate in country c, period t.
$d_{c,t}$	5-year decrement for country c, period t
$\varepsilon_{c,t}$	Distortion term added to the 5-year decrements
$\sigma^2_{c,t}$	Variance of the distortion terms in $t \neq \tau_c$
τ_c	Start period of the fertility transition for country c
λ_c	Start period of the recovery phase for country c
$\boldsymbol{\theta}_c$	Parameters of the double-logistic function for country c
d_c	Maximum annual decrement for country c
U_c	Start level of the fertility transition for country c
$\triangle_{ci}, i = 1, 2, 3, 4$	TFR ranges in which pace of fertility decline changes for country c
$g(\boldsymbol{\theta}_c, f_{c,t})$	5-year decrement for country c at TFR $f_{c,t}$
σ^2_0	Maximum variance of the distortions at $f = S$
S	TFR at which the distortions have max variance
a	Multiplier for the TFR (coeff. for linear decrease for $f > S$)
b	Multiplier for the TFR (coeff. for linear decrease for $f < S$)
$c_{1975}(t)$	Multiplier of the sd of the distortions
c	Multiplier of sd of the distortions before 1975
m_τ	Mean of distortion terms in start periods τ_c
s_τ	Standard deviation of distortion terms in start periods τ_c
χ	Hierarchical mean of logit-transformed maximum decline parameter d_c
ψ^2	Variance of logit-transformed maximum decline parameter d_c
p_{ci}	$\triangle_{ci}/(U_c - \triangle_{c4})$ for $i = 1, 2, 3$
γ_{ci}	Parameters to estimate the p_{ci}'s
α_i	Hierarchical mean of γ_{ci}'s for $i = 1, 2, 3$
δ^2_i	Variance of of γ_{ci}'s for $i = 1, 2, 3$
$\triangle_4$	Hierarchical mean of logit-transformed $\triangle_{c4}$'s
δ^2_4	Variance of logit-transformed $\triangle_{c4}$'s
ρ	Autoregressive parameter in AR(1) projection model
s	Standard deviation of AR(1) distortion terms in short-term projections
$s^{(a)}$	Standard deviation of AR(1) distortion terms in long-term projections
μ	Long-term mean in AR(1) projection model

9 APPENDIX: Results

9.1 Plots: Projections

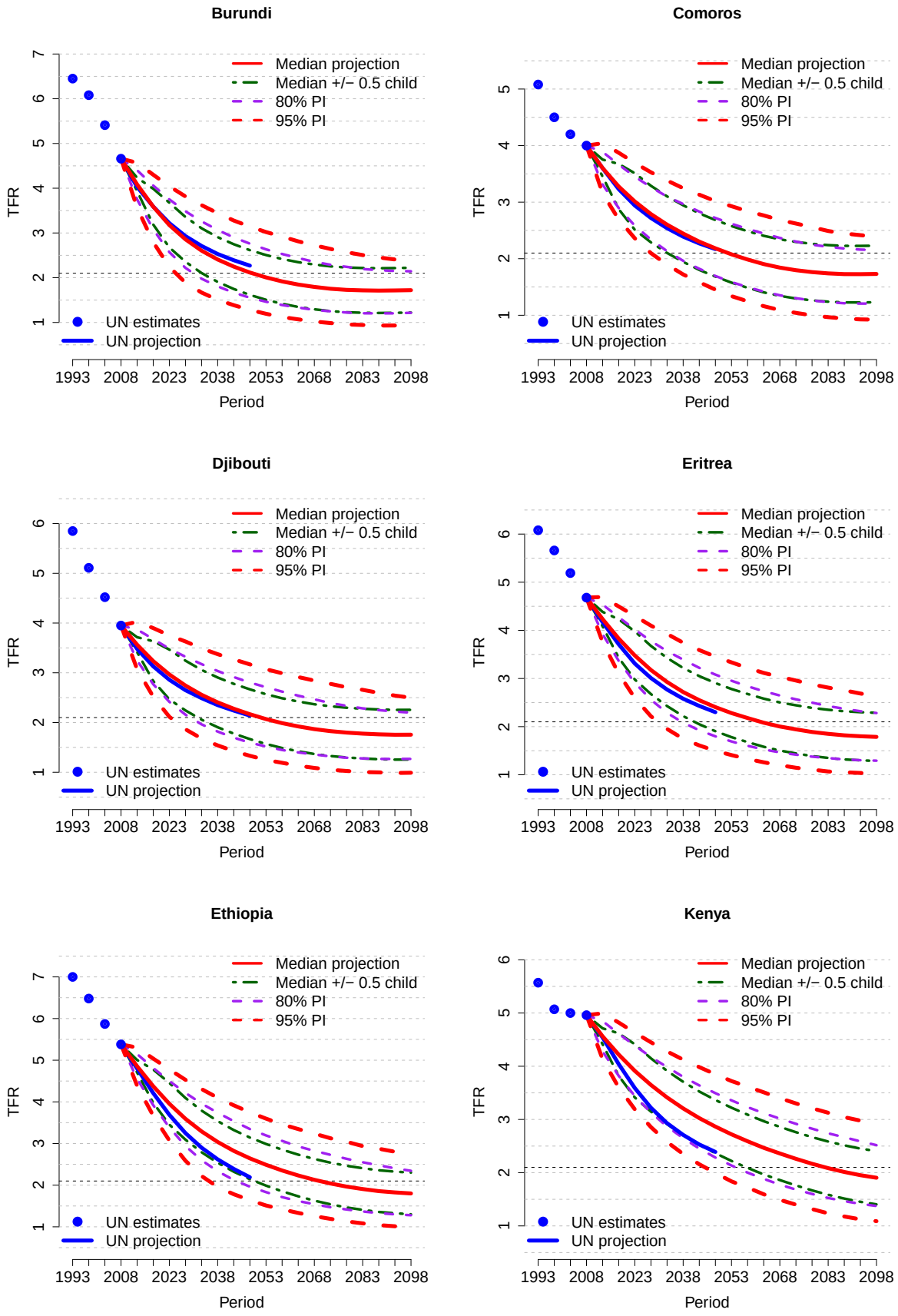

Figure 26: Projections for Burundi, Comoros, Djibouti, Eritrea, Ethiopia, Kenya

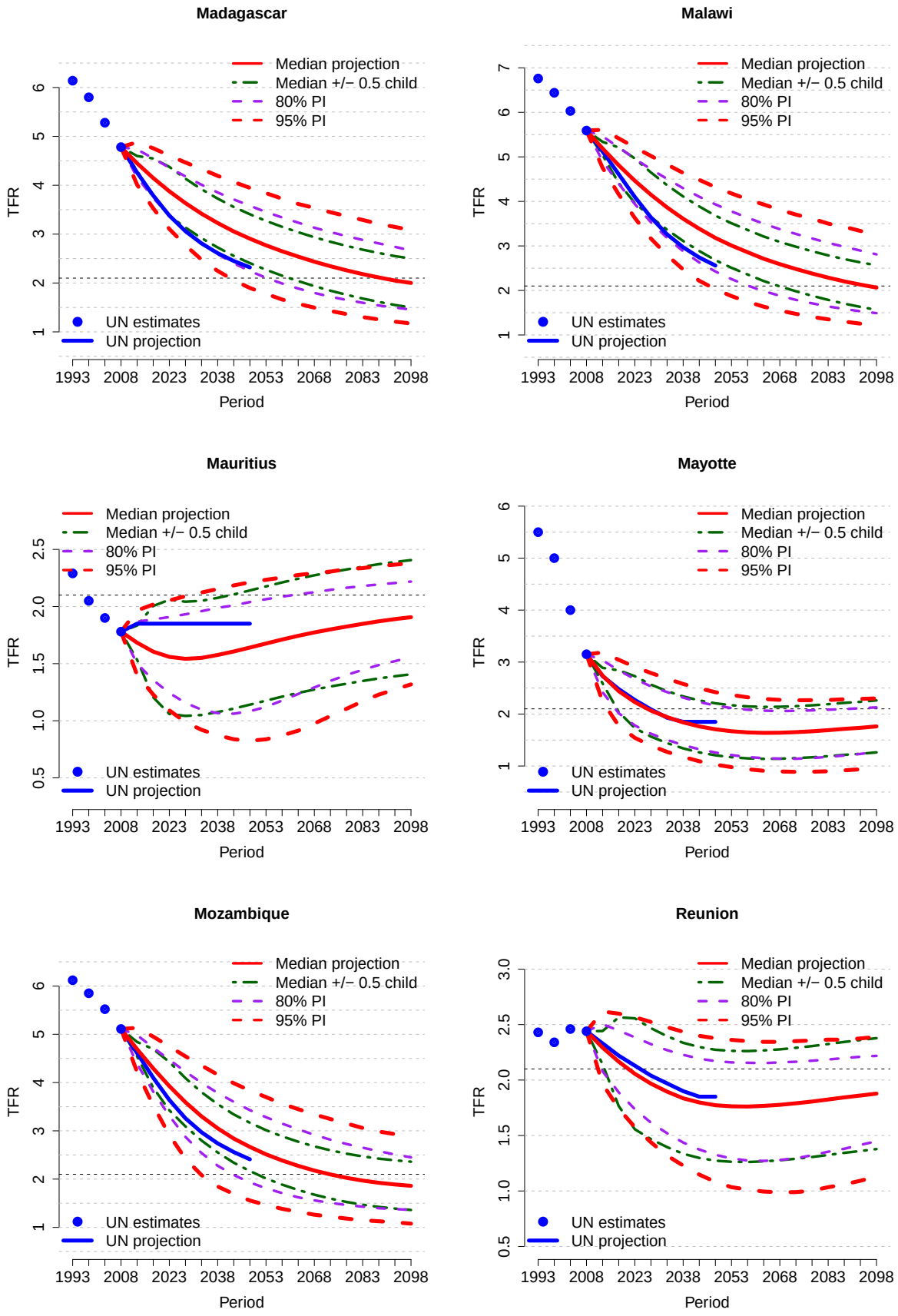

Figure 27: Projections for Madagascar, Malawi, Mauritius, Mayotte, Mozambique, Reunion

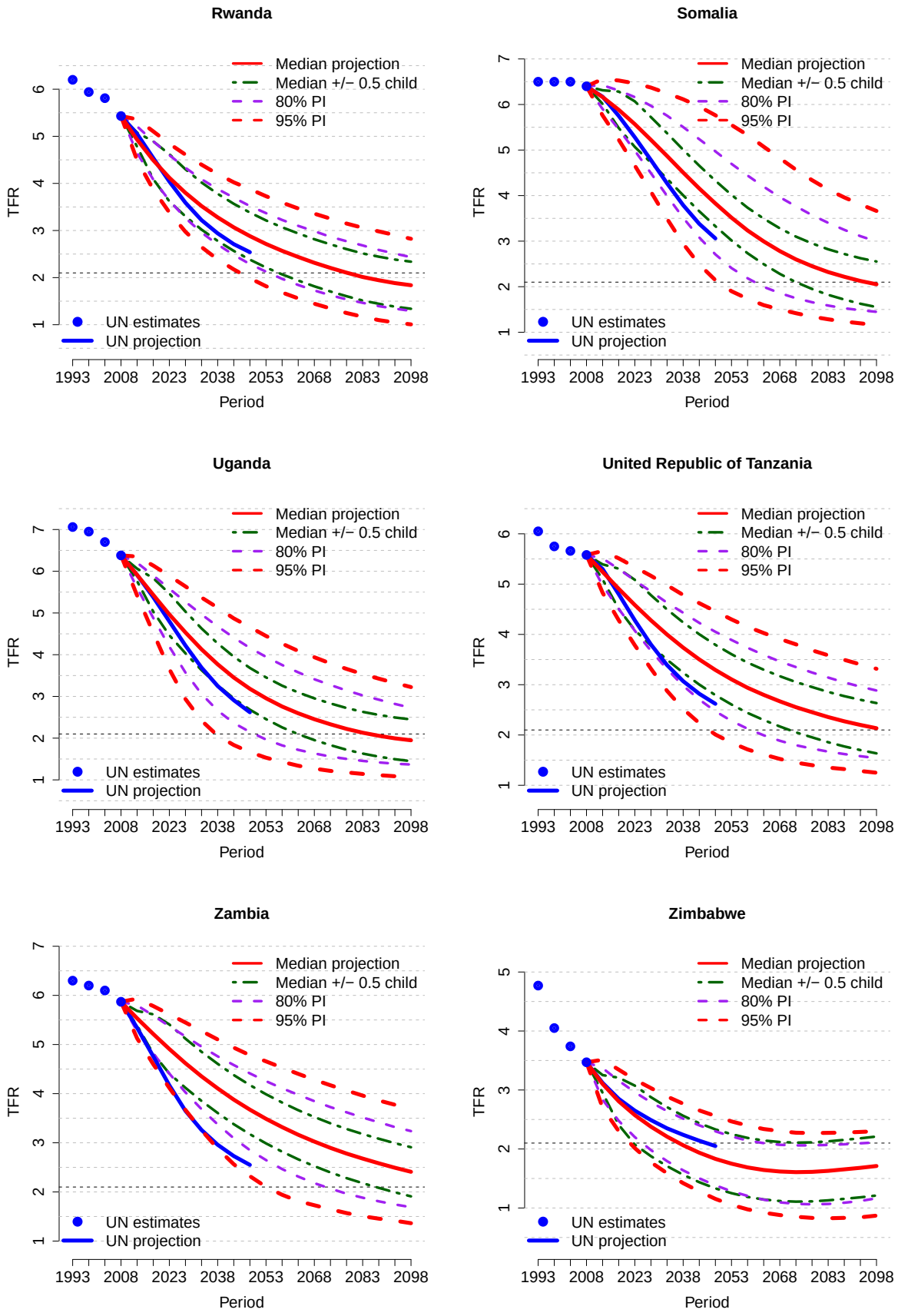

Figure 28: Projections for Rwanda, Somalia, Uganda, United Republic of Tanzania, Zambia, Zimbabwe

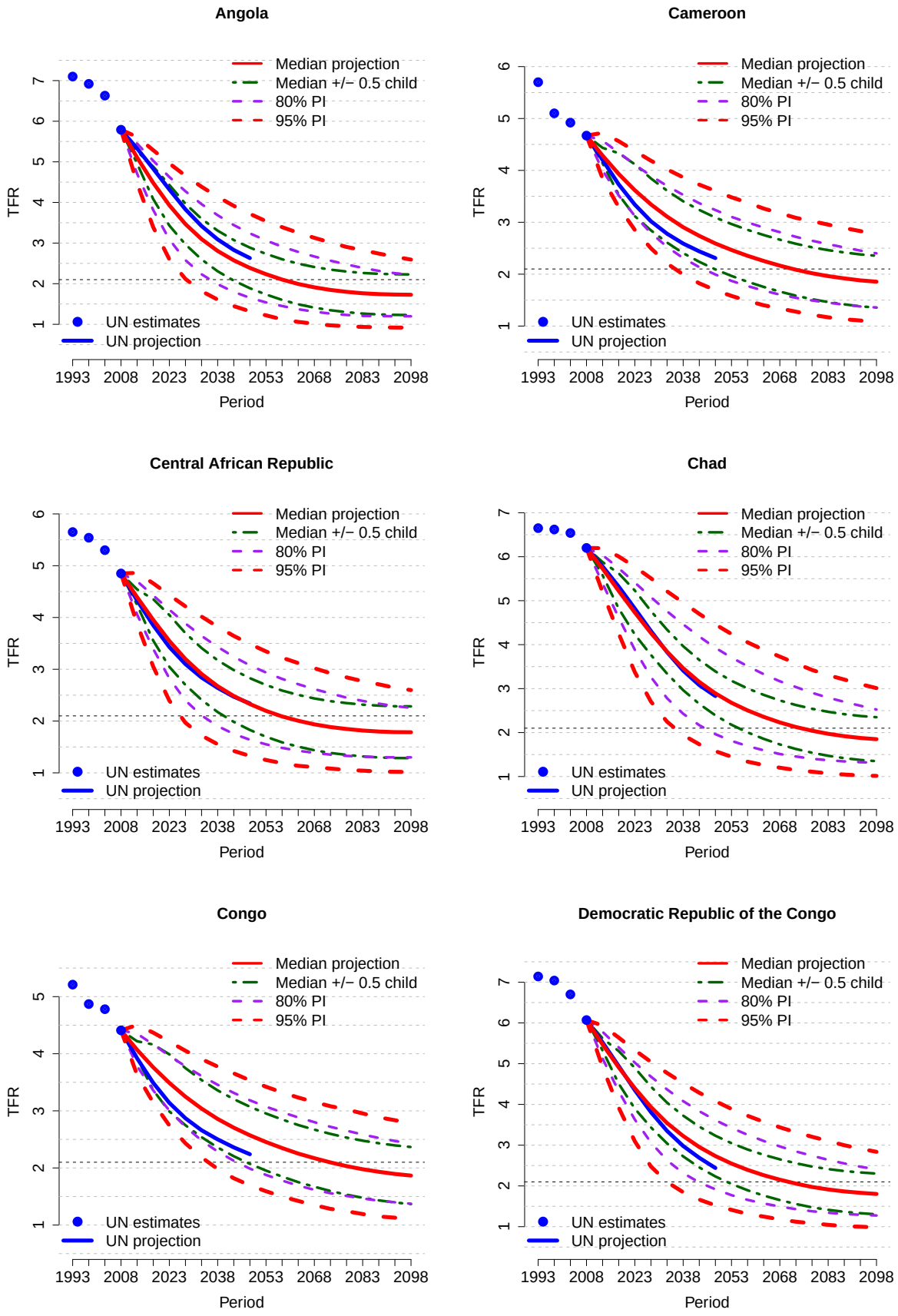

Figure 29: Projections for Angola, Cameroon, Central African Republic, Chad, Congo, Democratic Republic of the Congo

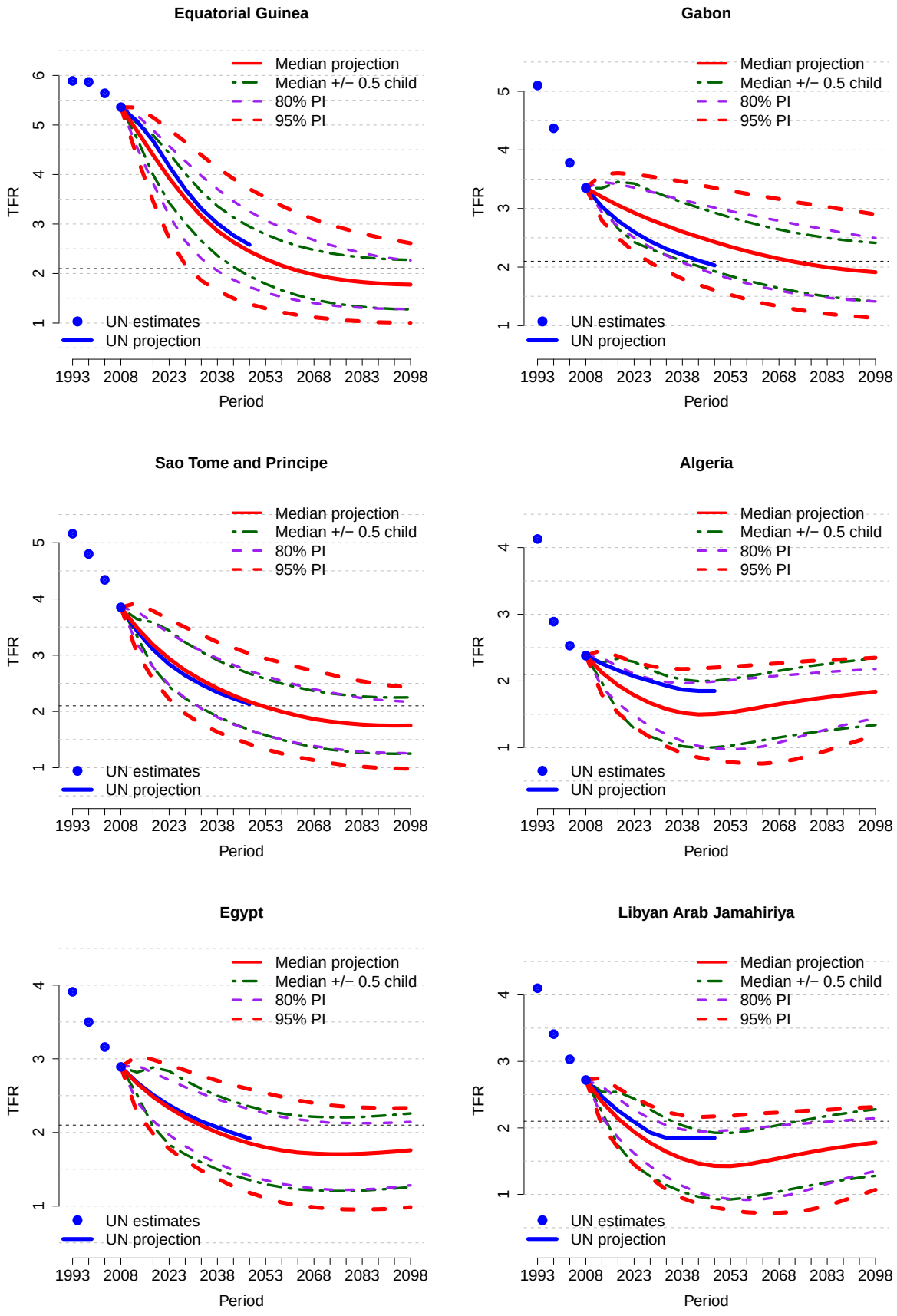

Figure 30: Projections for Equatorial Guinea, Gabon, Sao Tome and Principe, Algeria, Egypt, Libyan Arab Jamahiriya

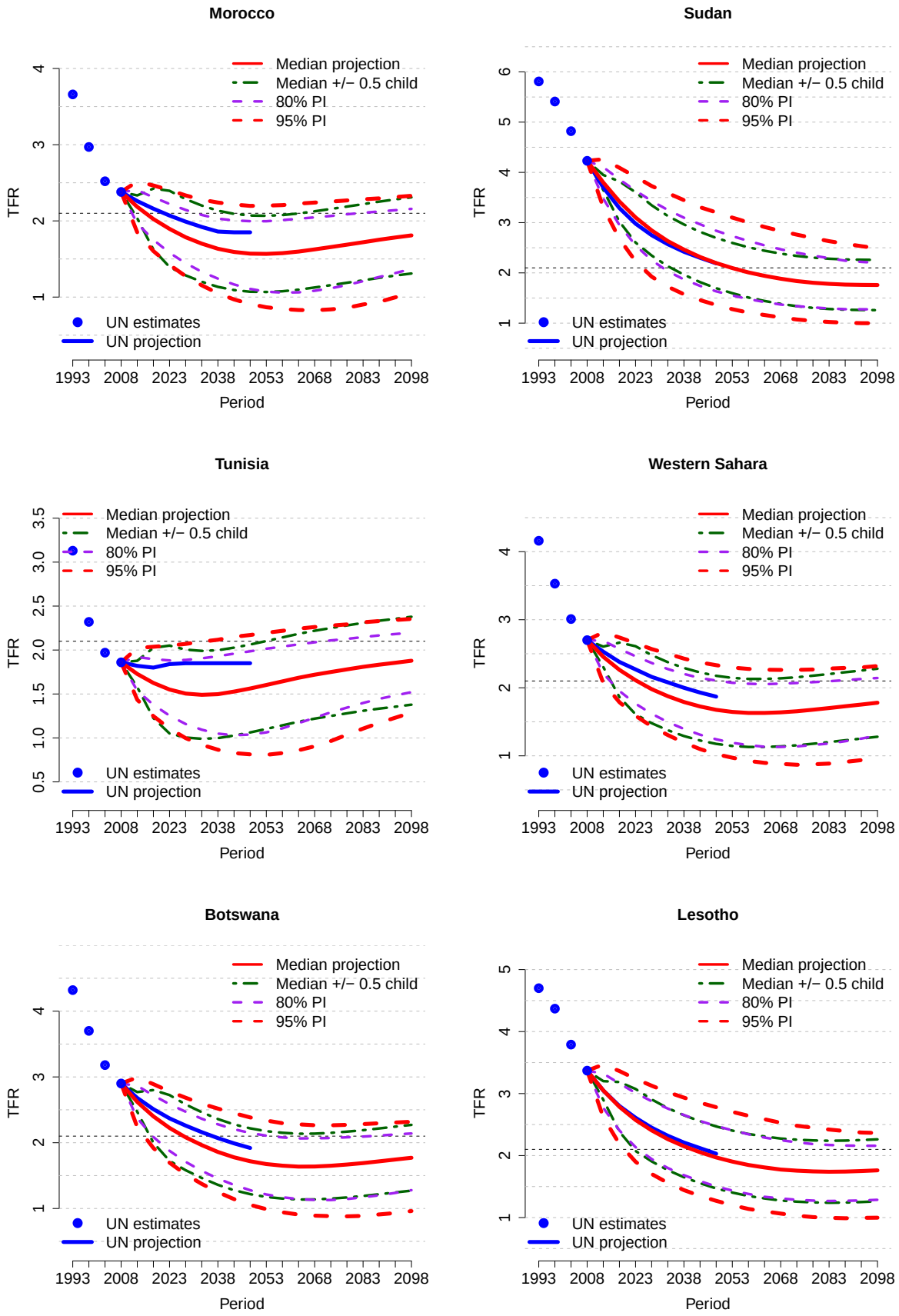

Figure 31: Projections for Morocco, Sudan, Tunisia, Western Sahara, Botswana, Lesotho

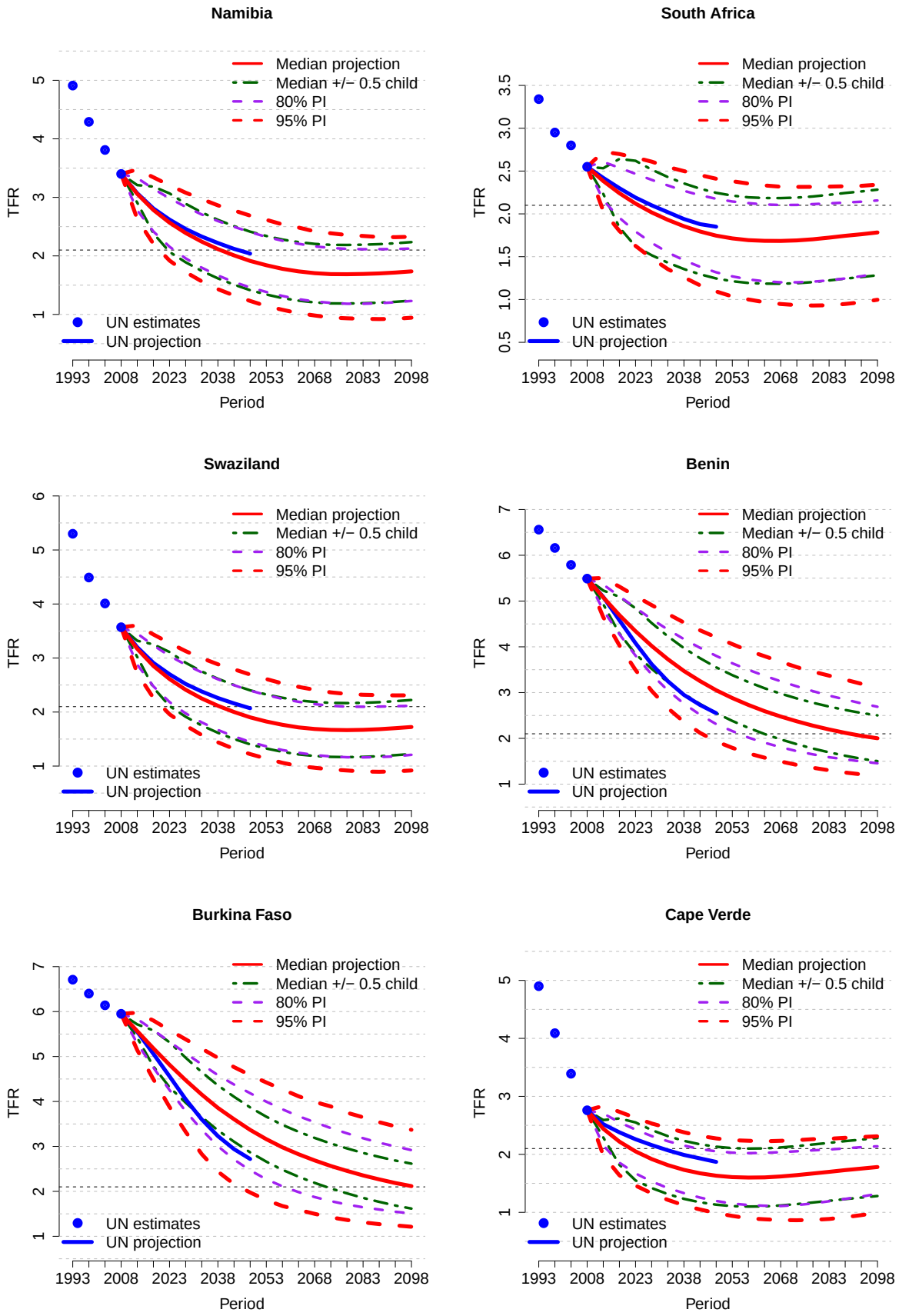

Figure 32: Projections for Namibia, South Africa, Swaziland, Benin, Burkina Faso, Cape Verde

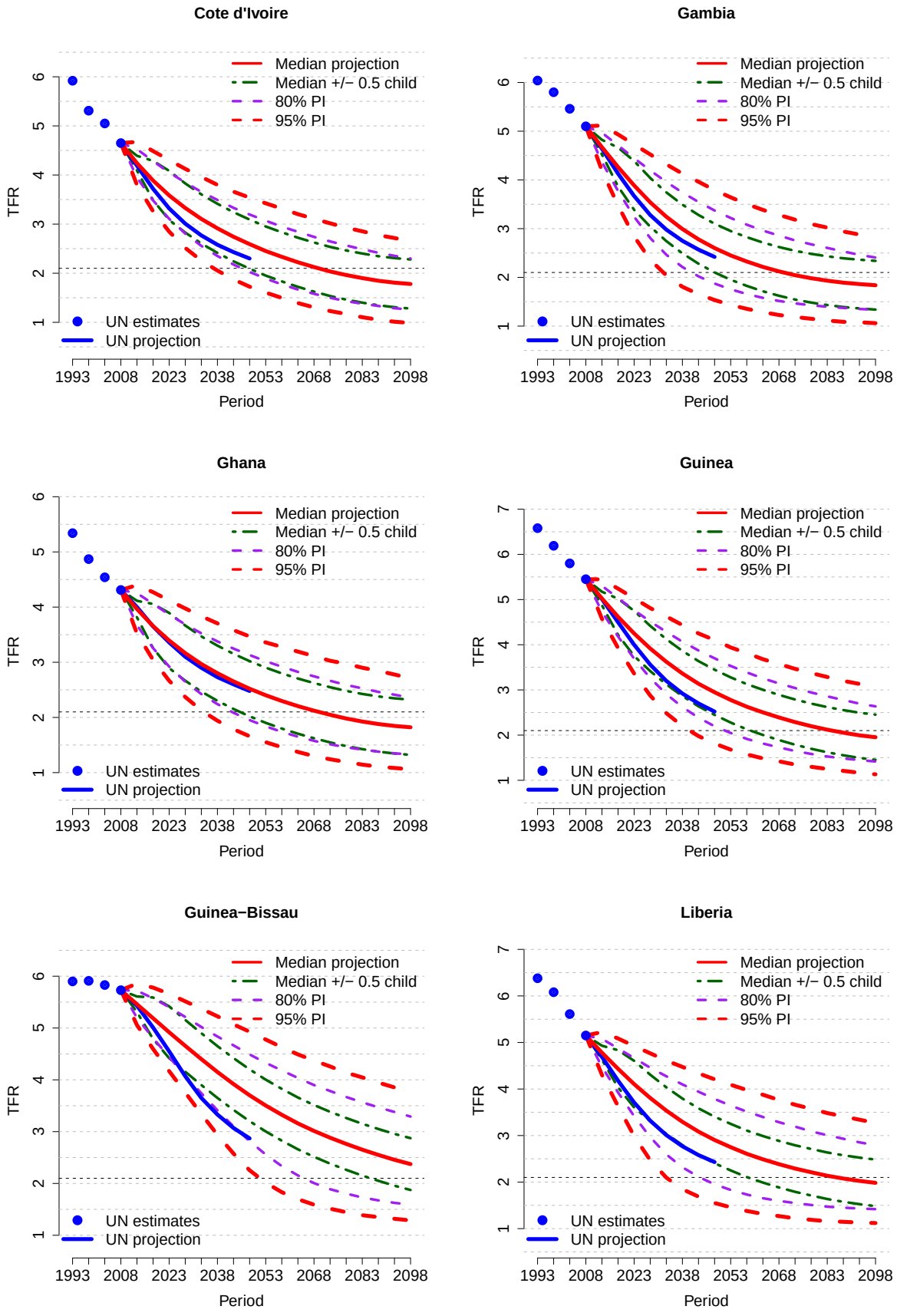

Figure 33: Projections for Cote d'Ivoire, Gambia, Ghana, Guinea, Guinea-Bissau, Liberia

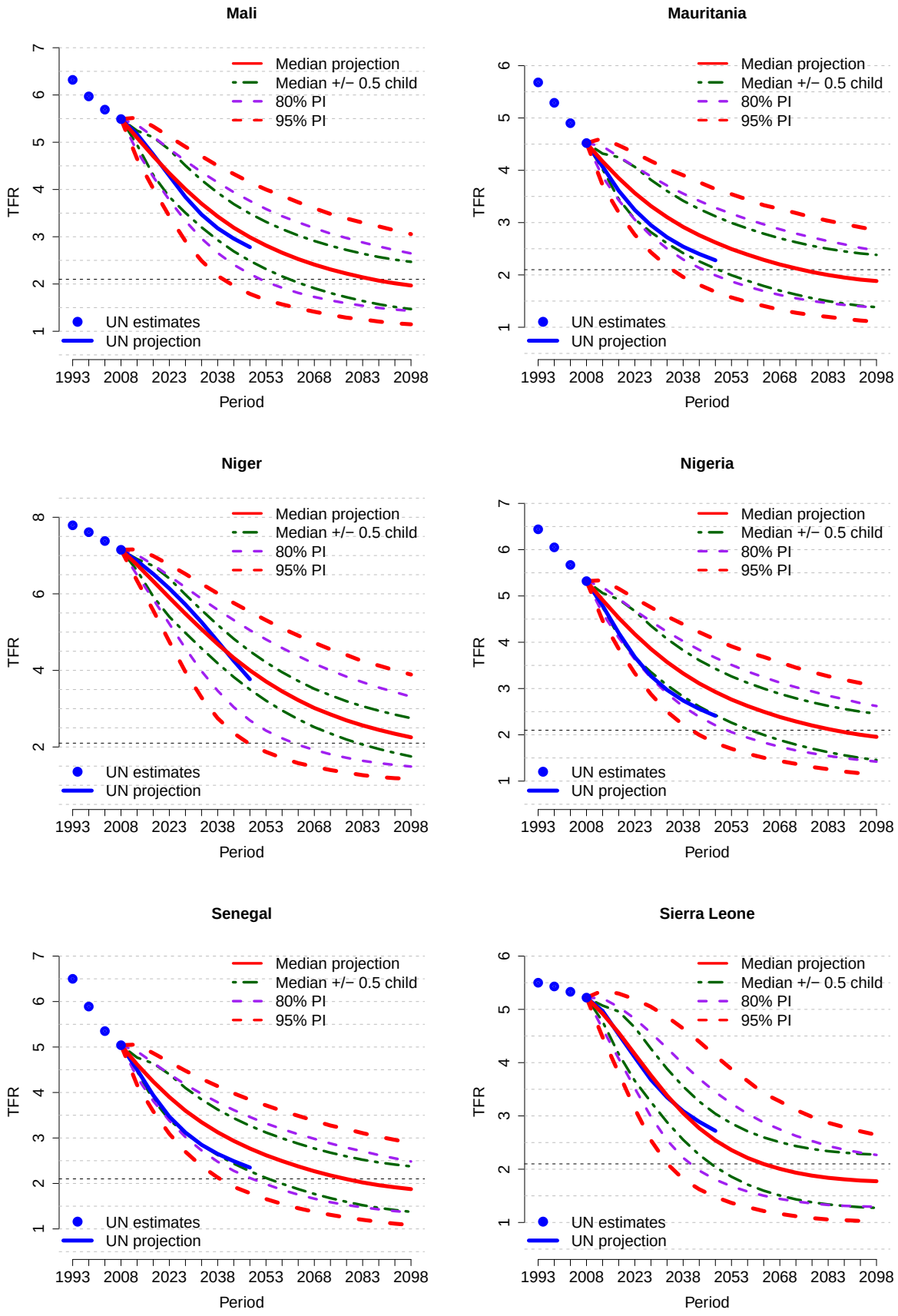

Figure 34: Projections for Mali, Mauritania, Niger, Nigeria, Senegal, Sierra Leone

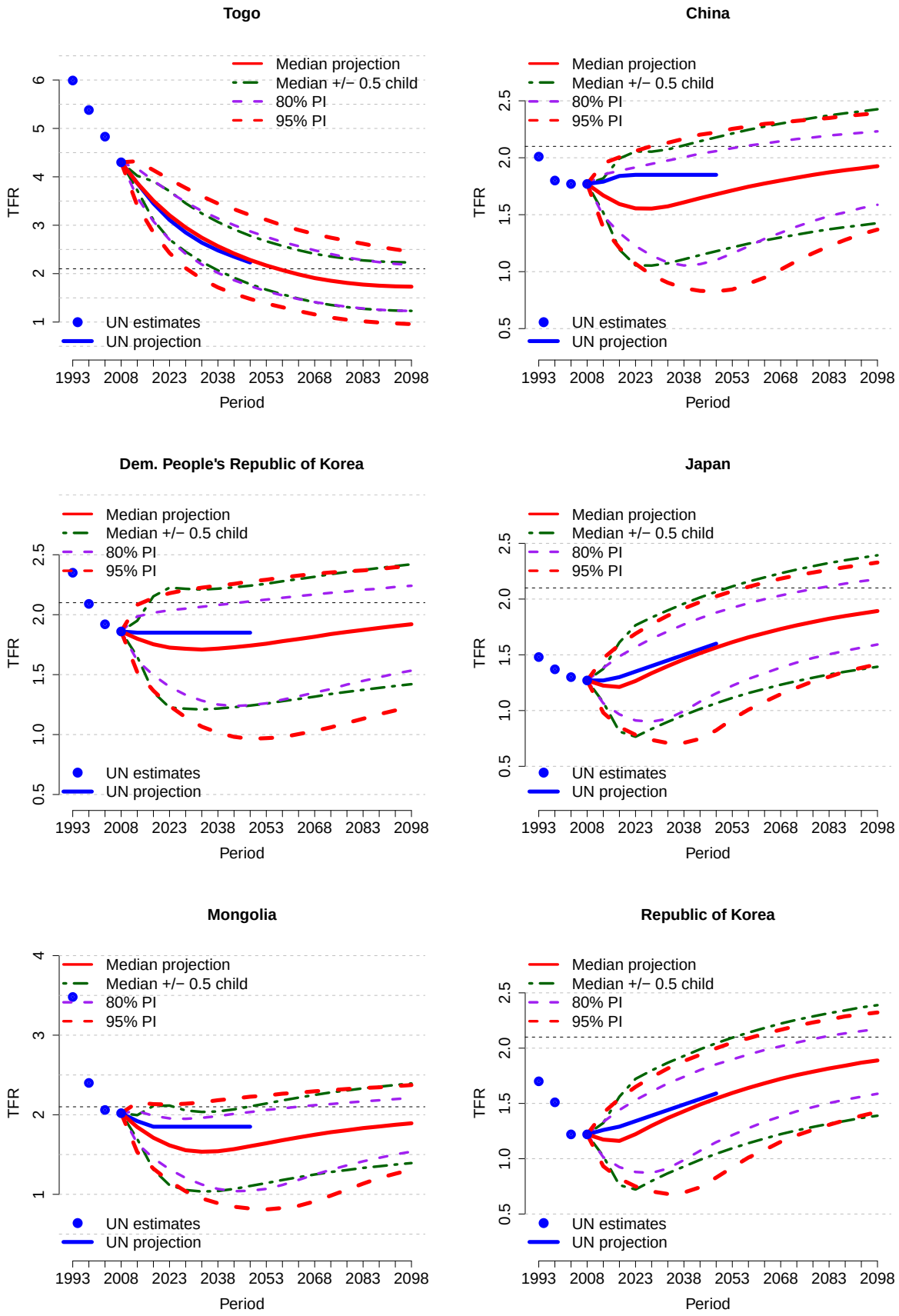

Figure 35: Projections for Togo, China, Dem. People's Republic of Korea, Japan, Mongolia, Republic of Korea

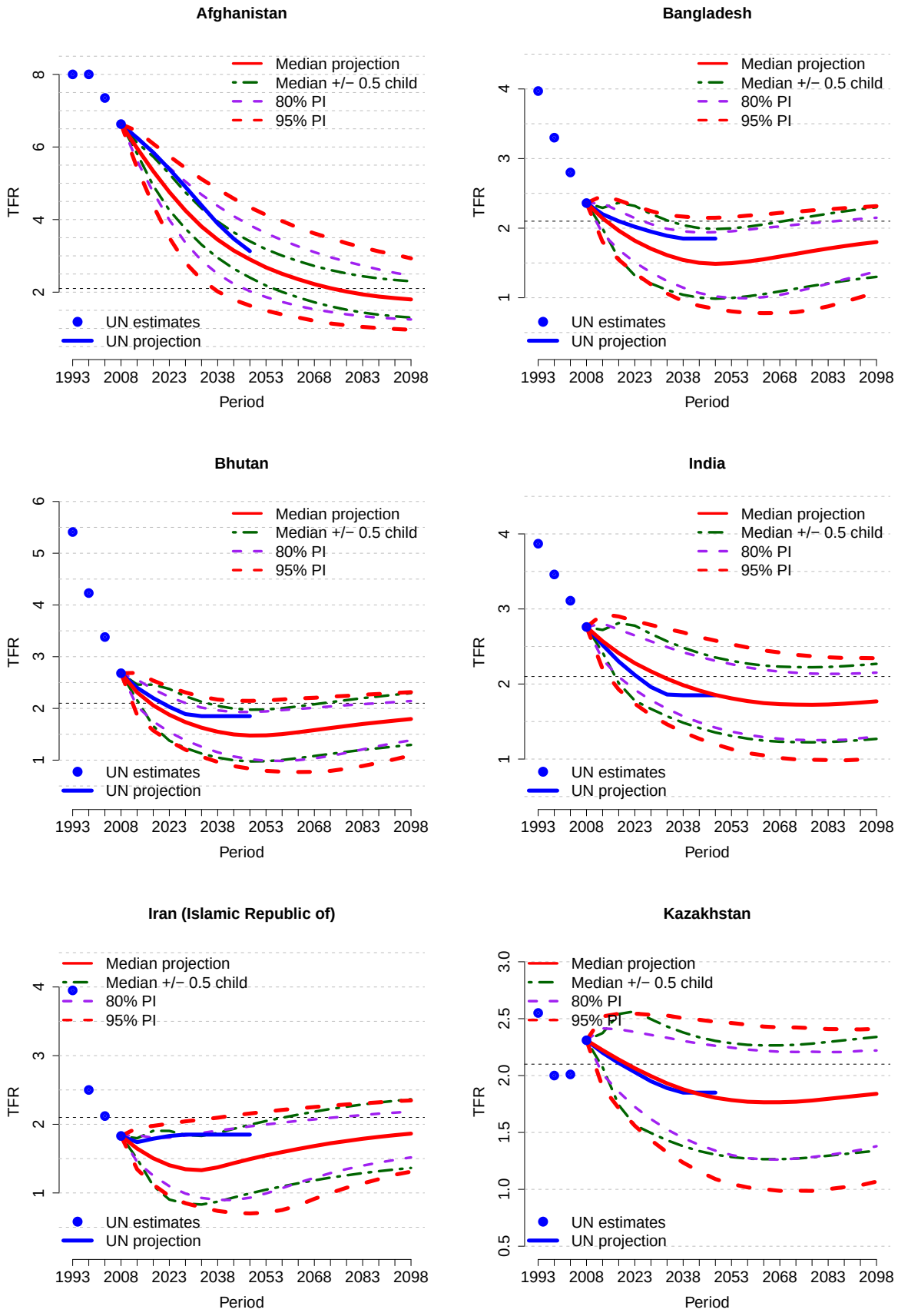

Figure 36: Projections for Afghanistan, Bangladesh, Bhutan, India, Iran (Islamic Republic of), Kazakhstan

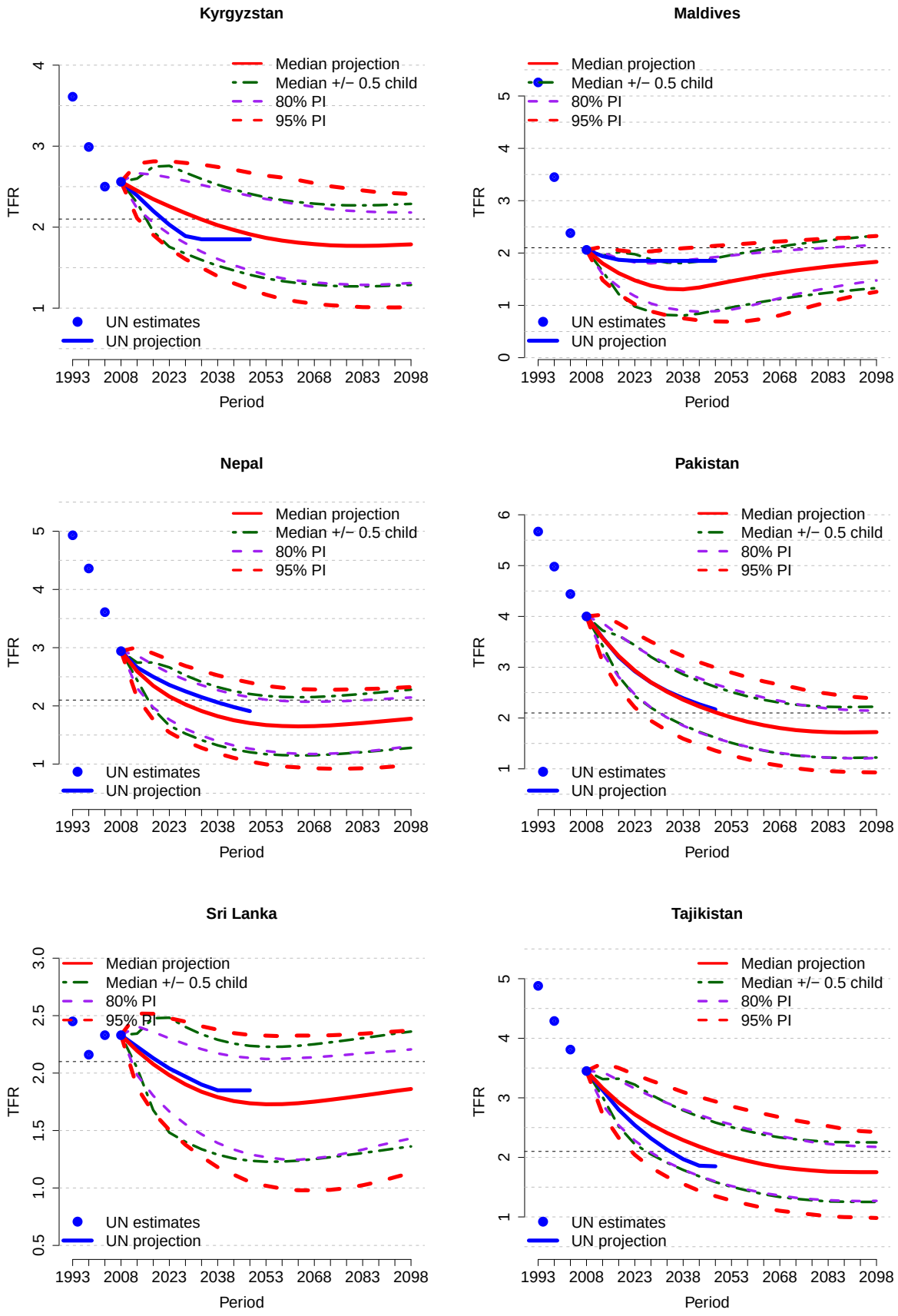

Figure 37: Projections for Kyrgyzstan, Maldives, Nepal, Pakistan, Sri Lanka, Tajikistan

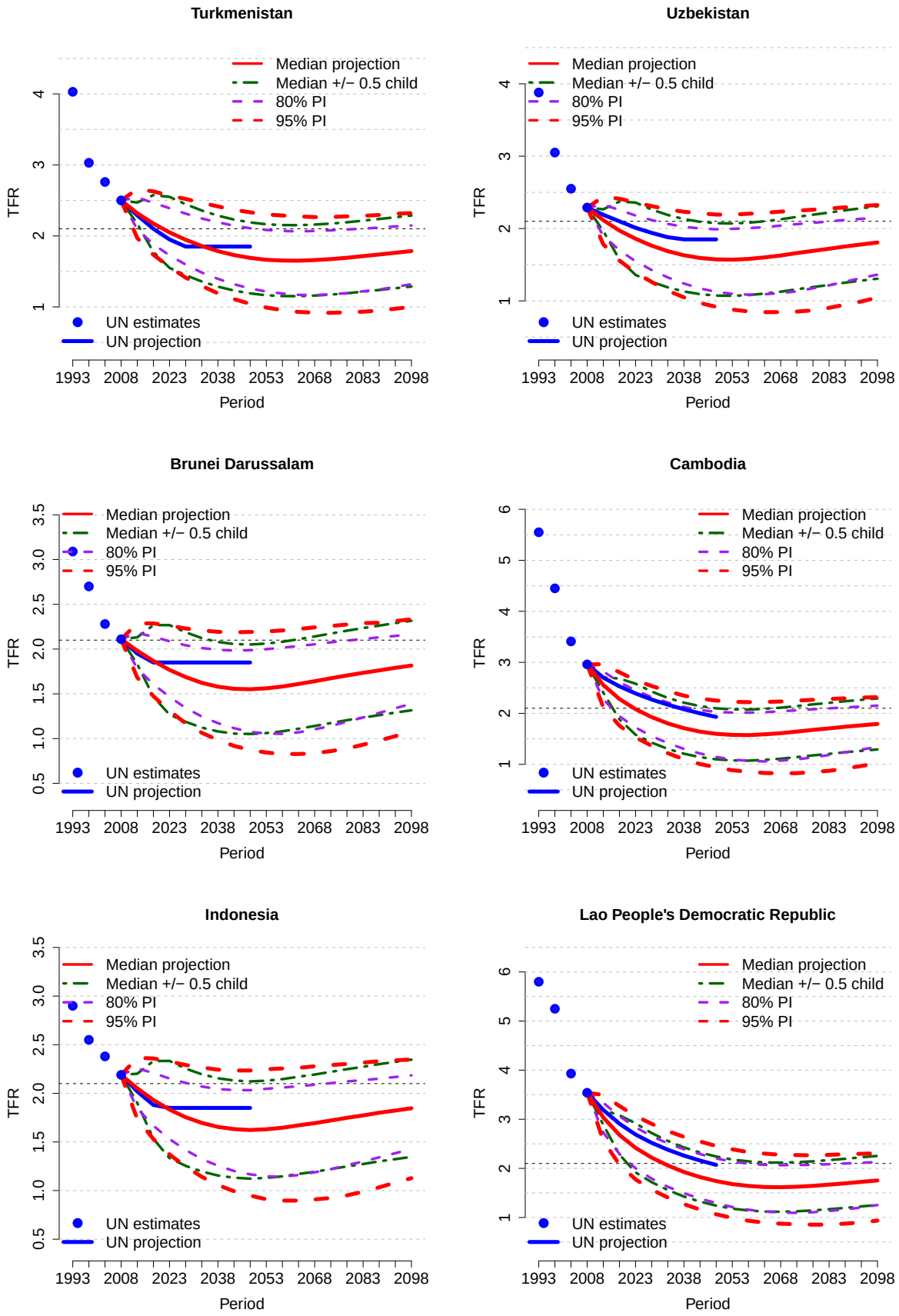

Figure 38: Projections for Turkmenistan, Uzbekistan, Brunei Darussalam, Cambodia, Indonesia, Lao People's Democratic Republic

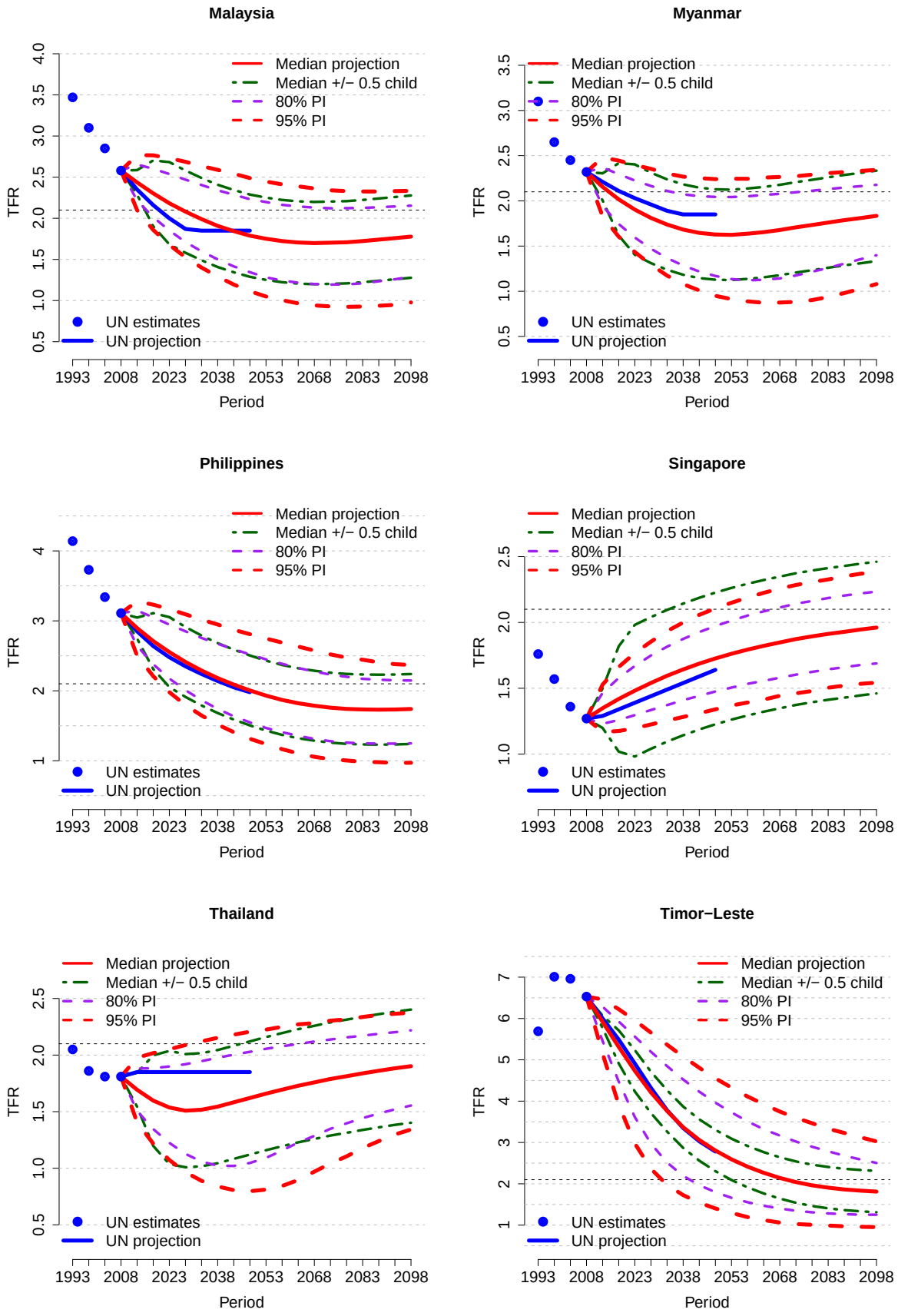

Figure 39: Projections for Malaysia, Myanmar, Philippines, Singapore, Thailand, Timor-Leste

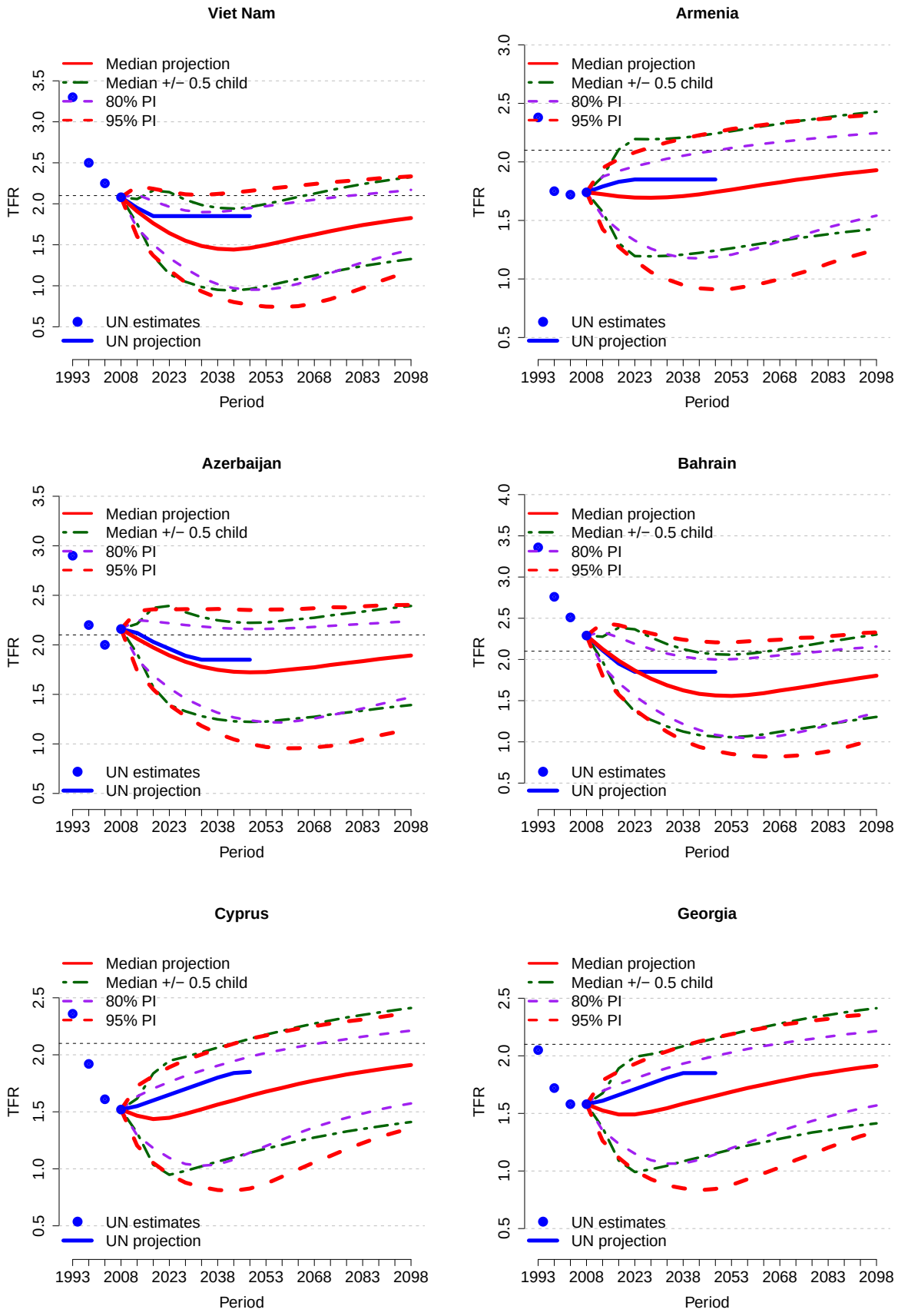

Figure 40: Projections for Viet Nam, Armenia, Azerbaijan, Bahrain, Cyprus, Georgia

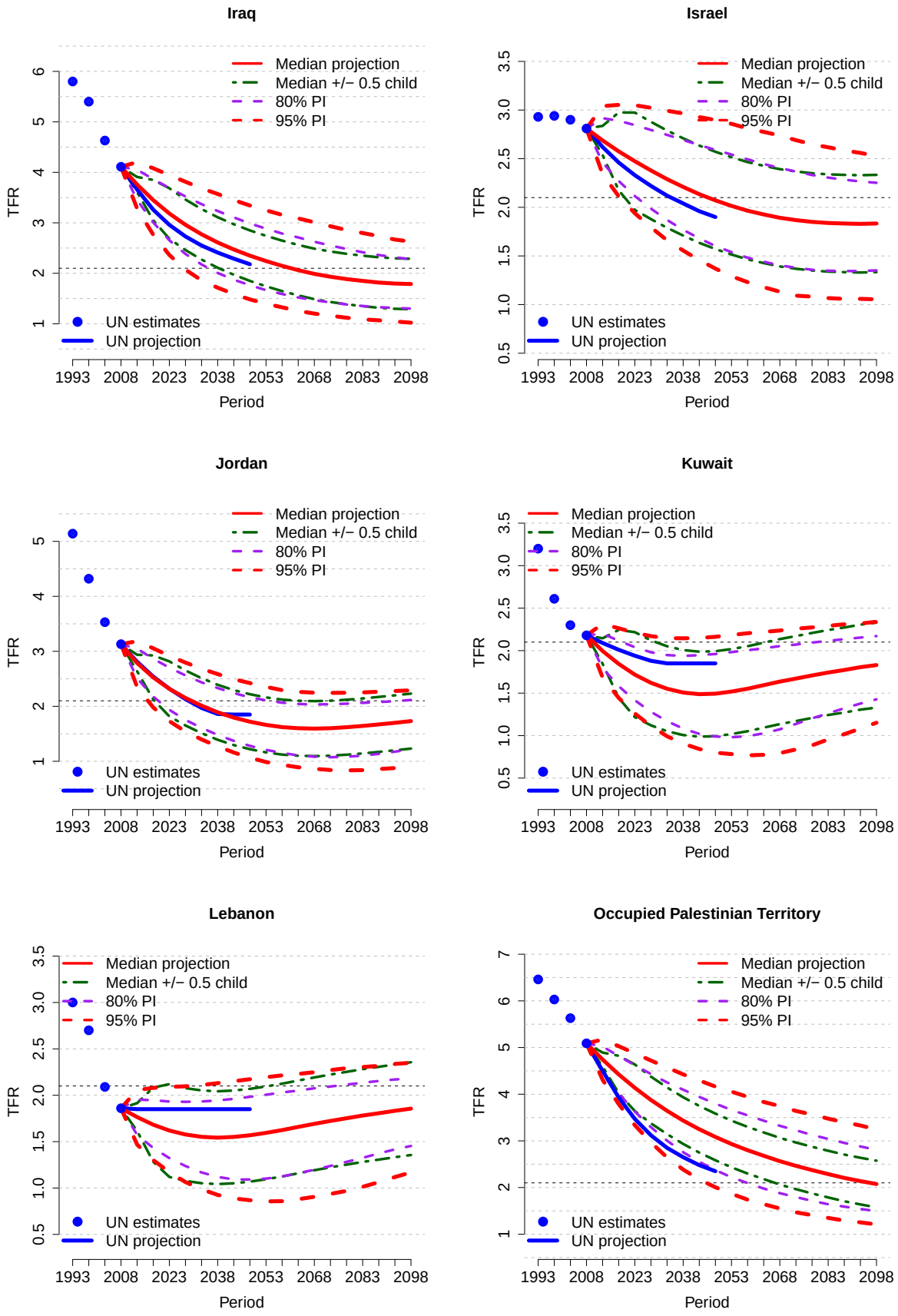

Figure 41: Projections for Iraq, Israel, Jordan, Kuwait, Lebanon, Occupied Palestinian Territory

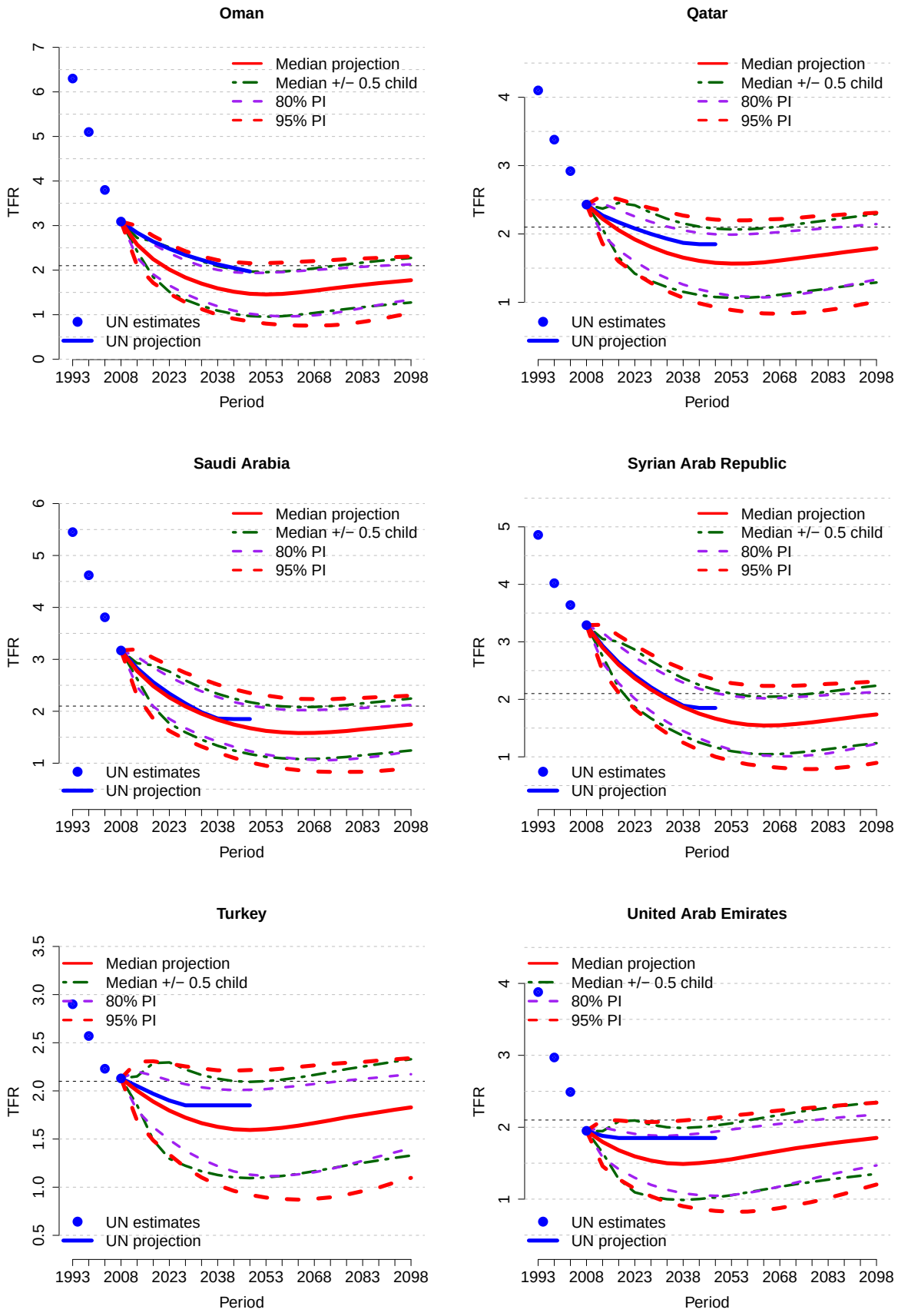

Figure 42: Projections for Oman, Qatar, Saudi Arabia, Syrian Arab Republic, Turkey, United Arab Emirates

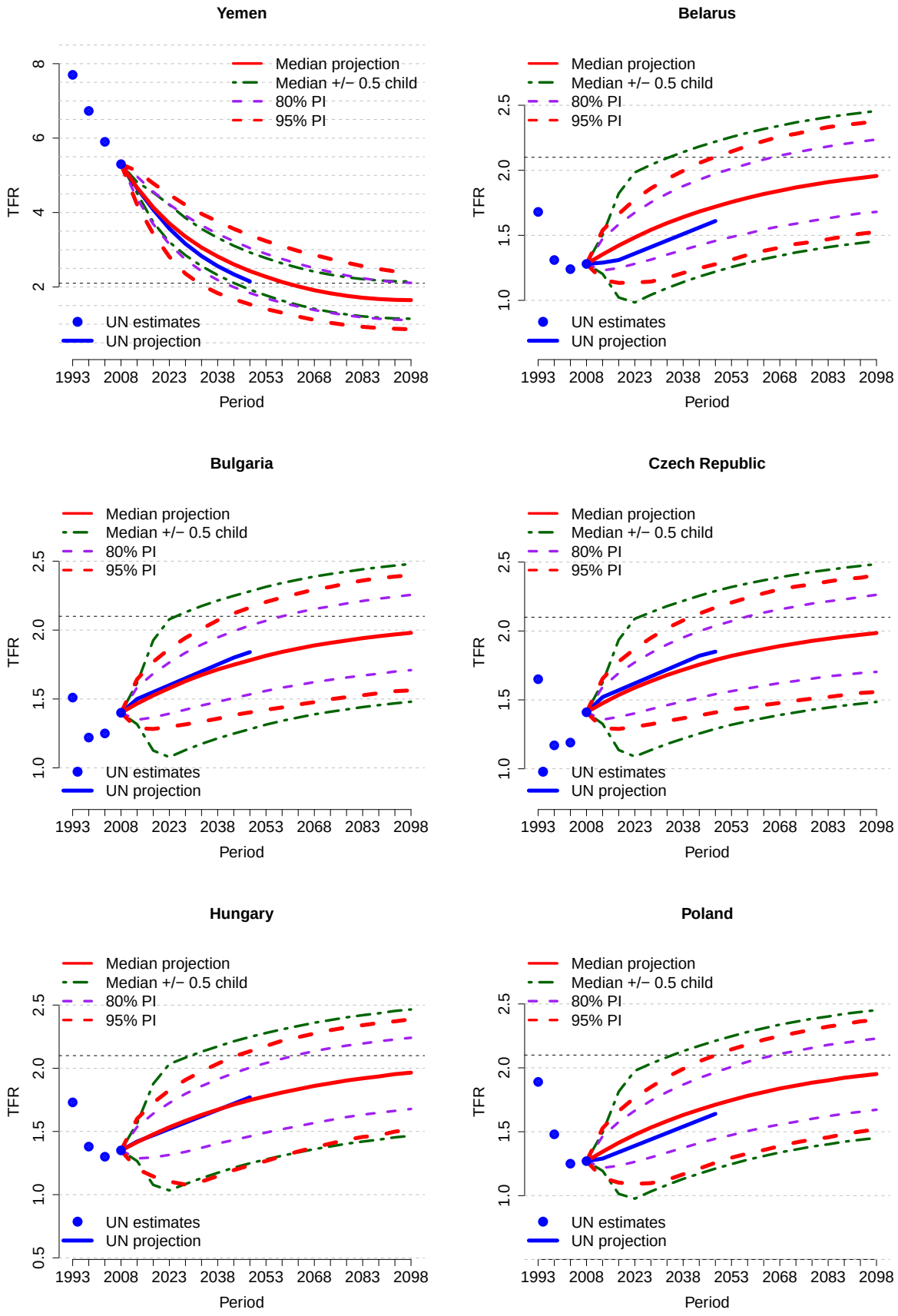

Figure 43: Projections for Yemen, Belarus, Bulgaria, Czech Republic, Hungary, Poland

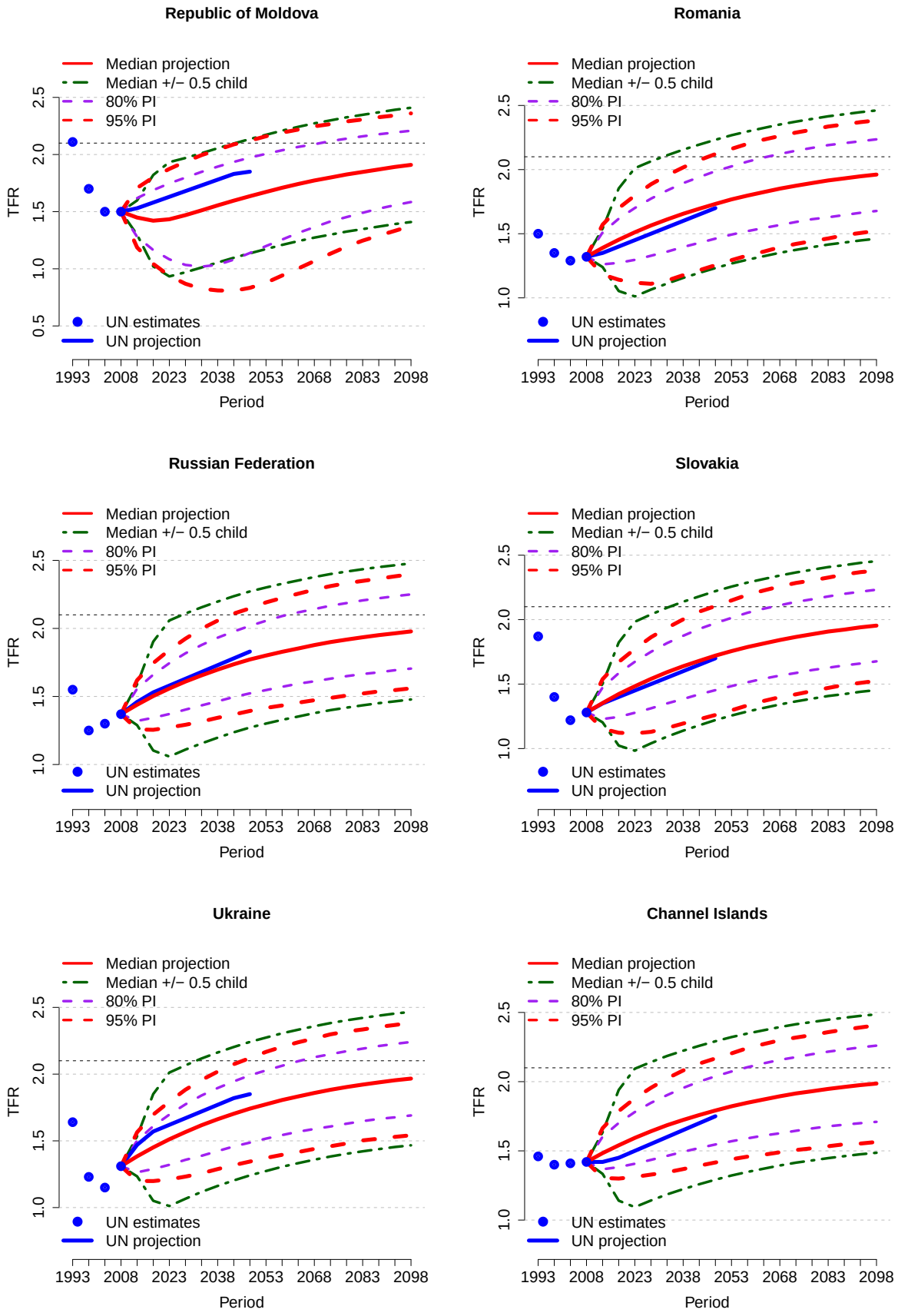

Figure 44: Projections for Republic of Moldova, Romania, Russian Federation, Slovakia, Ukraine, Channel Islands

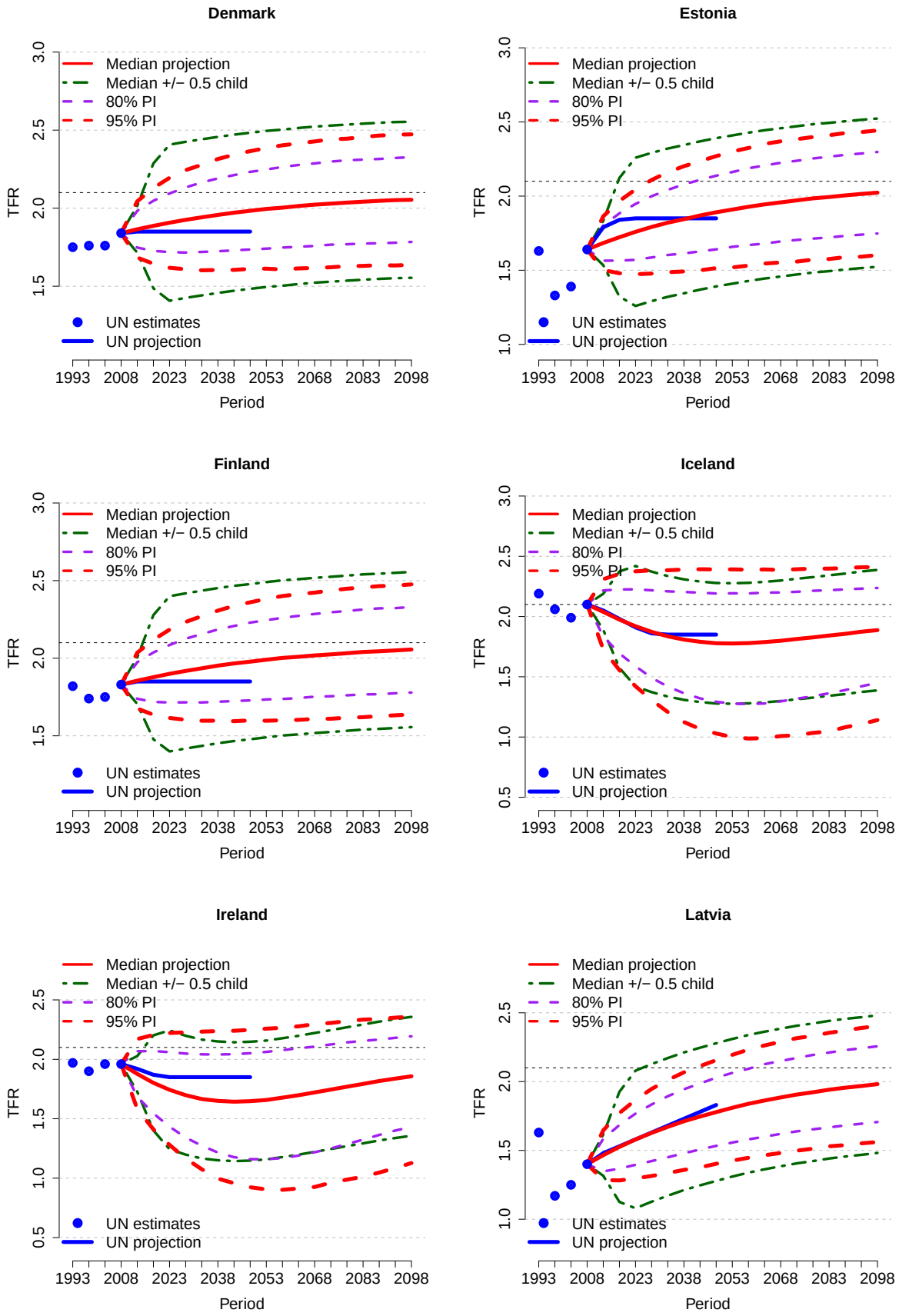

Figure 45: Projections for Denmark, Estonia, Finland, Iceland, Ireland, Latvia

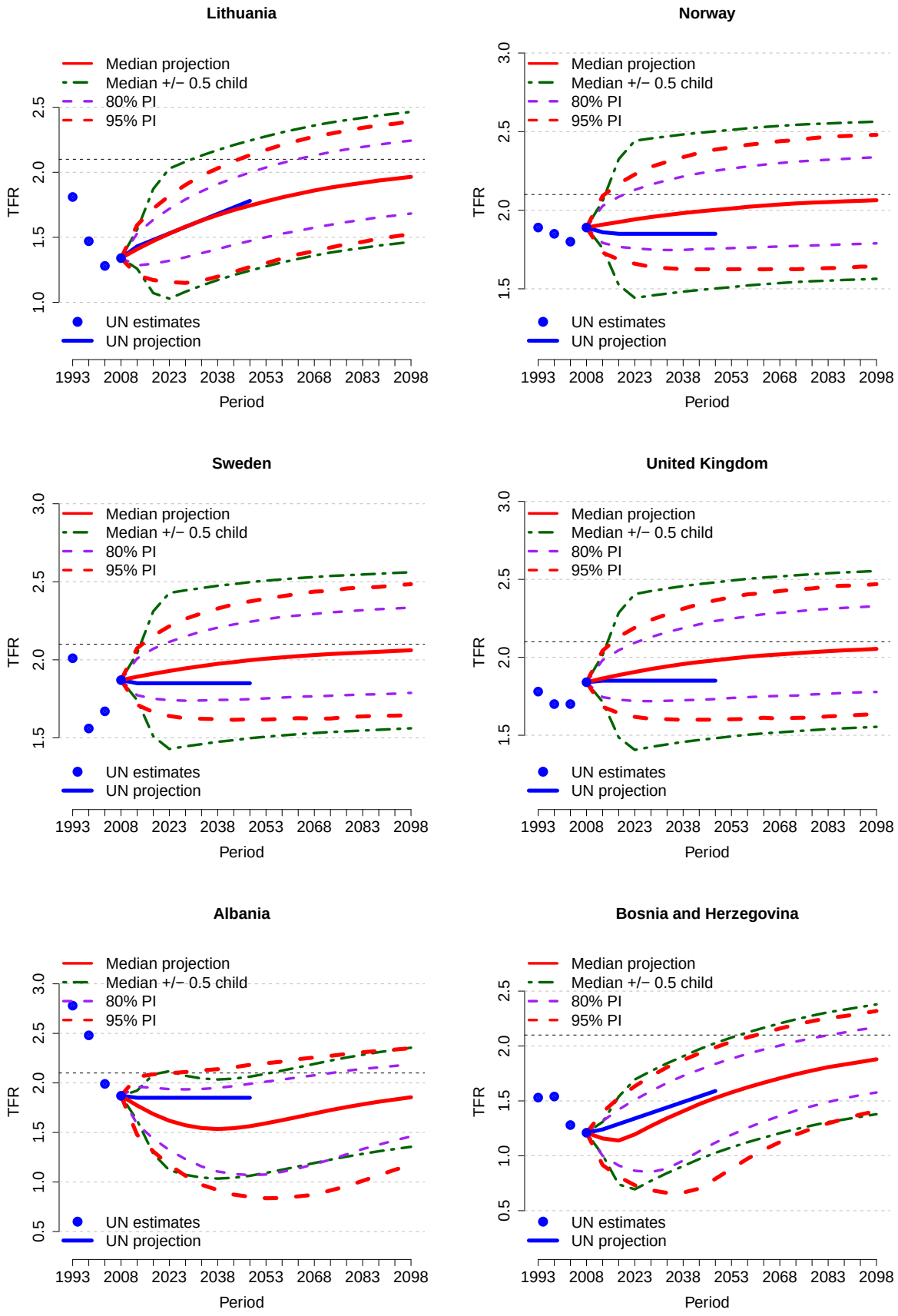

Figure 46: Projections for Lithuania, Norway, Sweden, United Kingdom, Albania, Bosnia and Herzegovina

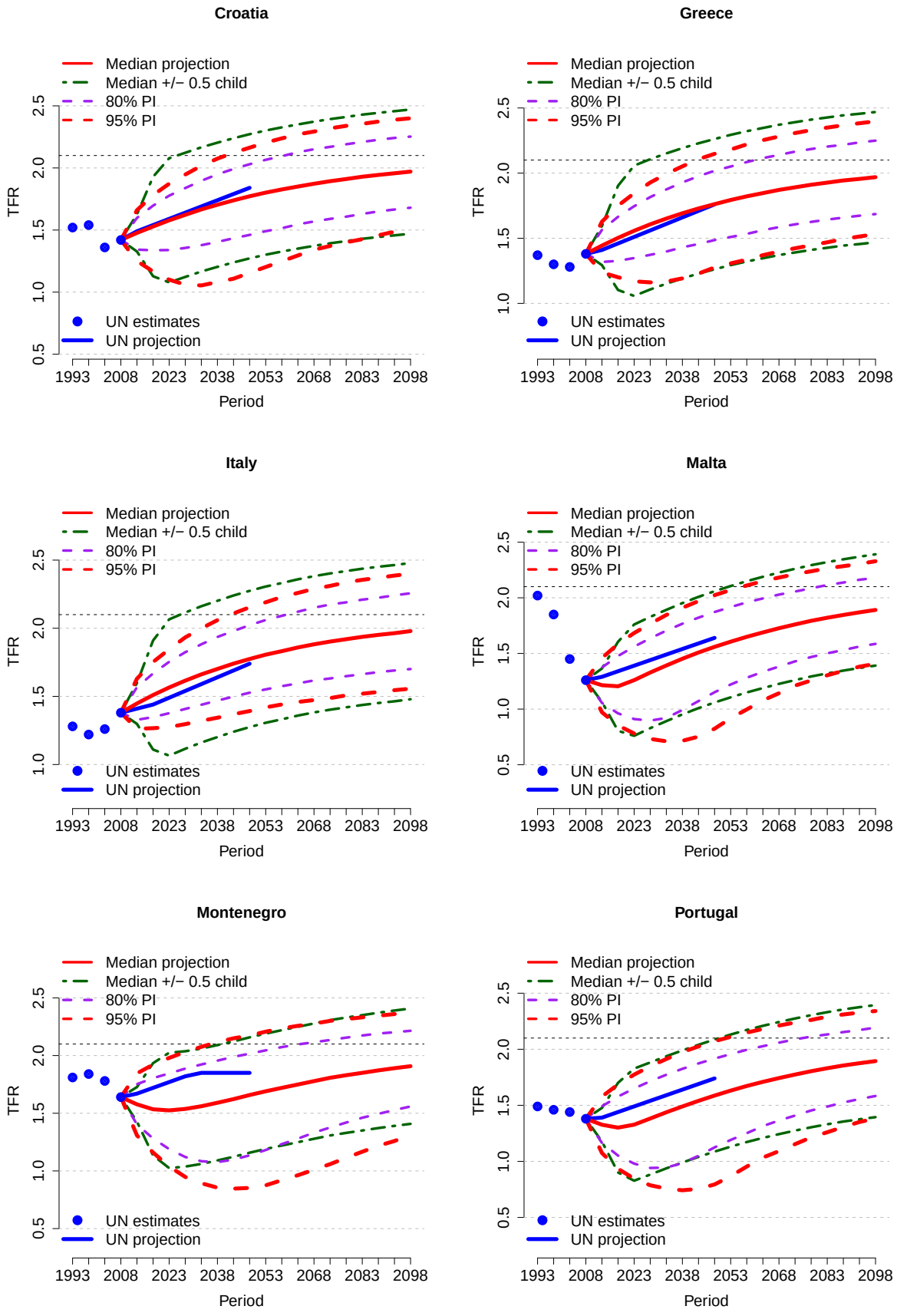

Figure 47: Projections for Croatia, Greece, Italy, Malta, Montenegro, Portugal

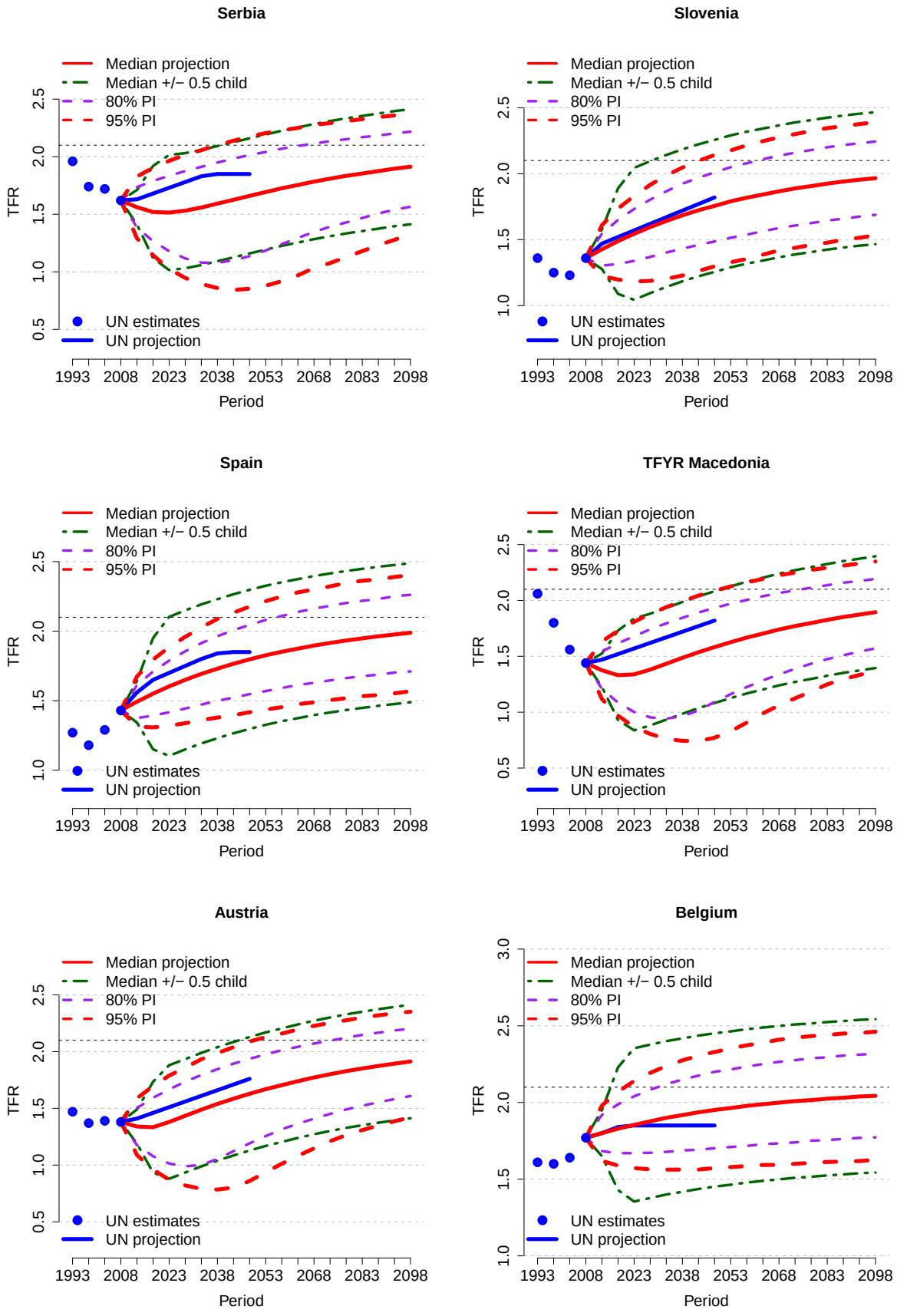

Figure 48: Projections for Serbia, Slovenia, Spain, TFYR Macedonia, Austria, Belgium

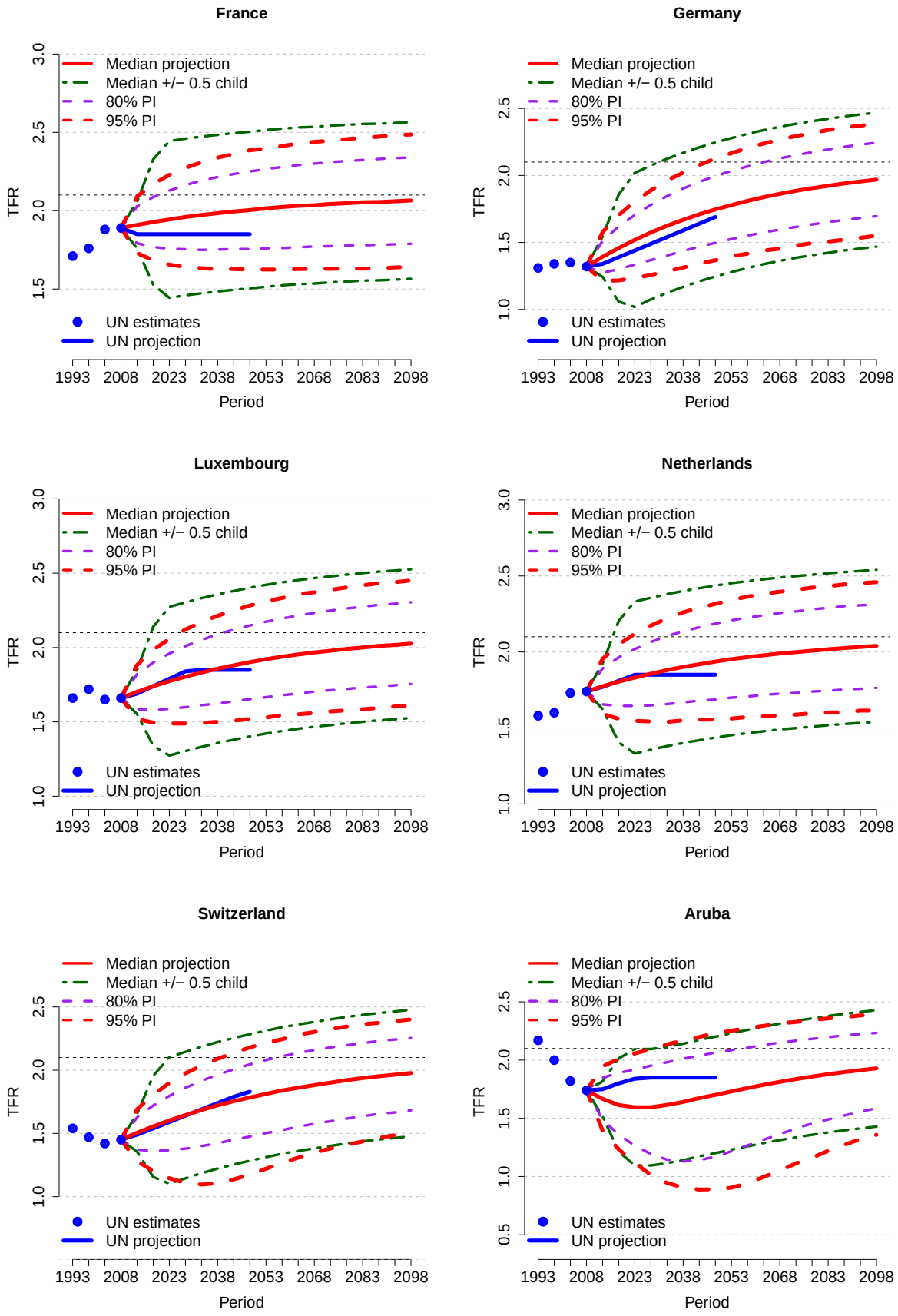

Figure 49: Projections for France, Germany, Luxembourg, Netherlands, Switzerland, Aruba

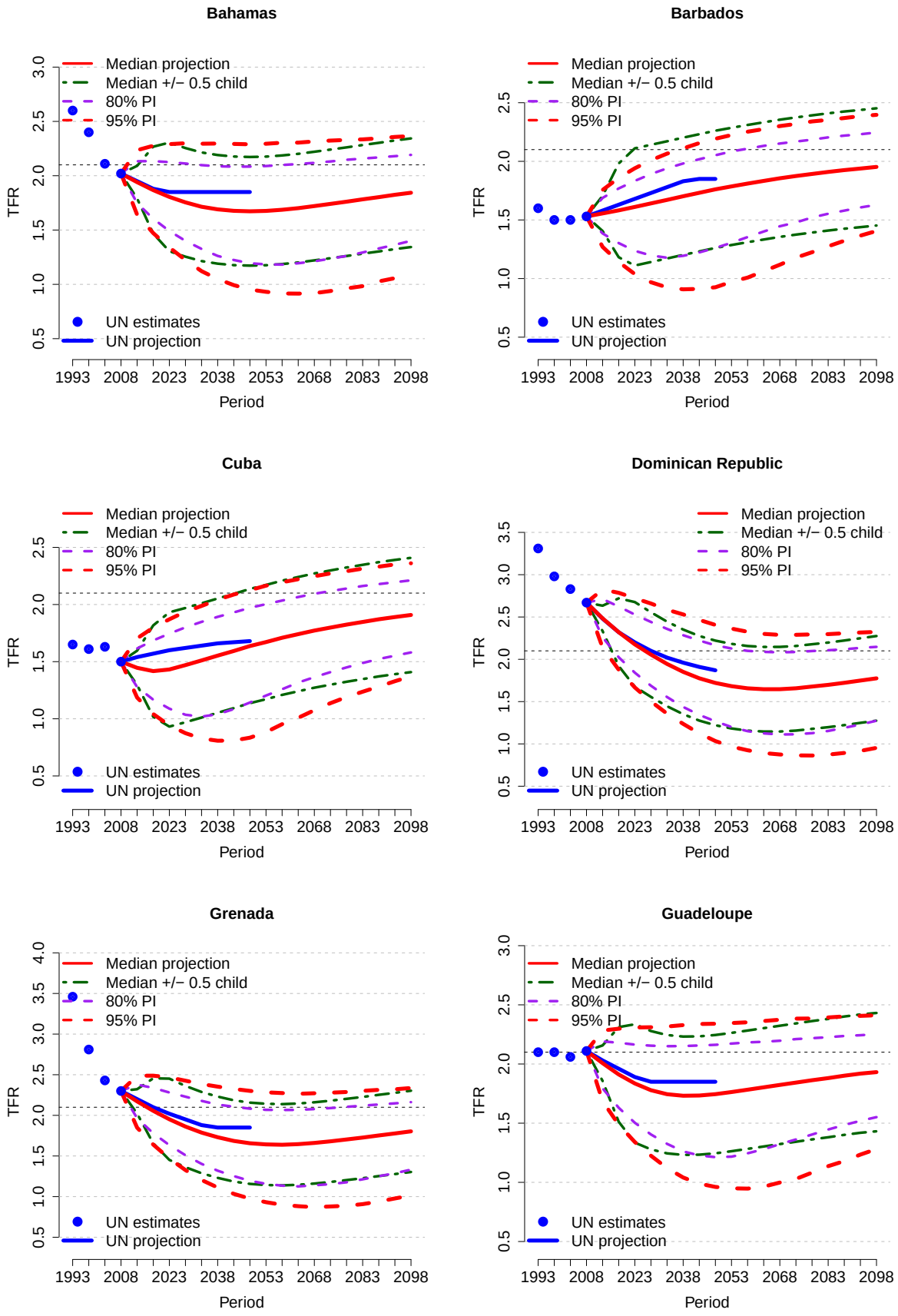

Figure 50: Projections for Bahamas, Barbados, Cuba, Dominican Republic, Grenada, Guadeloupe

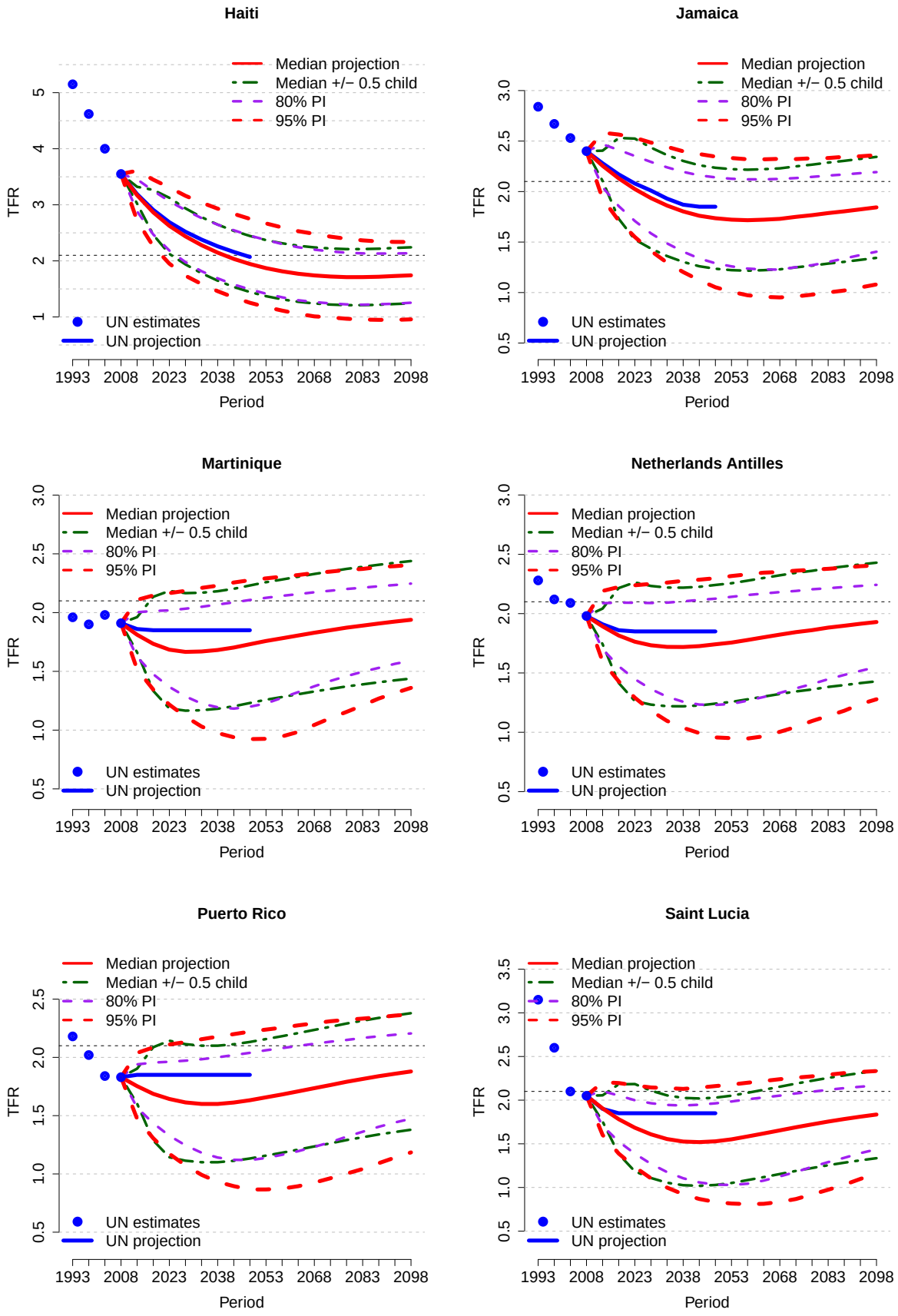

Figure 51: Projections for Haiti, Jamaica, Martinique, Netherlands Antilles, Puerto Rico, Saint Lucia

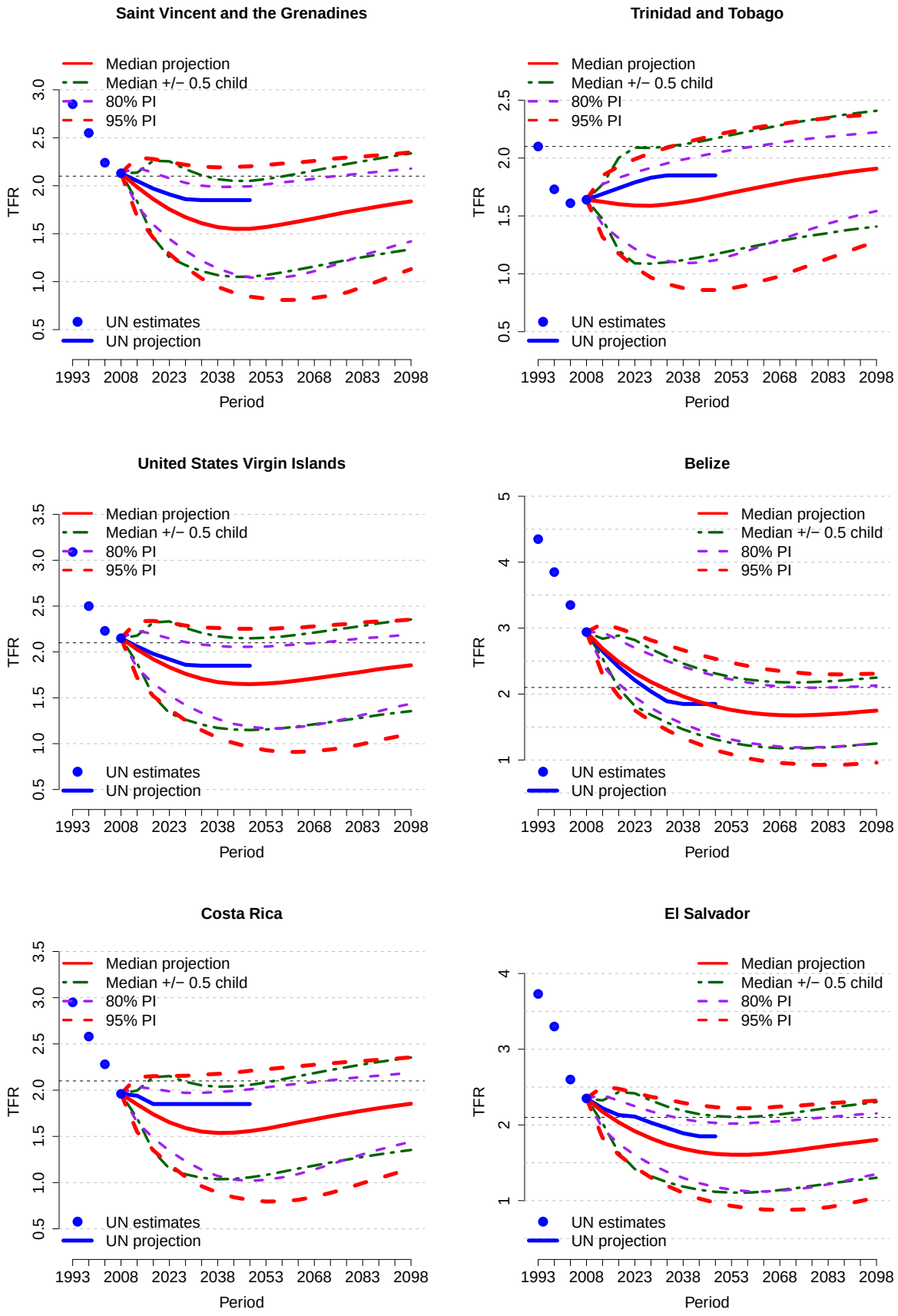

Figure 52: Projections for Saint Vincent and the Grenadines, Trinidad and Tobago, United States Virgin Islands, Belize, Costa Rica, El Salvador

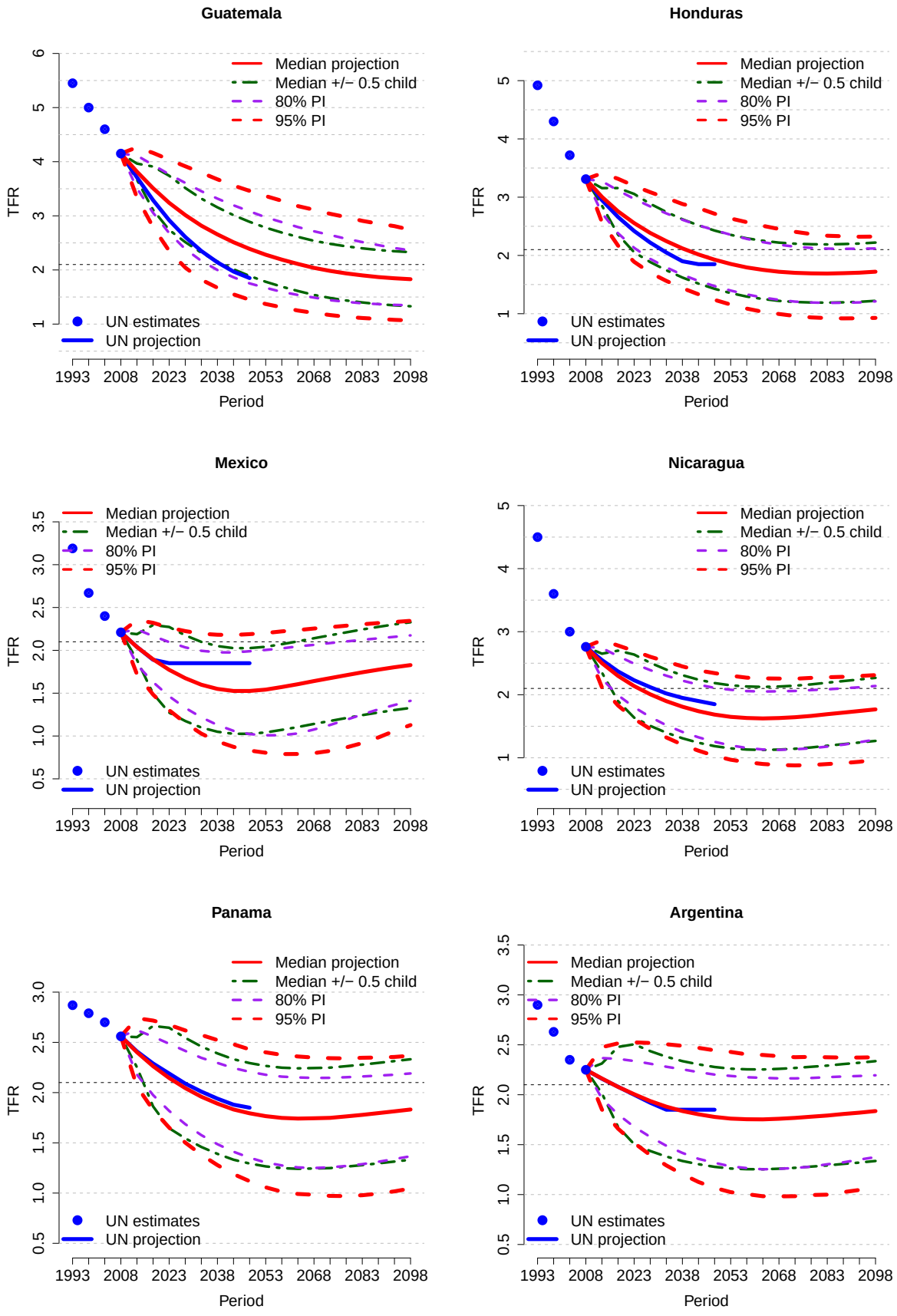

Figure 53: Projections for Guatemala, Honduras, Mexico, Nicaragua, Panama, Argentina

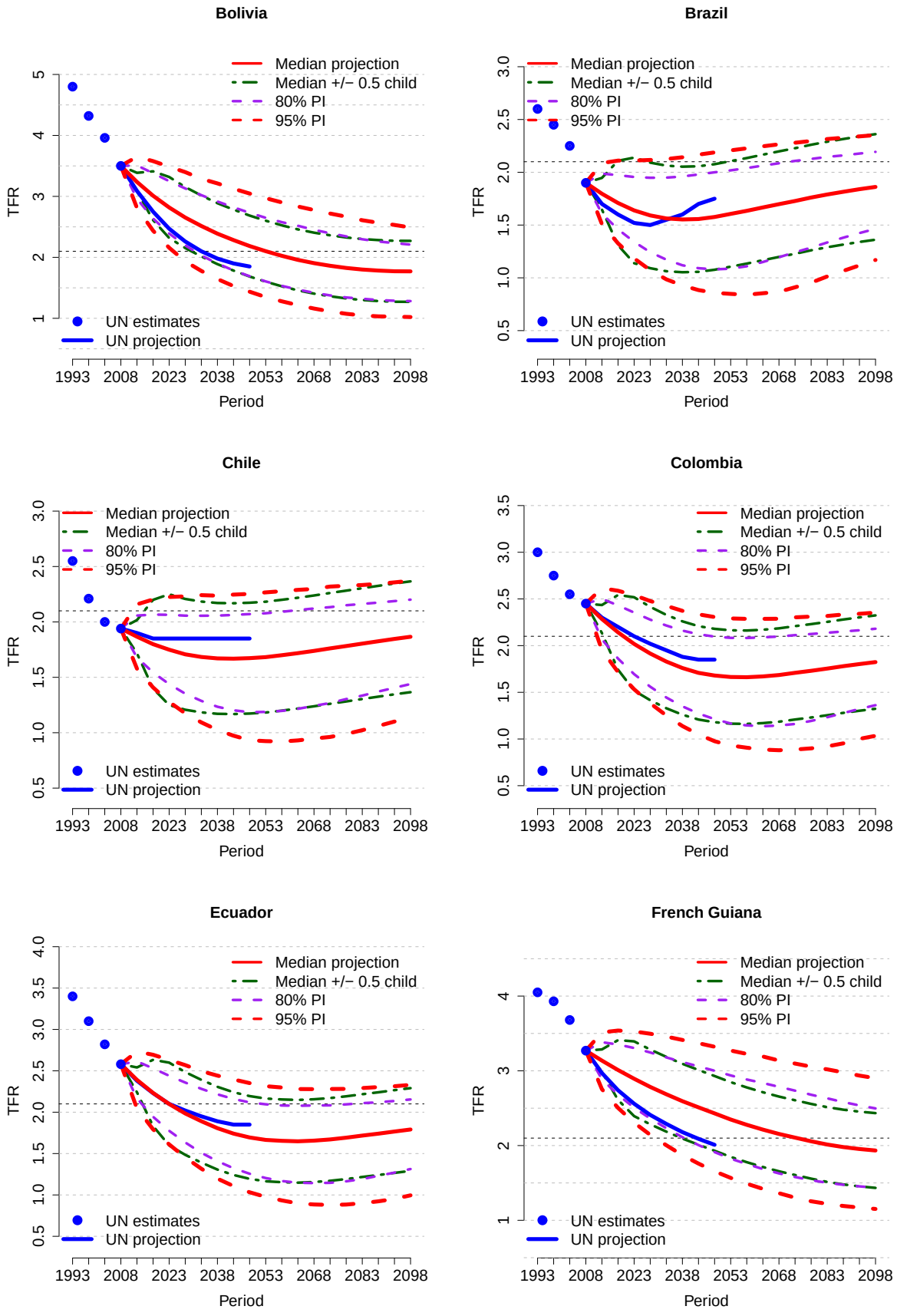

Figure 54: Projections for Bolivia, Brazil, Chile, Colombia, Ecuador, French Guiana

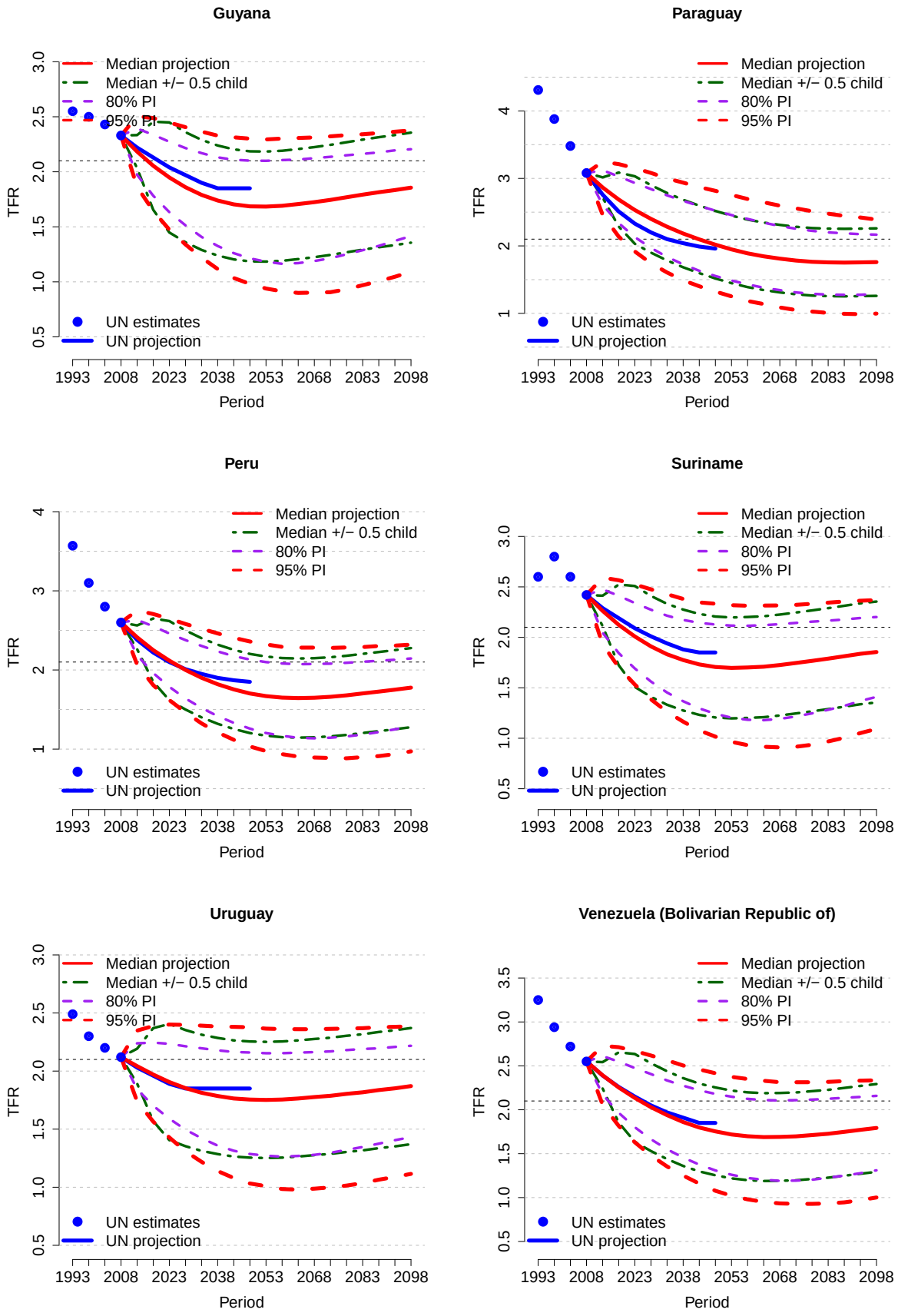

Figure 55: Projections for Guyana, Paraguay, Peru, Suriname, Uruguay, Venezuela (Bolivarian Republic of)

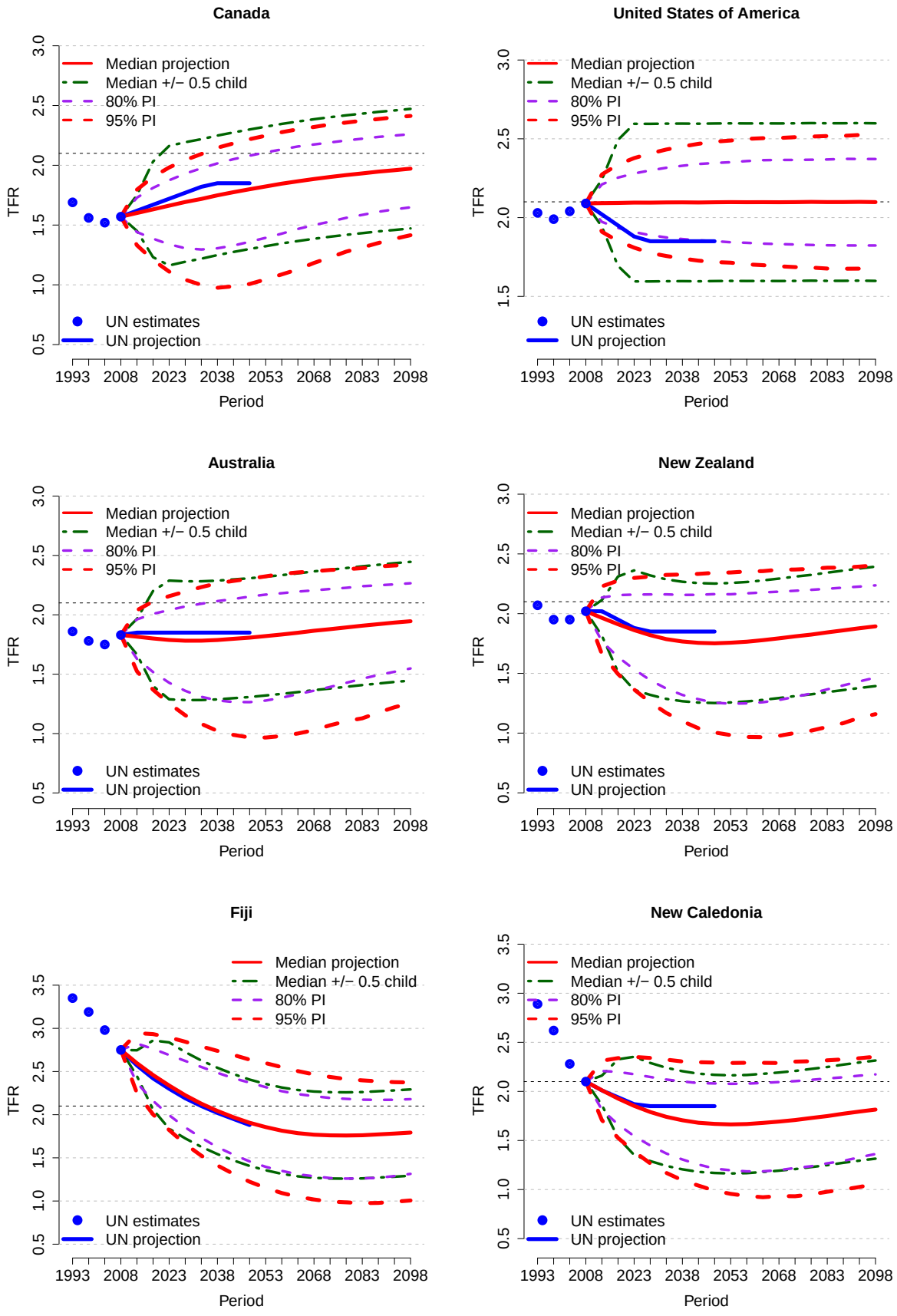

Figure 56: Projections for Canada, United States of America, Australia, New Zealand, Fiji, New Caledonia

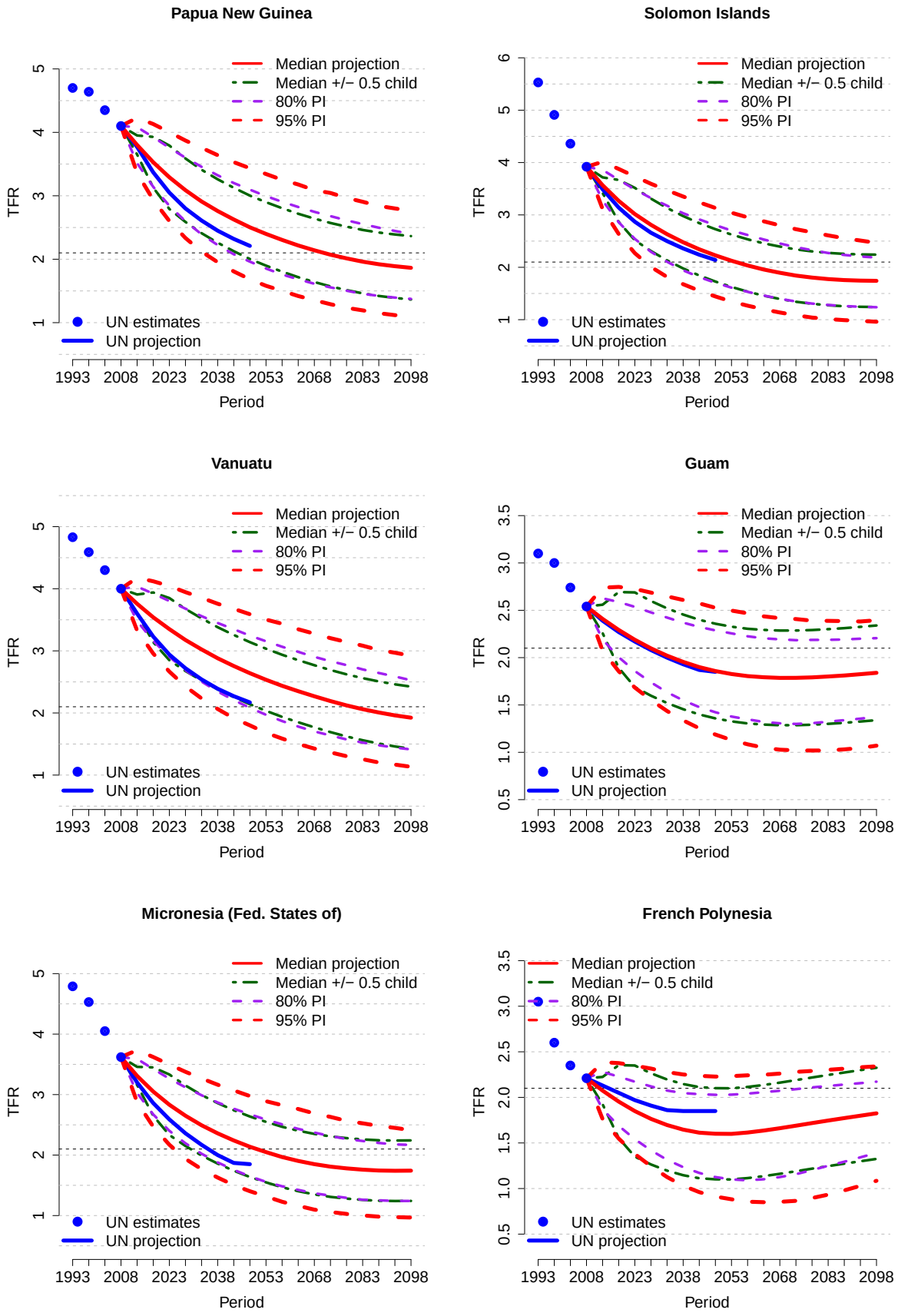

Figure 57: Projections for Papua New Guinea, Solomon Islands, Vanuatu, Guam, Micronesia (Fed. States of), French Polynesia

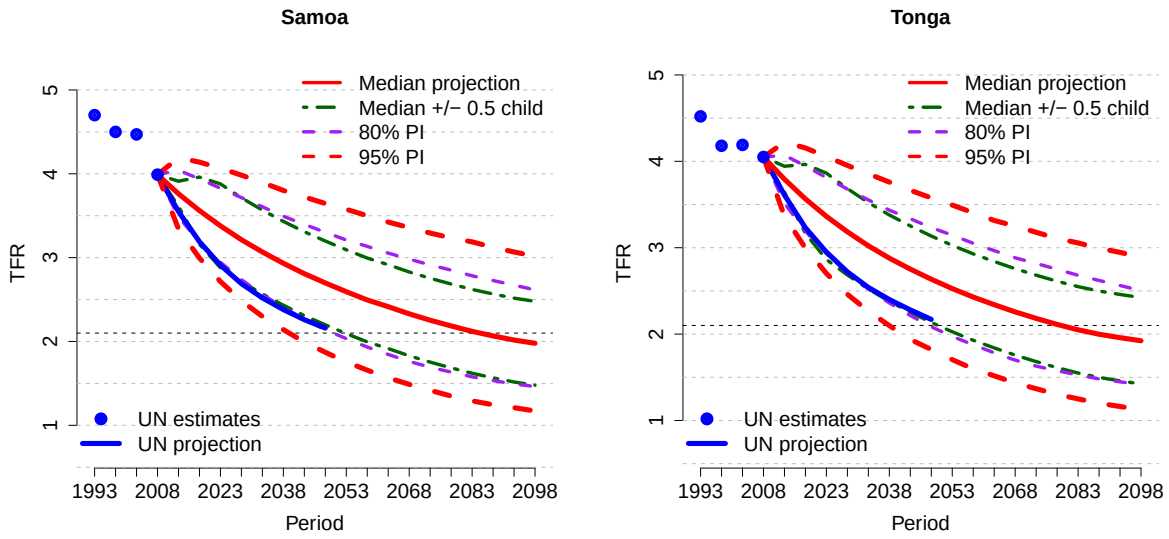

Figure 58: Projections for Samoa, Tonga

9.2 Plots: DL curves

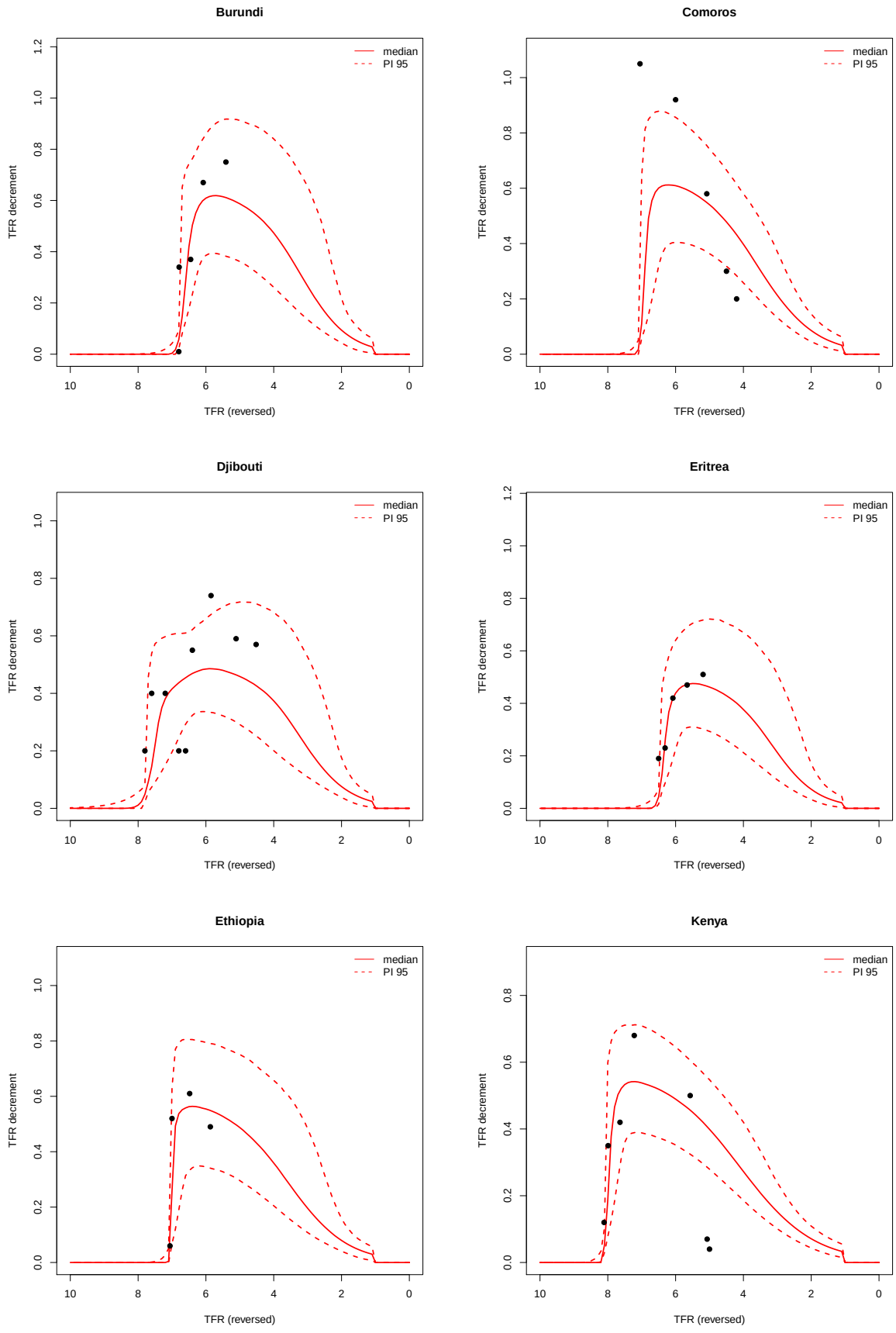

Figure 59: 95% Confidence and prediction intervals for the country-specific decline curves (red). The black dots are the observed decrements

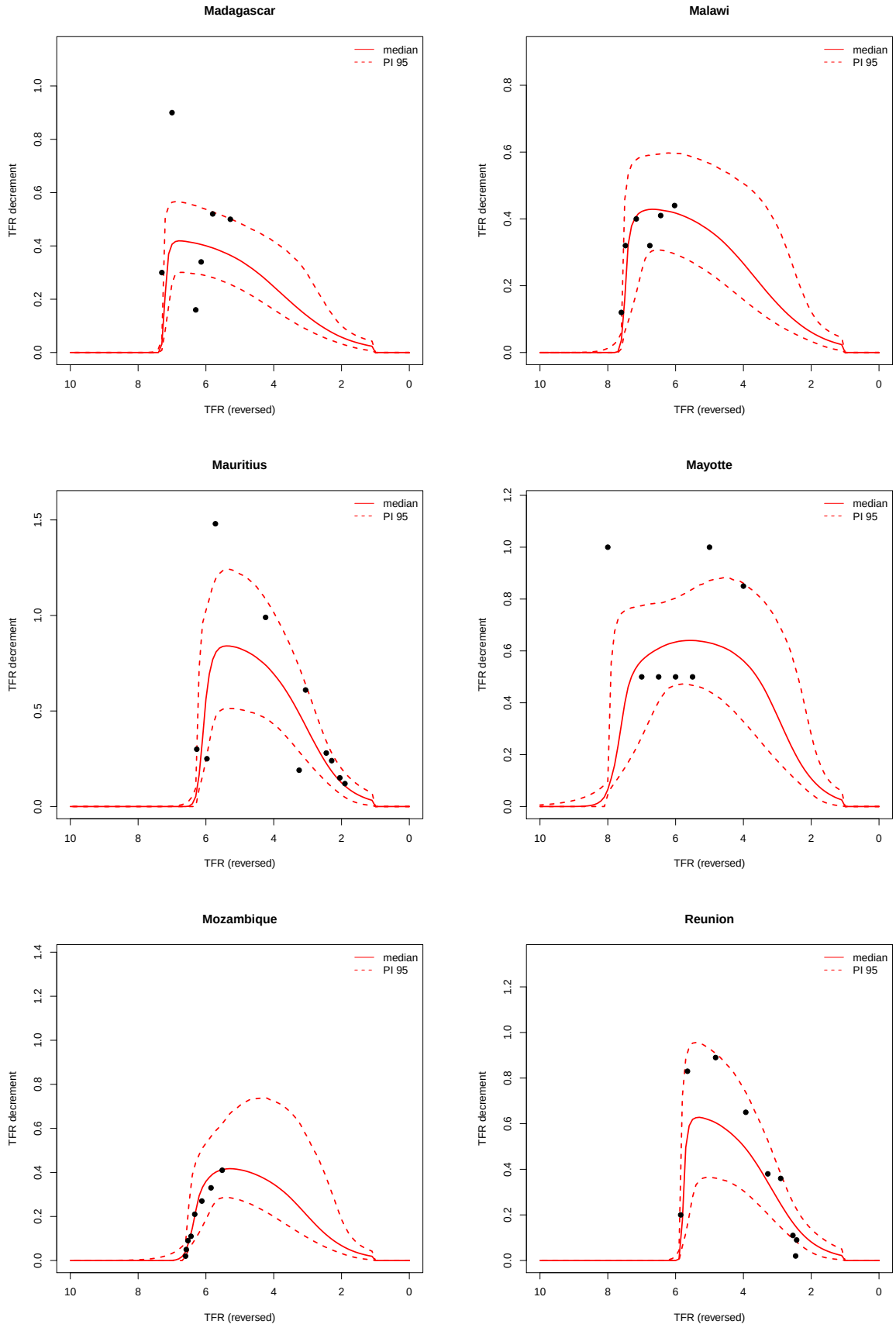

Figure 60: 95% Confidence and prediction intervals for the country-specific decline curves (red). The black dots are the observed decrements

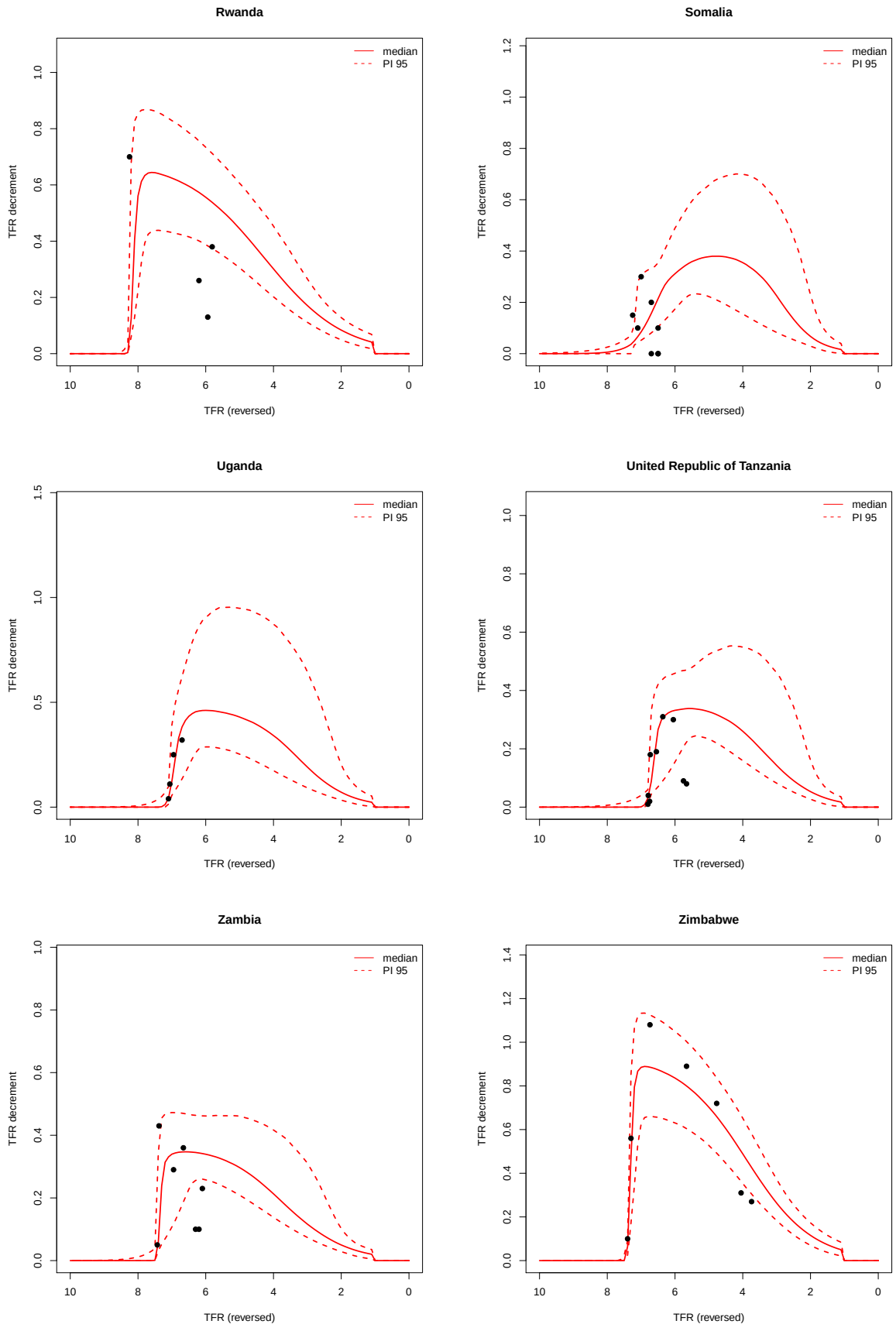

Figure 61: 95% Confidence and prediction intervals for the country-specific decline curves (red). The black dots are the observed decrements

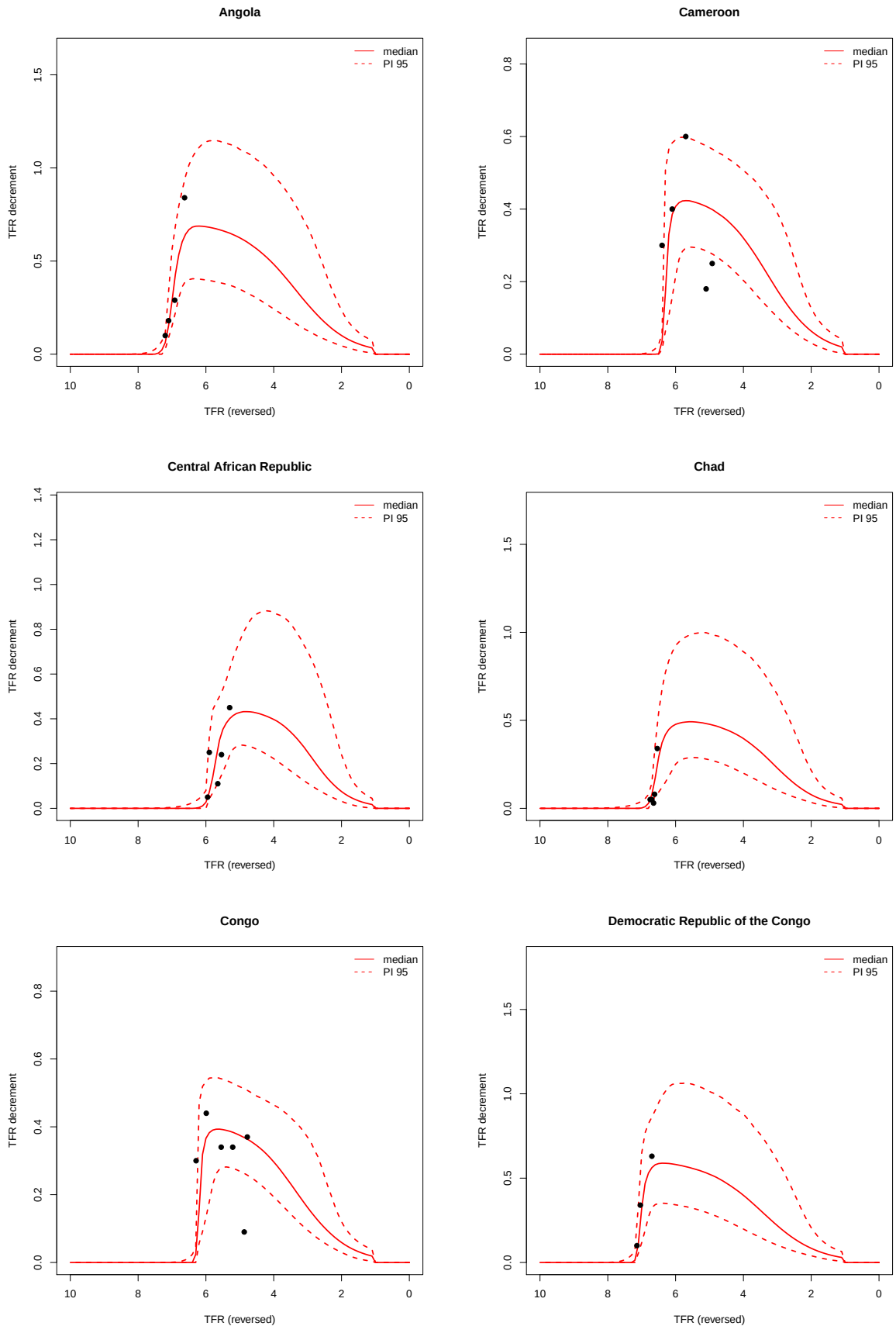

Figure 62: 95% Confidence and prediction intervals for the country-specific decline curves (red). The black dots are the observed decrements

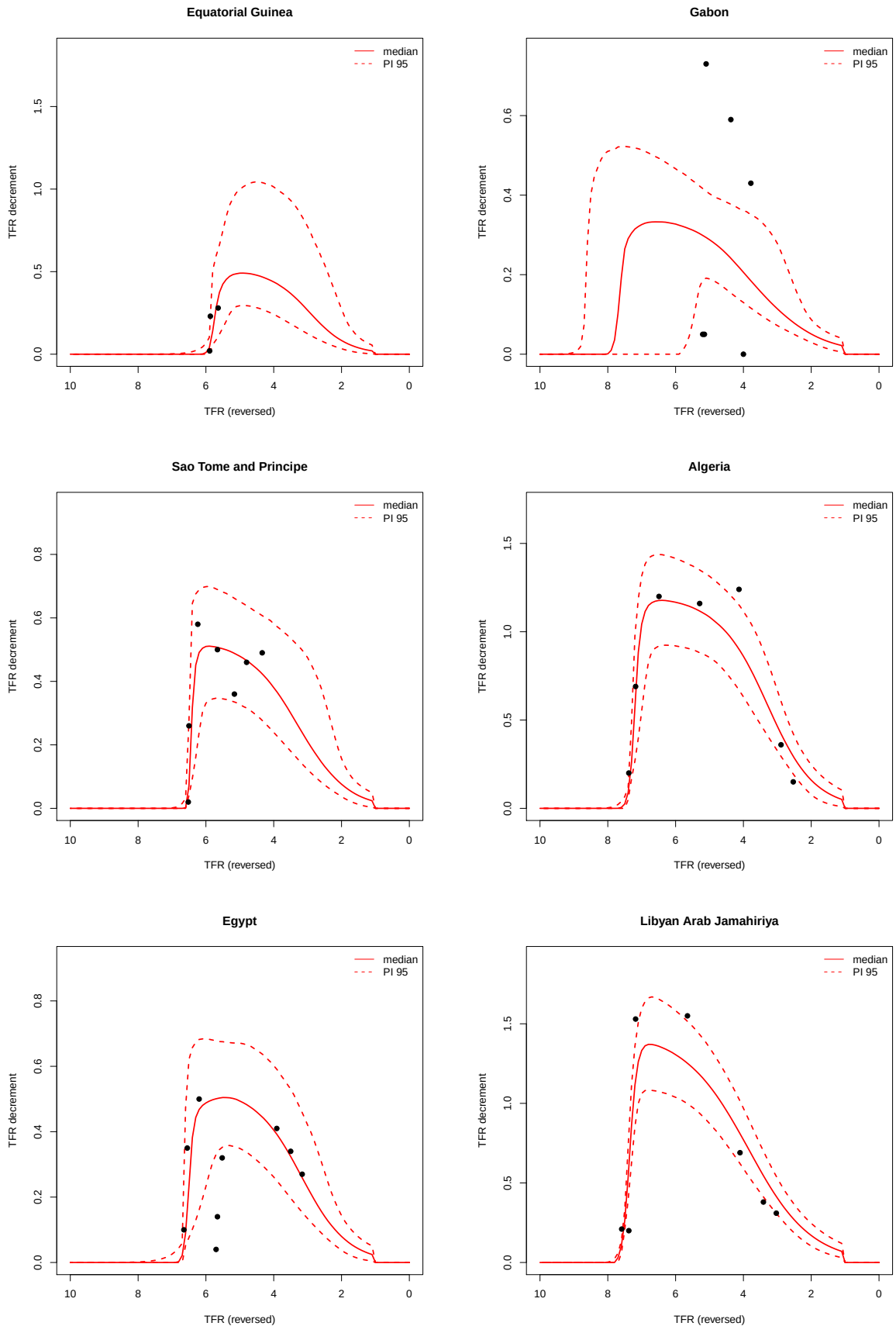

Figure 63: 95% Confidence and prediction intervals for the country-specific decline curves (red). The black dots are the observed decrements

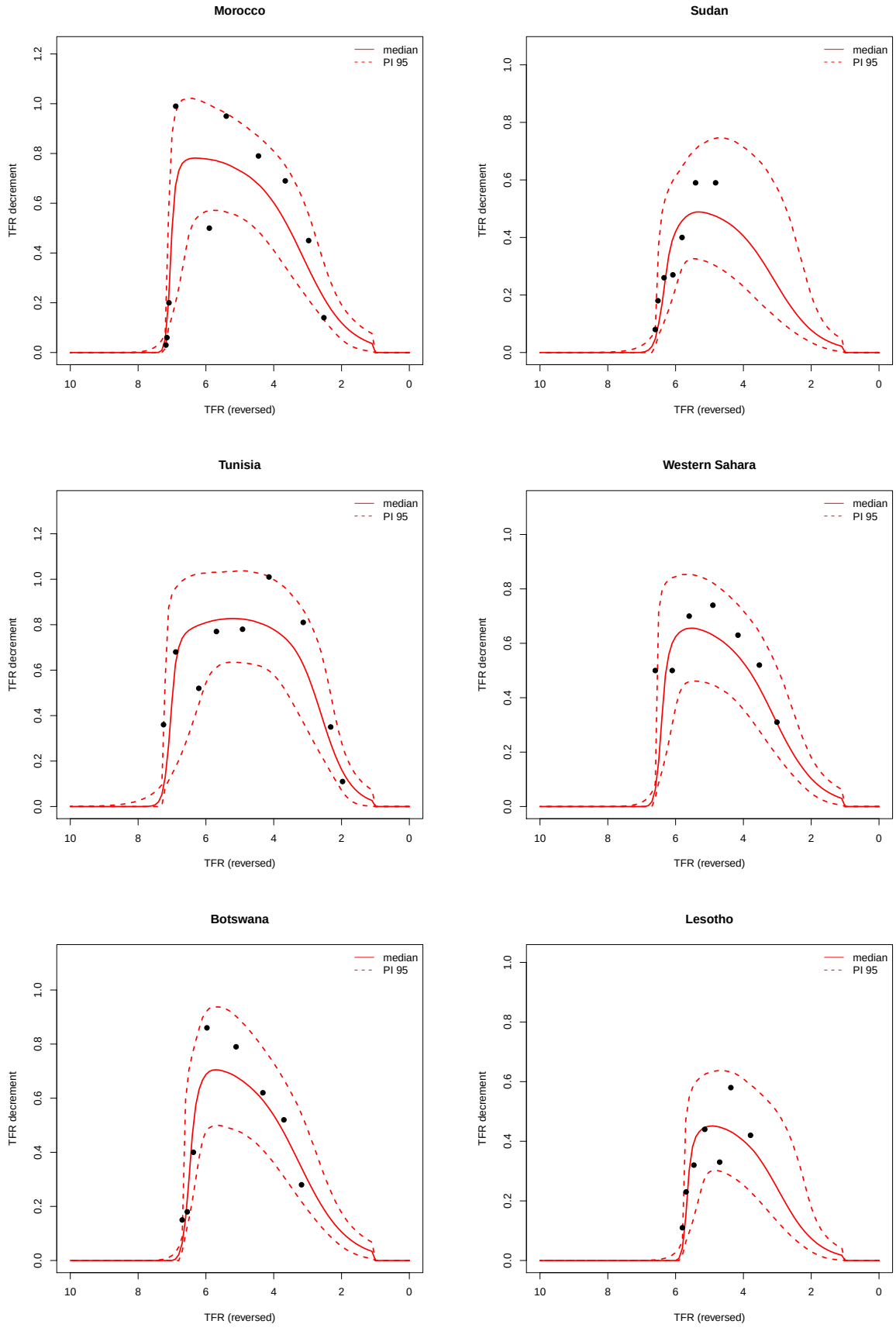

Figure 64: 95% Confidence and prediction intervals for the country-specific decline curves (red). The black dots are the observed decrements

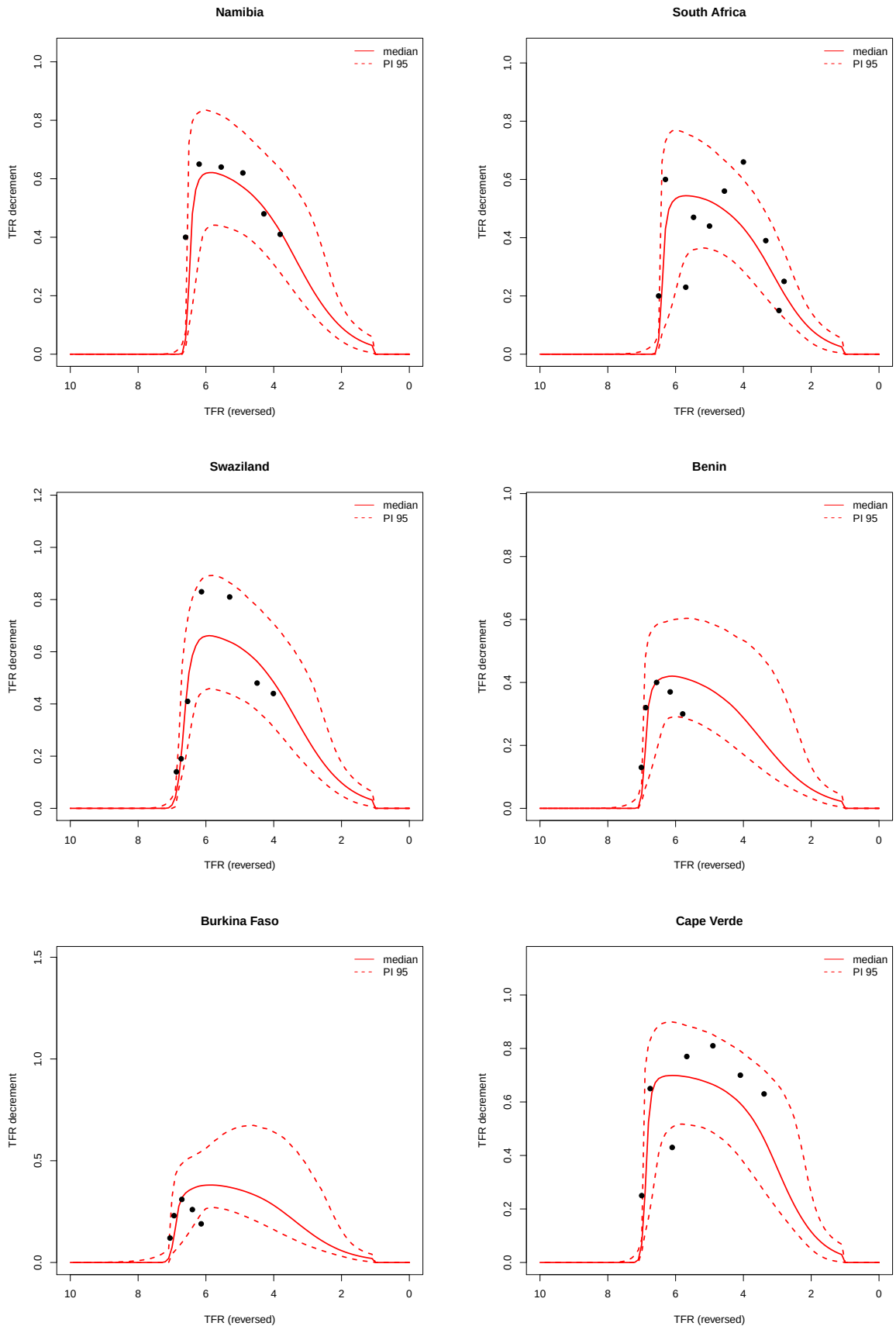

Figure 65: 95% Confidence and prediction intervals for the country-specific decline curves (red). The black dots are the observed decrements

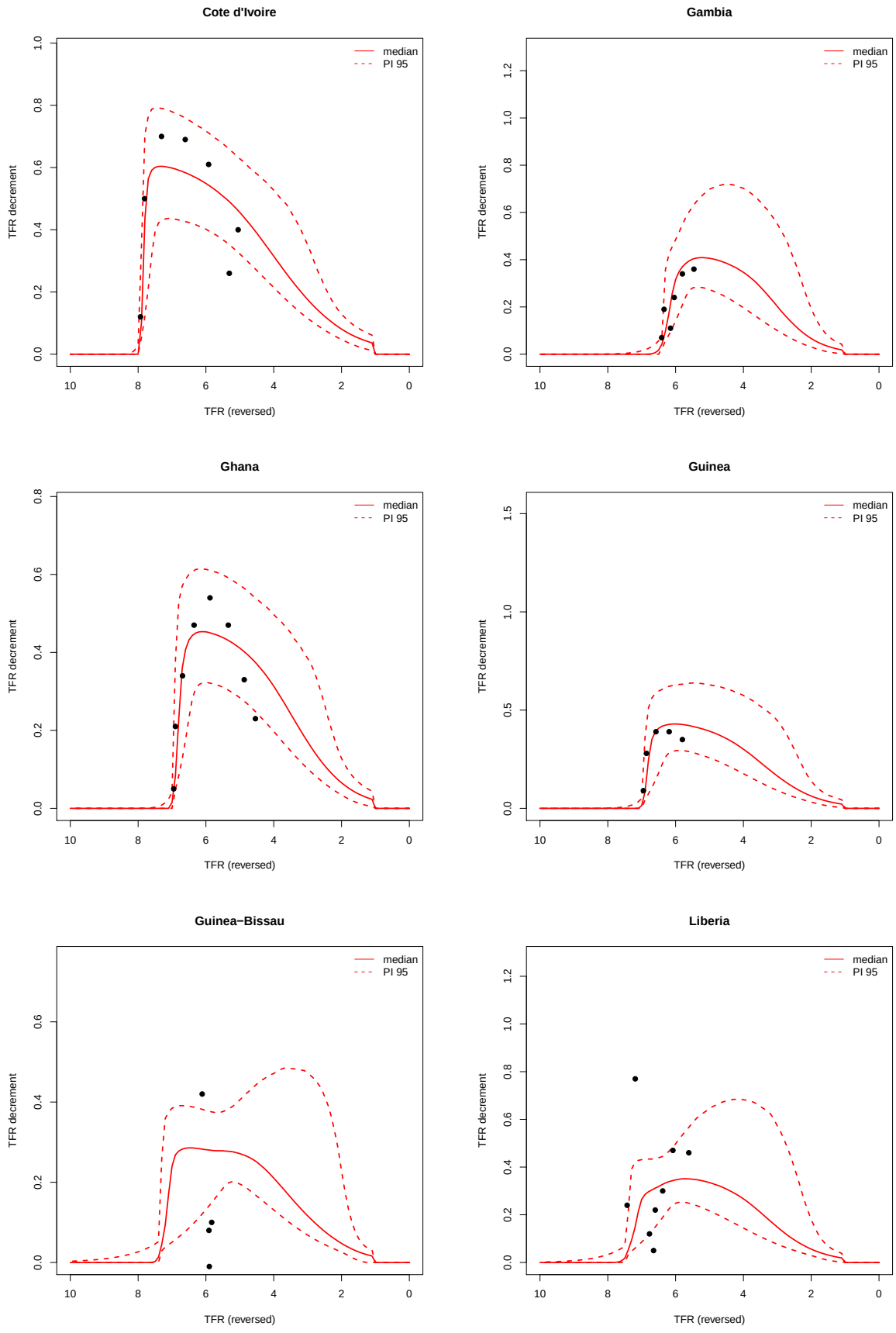

Figure 66: 95% Confidence and prediction intervals for the country-specific decline curves (red). The black dots are the observed decrements

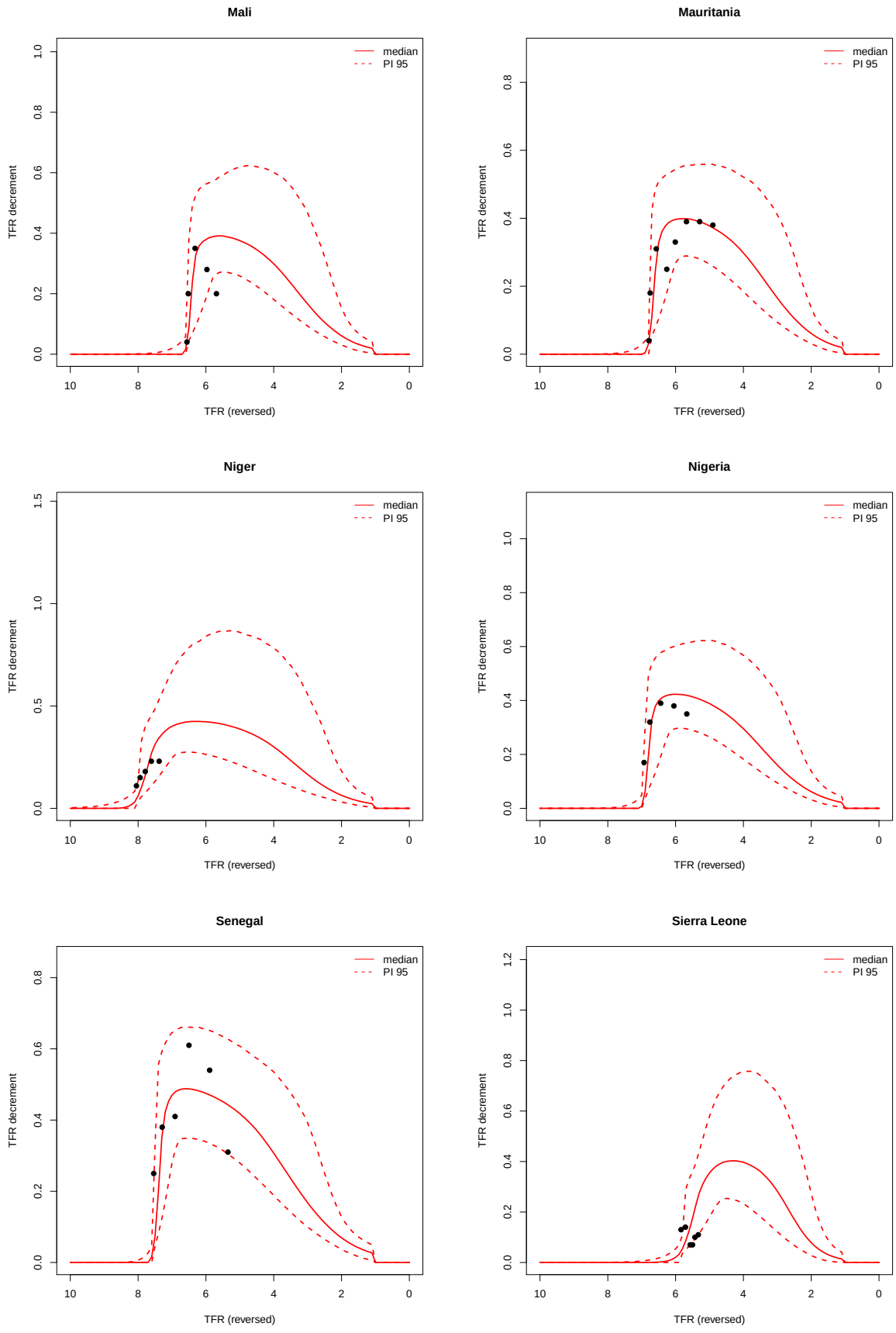

Figure 67: 95% Confidence and prediction intervals for the country-specific decline curves (red). The black dots are the observed decrements

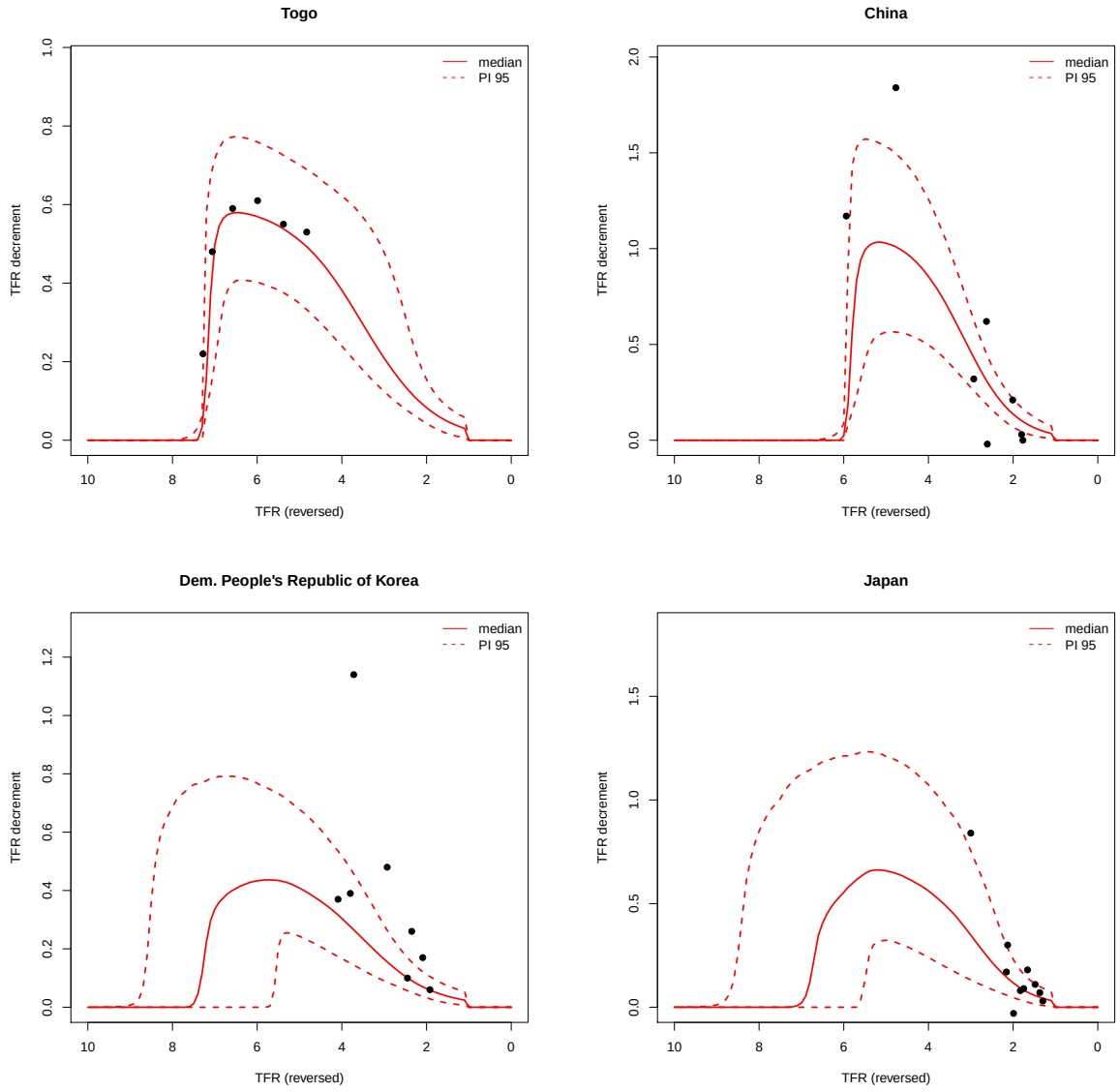

Figure 68: 95% Confidence and prediction intervals for the country-specific decline curves (red). The black dots are the observed decrements

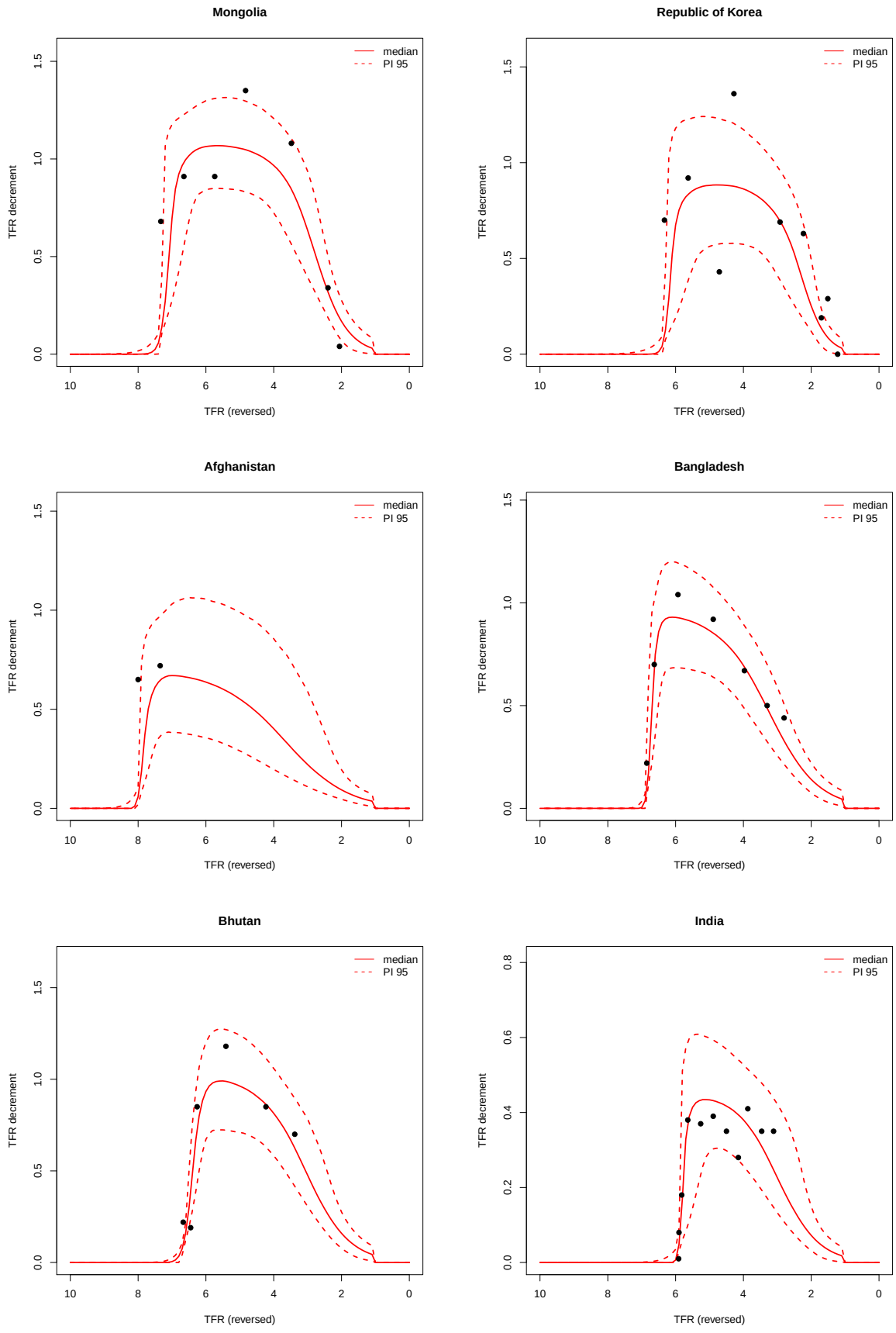

Figure 69: 95% Confidence and prediction intervals for the country-specific decline curves (red). The black dots are the observed decrements

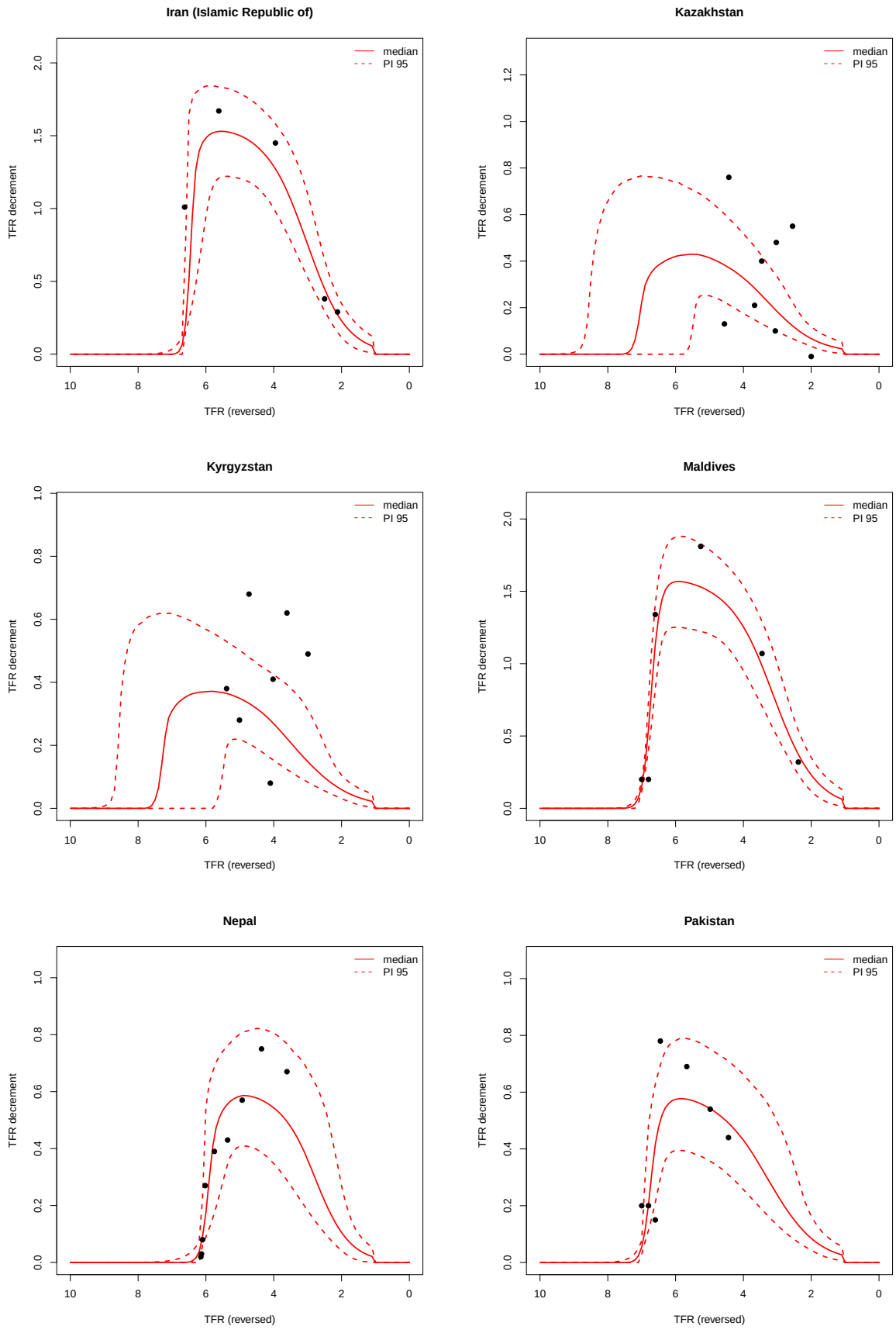

Figure 70: 95% Confidence and prediction intervals for the country-specific decline curves (red). The black dots are the observed decrements

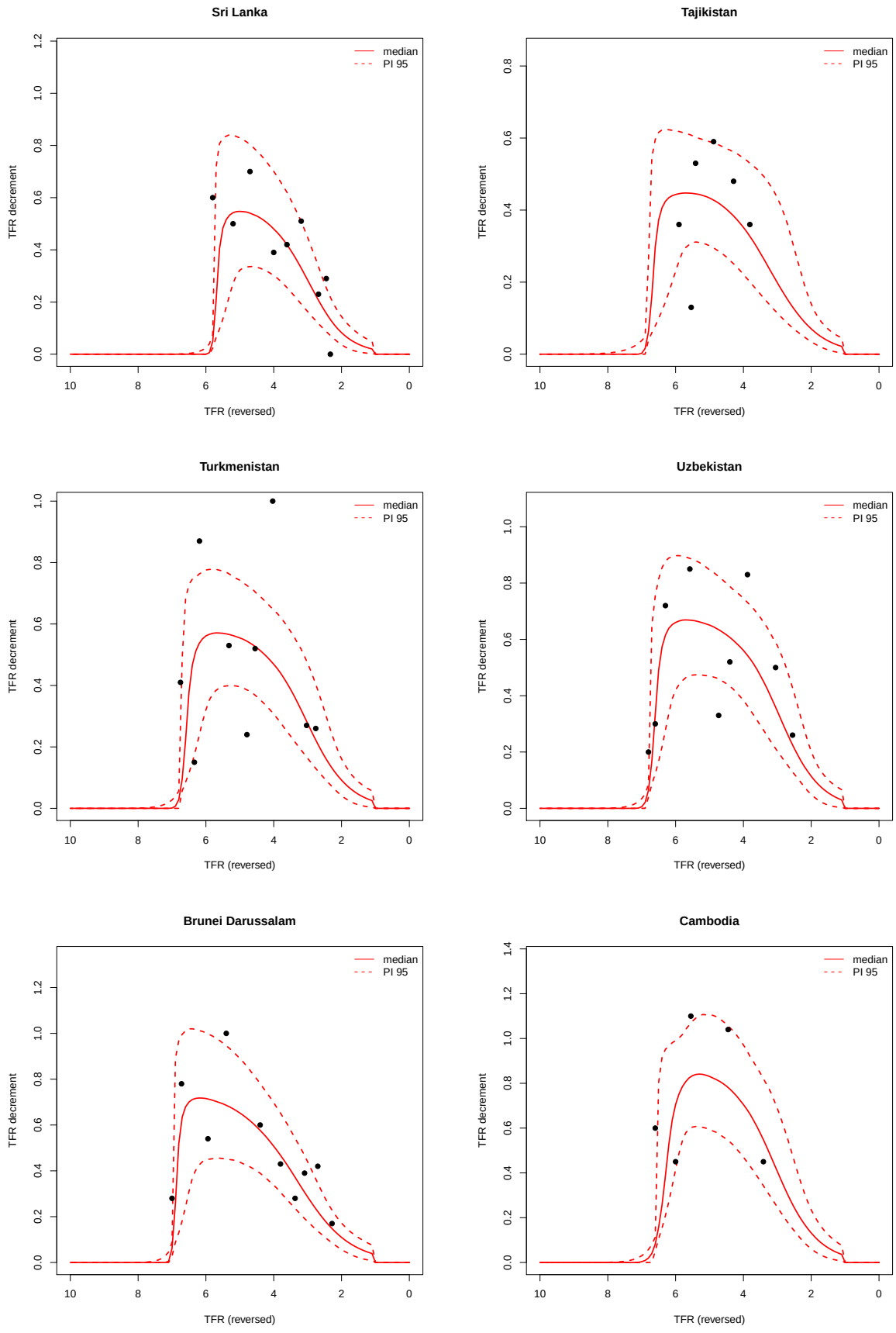

Figure 71: 95% Confidence and prediction intervals for the country-specific decline curves (red). The black dots are the observed decrements

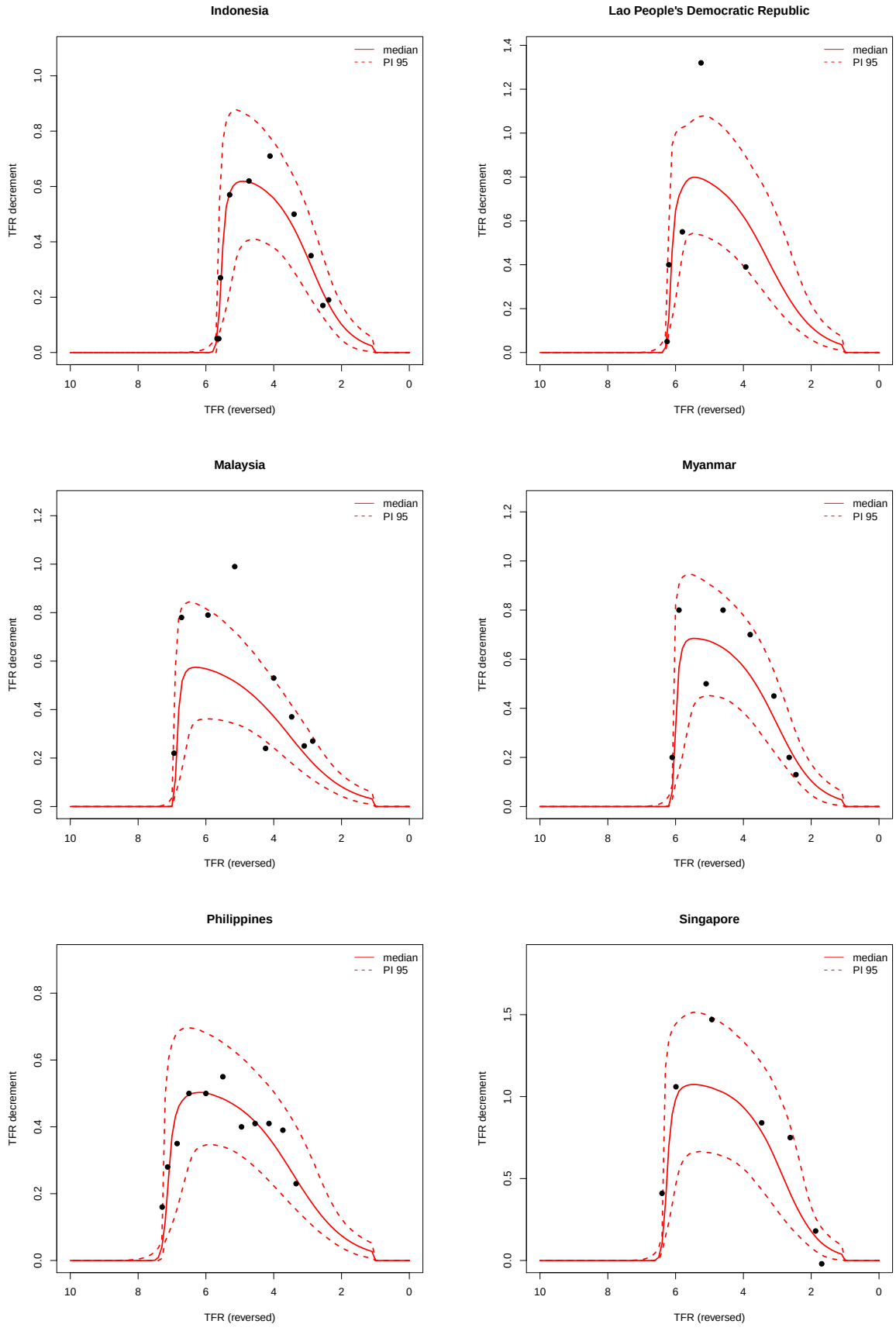

Figure 72: 95% Confidence and prediction intervals for the country-specific decline curves (red). The black dots are the observed decrements

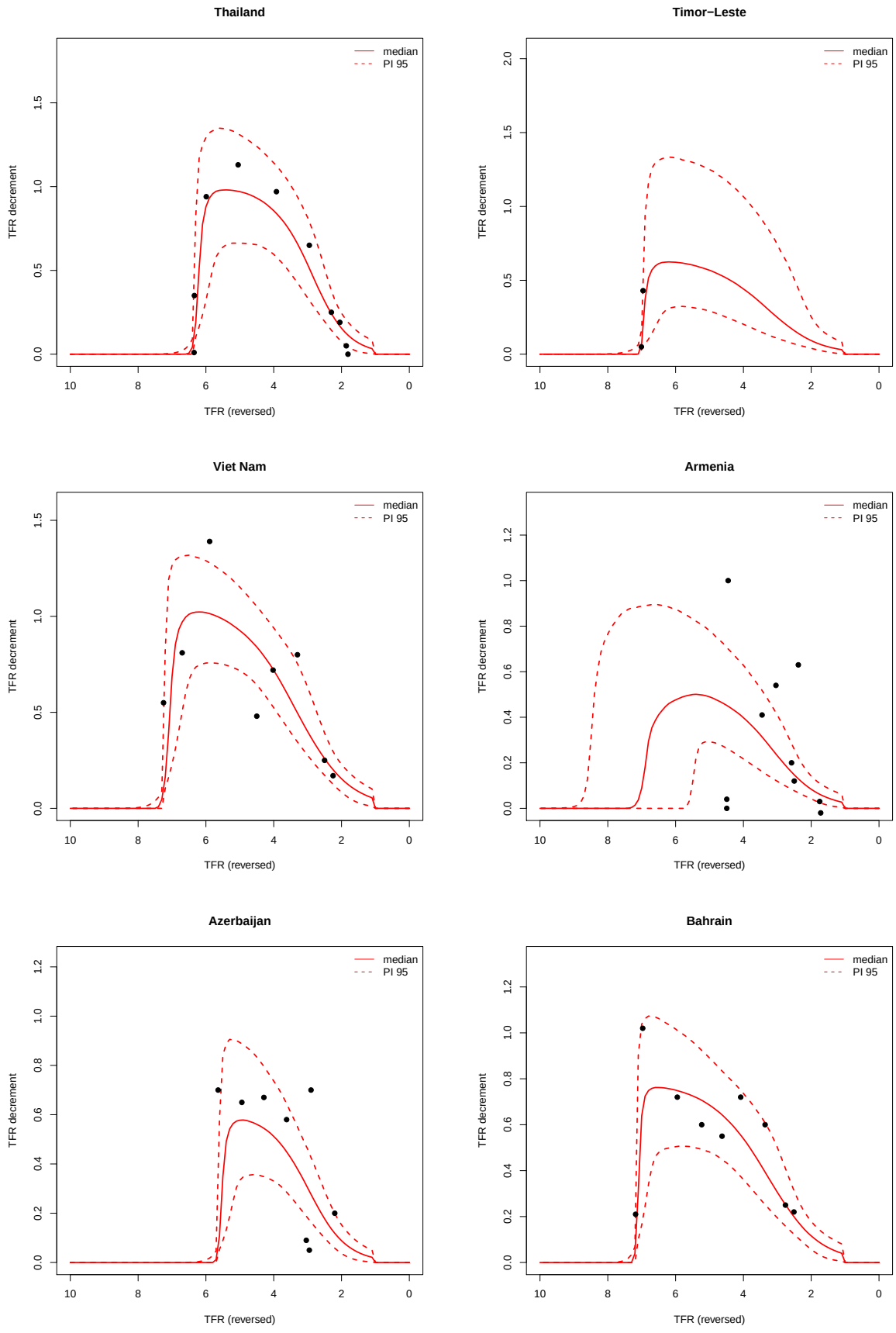

Figure 73: 95% Confidence and prediction intervals for the country-specific decline curves (red). The black dots are the observed decrements

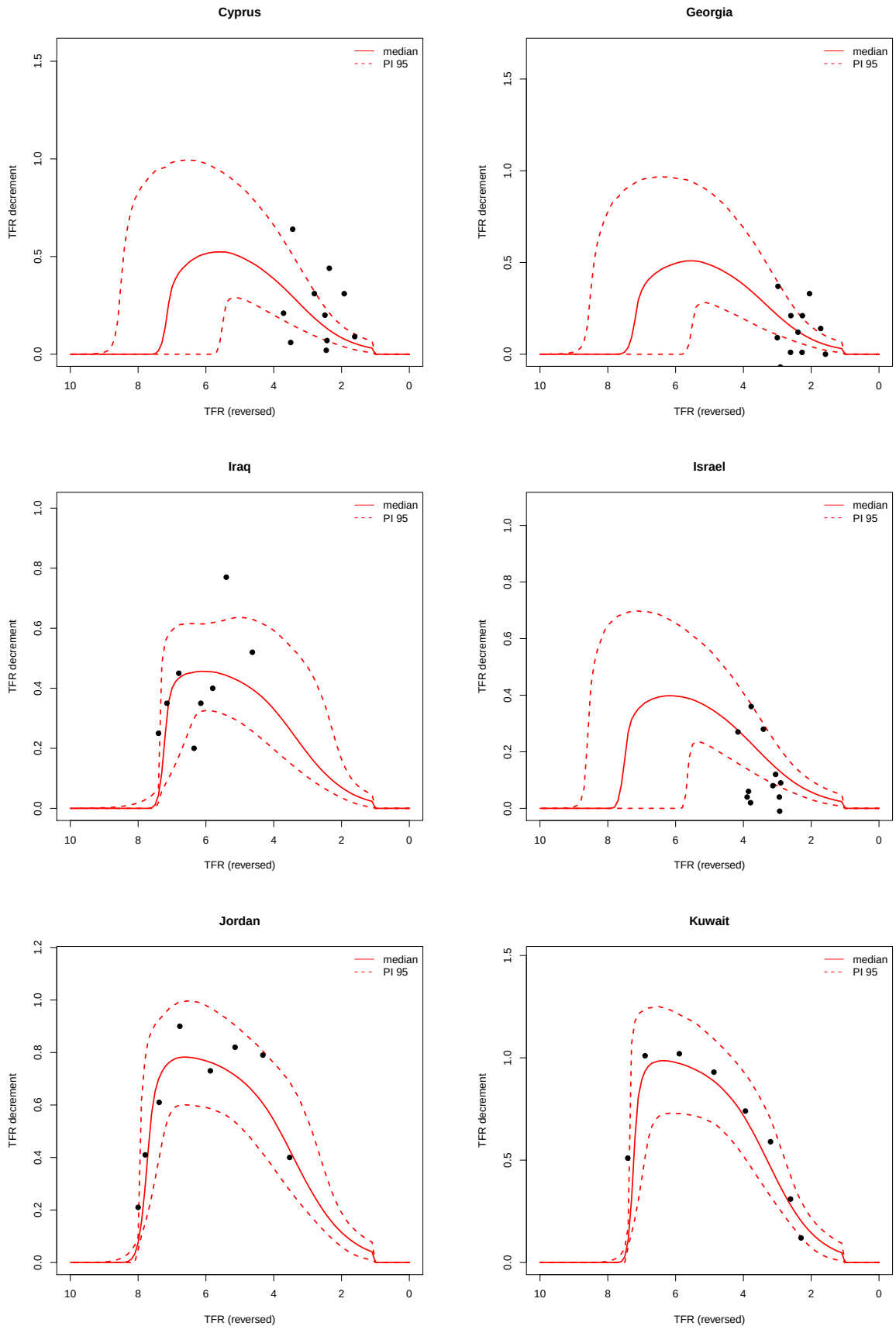

Figure 74: 95% Confidence and prediction intervals for the country-specific decline curves (red). The black dots are the observed decrements

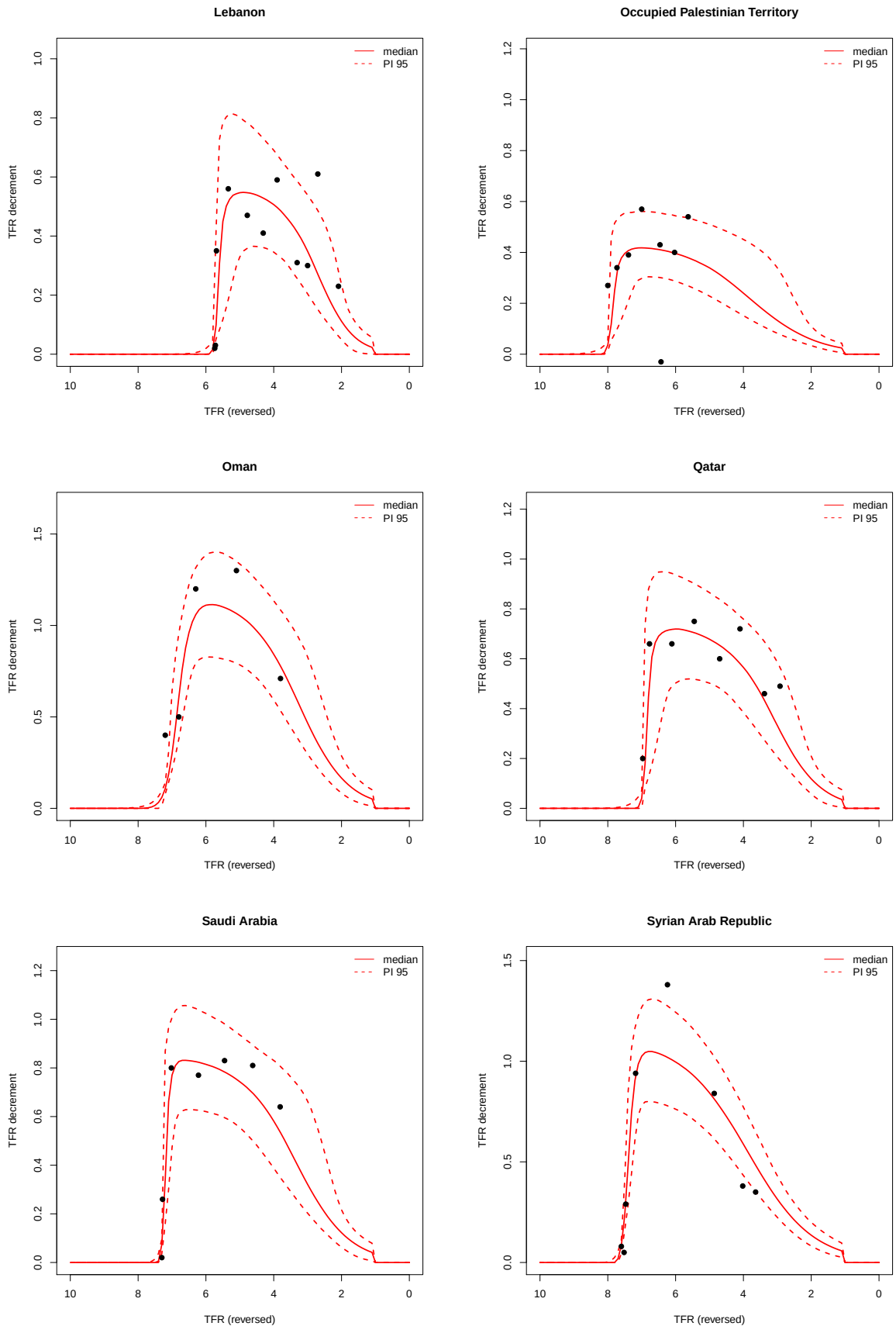

Figure 75: 95% Confidence and prediction intervals for the country-specific decline curves (red). The black dots are the observed decrements

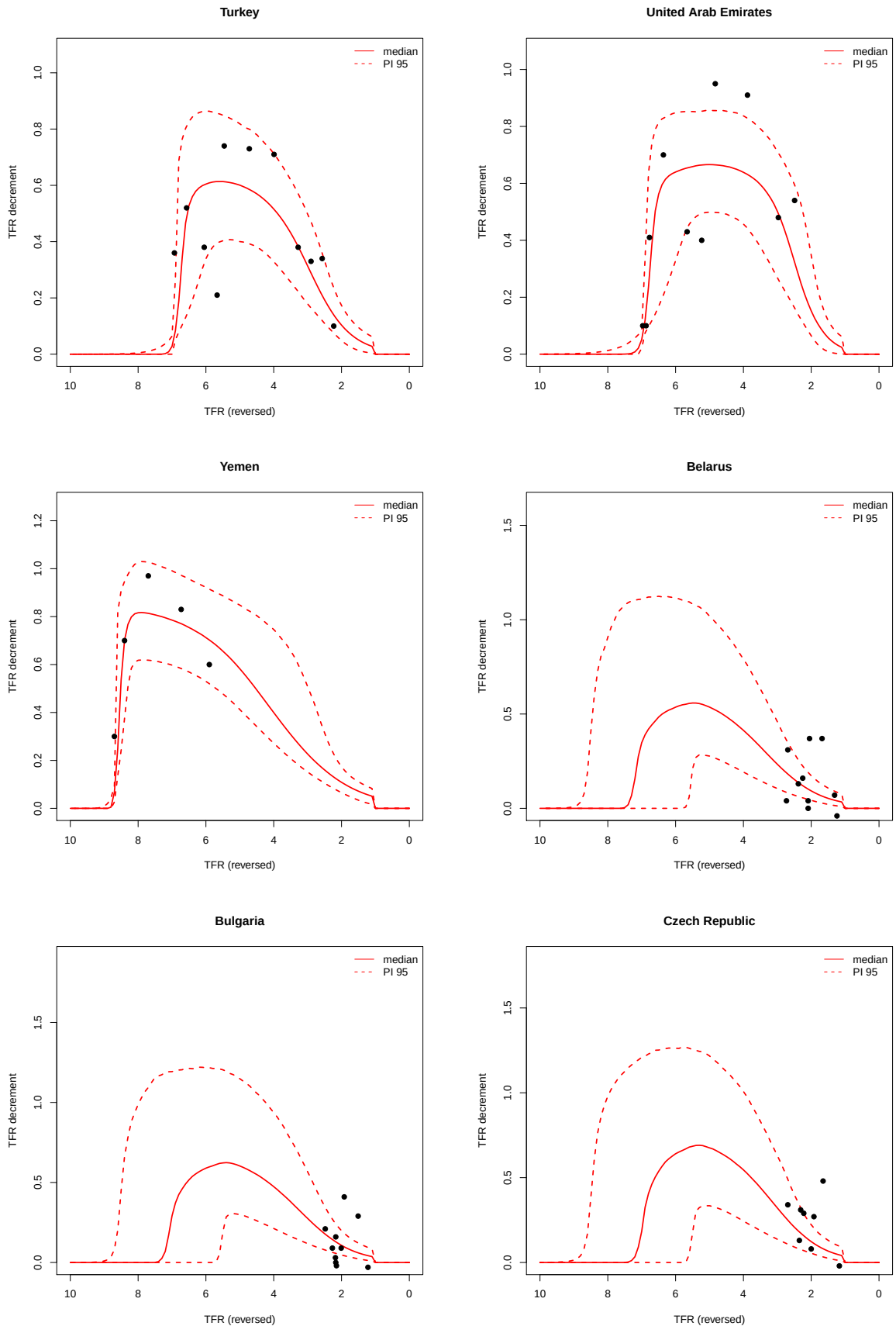

Figure 76: 95% Confidence and prediction intervals for the country-specific decline curves (red). The black dots are the observed decrements

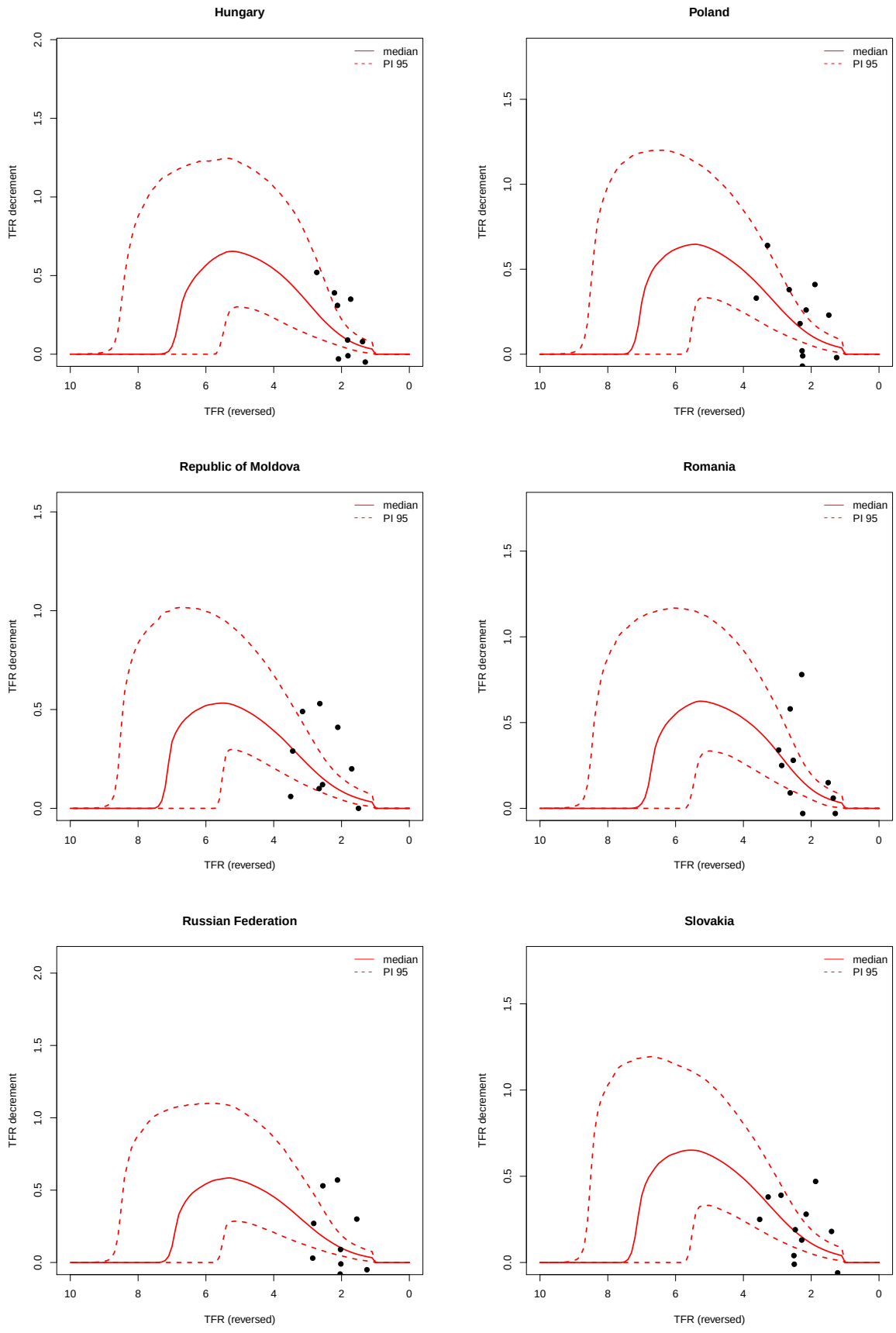

Figure 77: 95% Confidence and prediction intervals for the country-specific decline curves (red). The black dots are the observed decrements

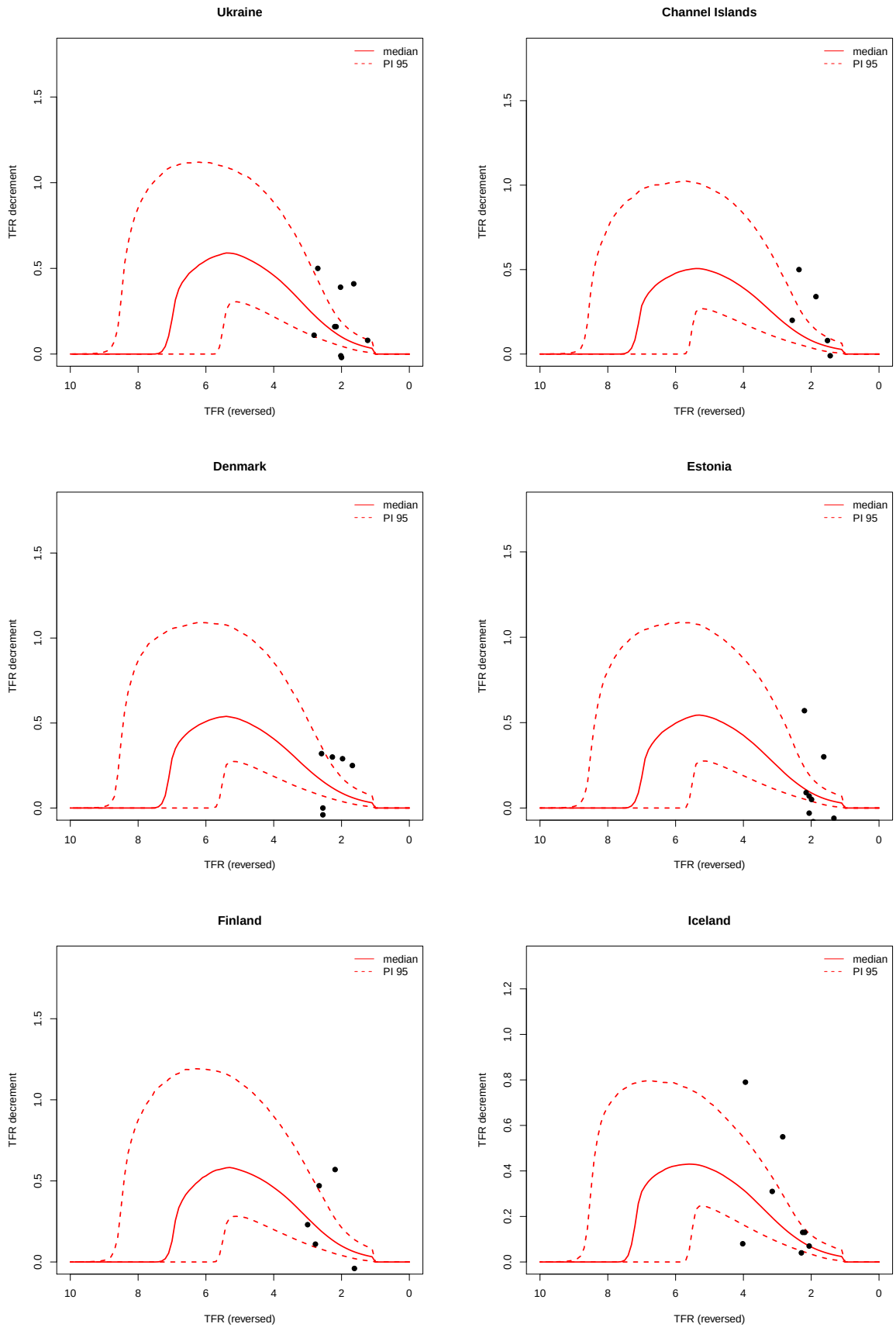

Figure 78: 95% Confidence and prediction intervals for the country-specific decline curves (red). The black dots are the observed decrements

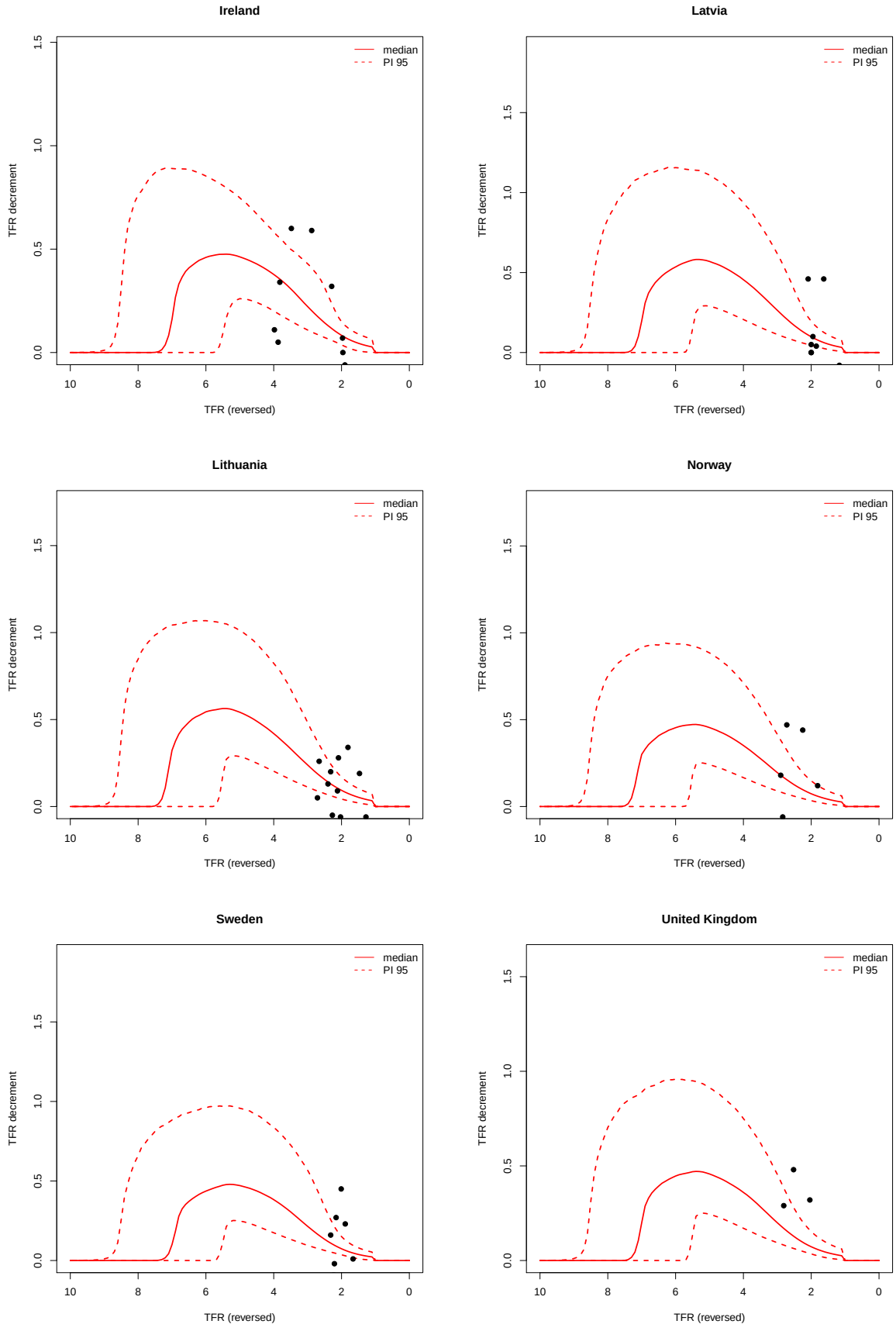

Figure 79: 95% Confidence and prediction intervals for the country-specific decline curves (red). The black dots are the observed decrements

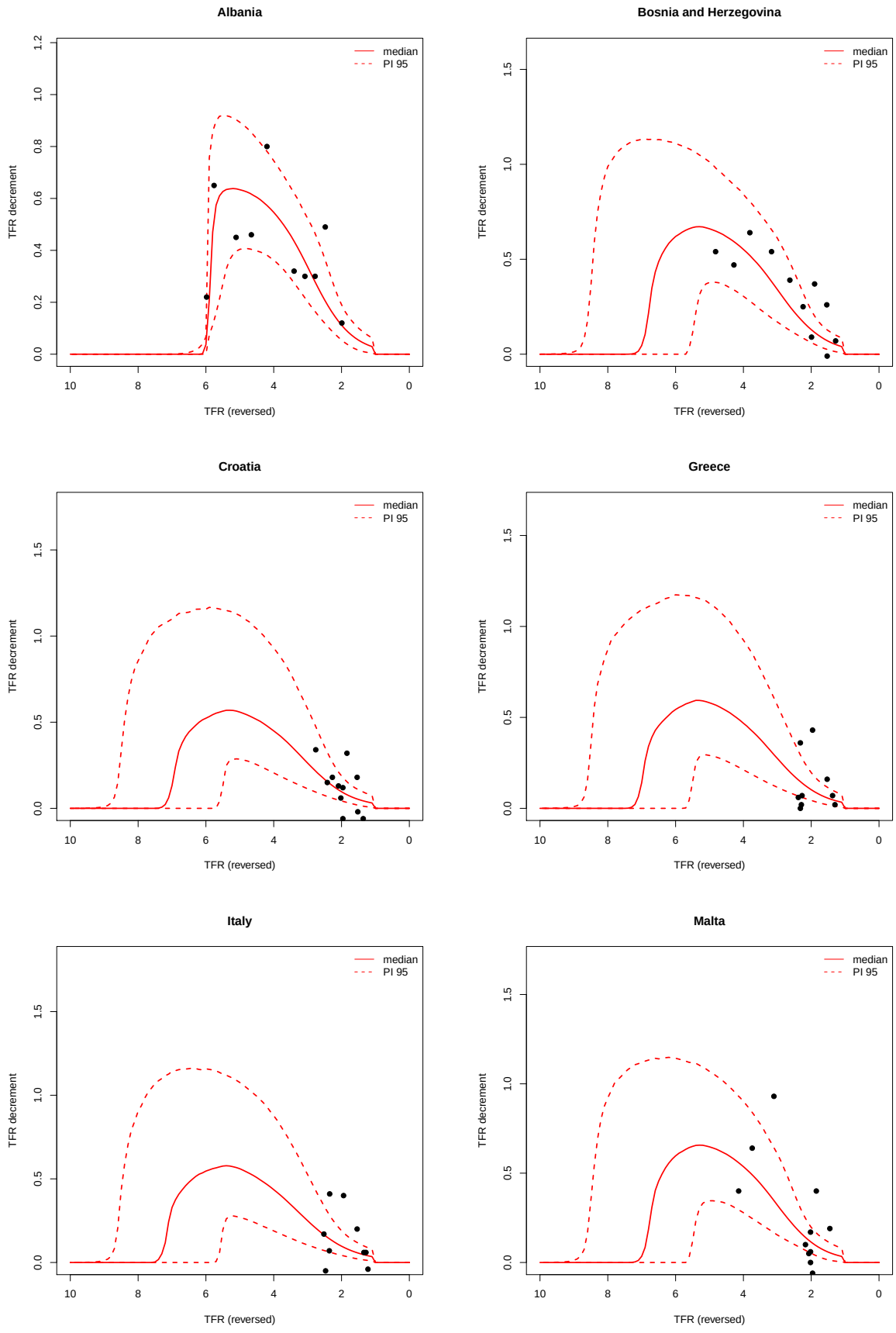

Figure 80: 95% Confidence and prediction intervals for the country-specific decline curves (red). The black dots are the observed decrements

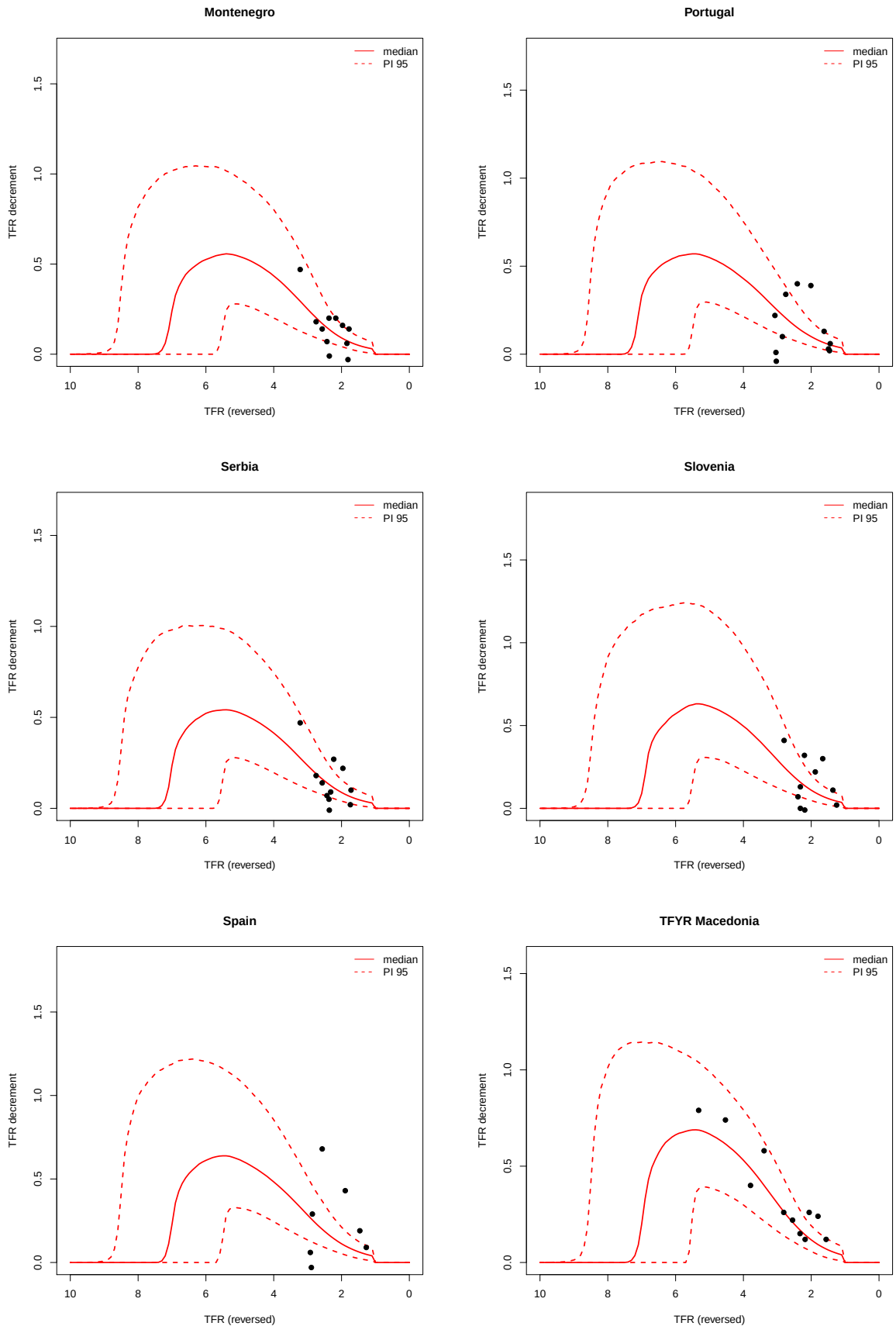

Figure 81: 95% Confidence and prediction intervals for the country-specific decline curves (red). The black dots are the observed decrements

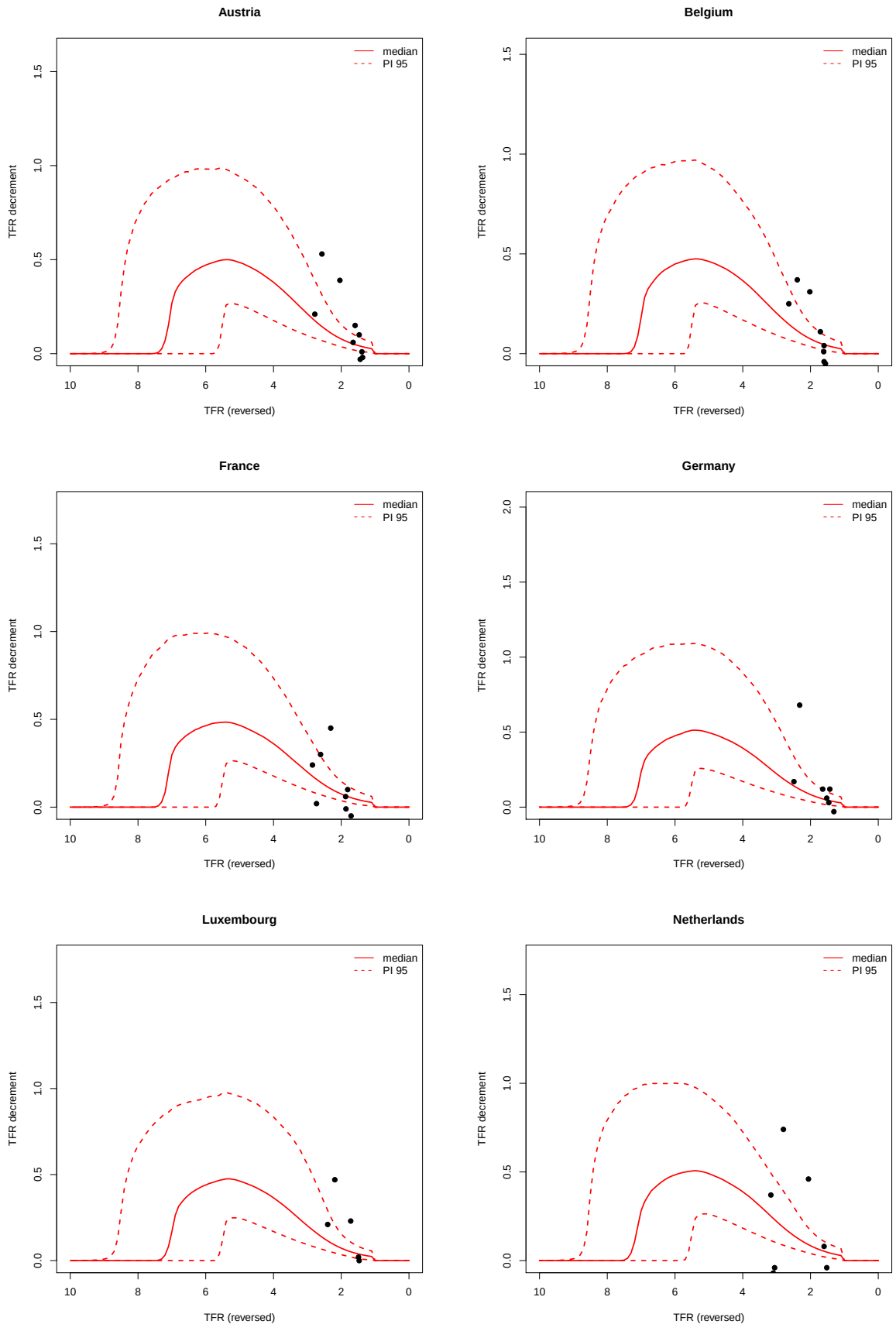

Figure 82: 95% Confidence and prediction intervals for the country-specific decline curves (red). The black dots are the observed decrements

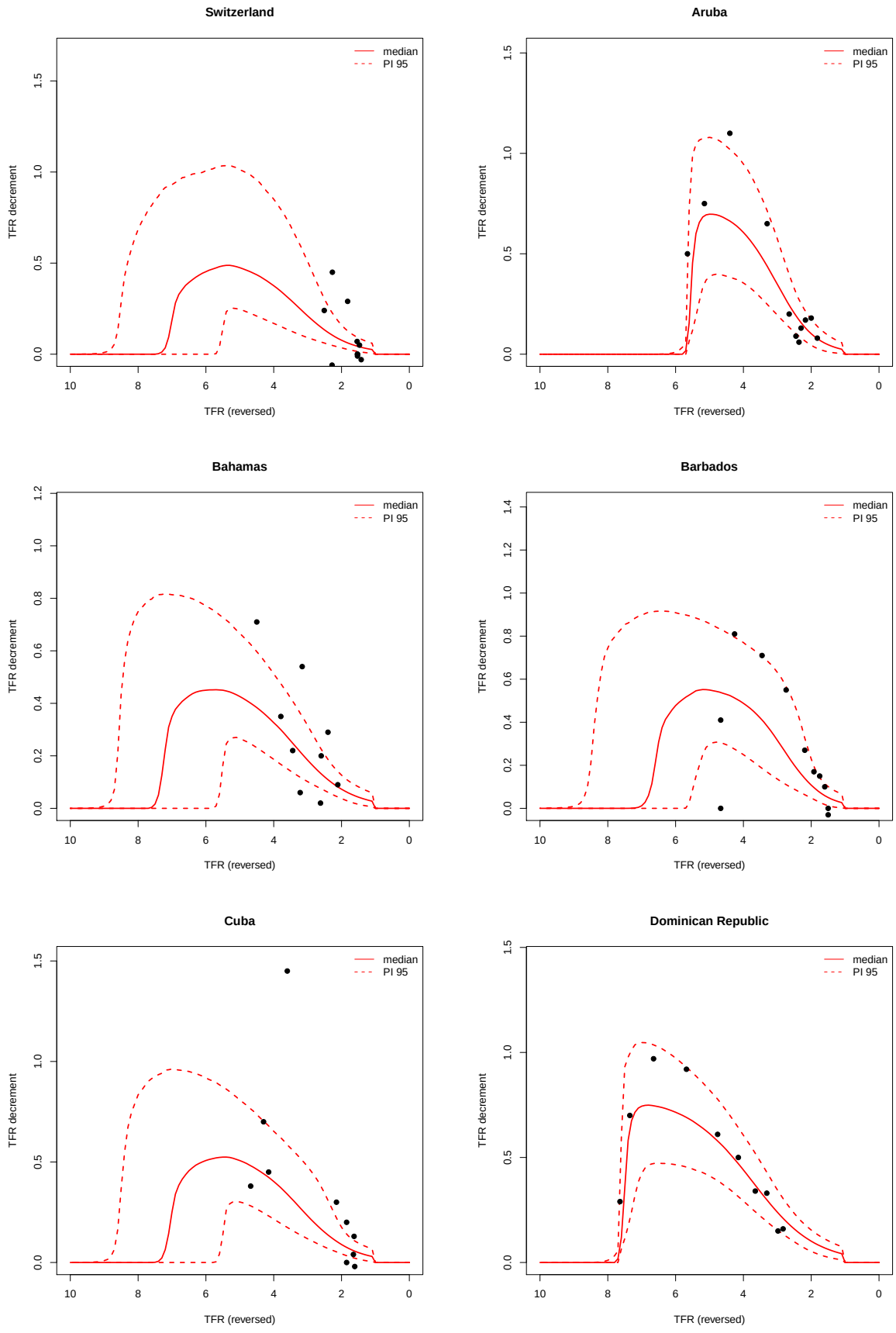

Figure 83: 95% Confidence and prediction intervals for the country-specific decline curves (red). The black dots are the observed decrements

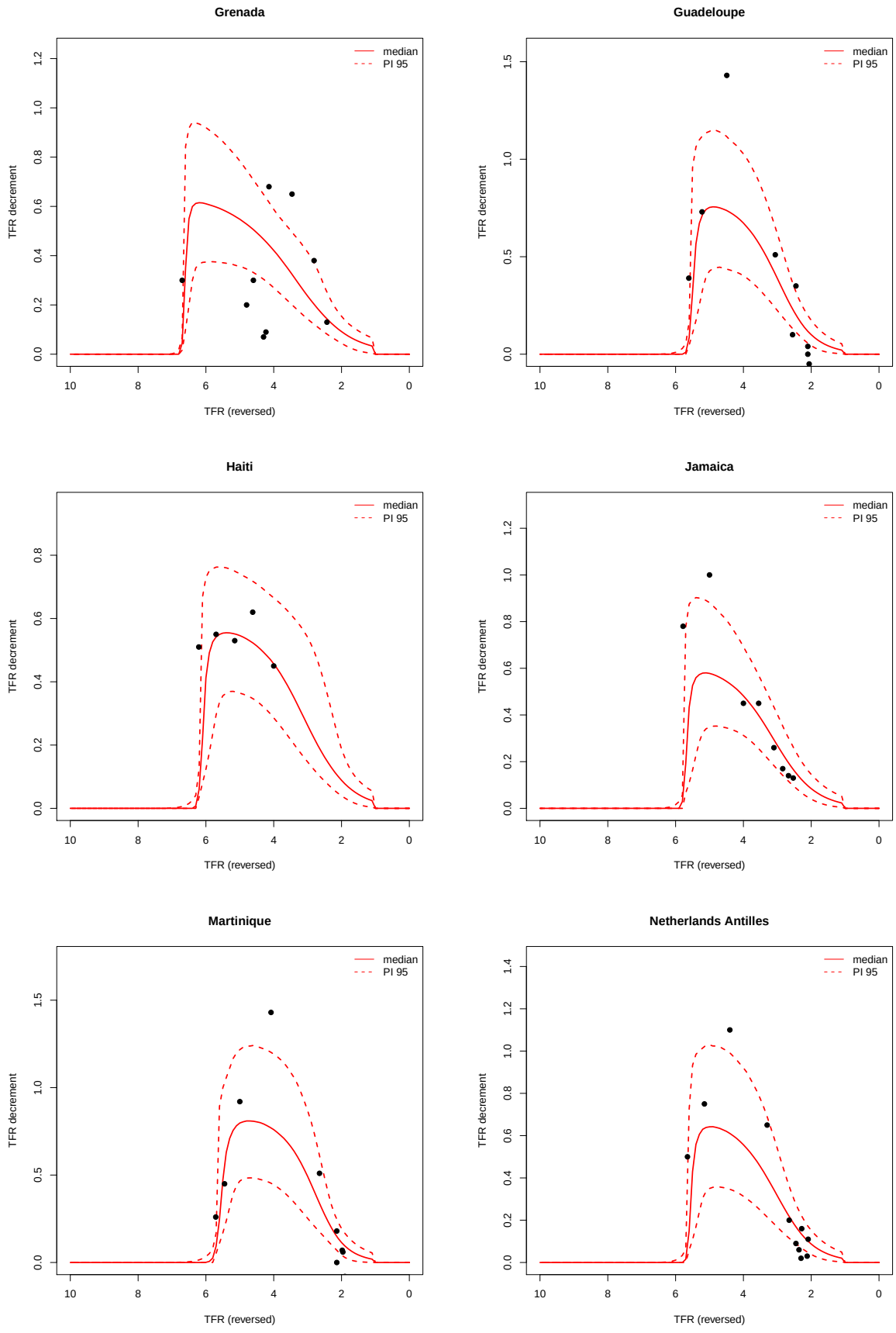

Figure 84: 95% Confidence and prediction intervals for the country-specific decline curves (red). The black dots are the observed decrements

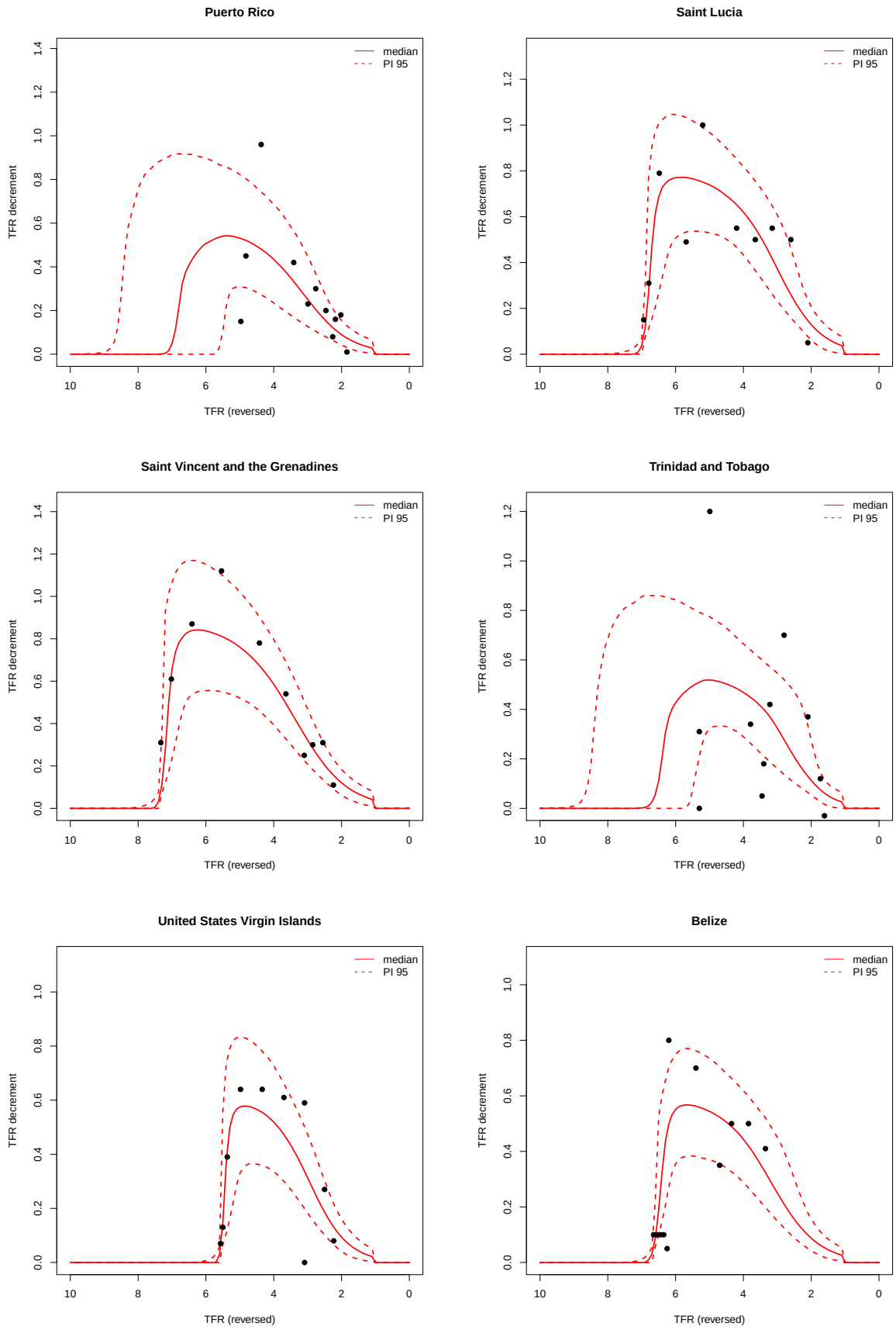

Figure 85: 95% Confidence and prediction intervals for the country-specific decline curves (red). The black dots are the observed decrements

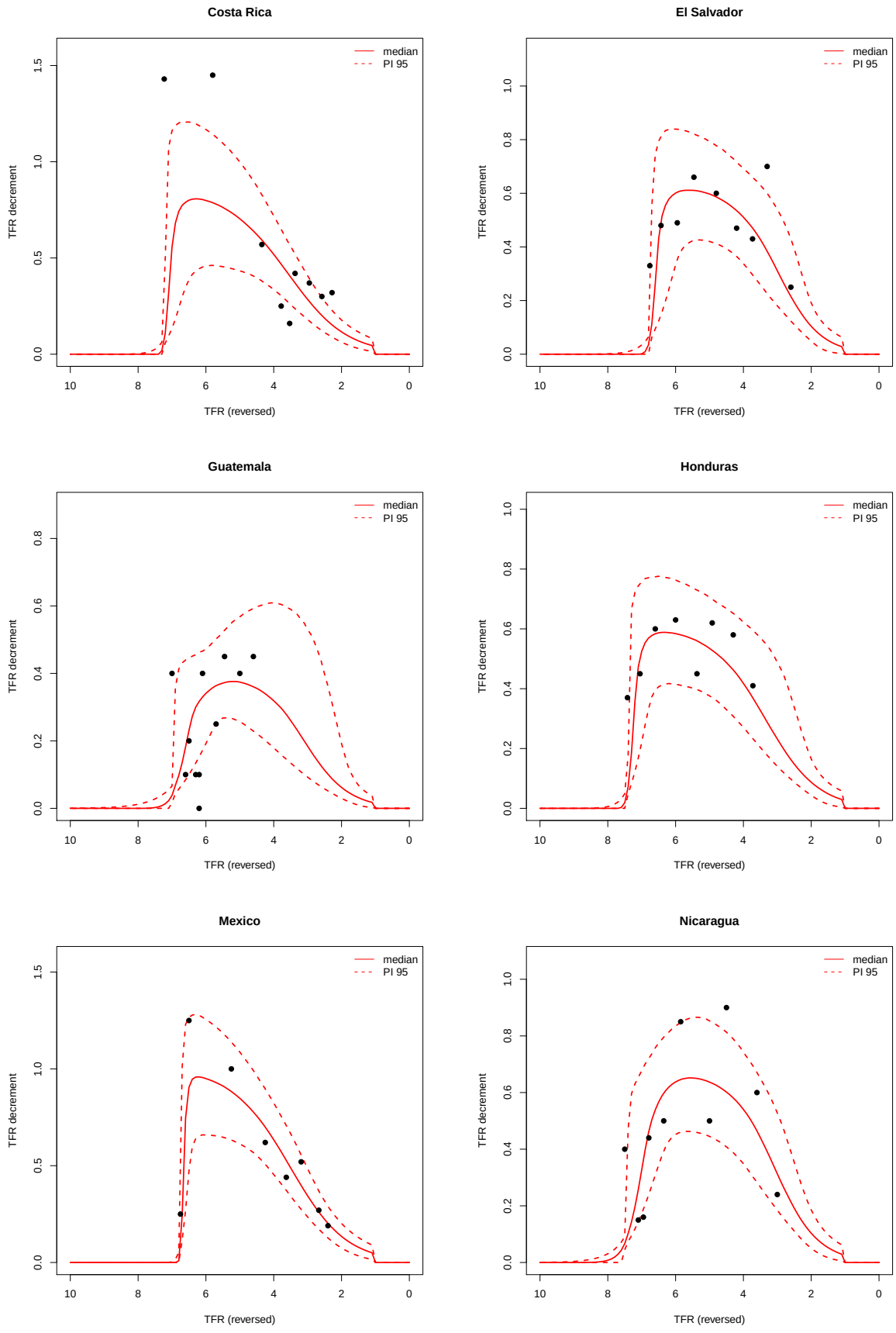

Figure 86: 95% Confidence and prediction intervals for the country-specific decline curves (red). The black dots are the observed decrements

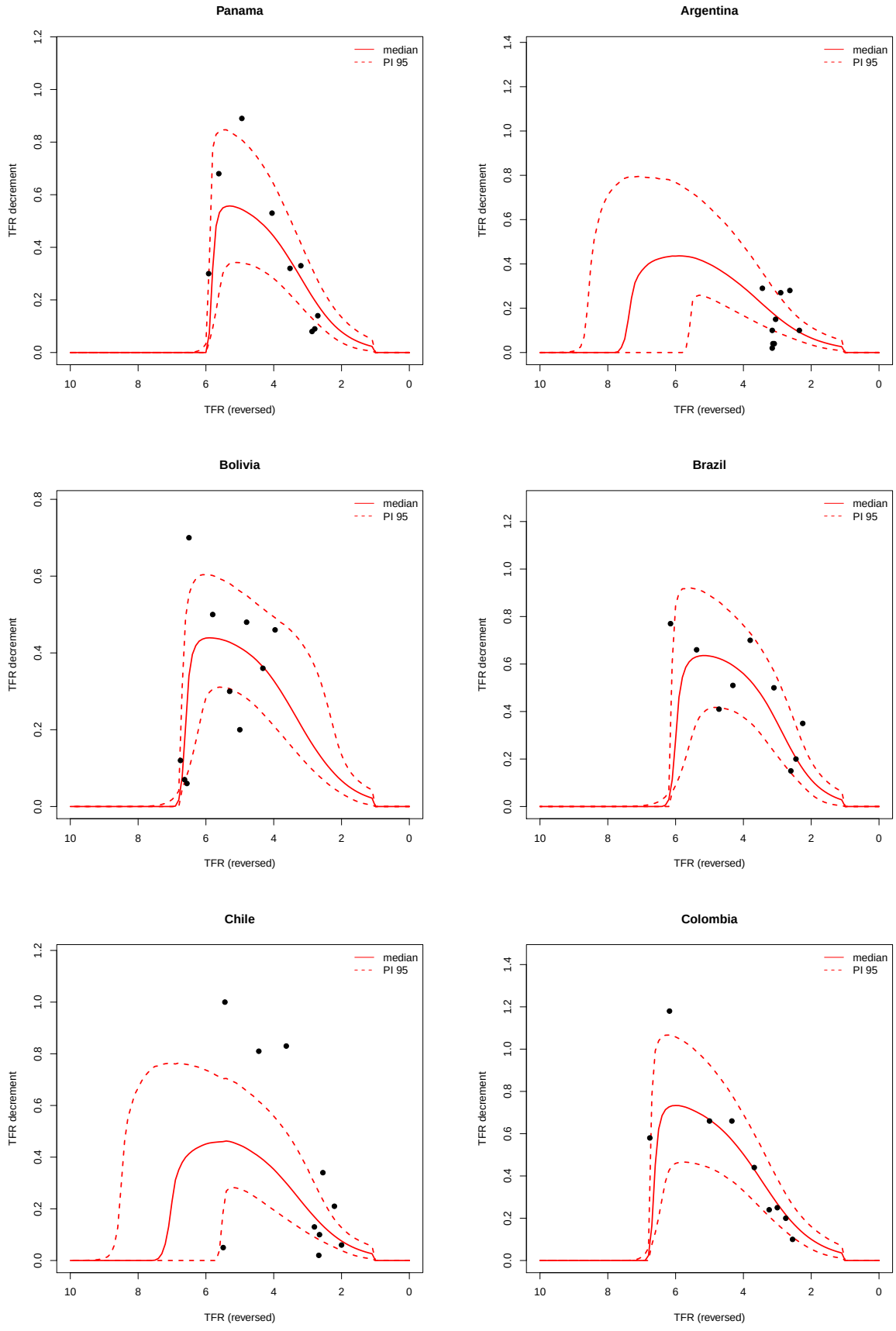

Figure 87: 95% Confidence and prediction intervals for the country-specific decline curves (red). The black dots are the observed decrements

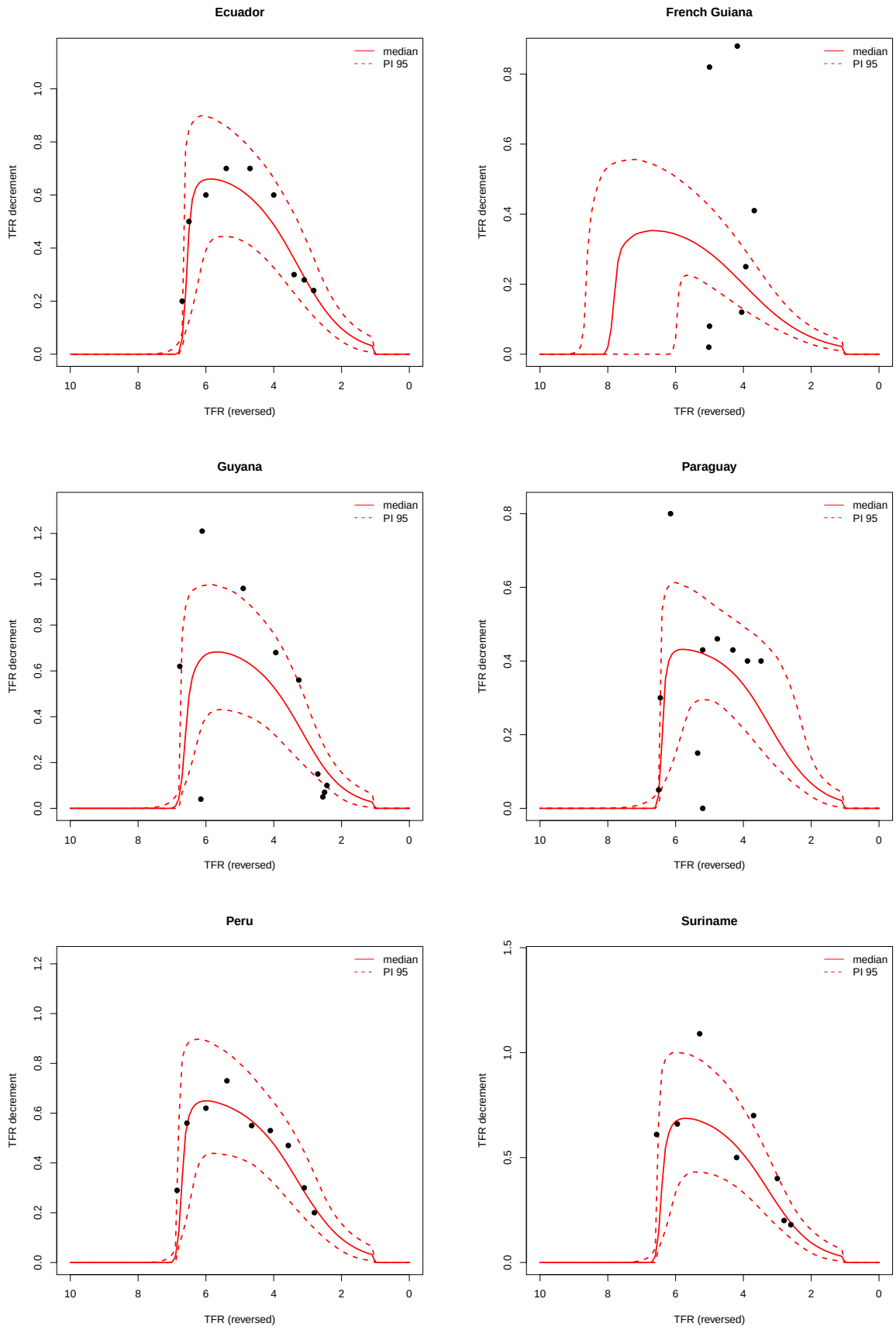

Figure 88: 95% Confidence and prediction intervals for the country-specific decline curves (red). The black dots are the observed decrements

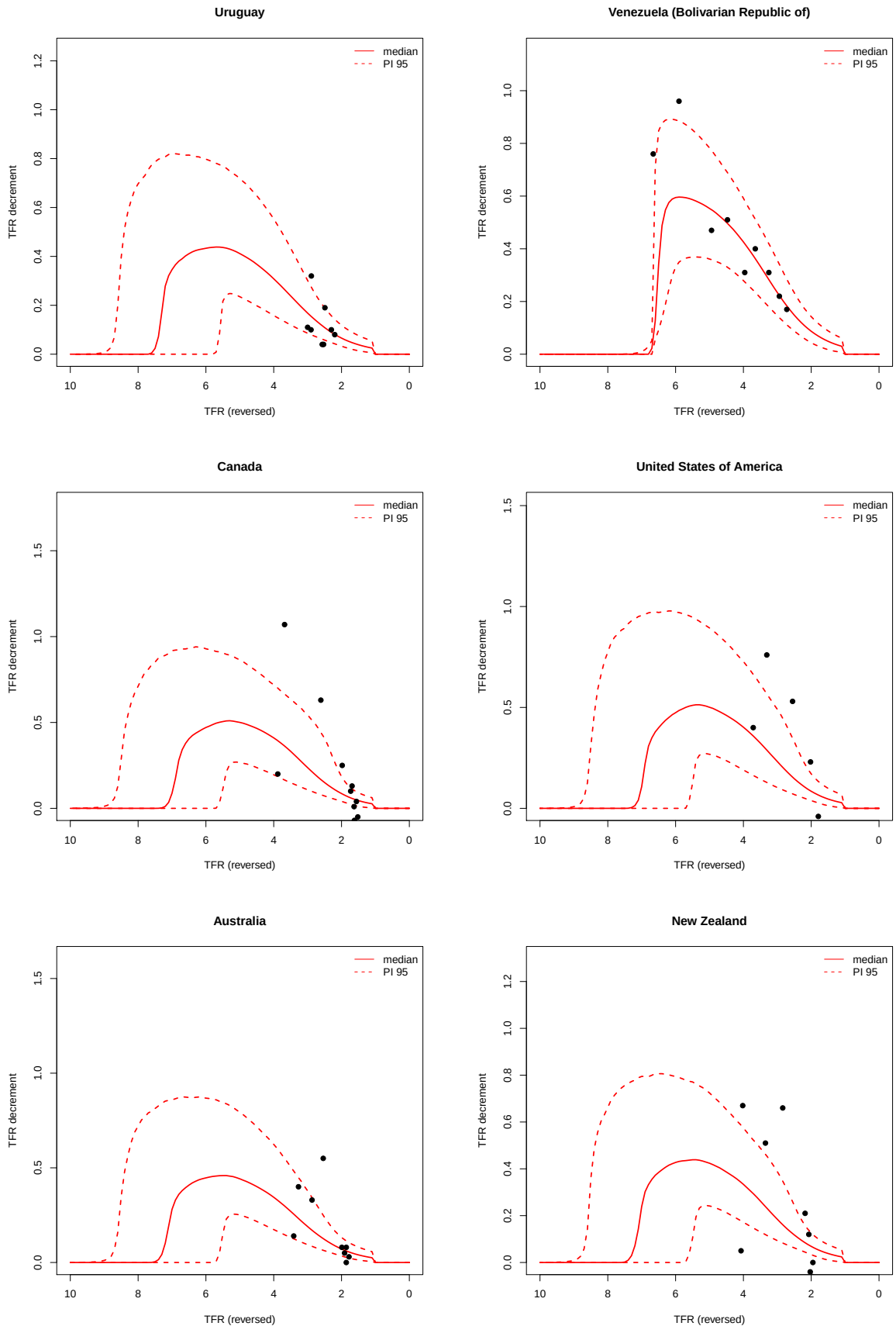

Figure 89: 95% Confidence and prediction intervals for the country-specific decline curves (red). The black dots are the observed decrements

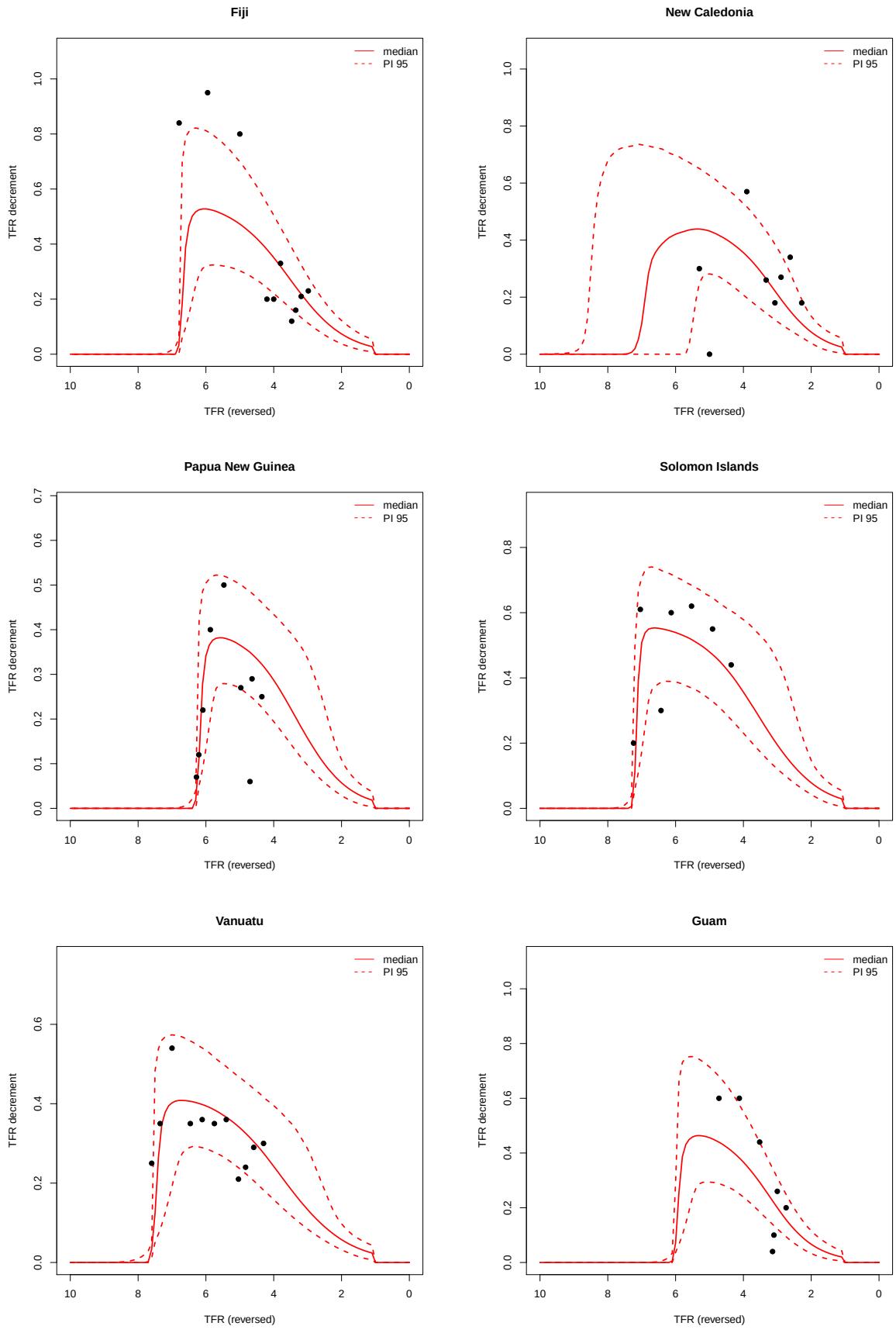

Figure 90: 95% Confidence and prediction intervals for the country-specific decline curves (red). The black dots are the observed decrements

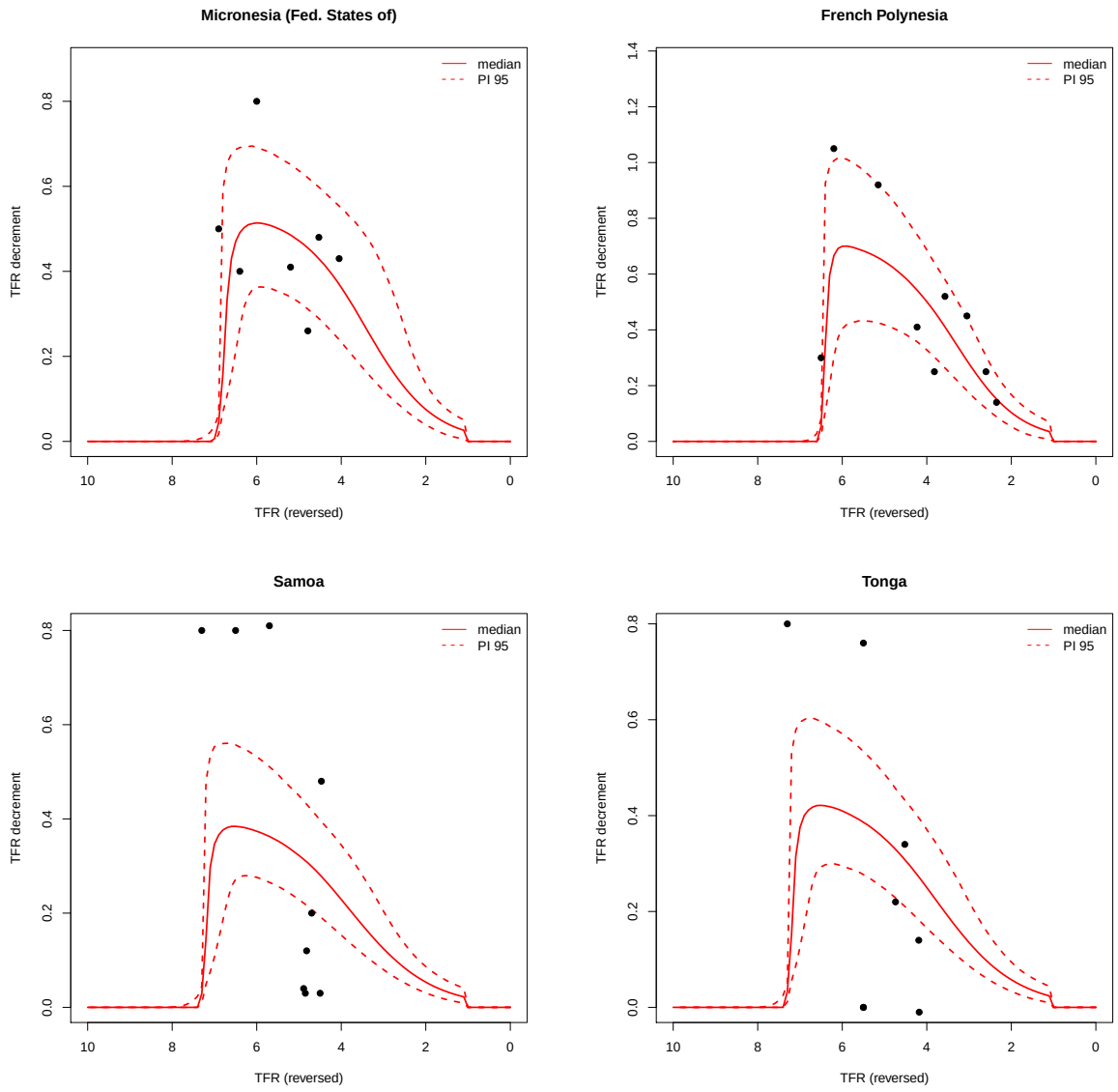

Figure 91: 95% Confidence and prediction intervals for the country-specific decline curves (red). The black dots are the observed decrements

9.3 Plots: Out-of-sample in 1980

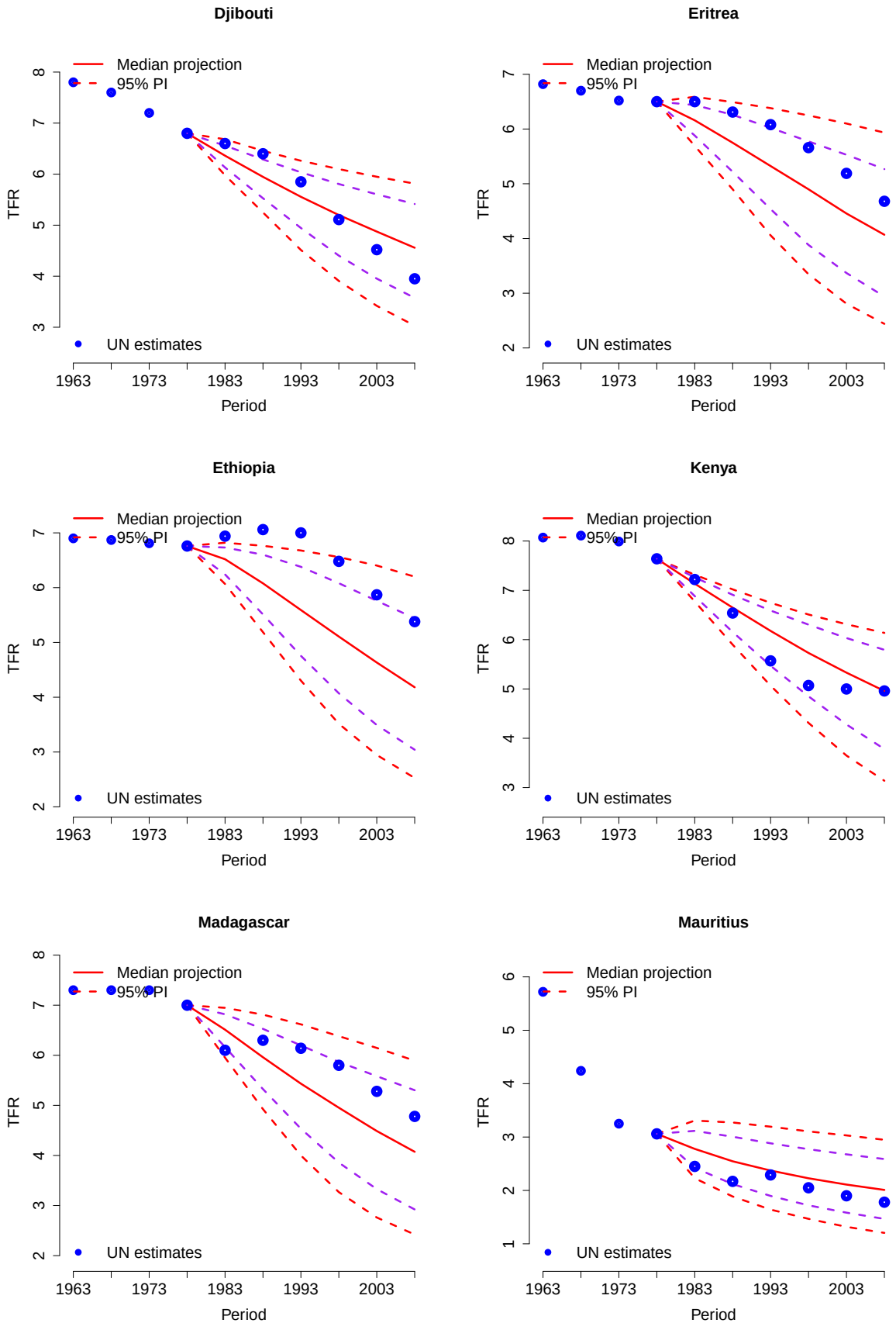

Figure 92: Out-of-sample in 1980

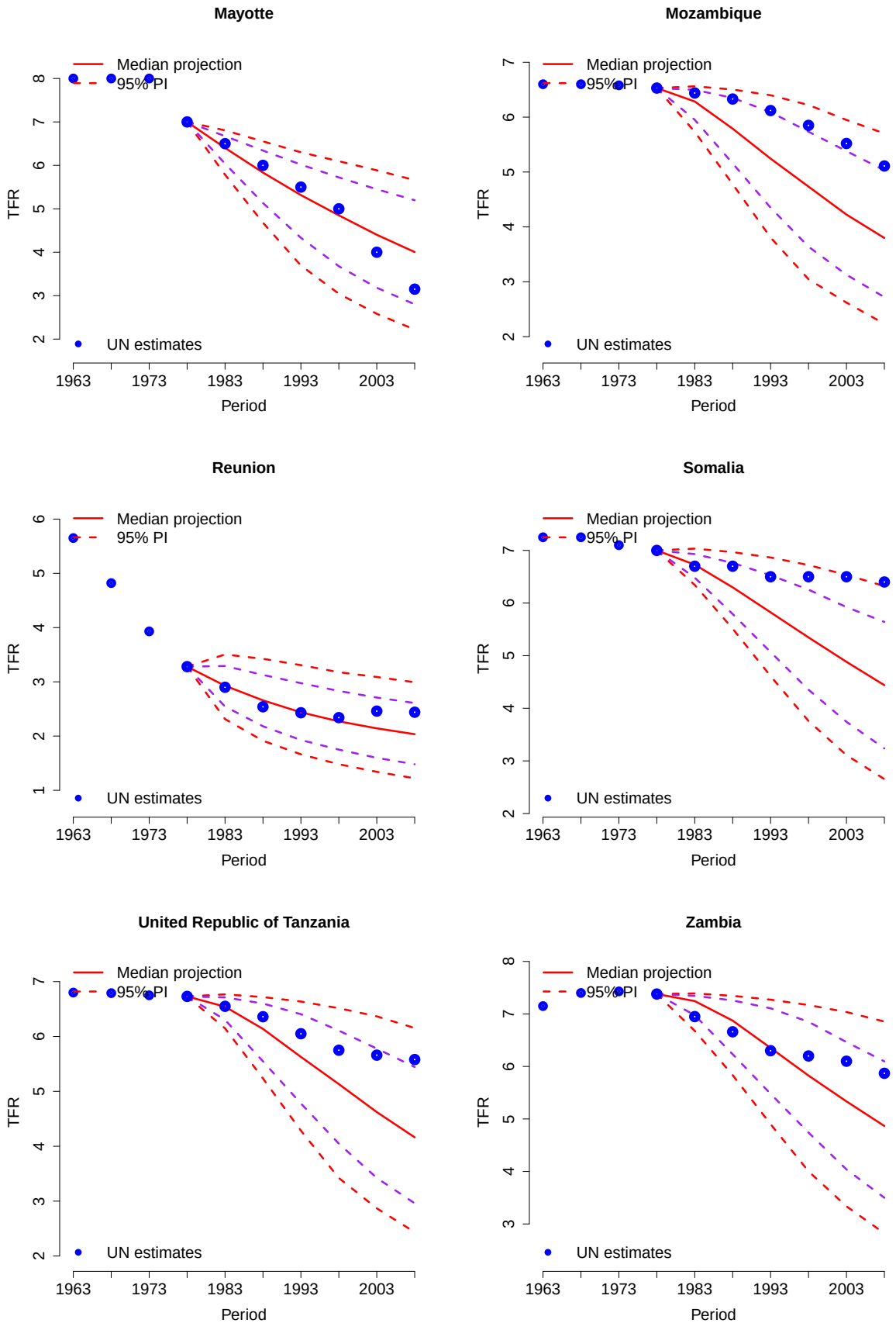

Figure 93: Out-of-sample in 1980

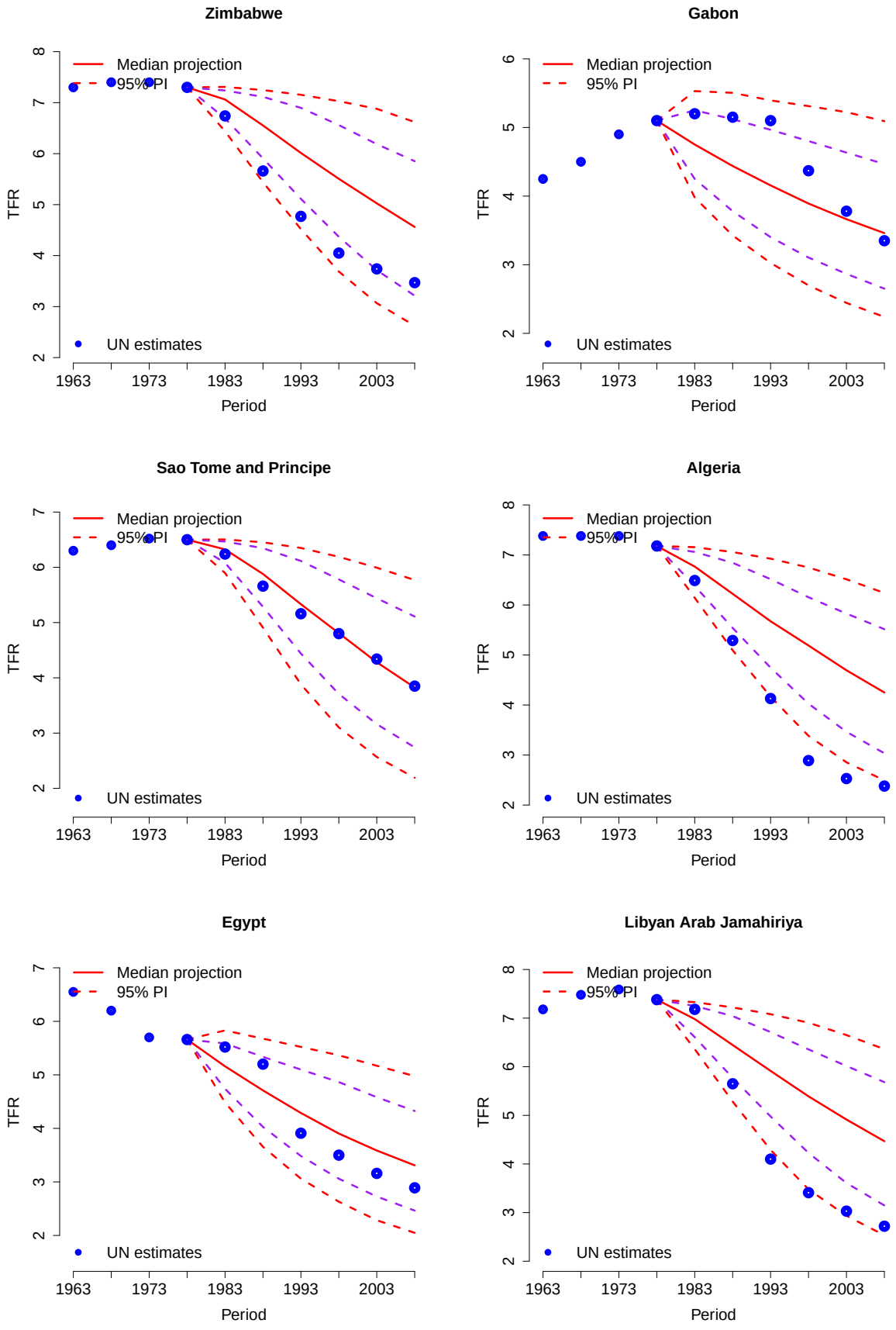

Figure 94: Out-of-sample in 1980

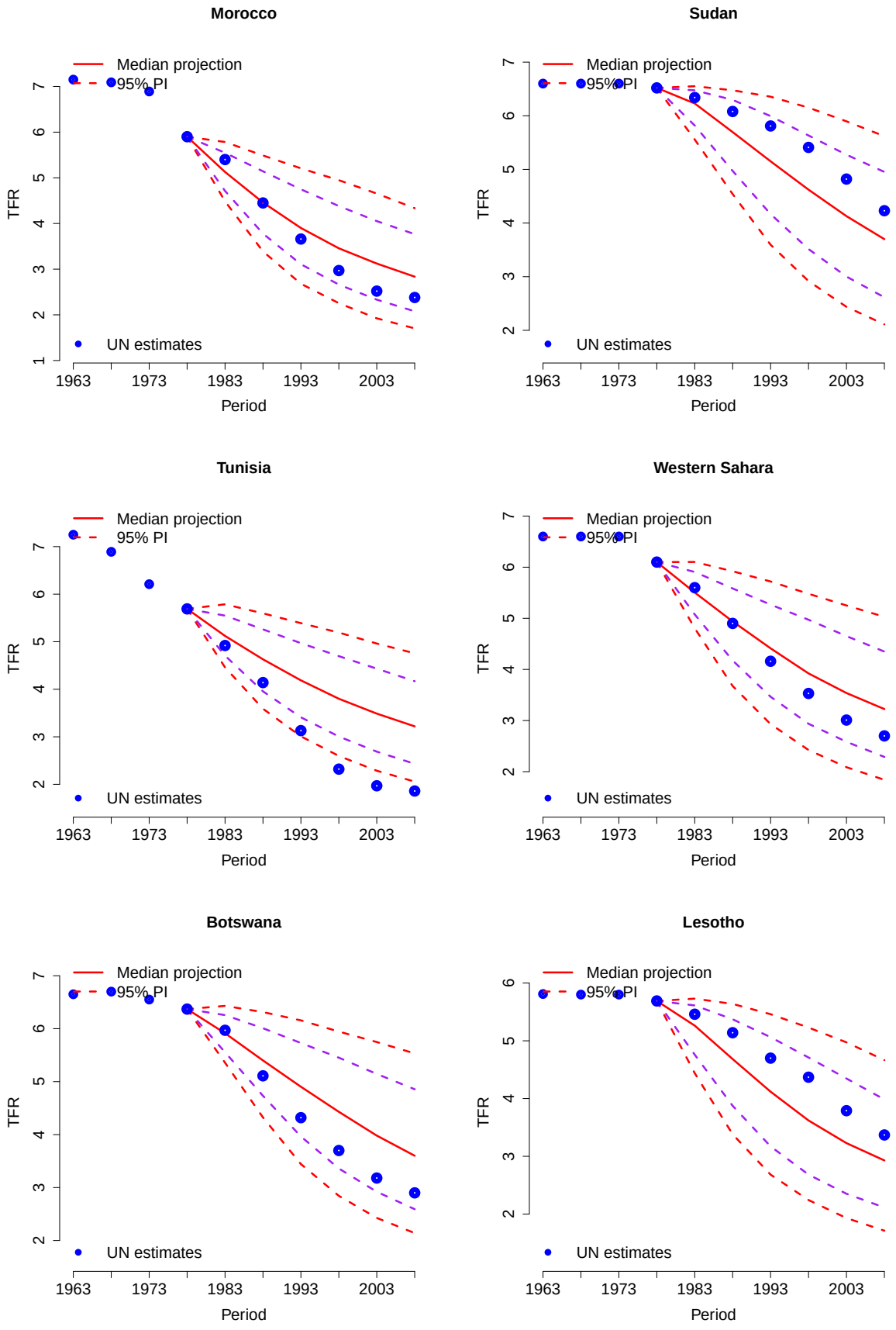

Figure 95: Out-of-sample in 1980

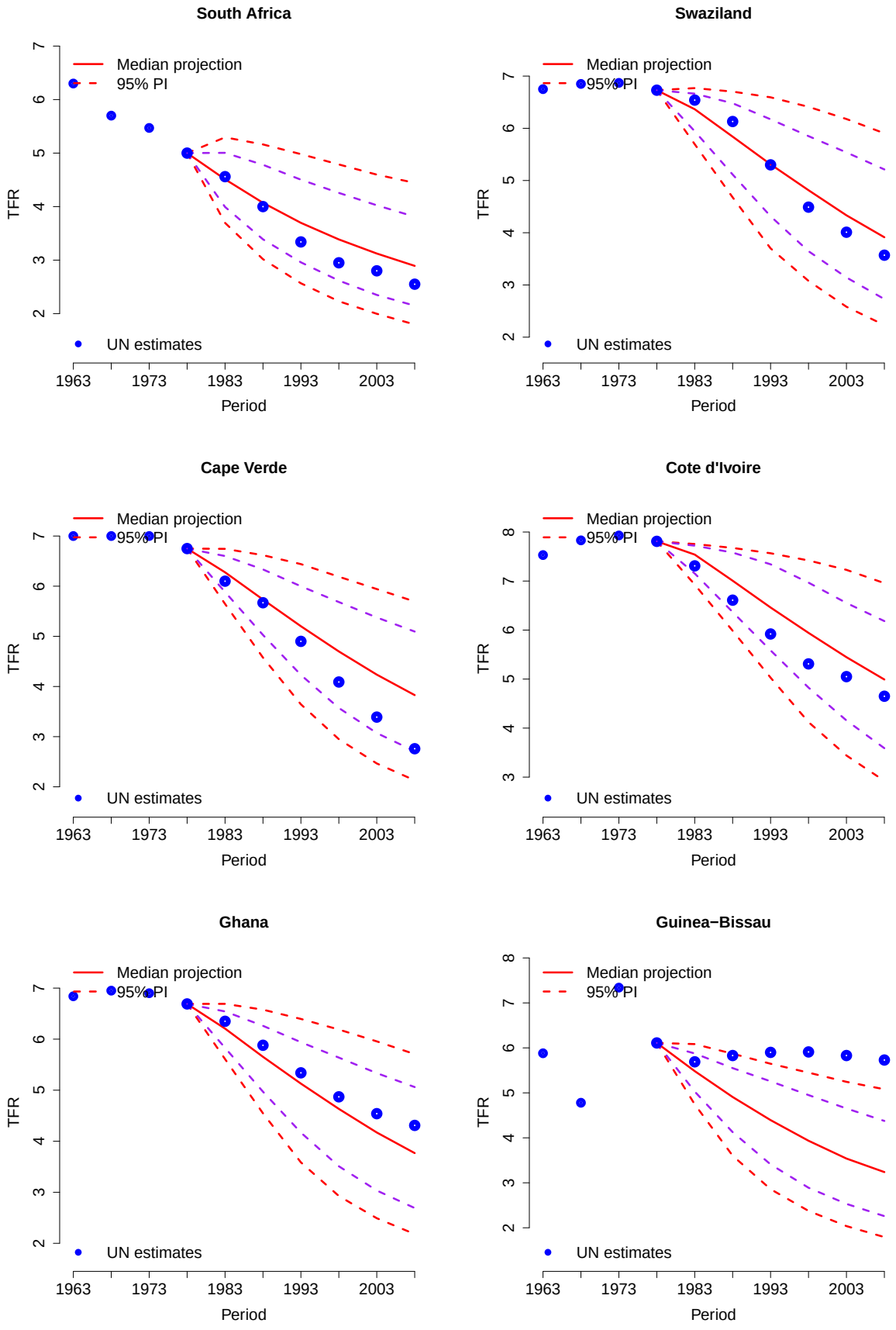

Figure 96: Out-of-sample in 1980

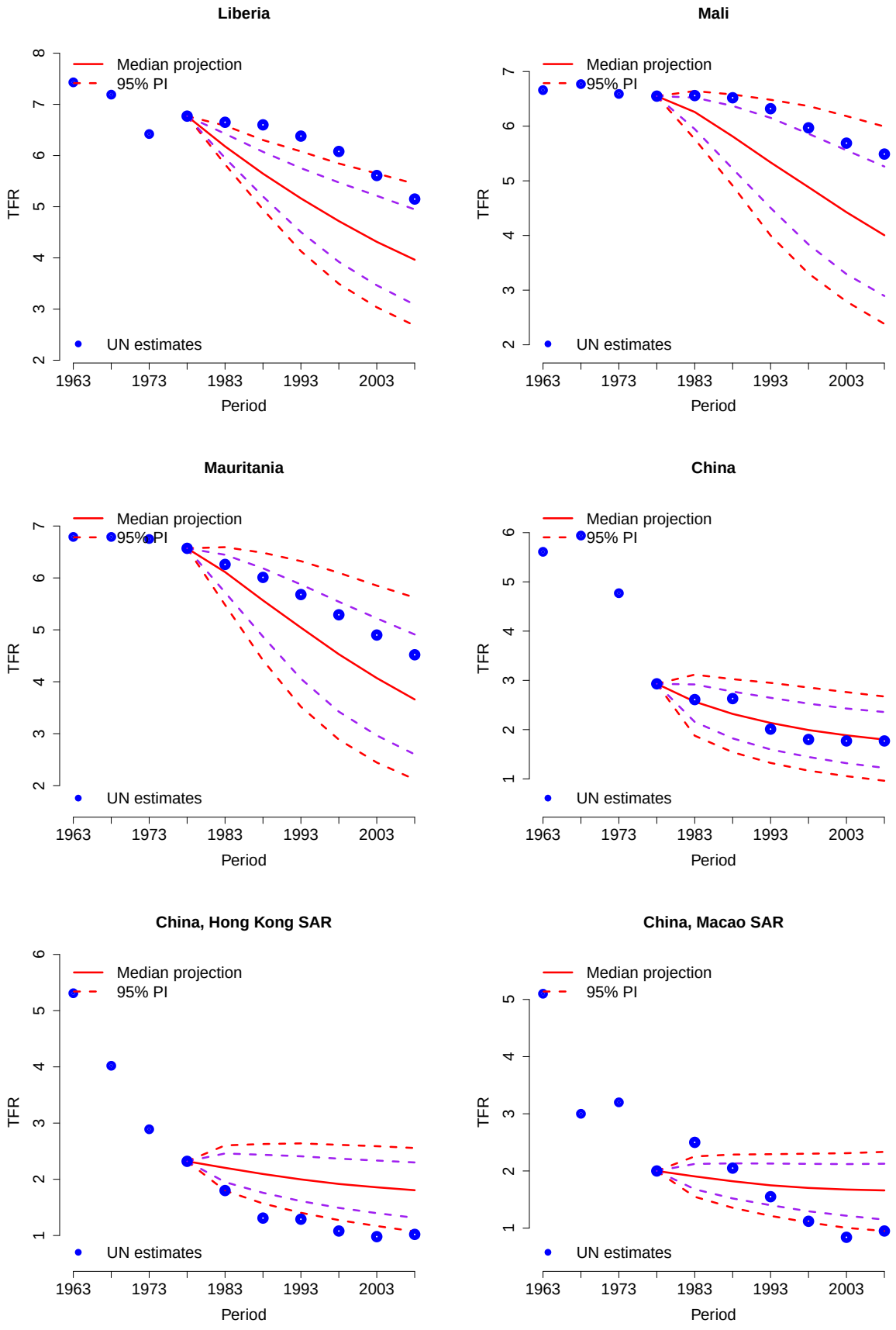

Figure 97: Out-of-sample in 1980

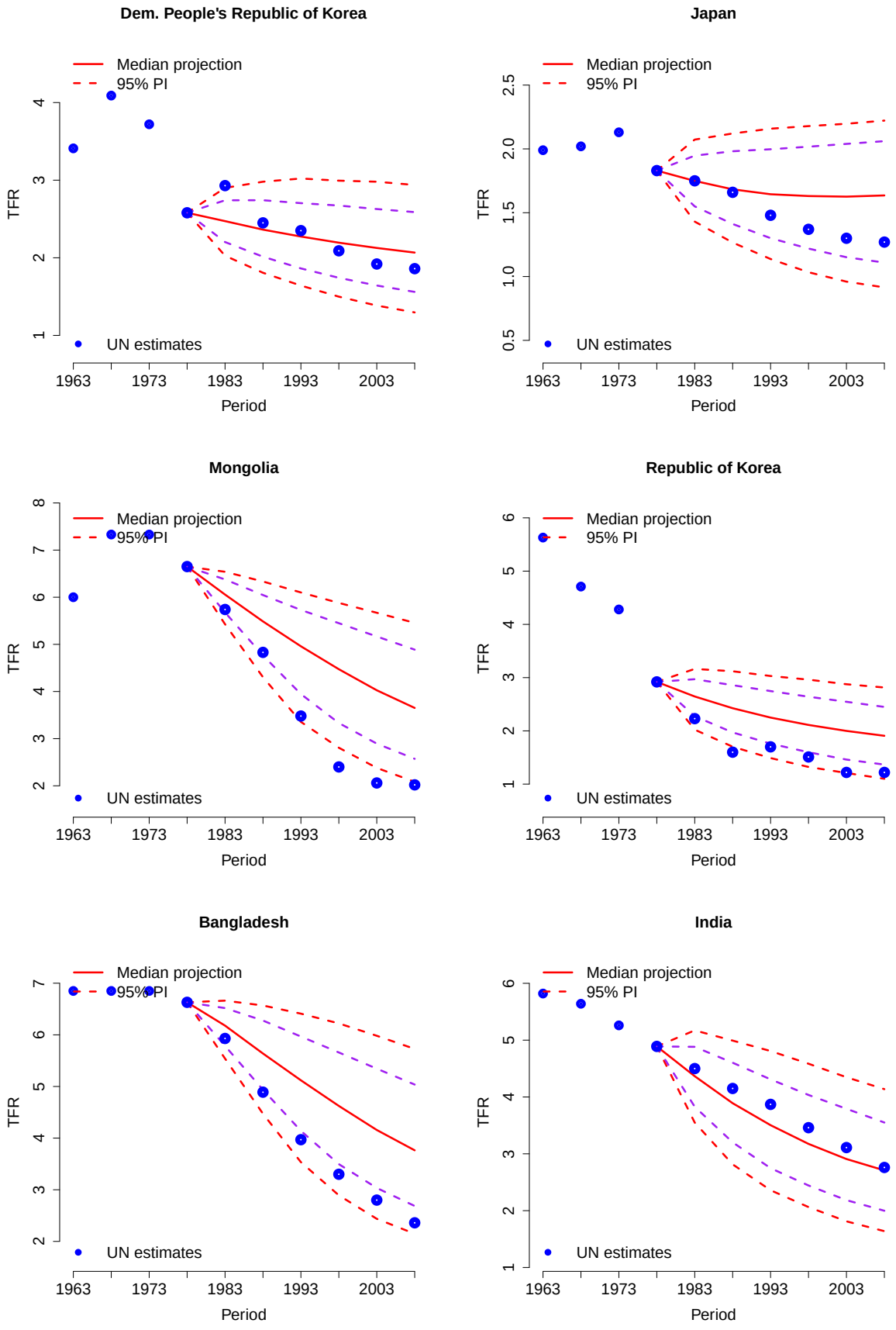

Figure 98: Out-of-sample in 1980

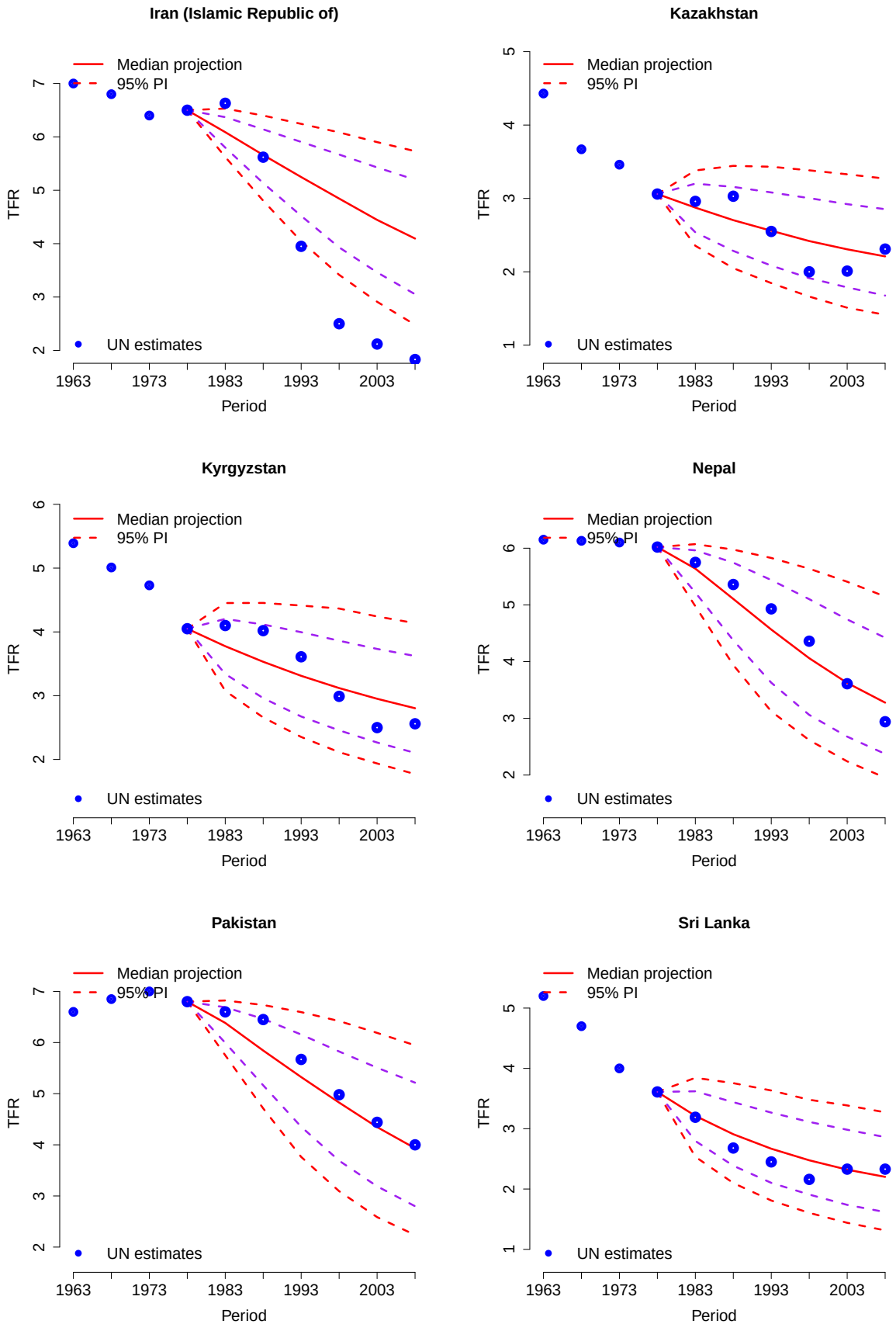

Figure 99: Out-of-sample in 1980

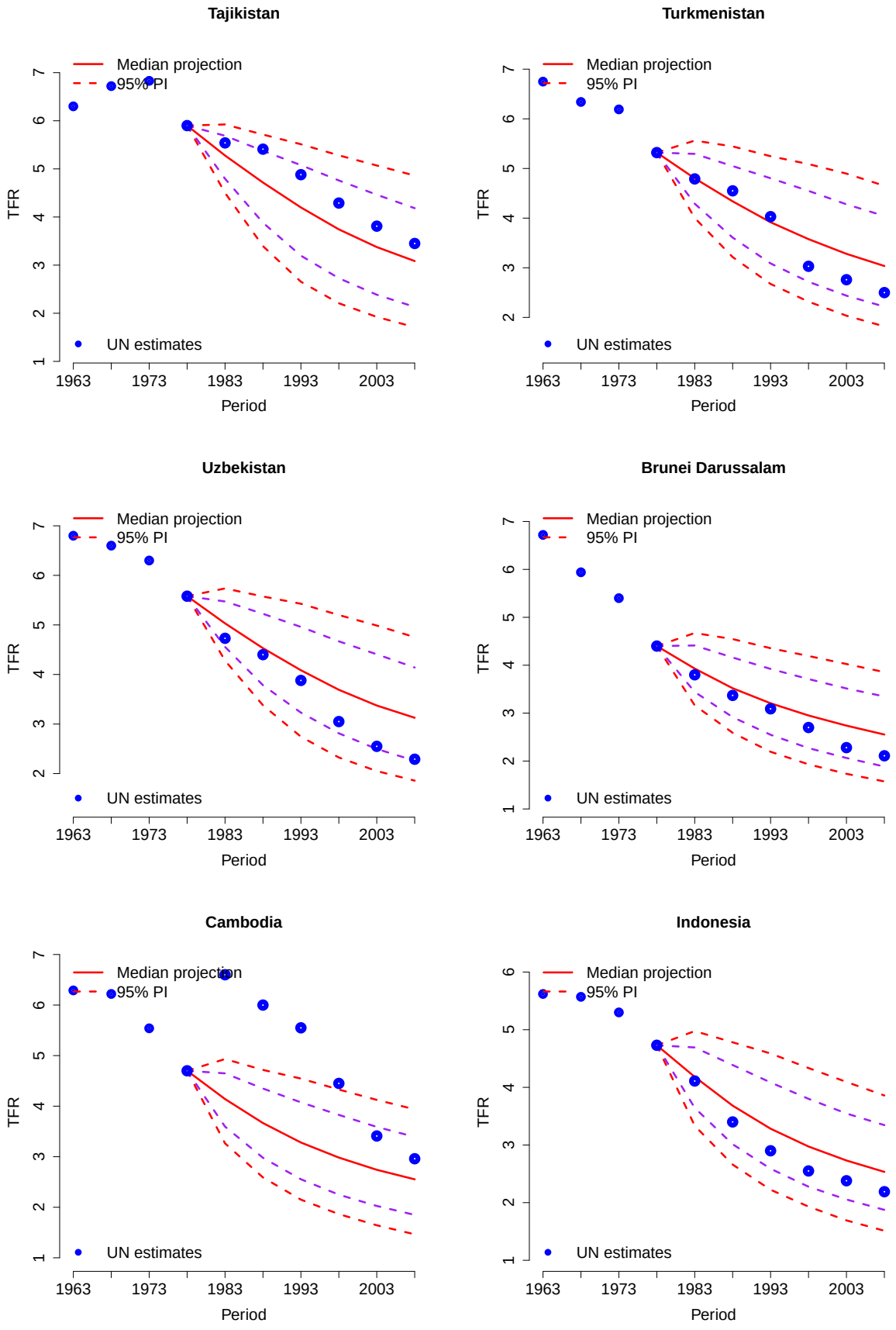

Figure 100: Out-of-sample in 1980

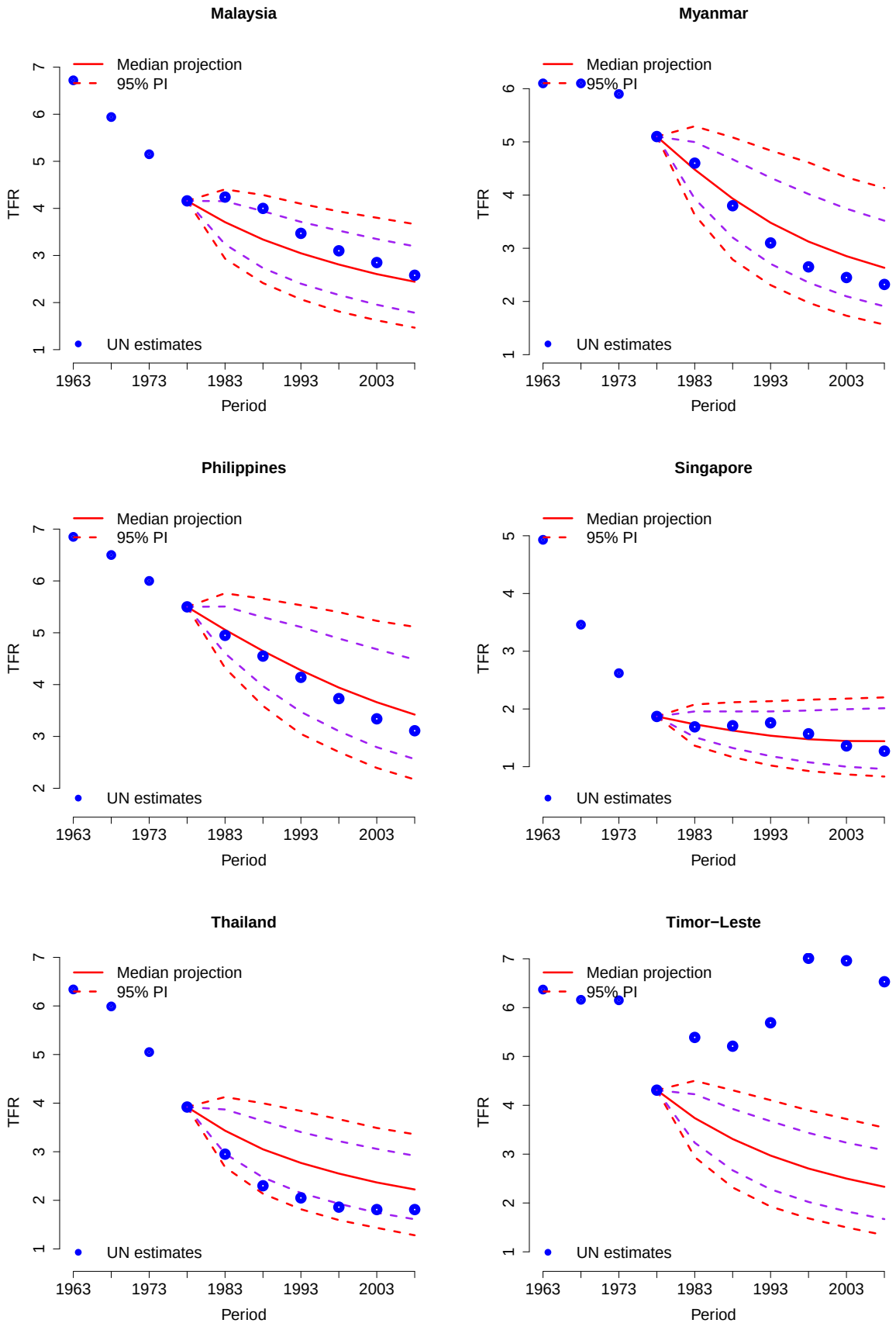

Figure 101: Out-of-sample in 1980

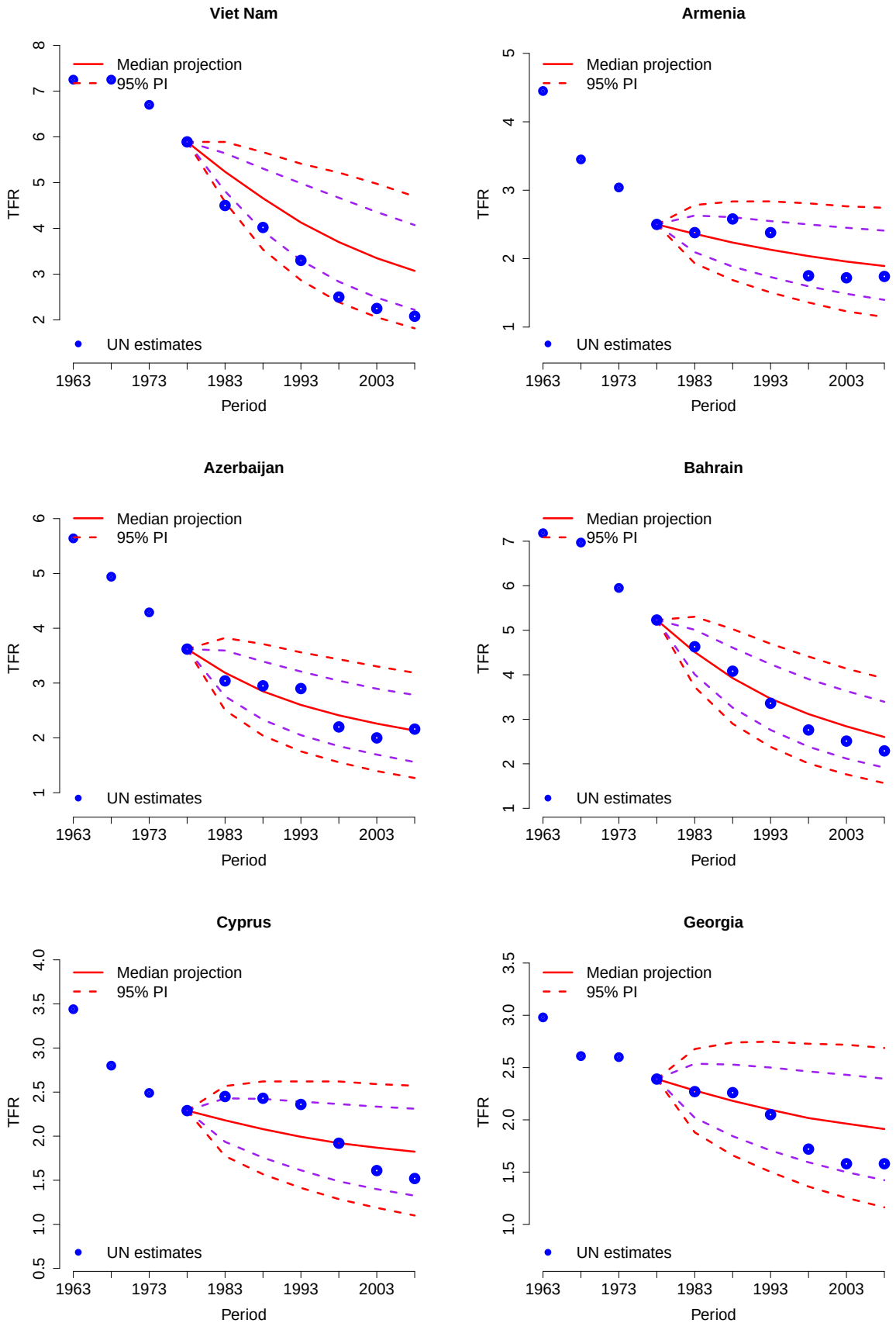

Figure 102: Out-of-sample in 1980

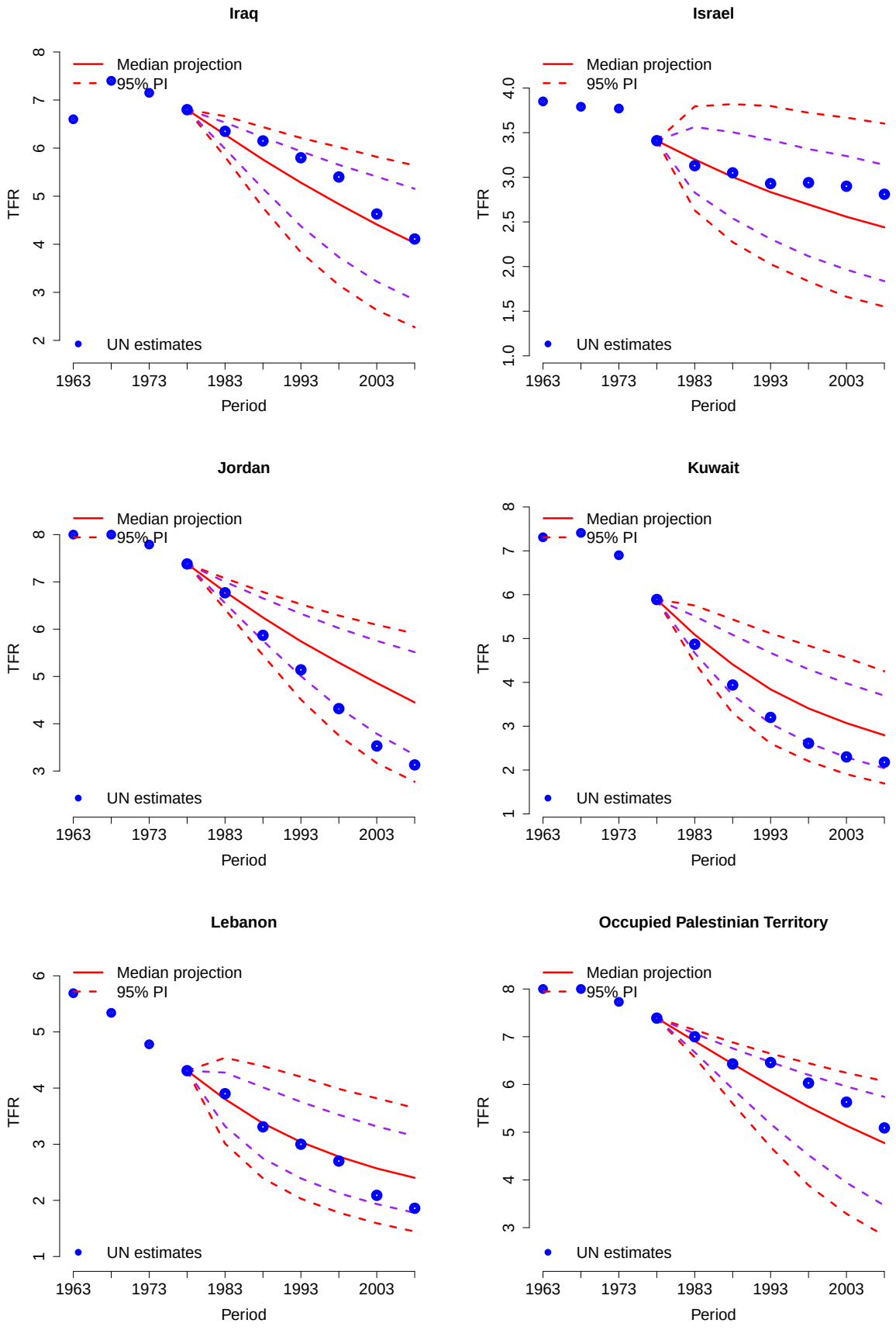

Figure 103: Out-of-sample in 1980

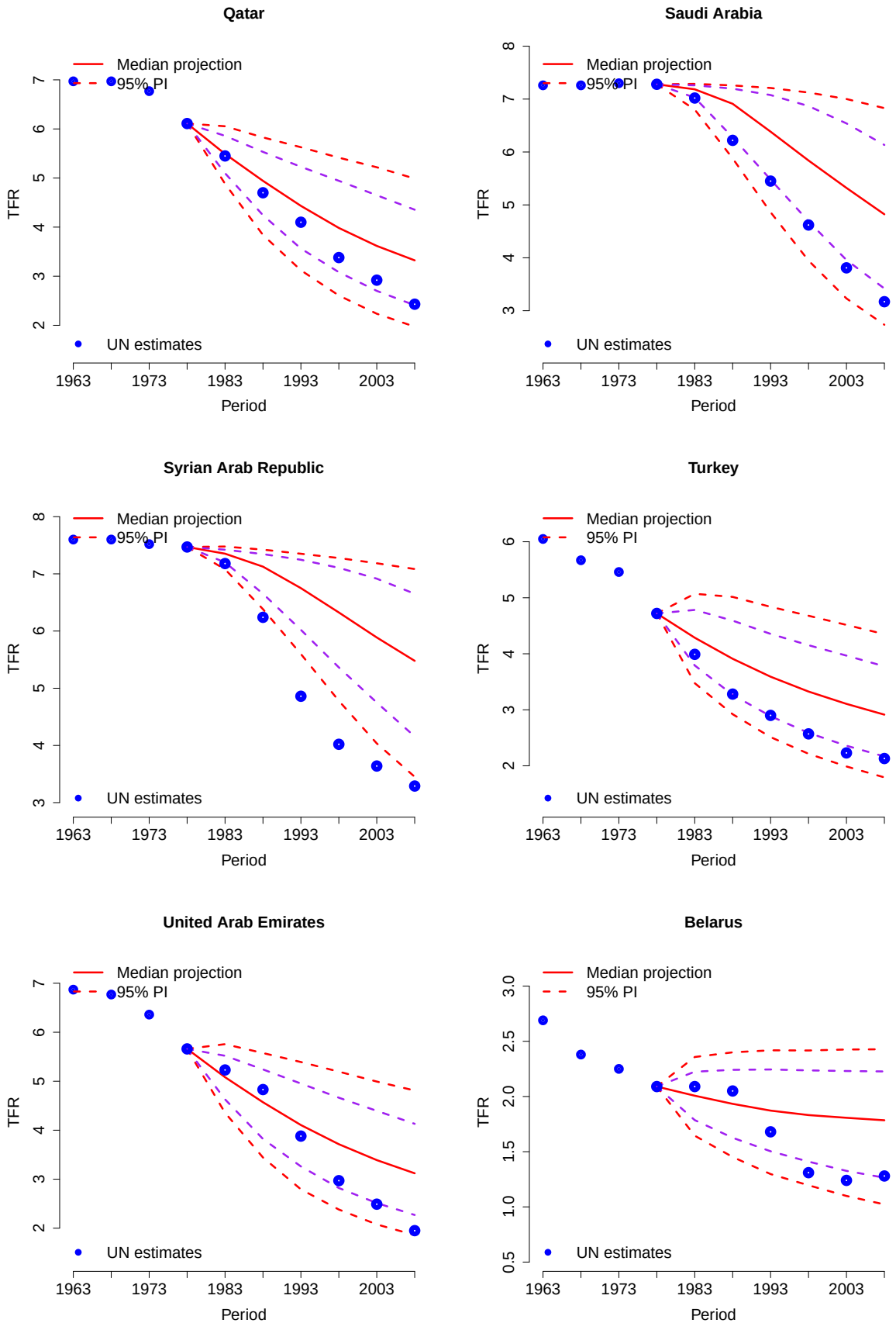

Figure 104: Out-of-sample in 1980

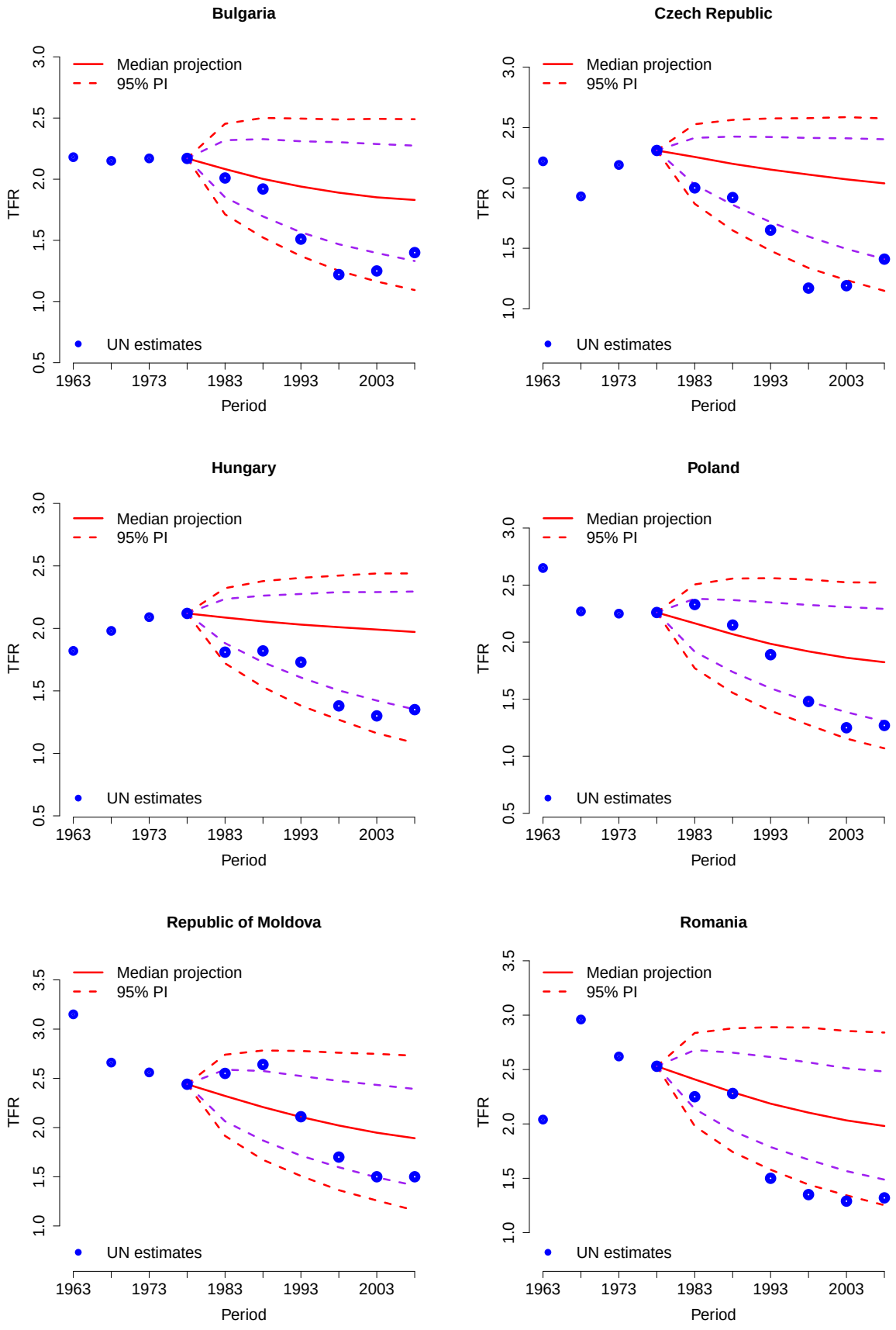

Figure 105: Out-of-sample in 1980

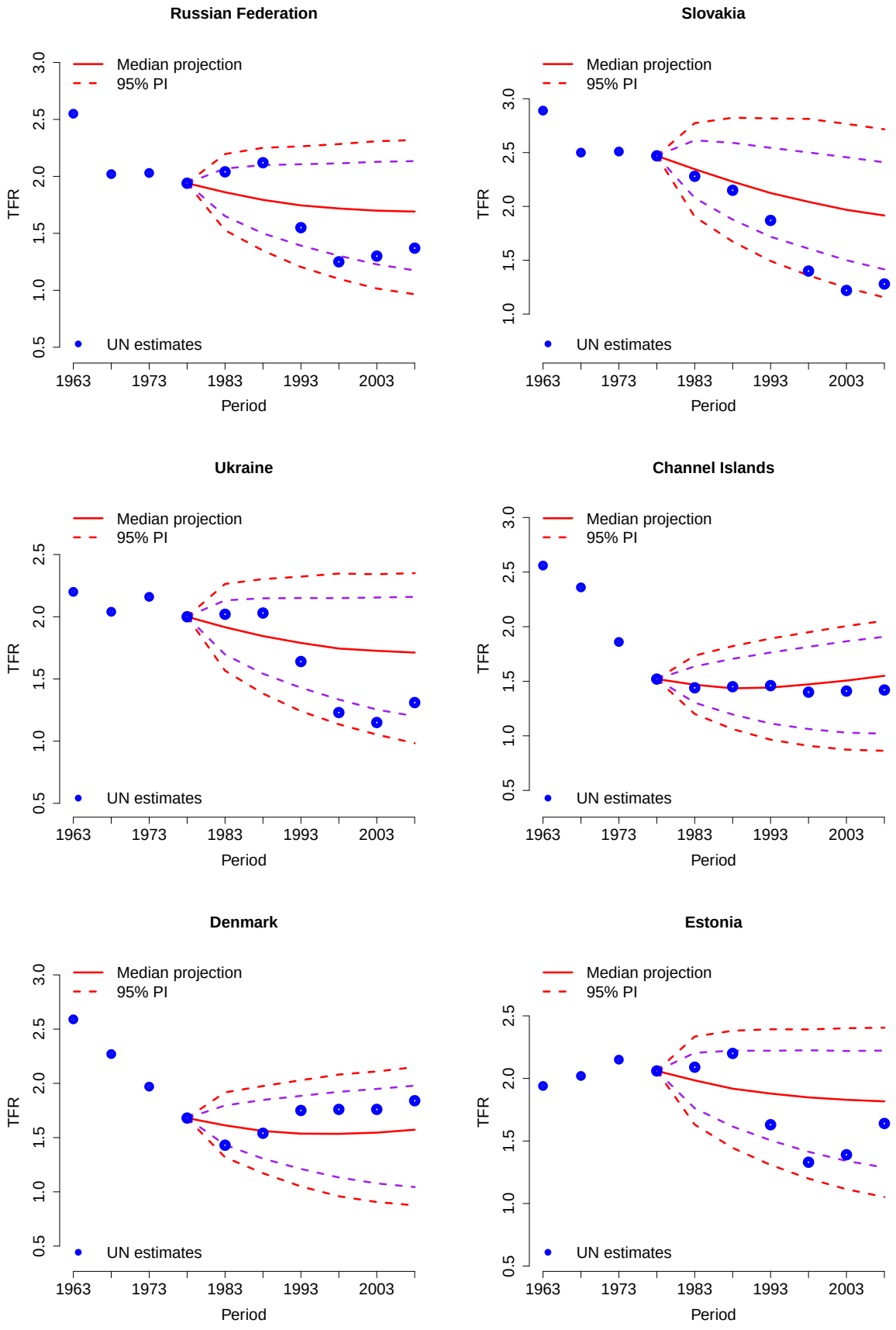

Figure 106: Out-of-sample in 1980

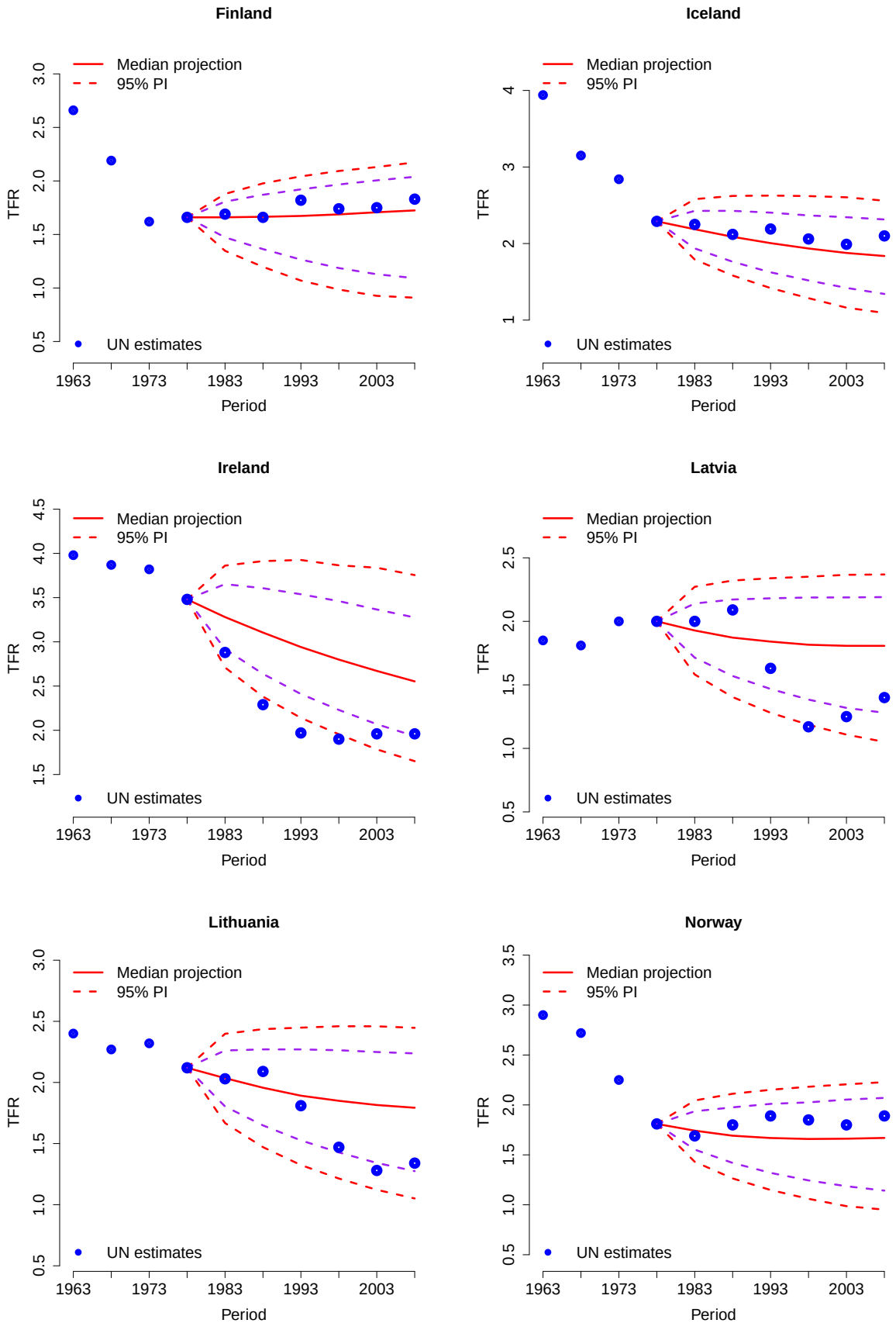

Figure 107: Out-of-sample in 1980

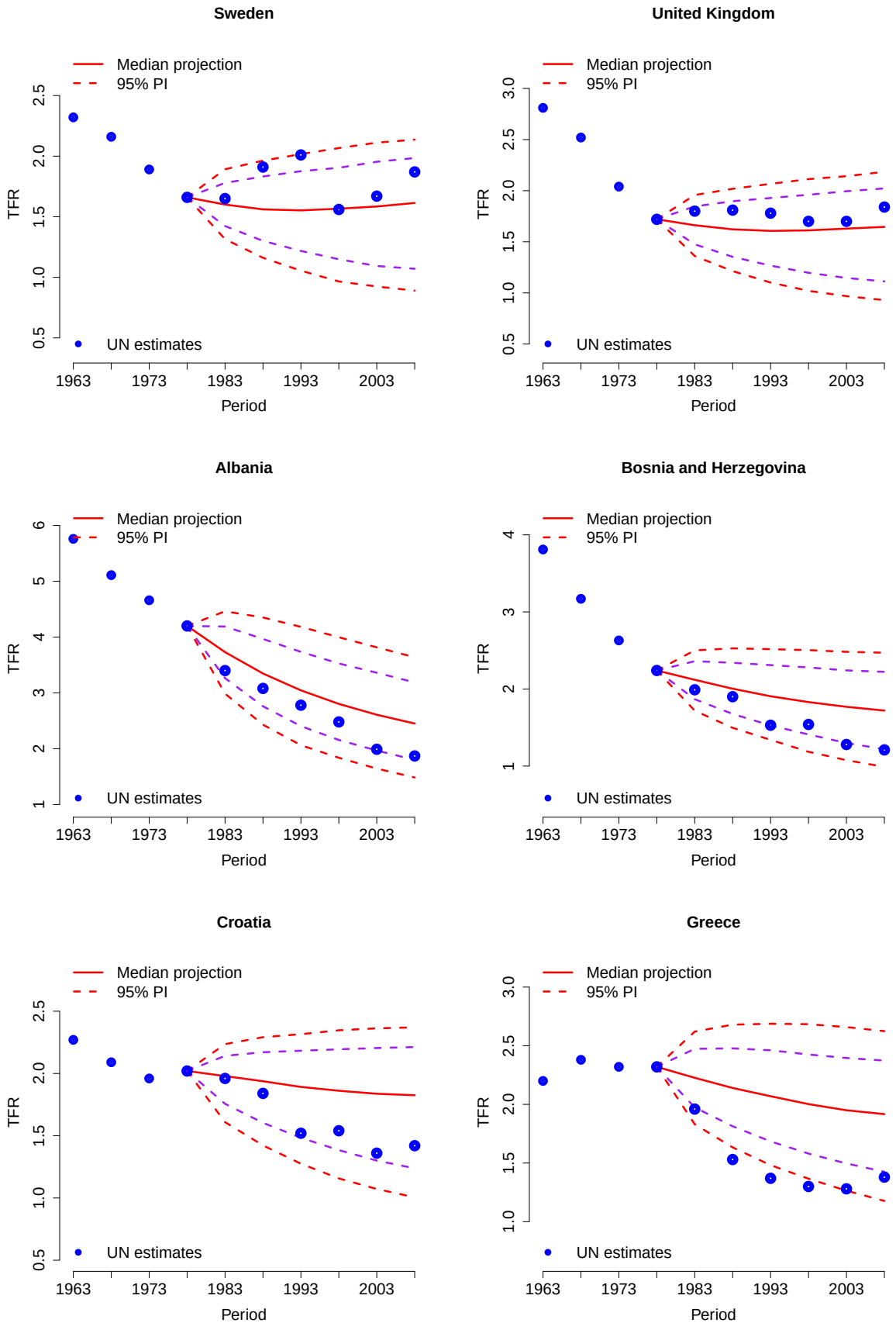

Figure 108: Out-of-sample in 1980

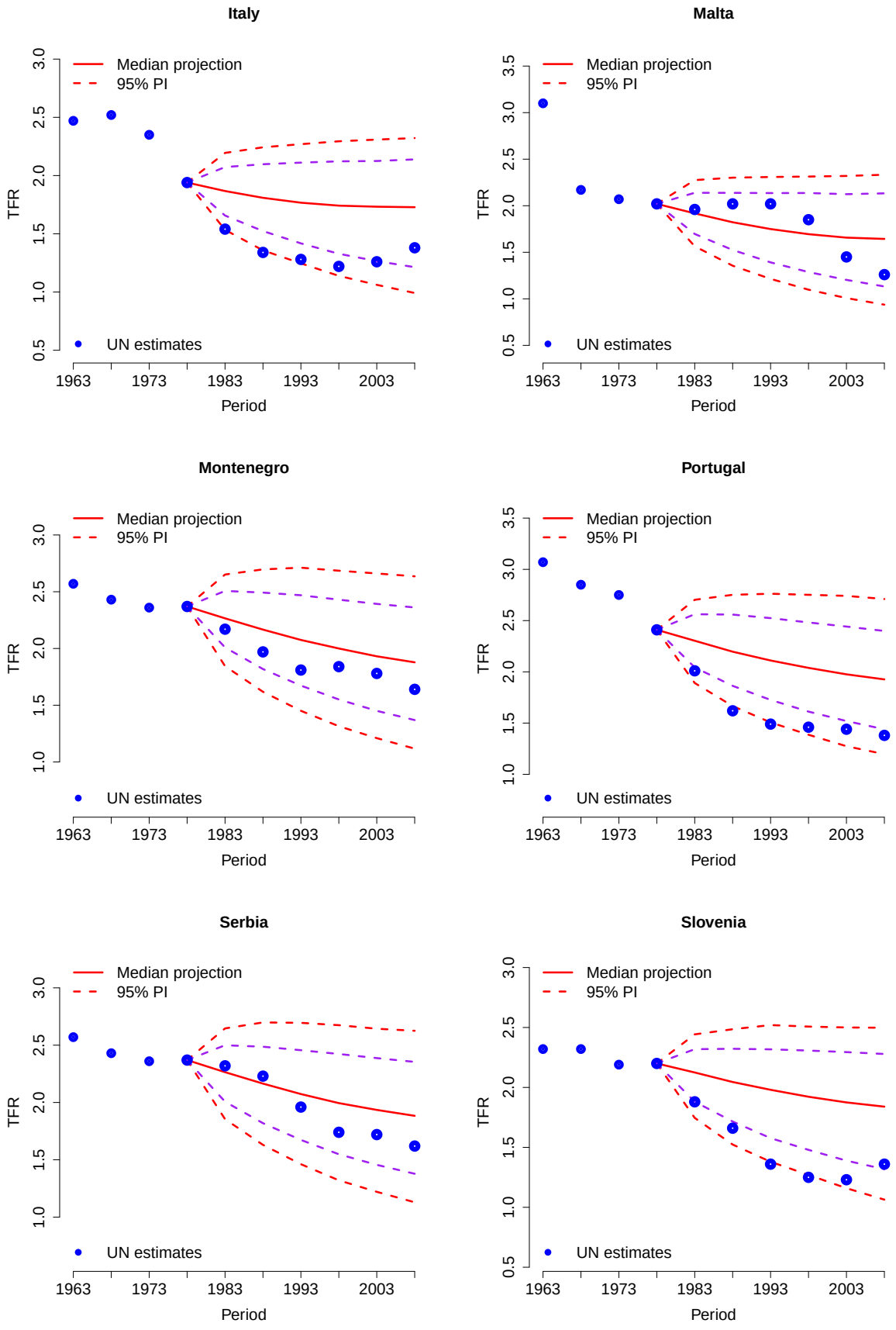

Figure 109: Out-of-sample in 1980

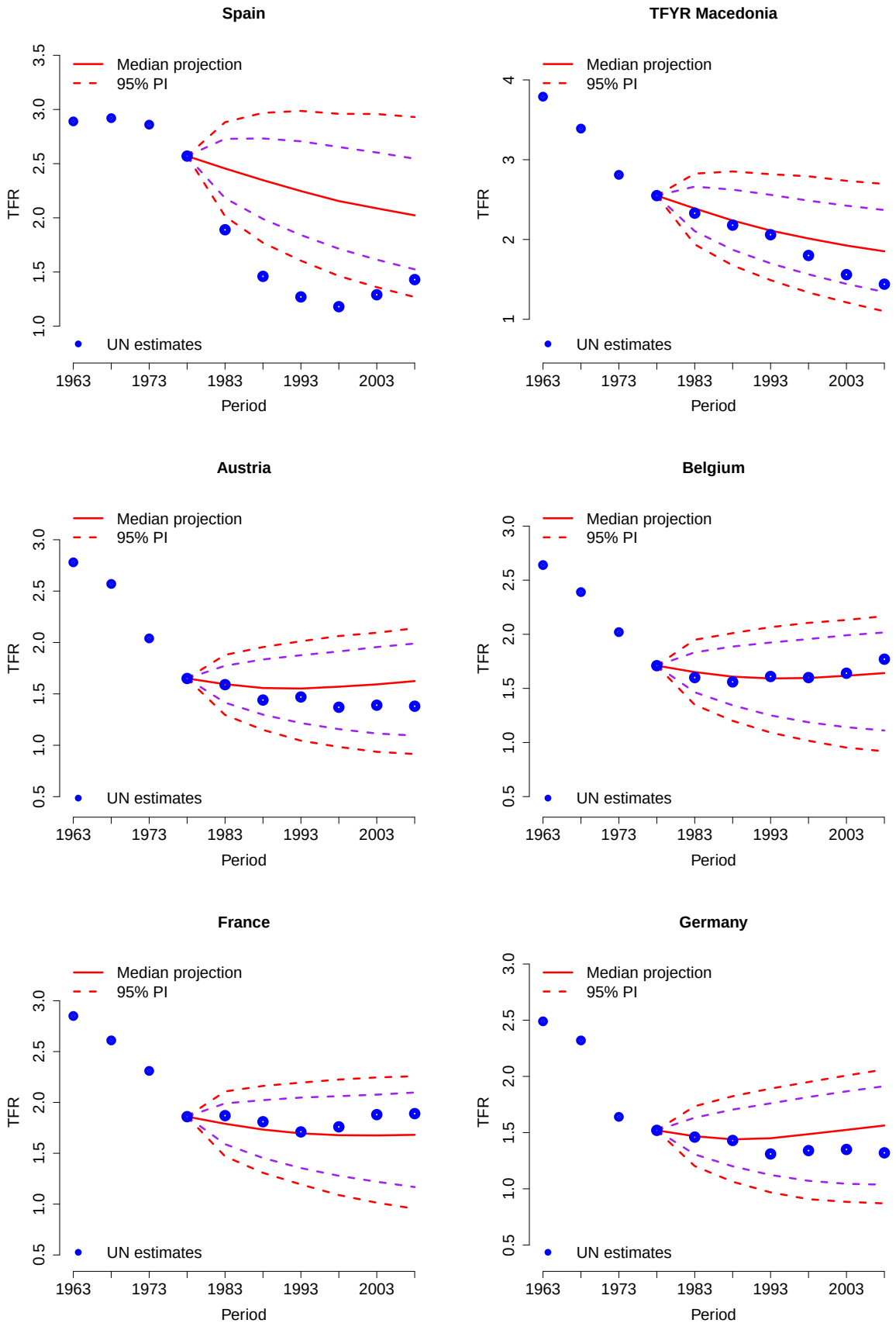

Figure 110: Out-of-sample in 1980

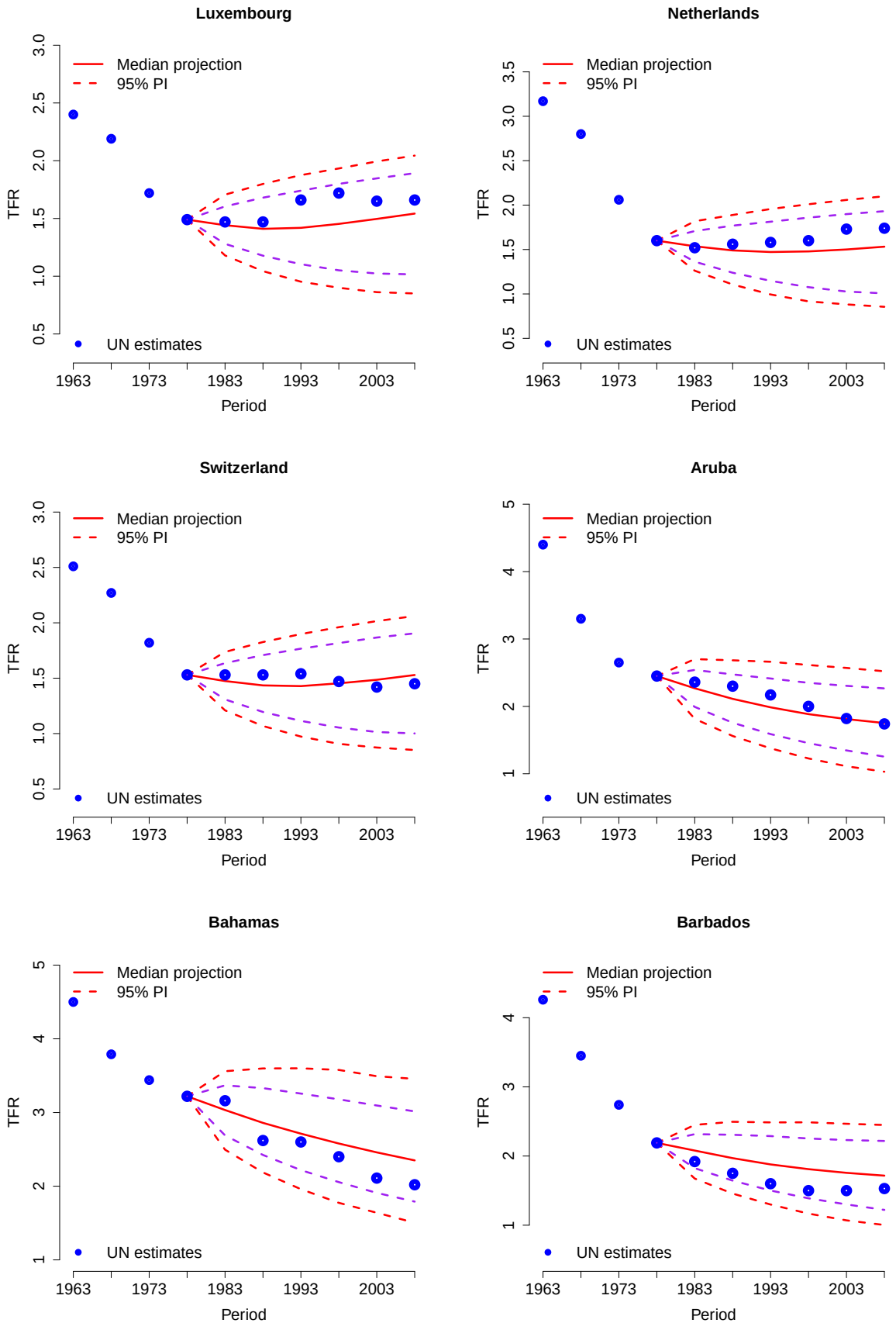

Figure 111: Out-of-sample in 1980

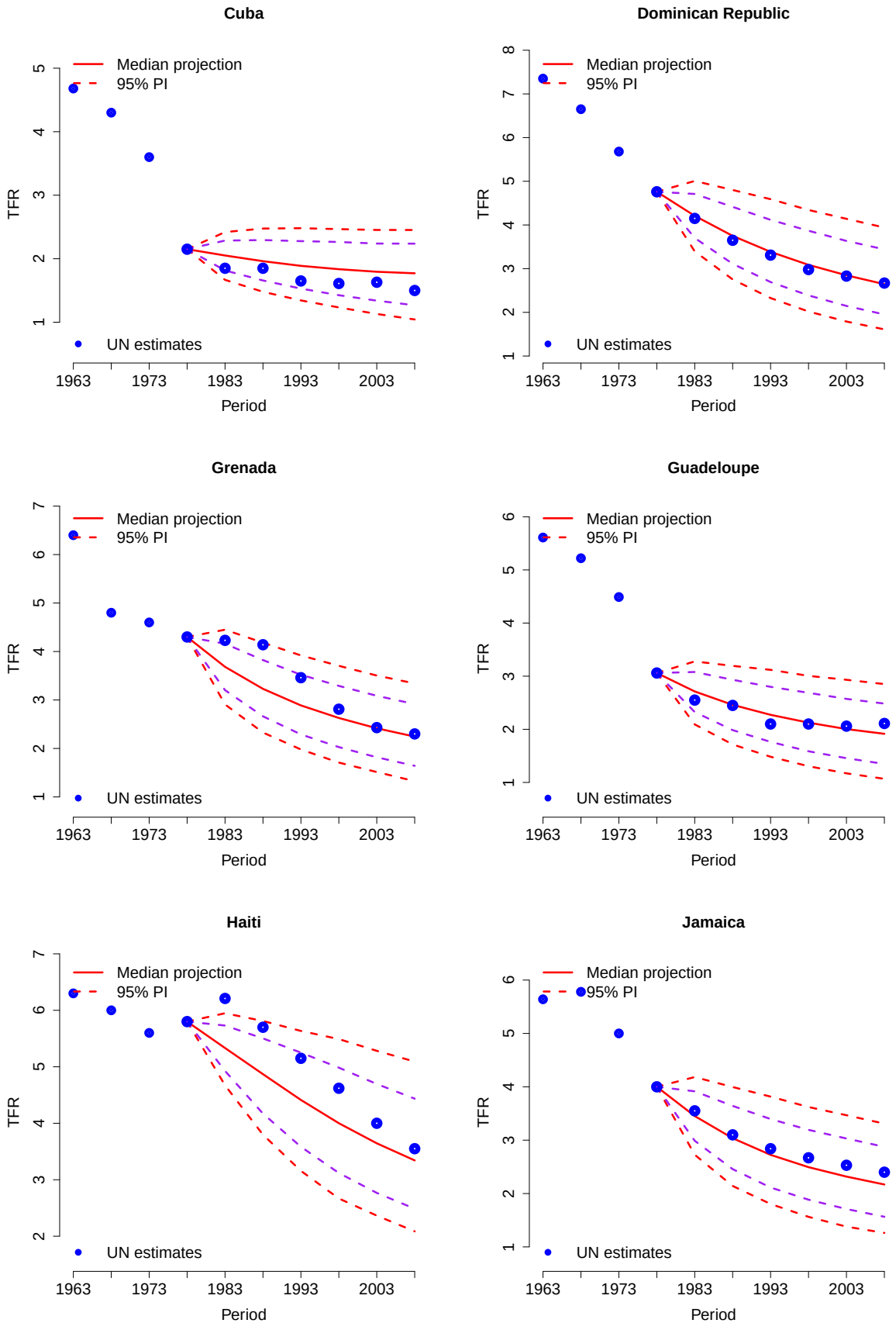

Figure 112: Out-of-sample in 1980

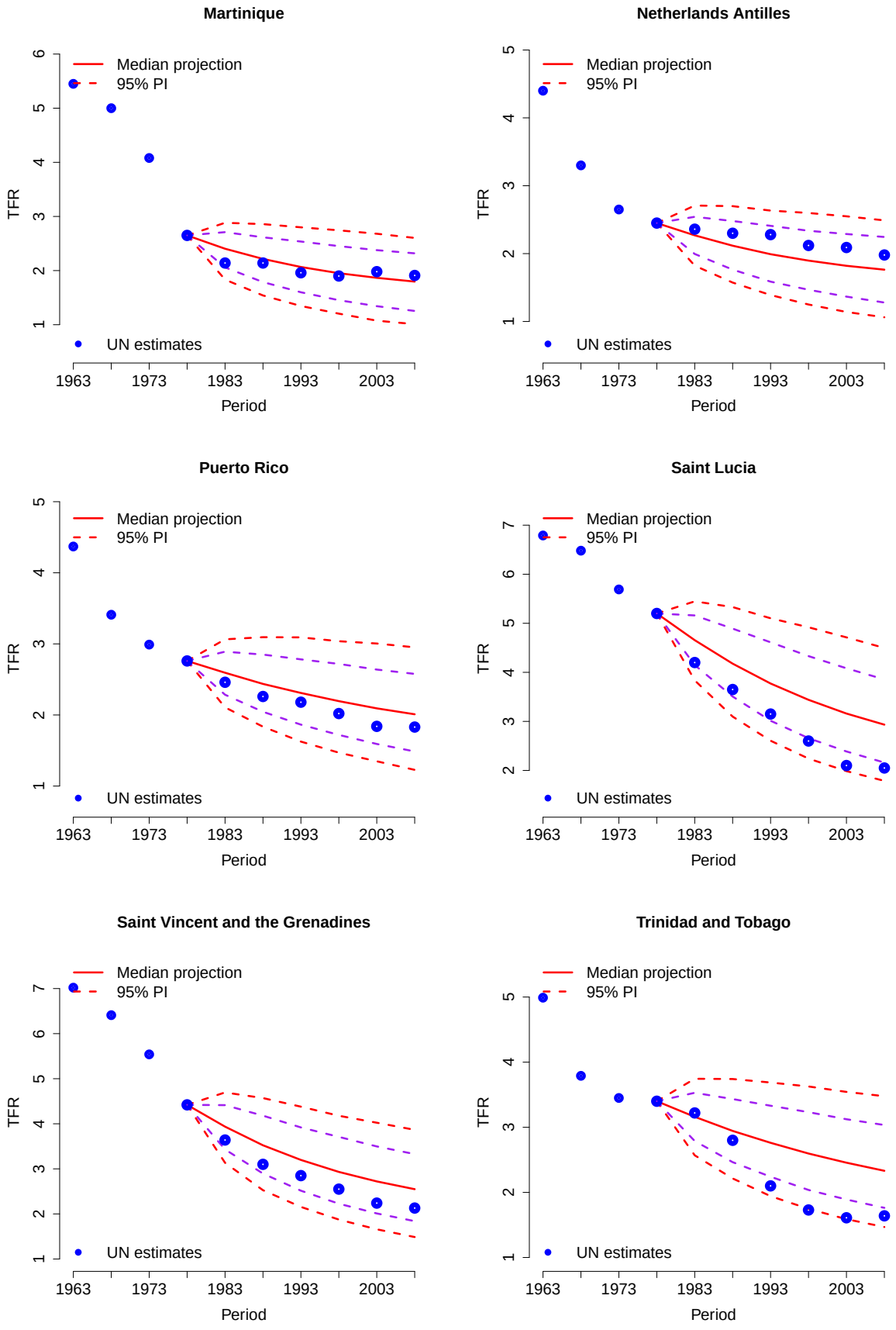

Figure 113: Out-of-sample in 1980

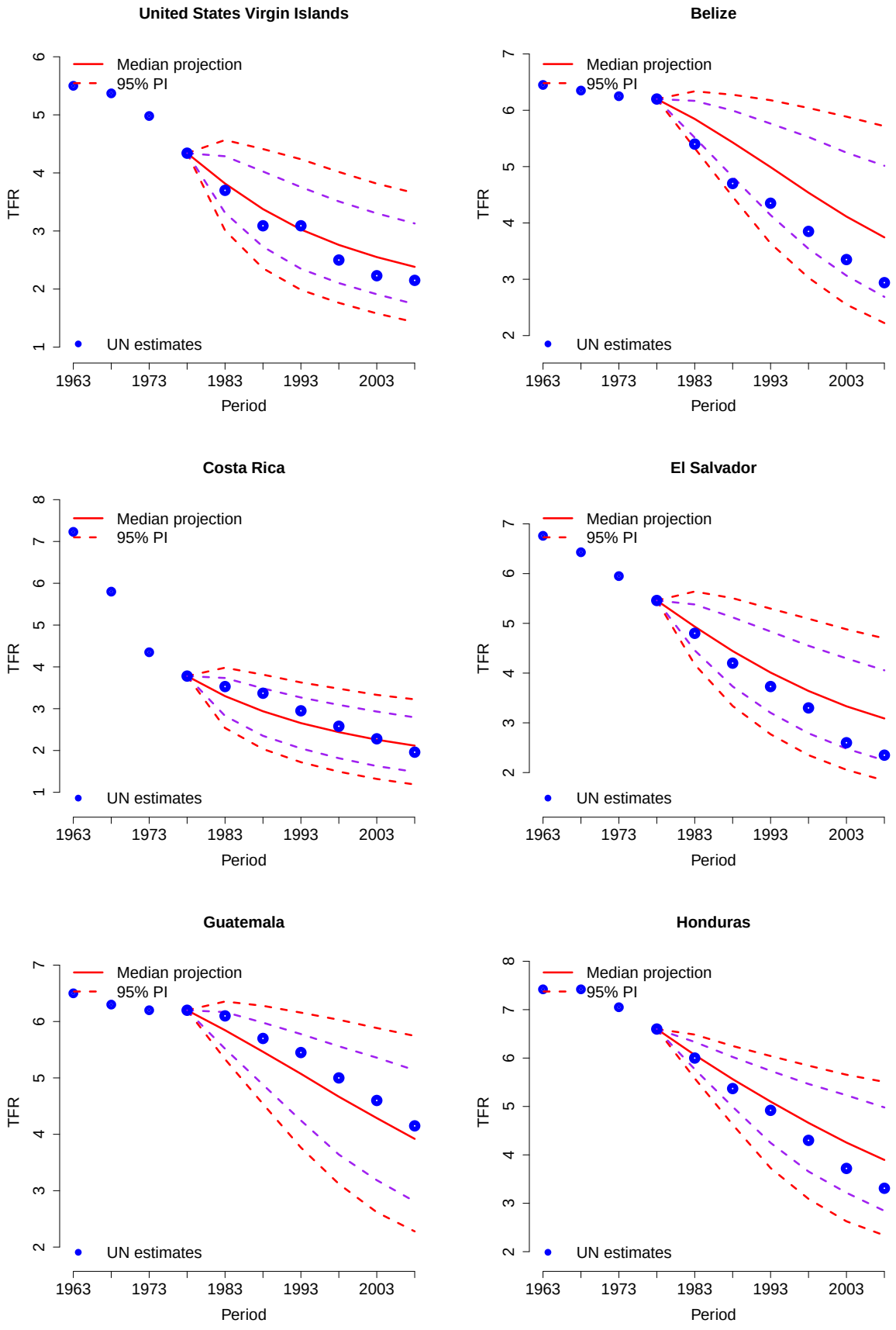

Figure 114: Out-of-sample in 1980

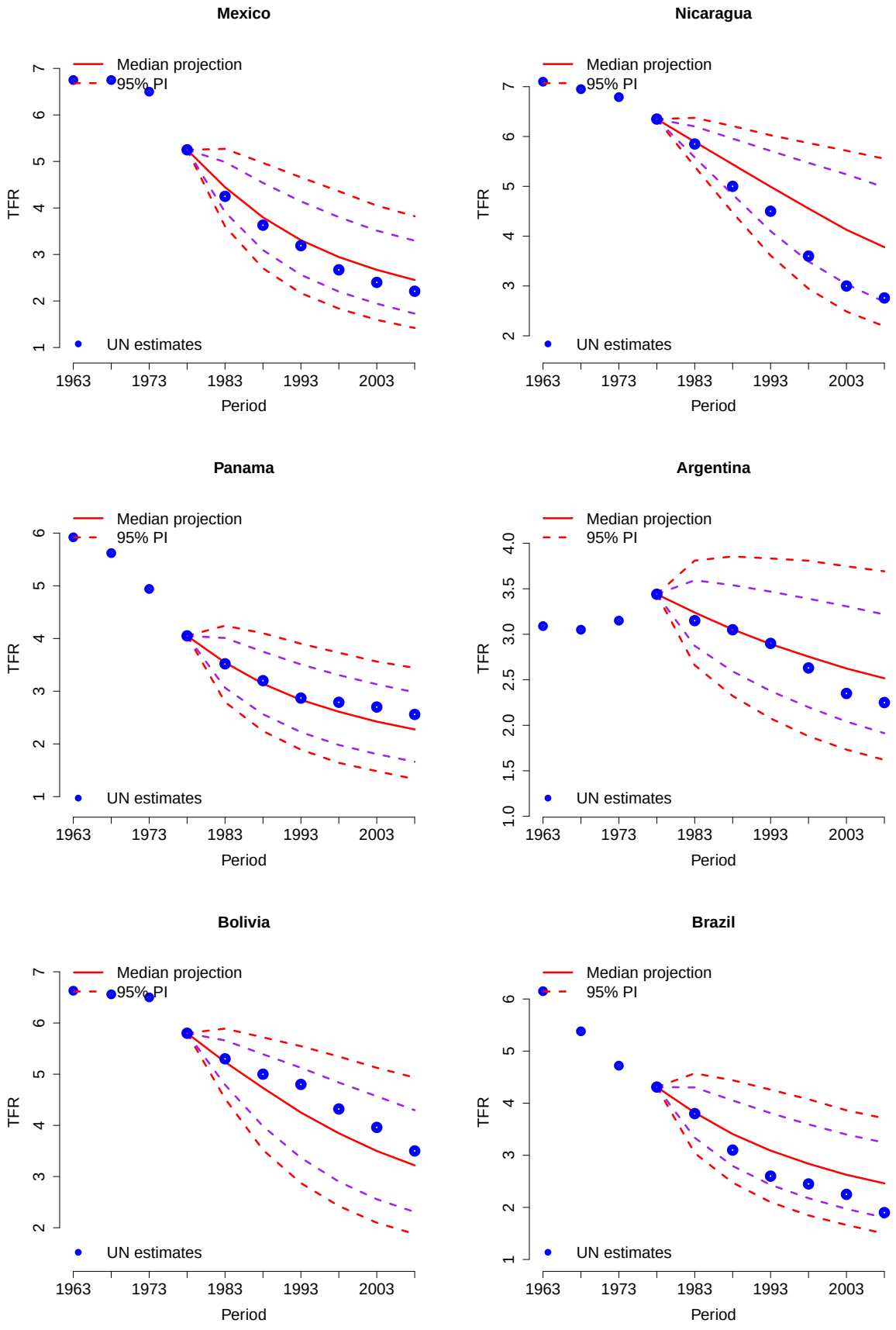

Figure 115: Out-of-sample in 1980

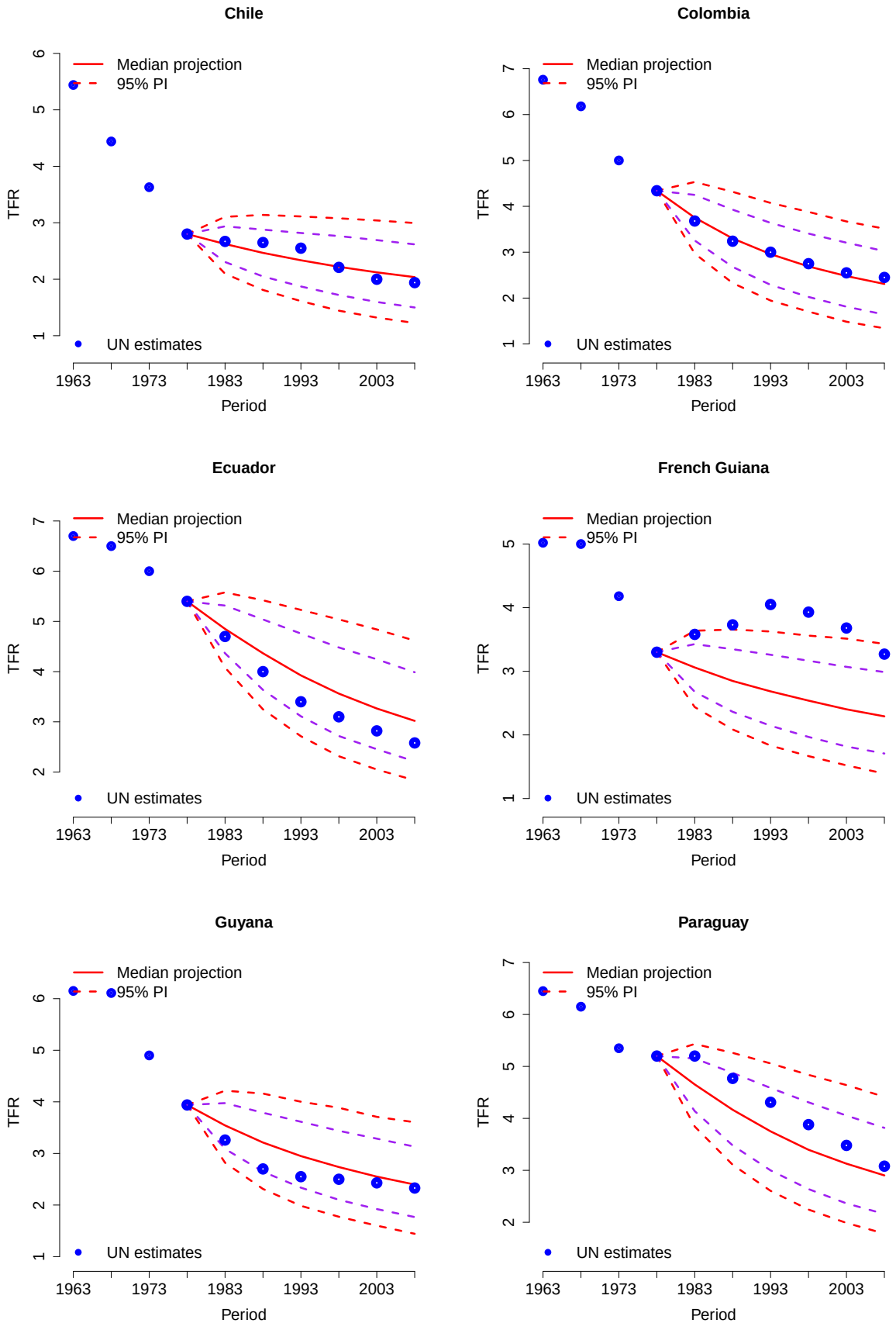

Figure 116: Out-of-sample in 1980

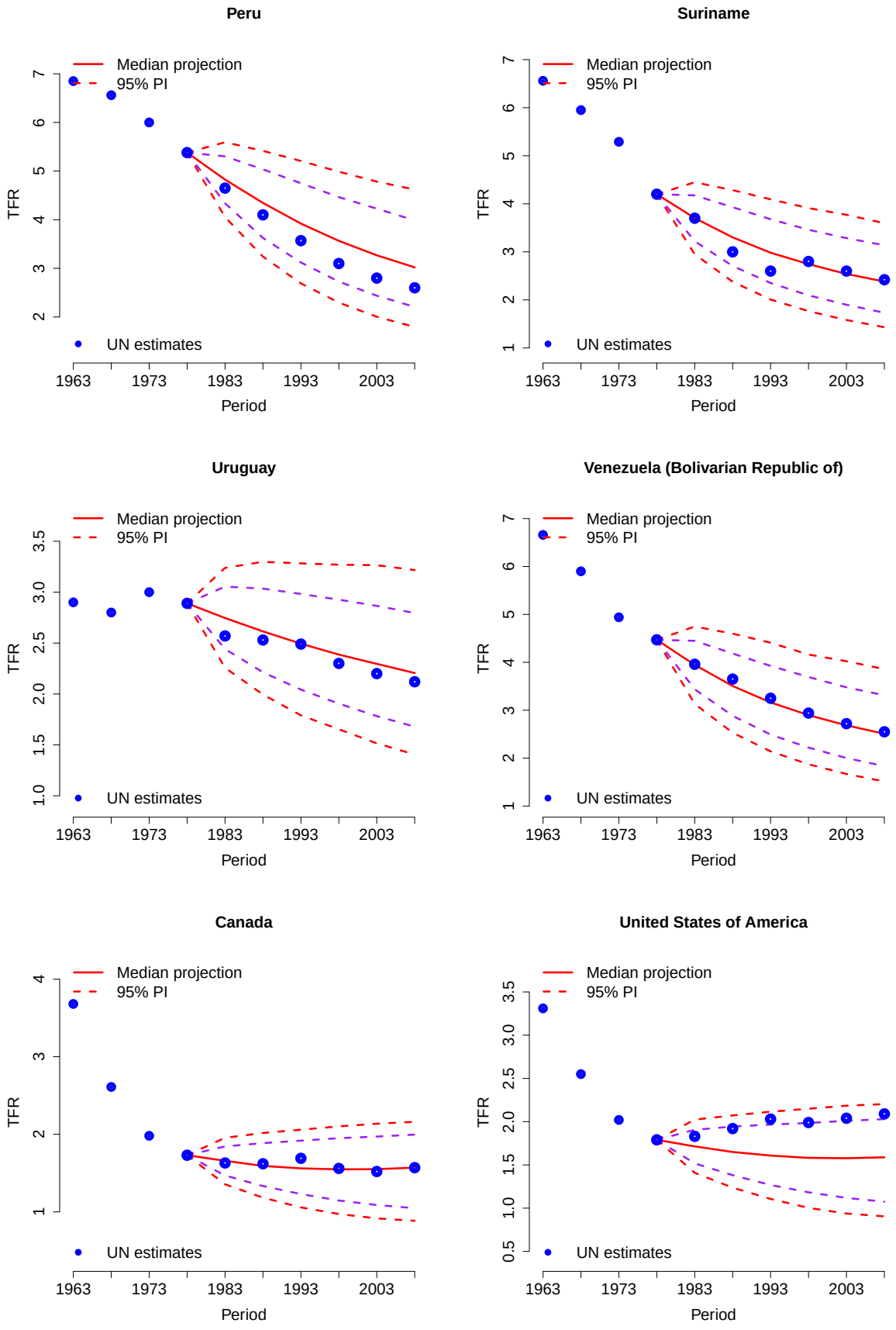

Figure 117: Out-of-sample in 1980

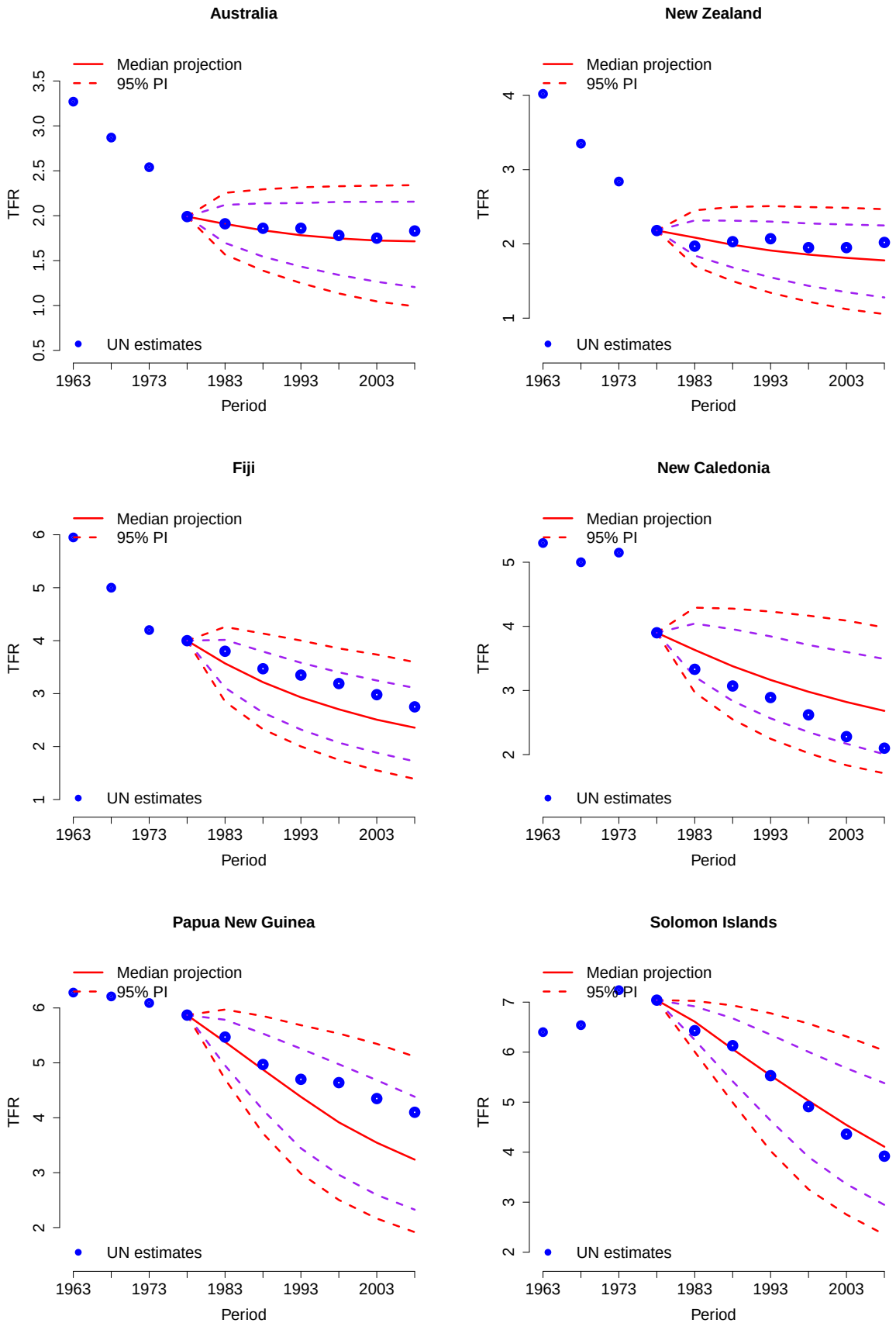

Figure 118: Out-of-sample in 1980

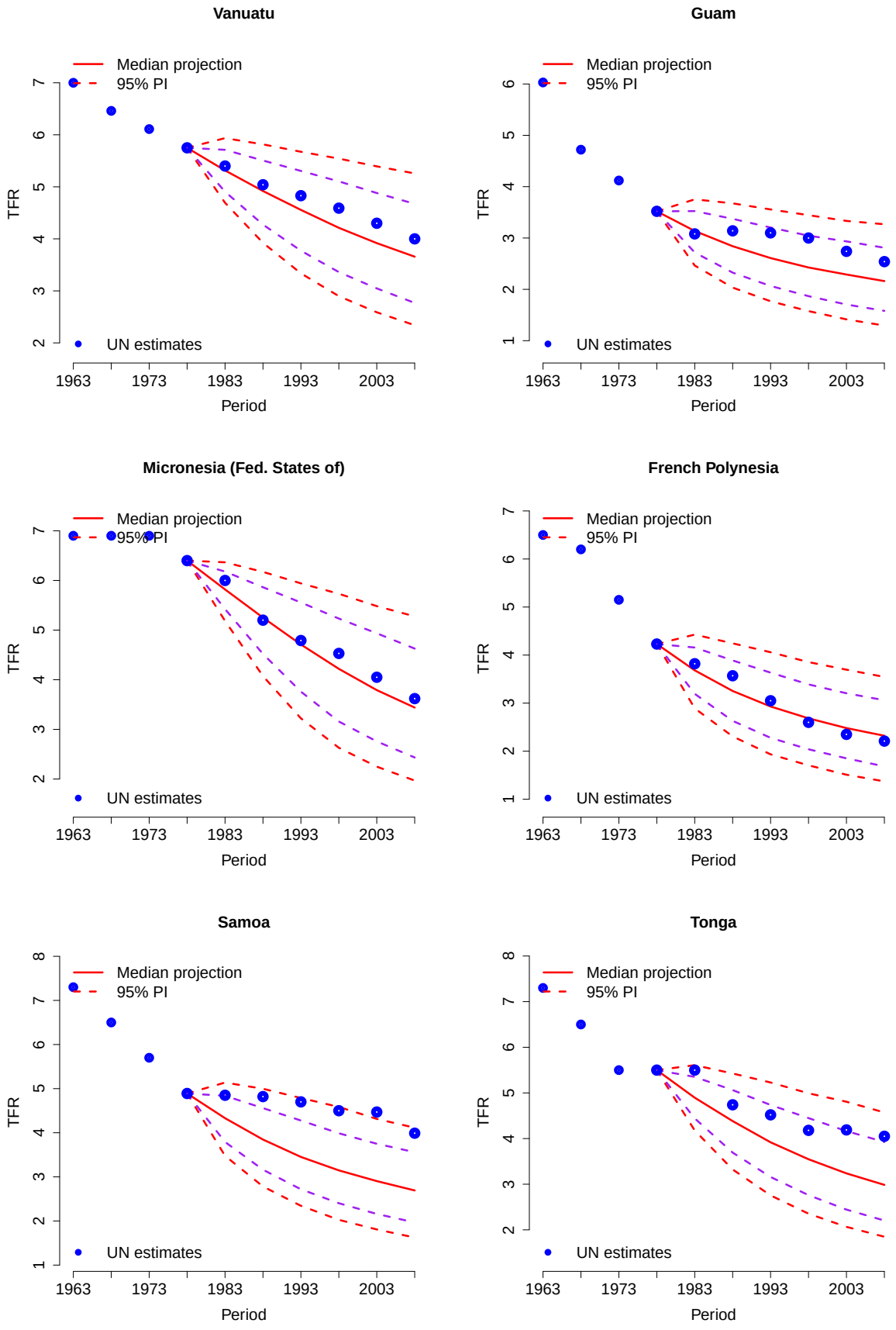

Figure 119: Out-of-sample in 1980

9.4 Plots: Out-of-sample in 1995

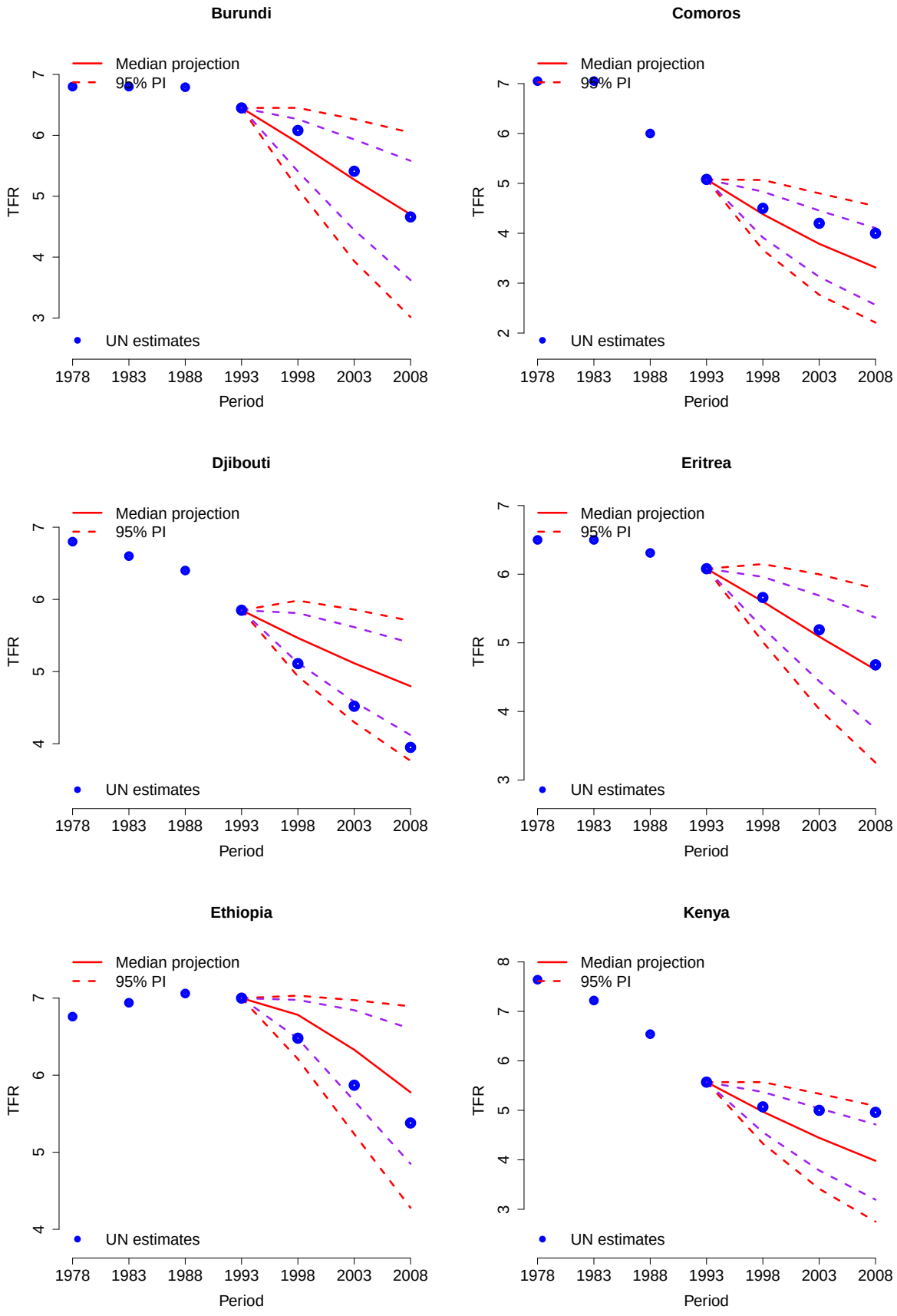

Figure 120: Out-of-sample in 1995

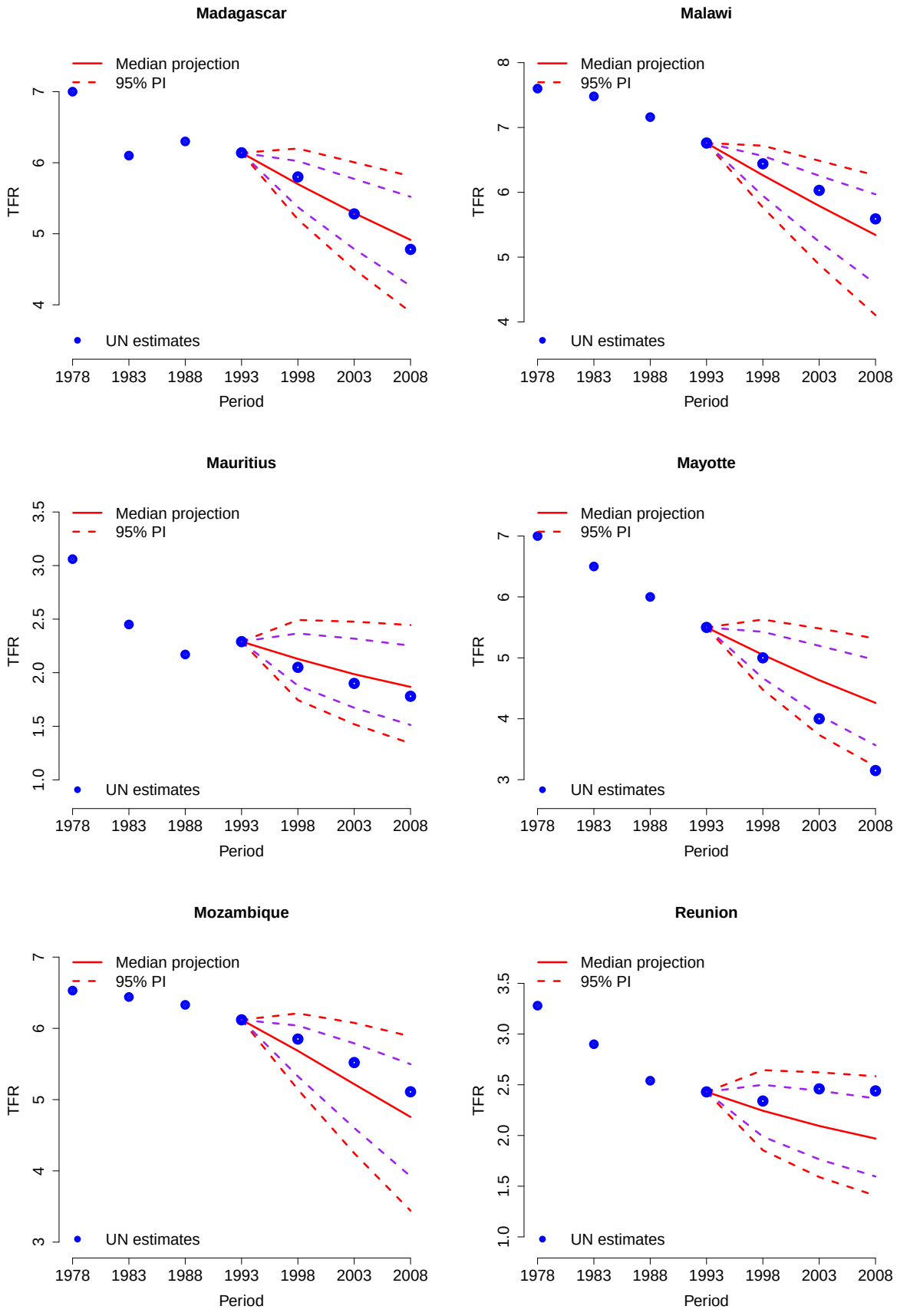

Figure 121: Out-of-sample in 1995

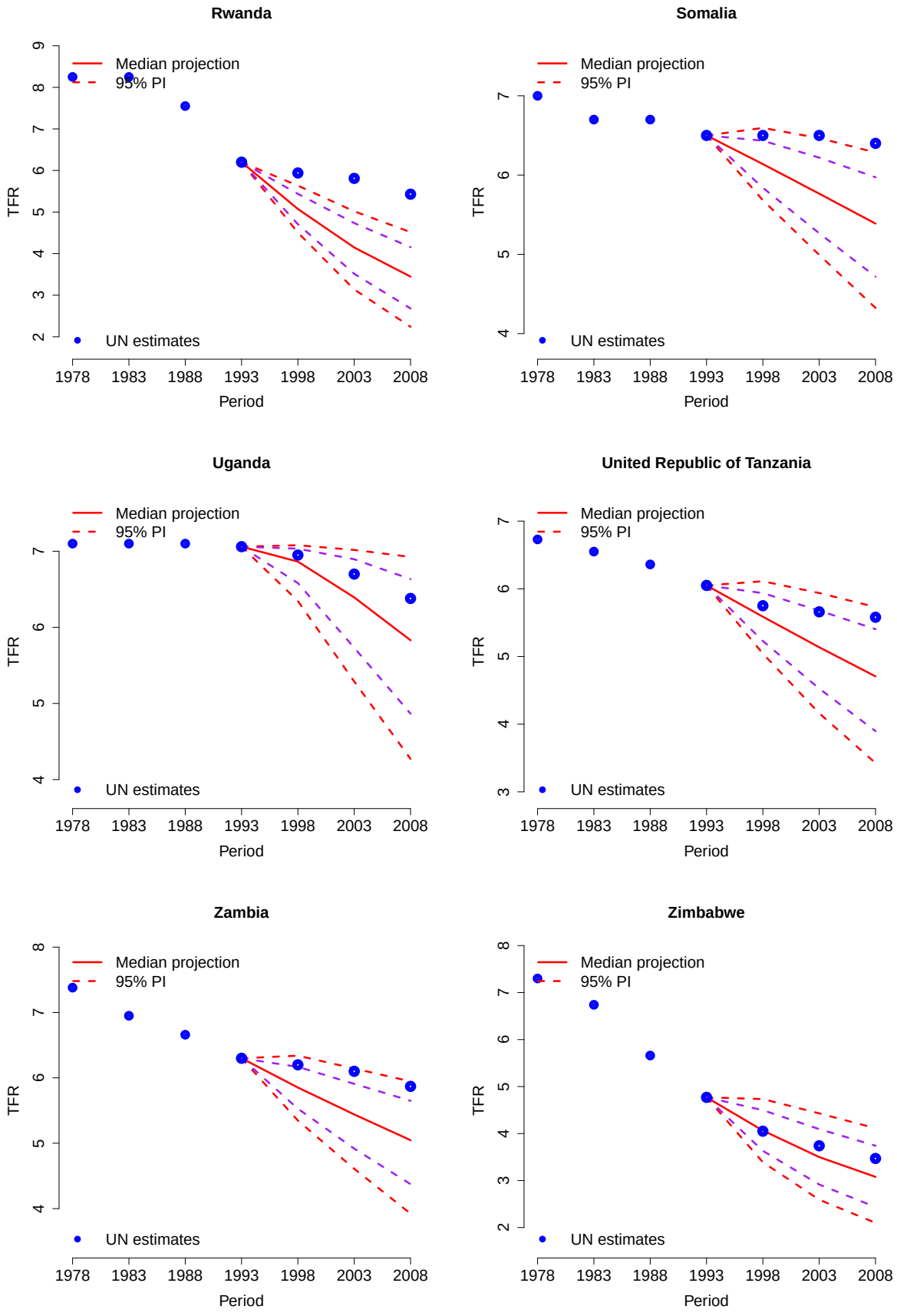

Figure 122: Out-of-sample in 1995

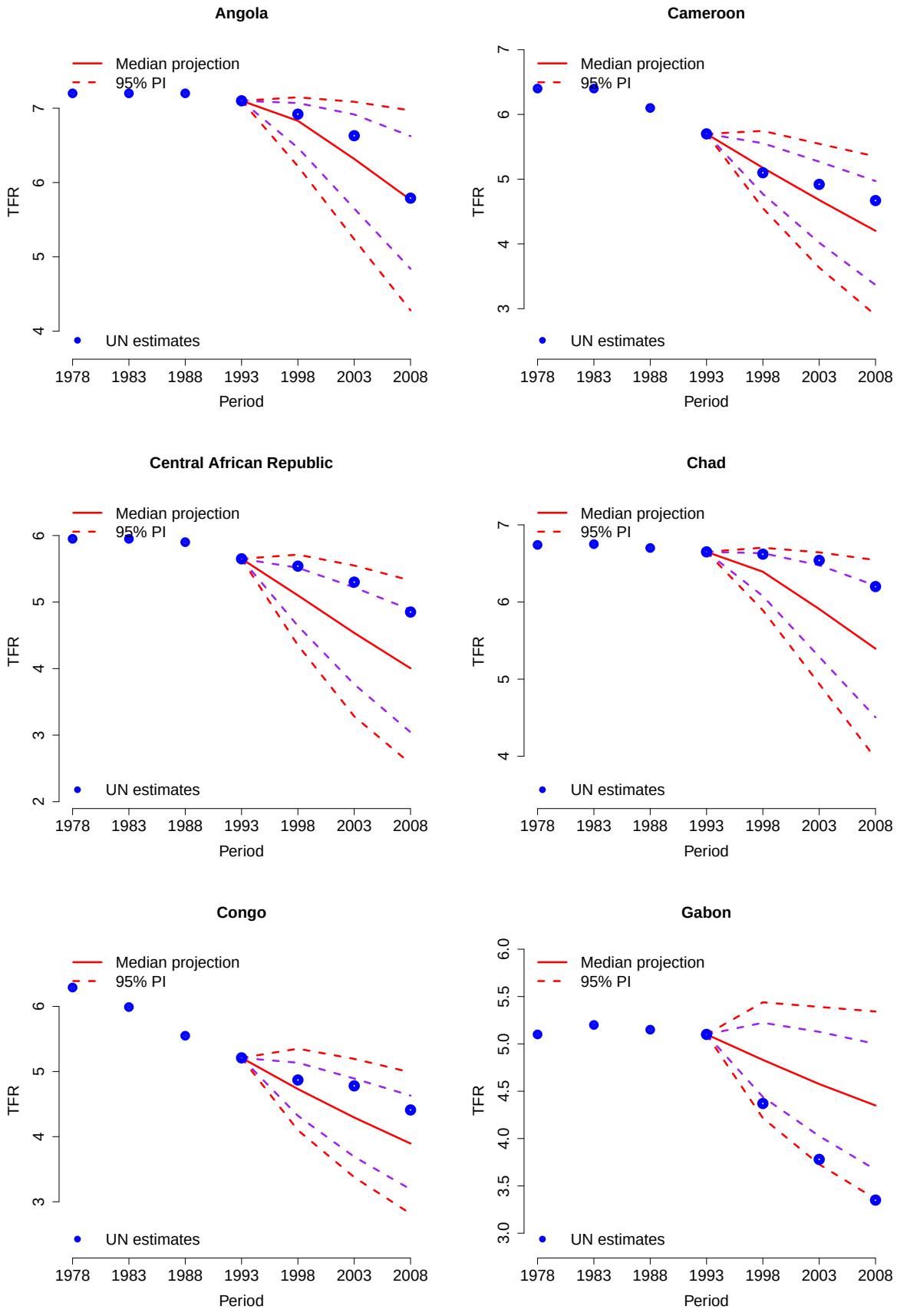

Figure 123: Out-of-sample in 1995

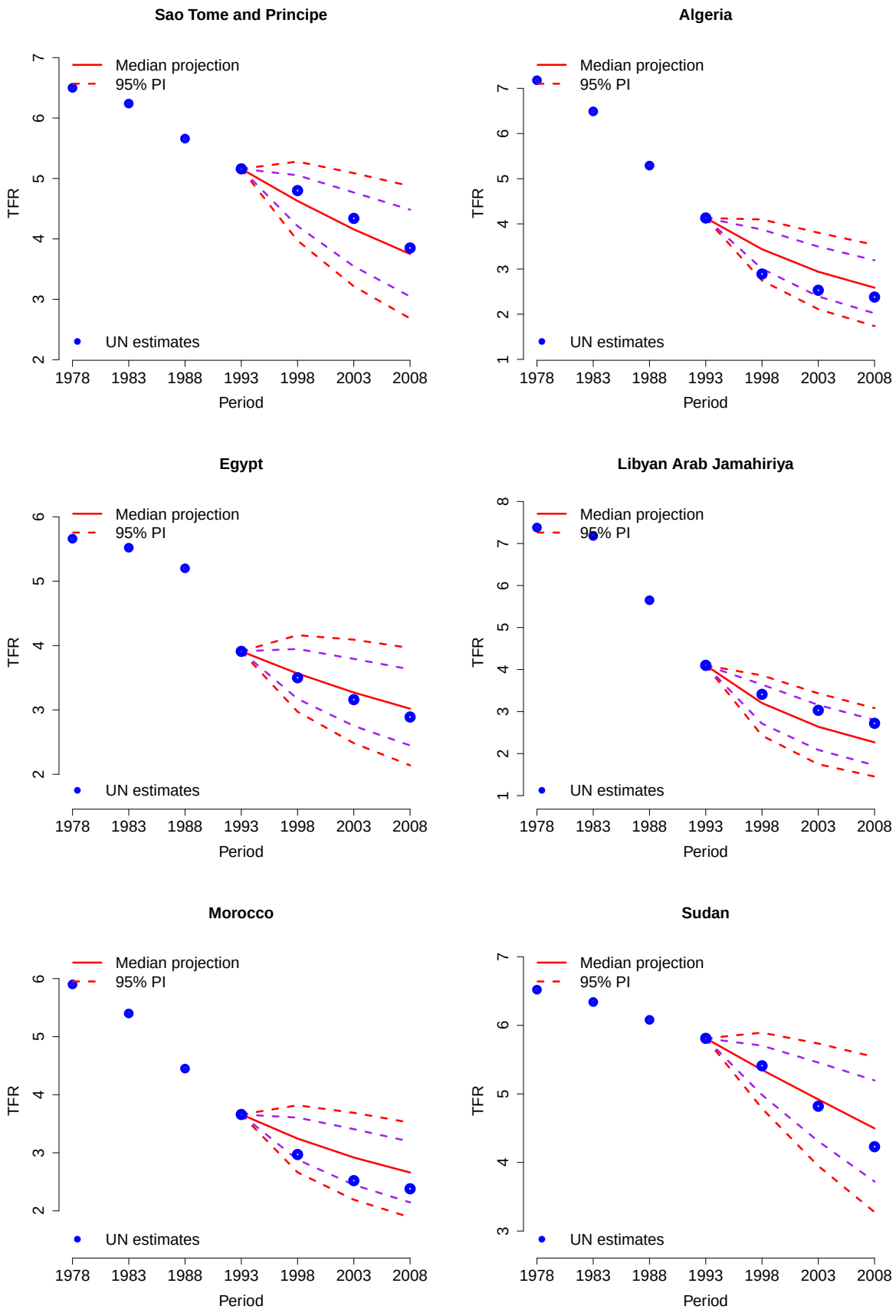

Figure 124: Out-of-sample in 1995

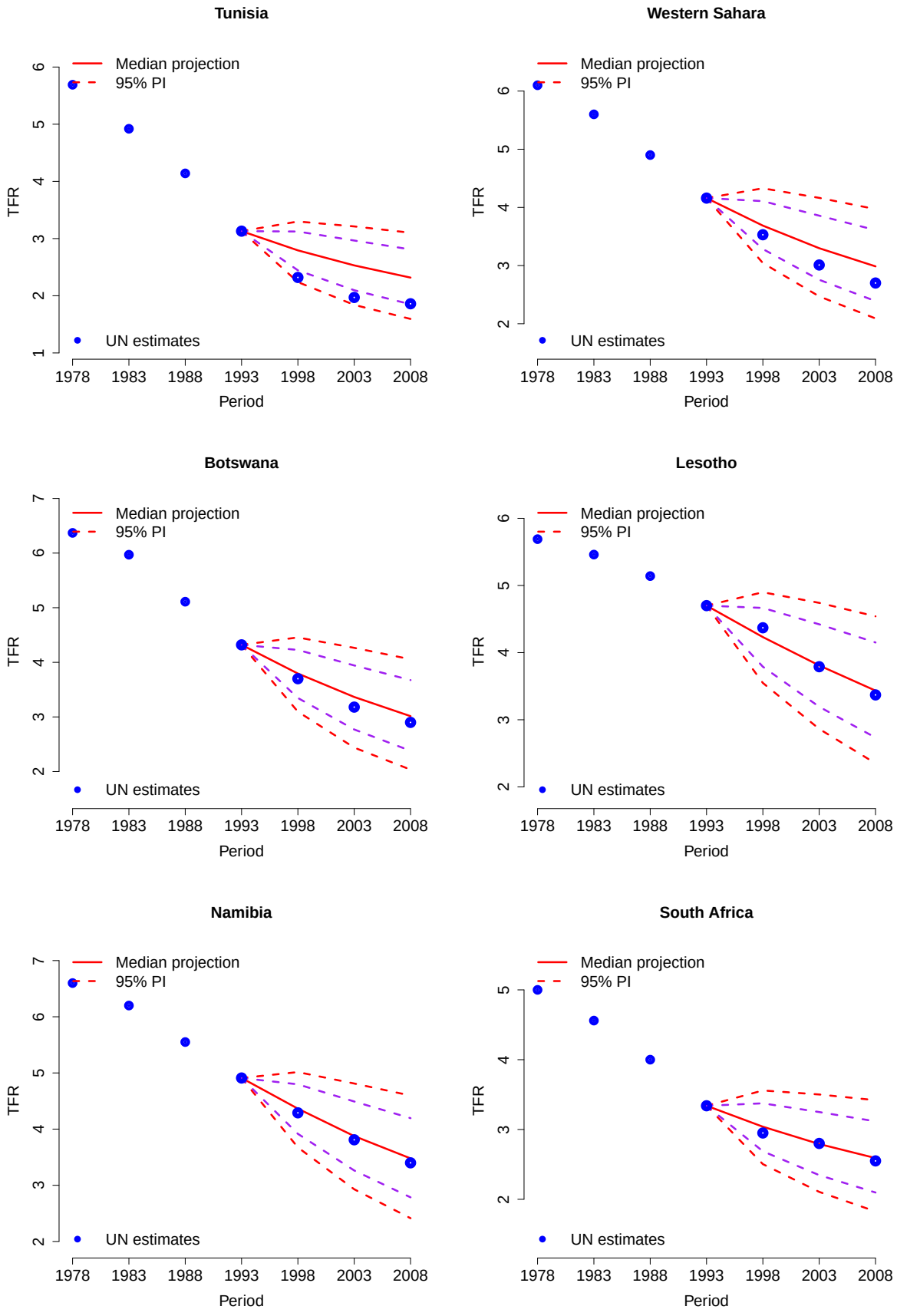

Figure 125: Out-of-sample in 1995

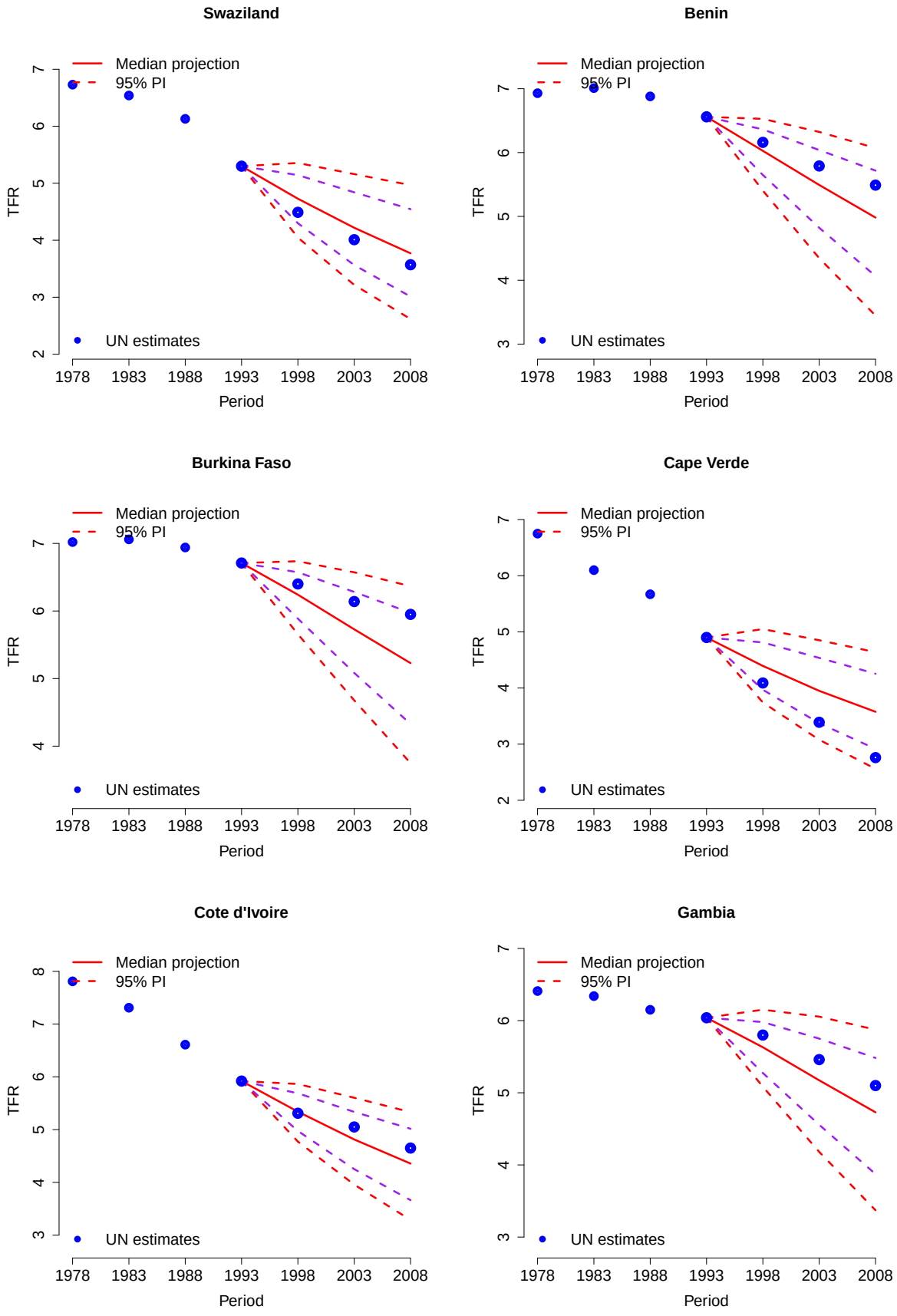

Figure 126: Out-of-sample in 1995

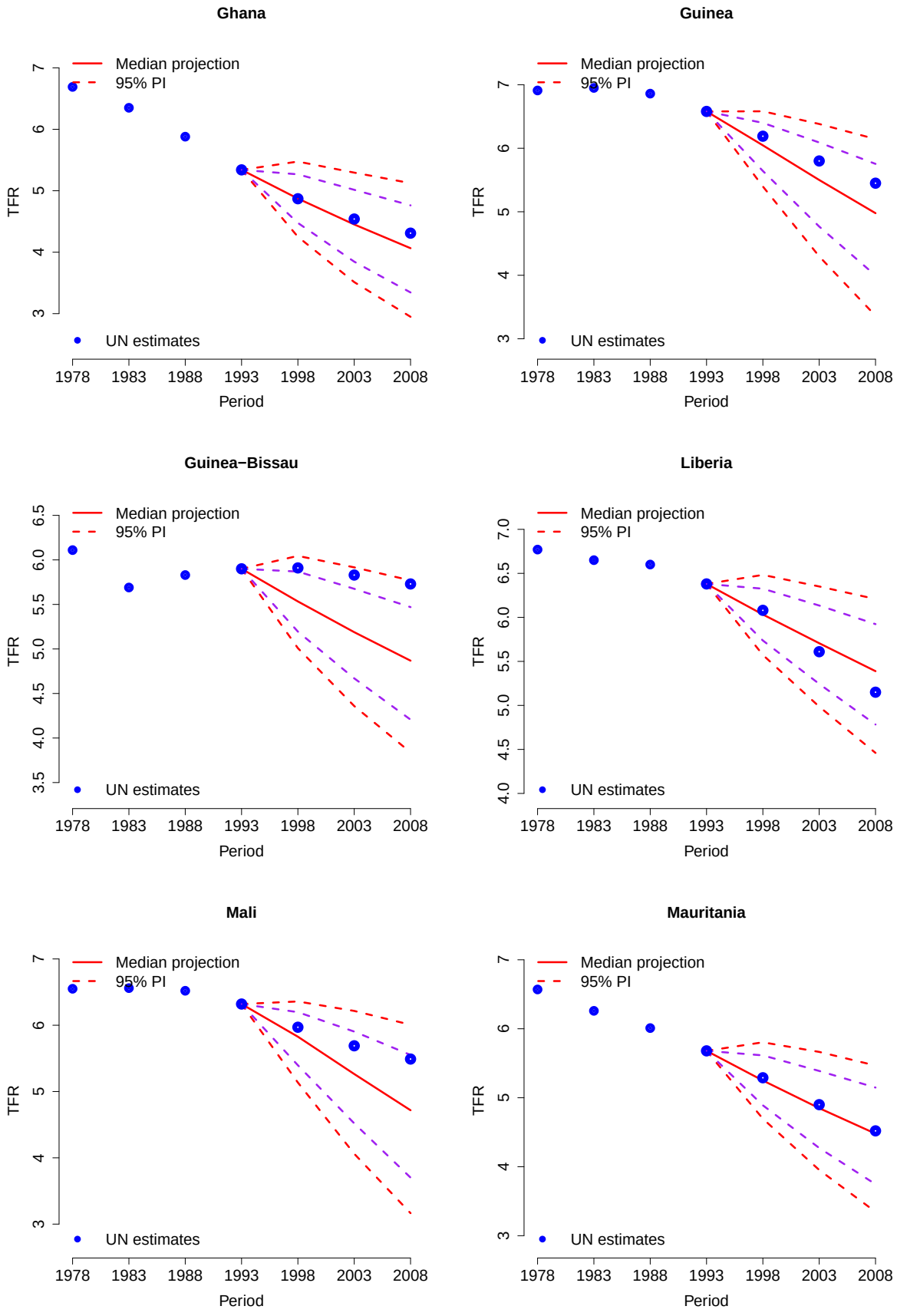

Figure 127: Out-of-sample in 1995

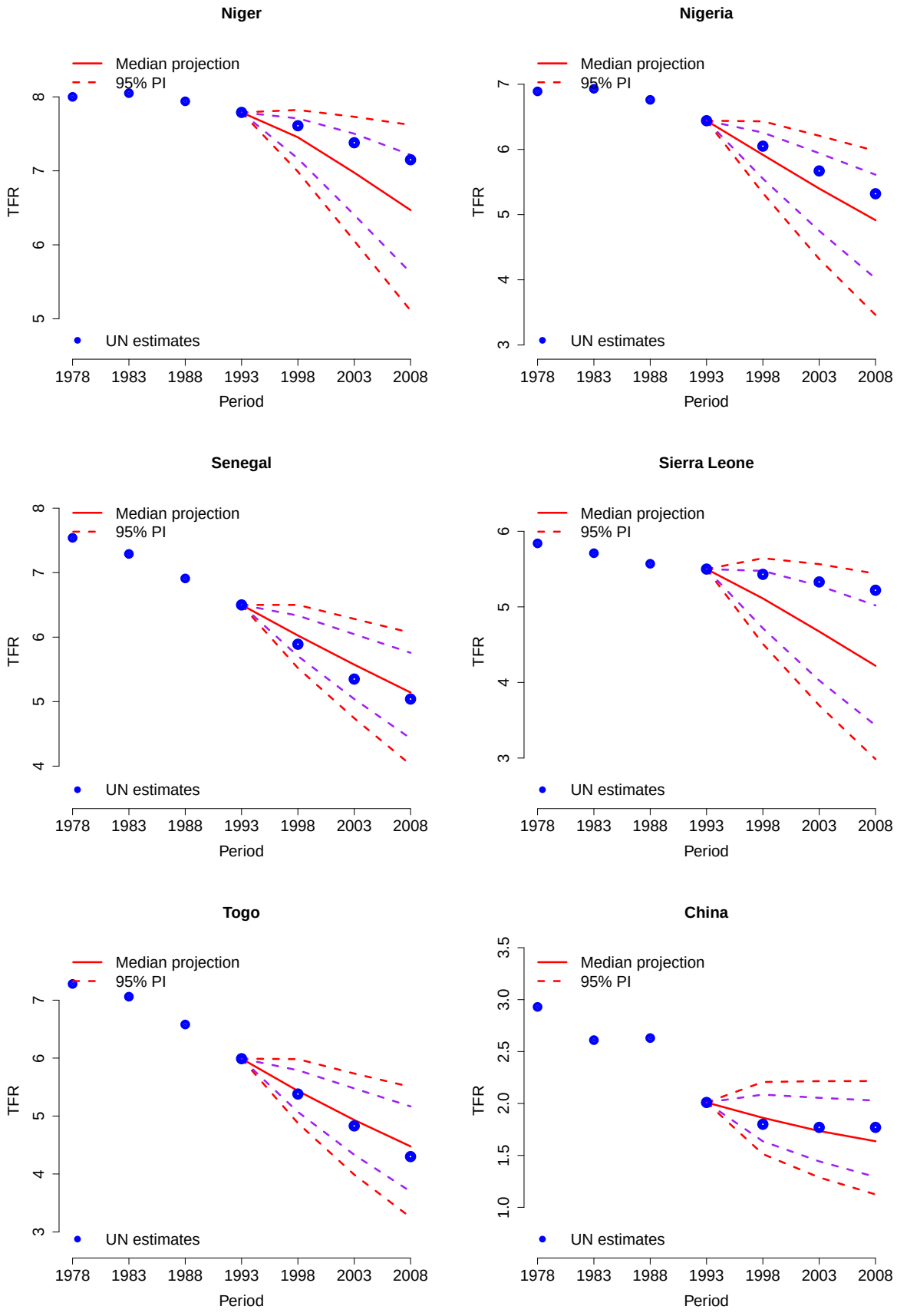

Figure 128: Out-of-sample in 1995

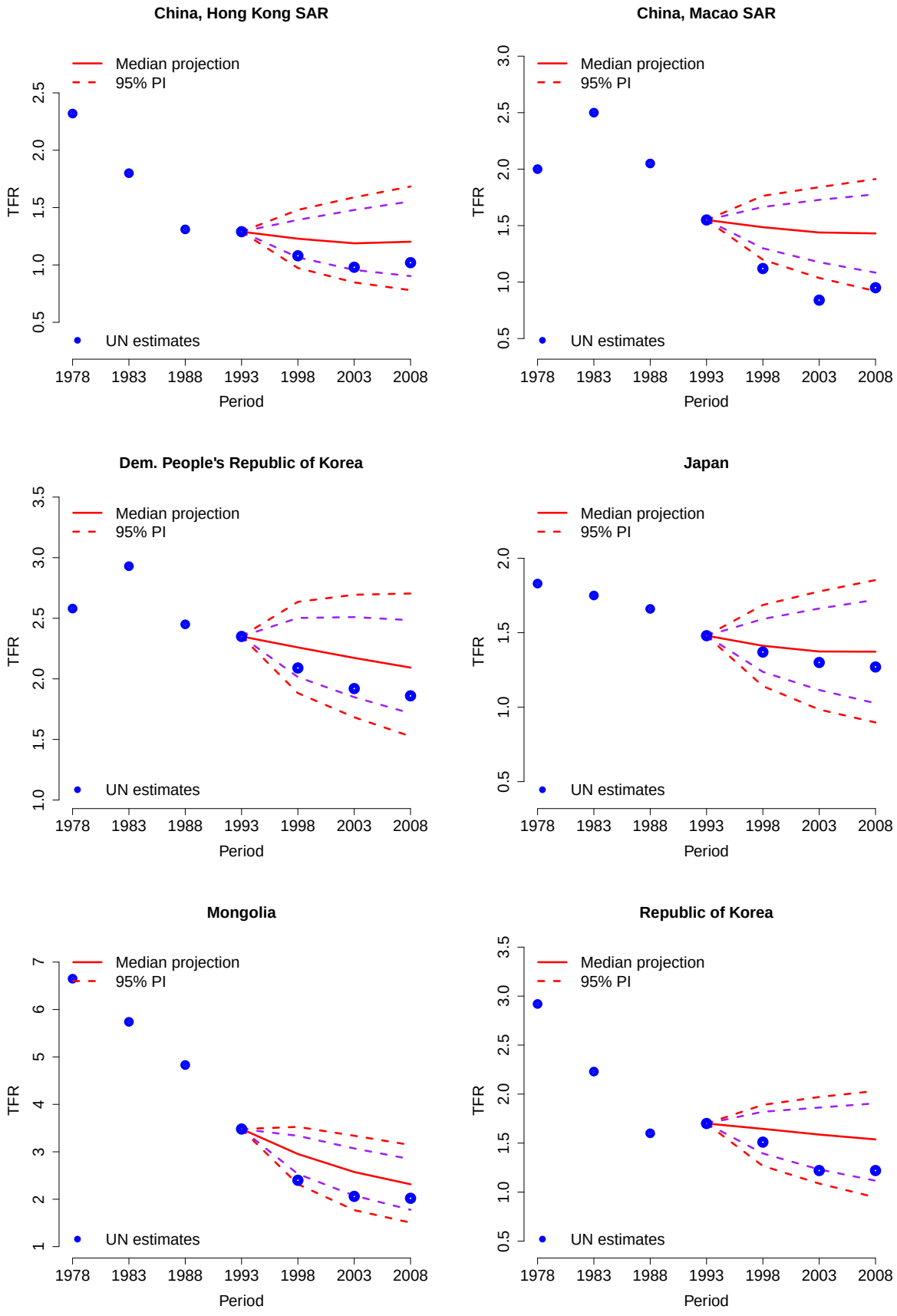

Figure 129: Out-of-sample in 1995

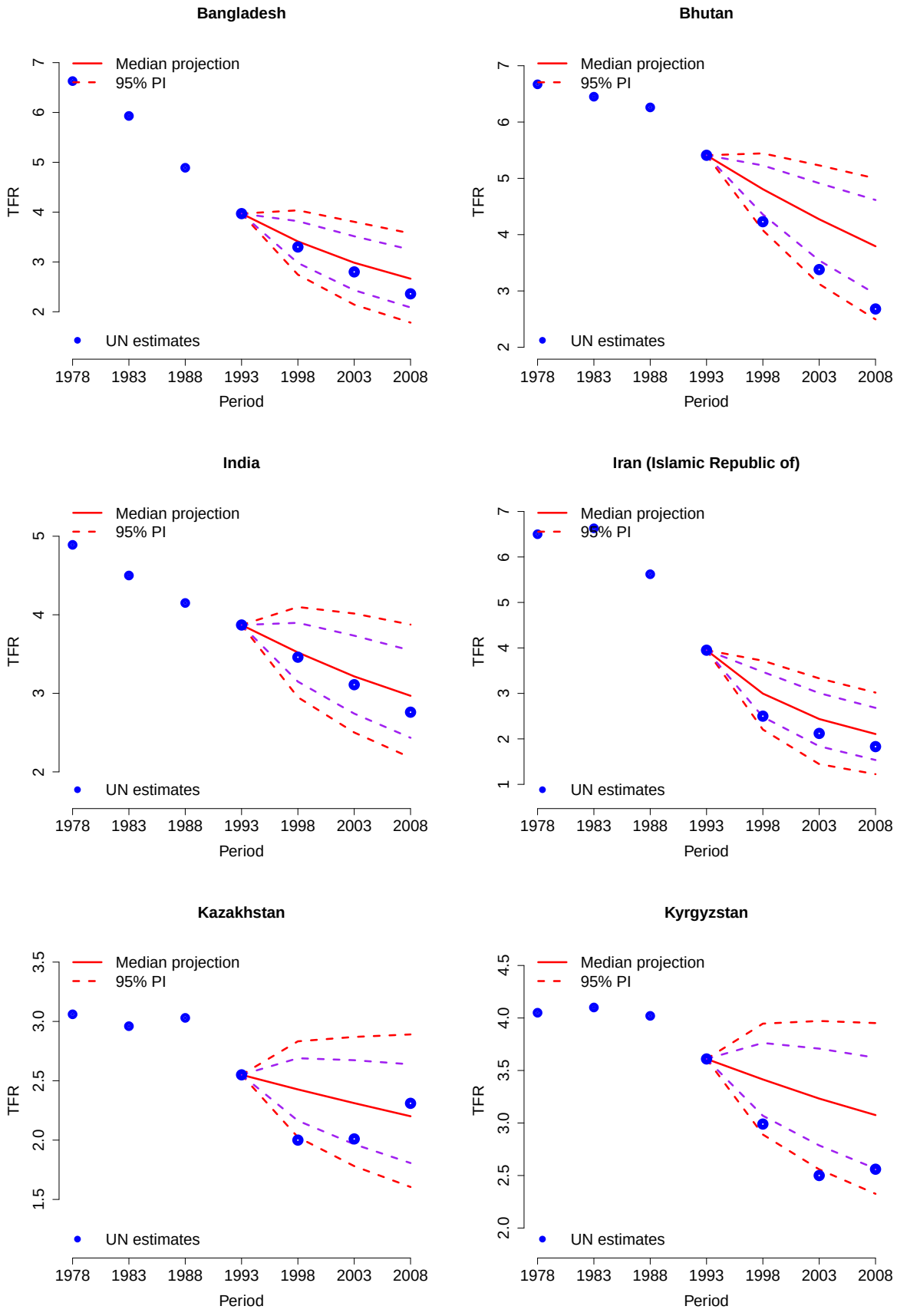

Figure 130: Out-of-sample in 1995

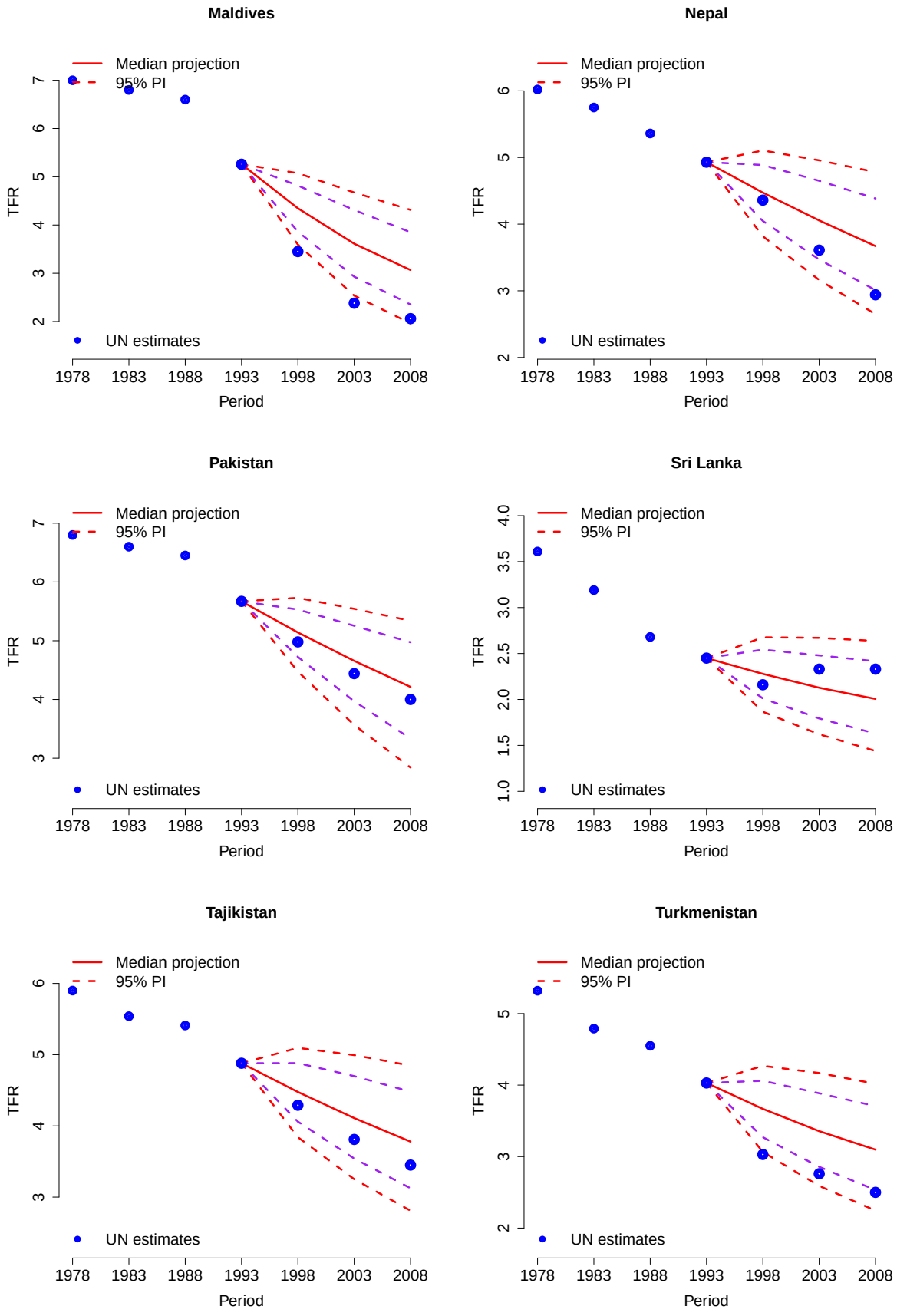

Figure 131: Out-of-sample in 1995

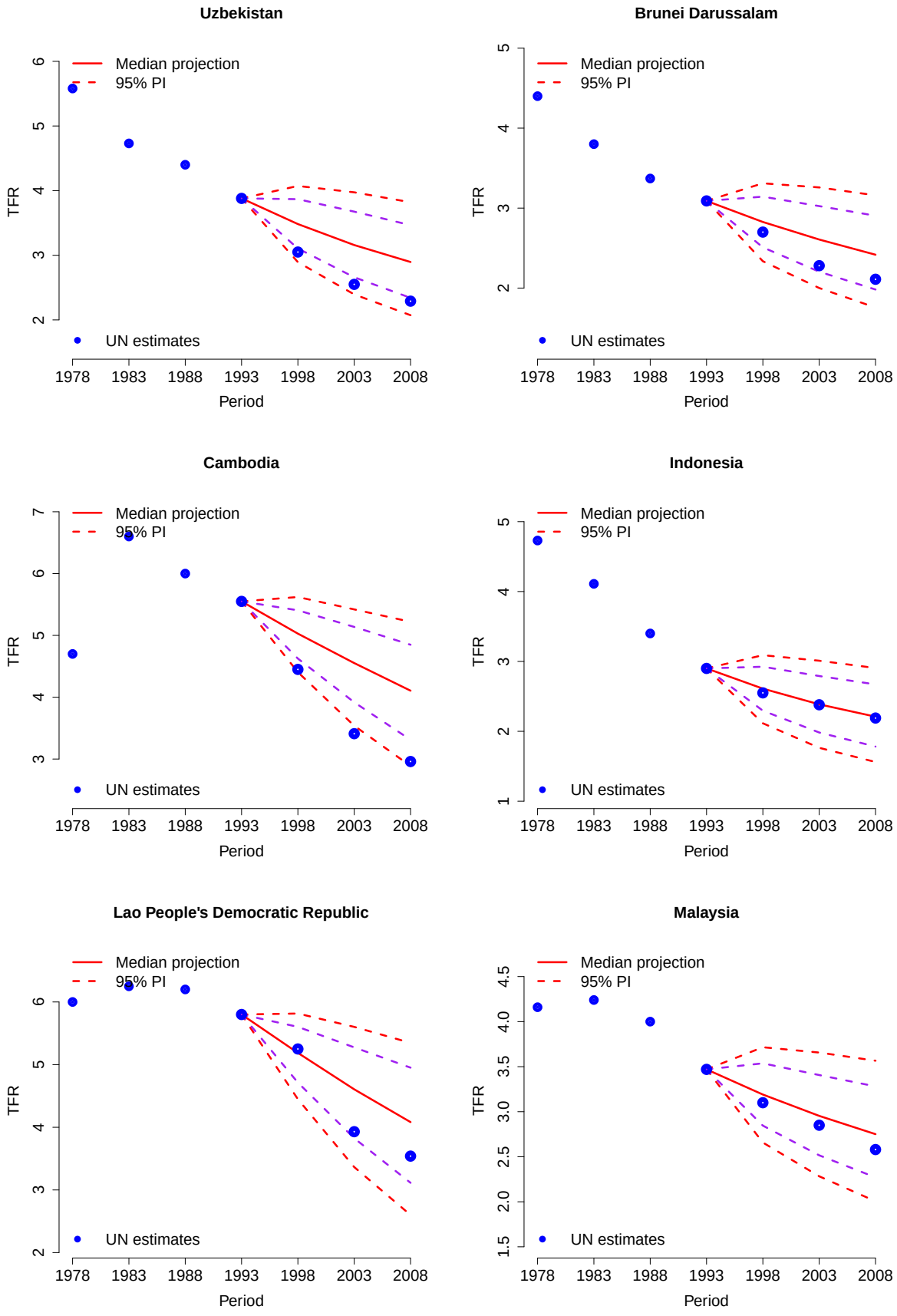

Figure 132: Out-of-sample in 1995

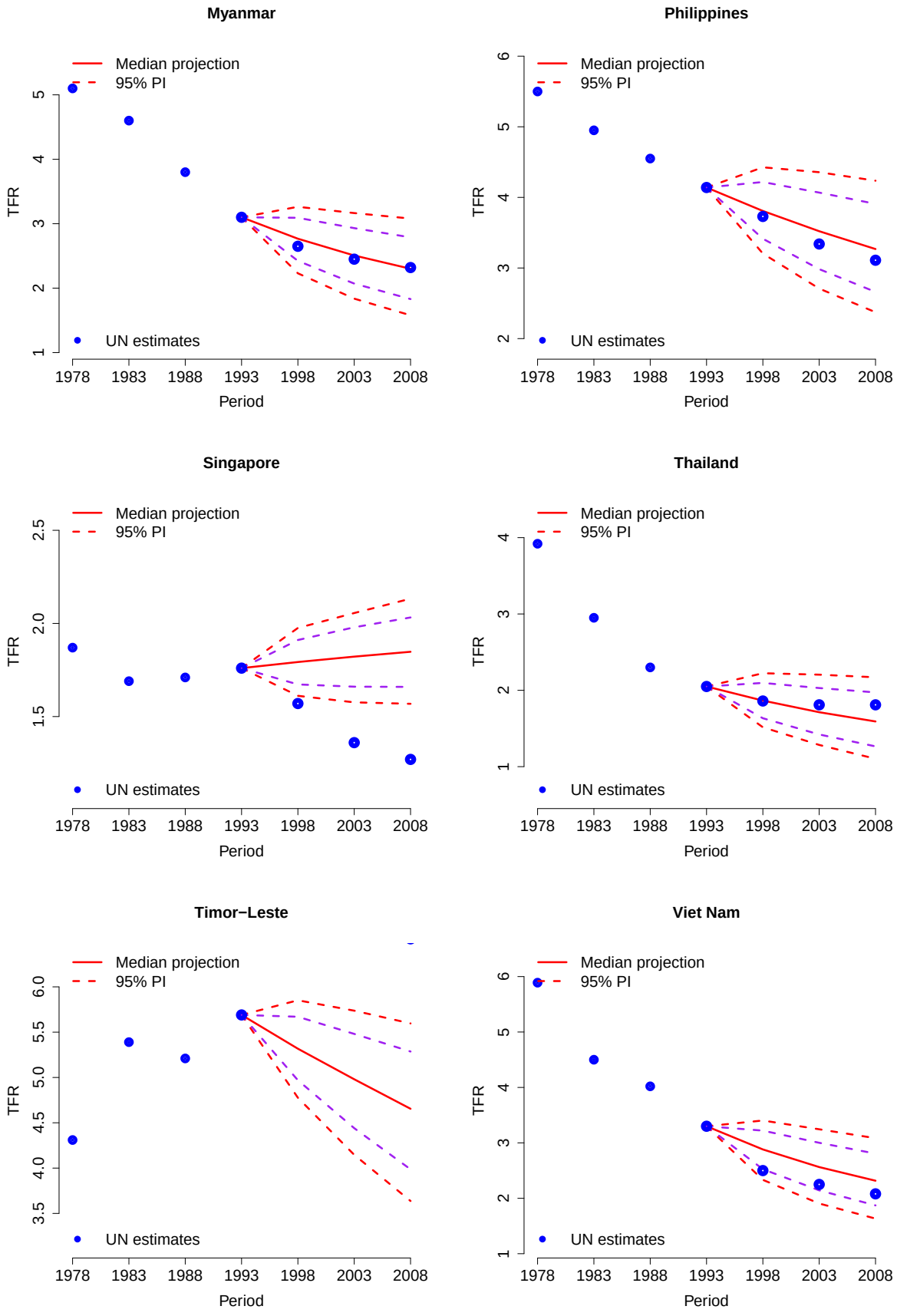

Figure 133: Out-of-sample in 1995

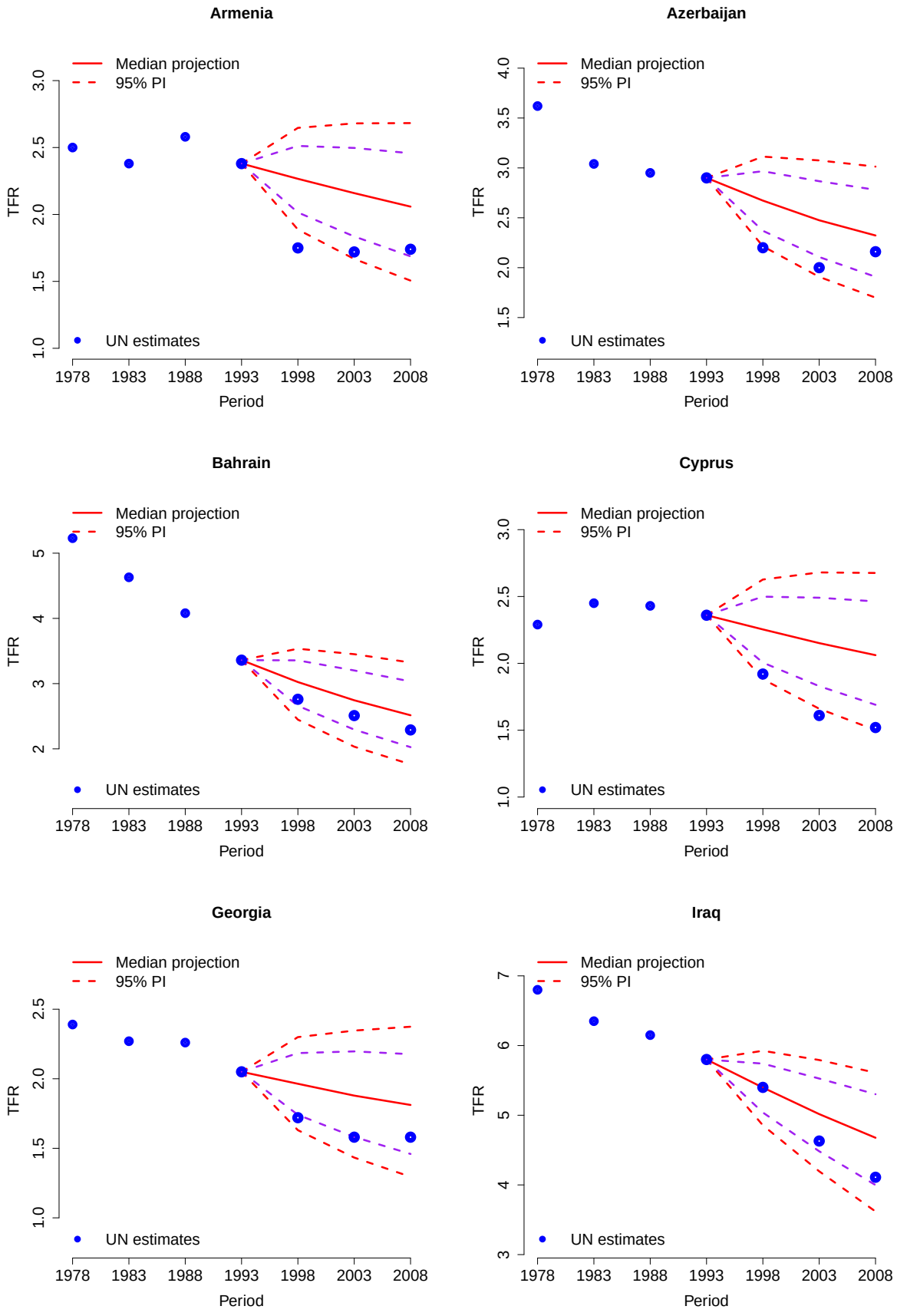

Figure 134: Out-of-sample in 1995

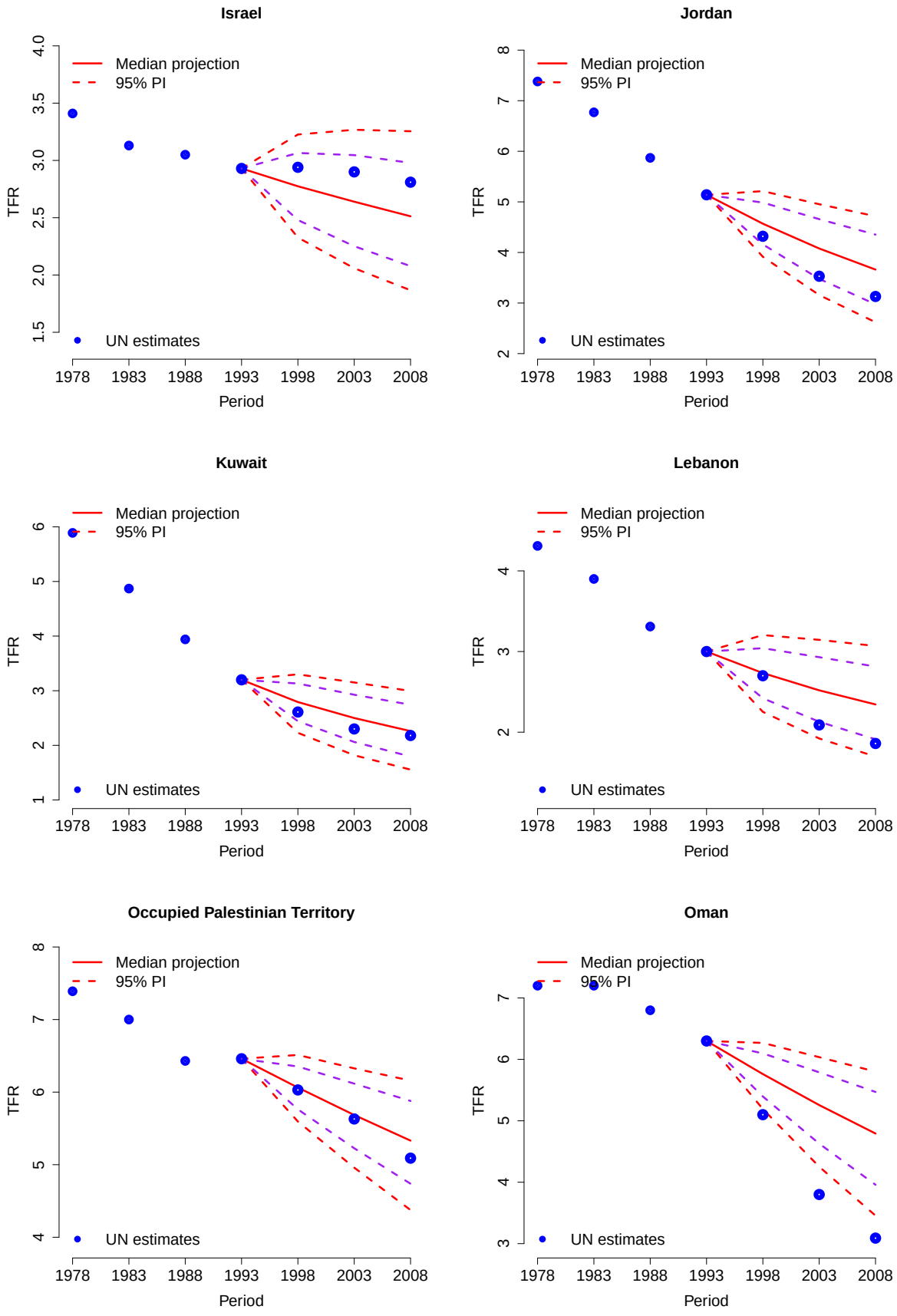

Figure 135: Out-of-sample in 1995

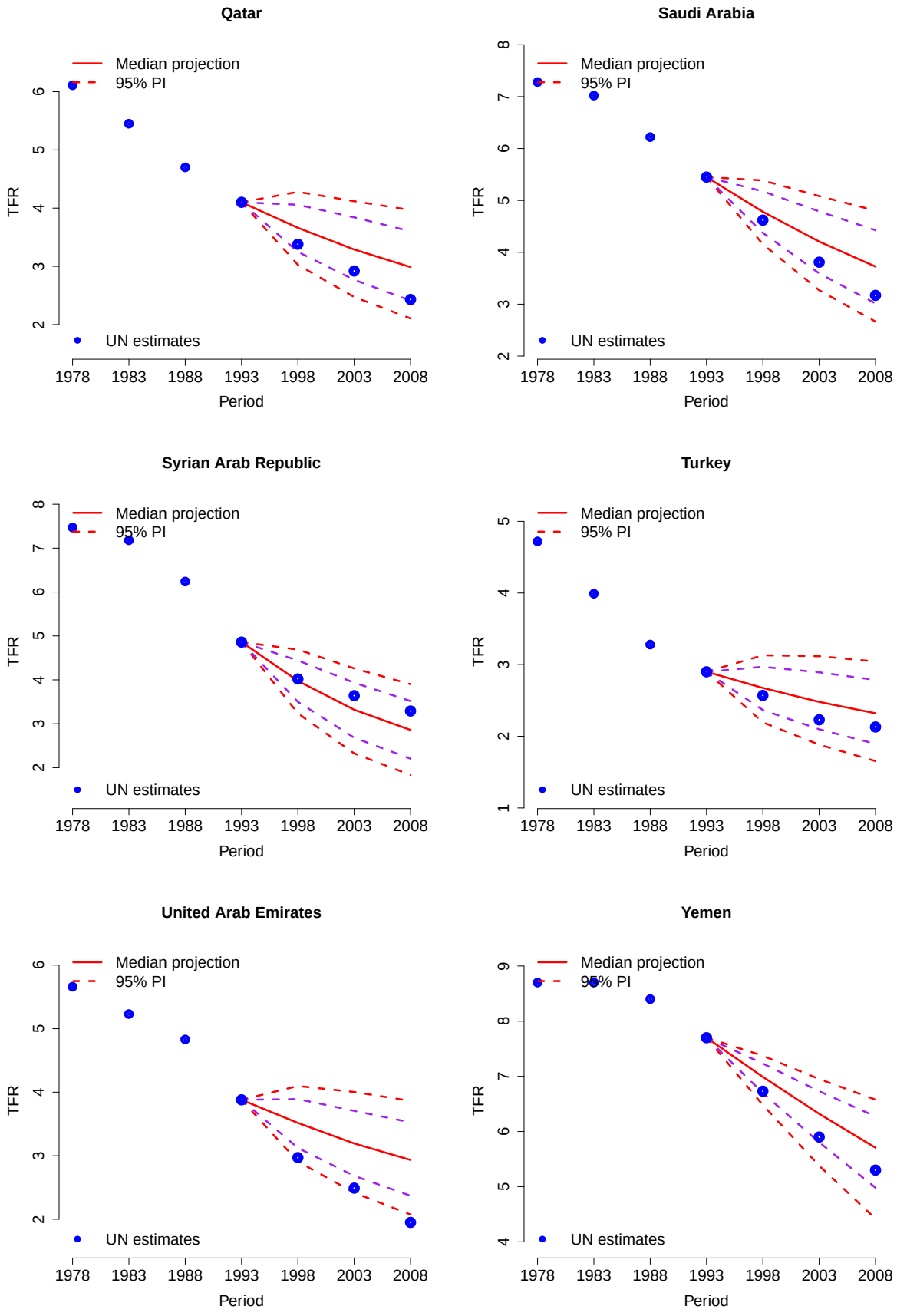

Figure 136: Out-of-sample in 1995

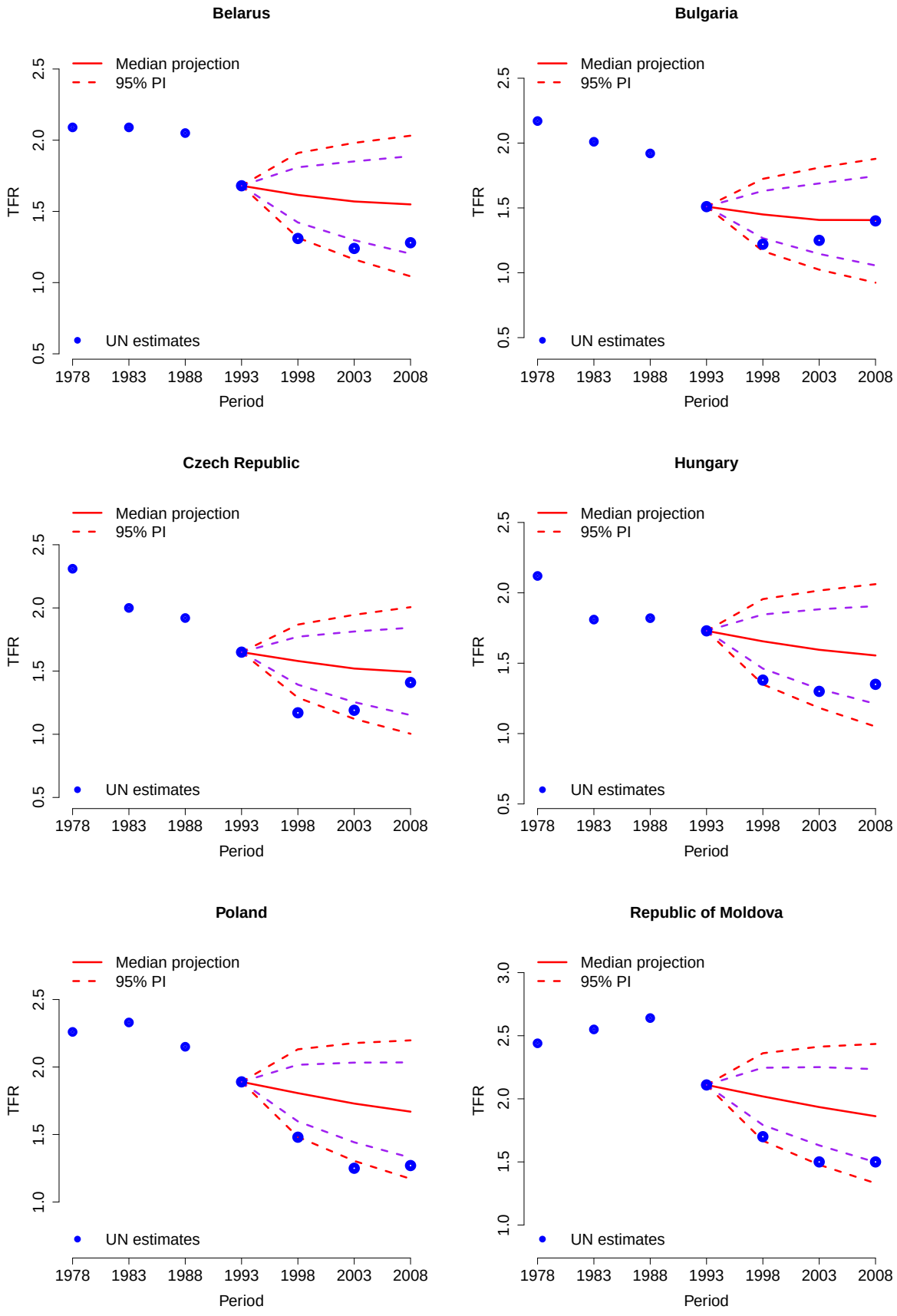

Figure 137: Out-of-sample in 1995

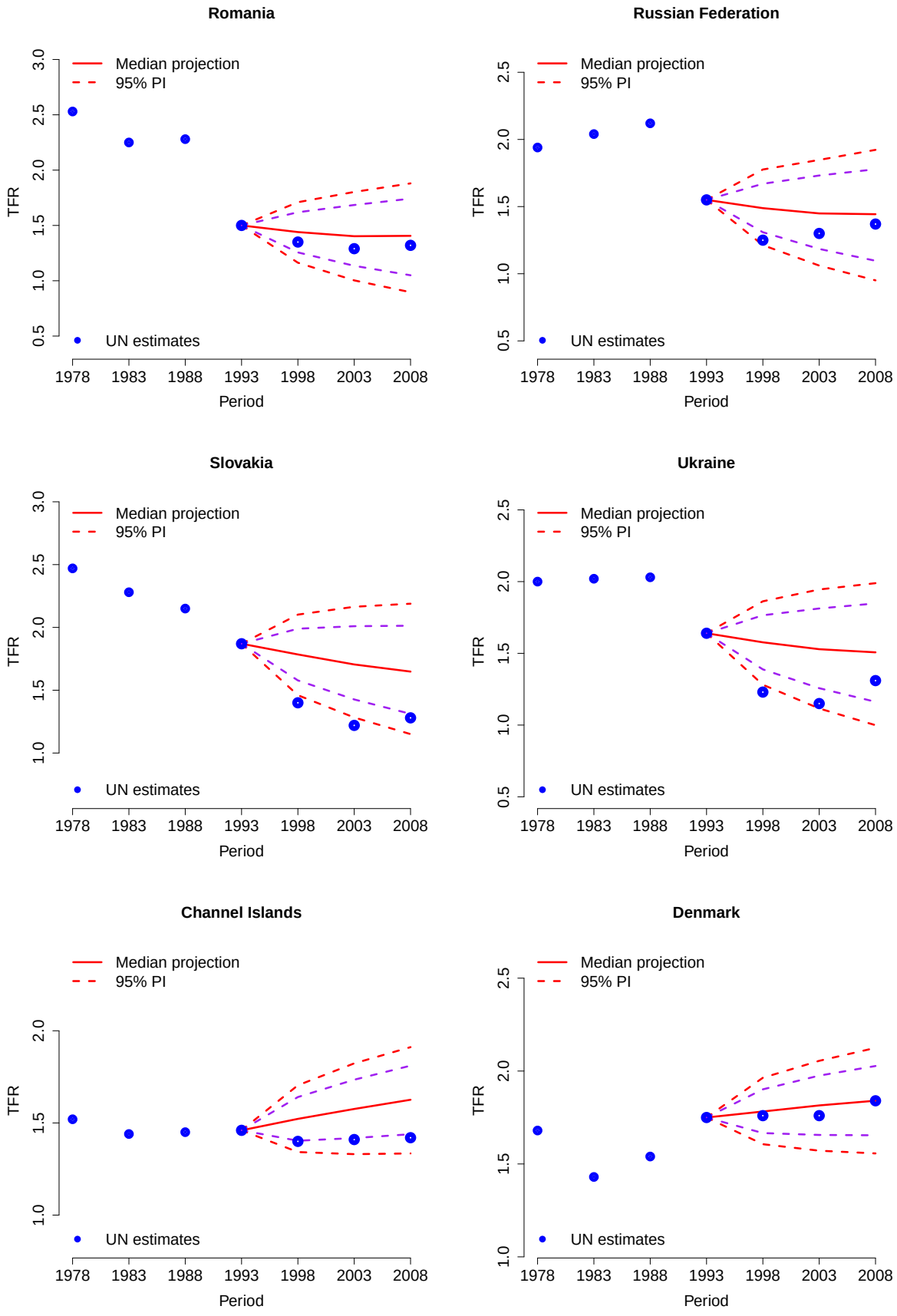

Figure 138: Out-of-sample in 1995

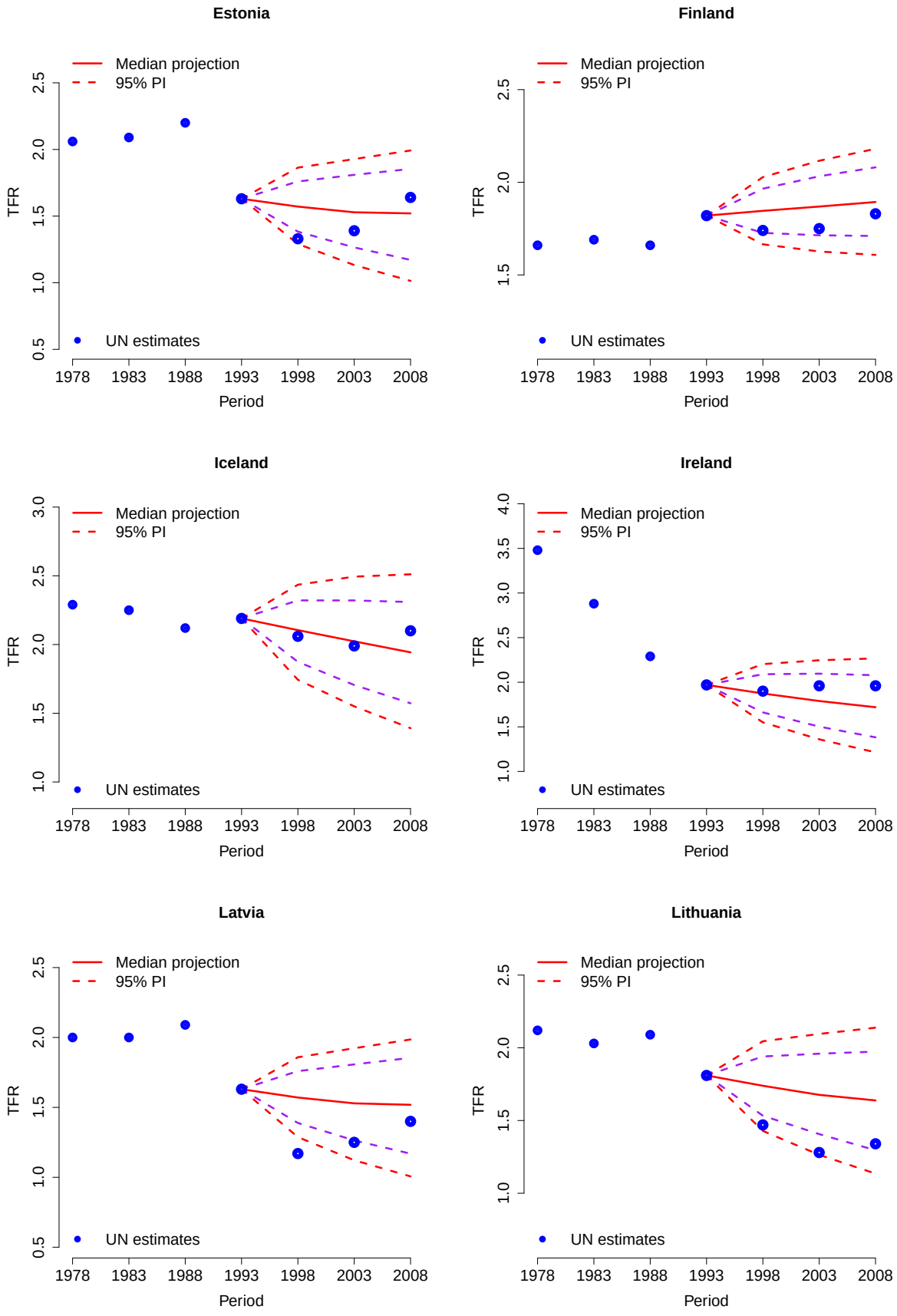

Figure 139: Out-of-sample in 1995

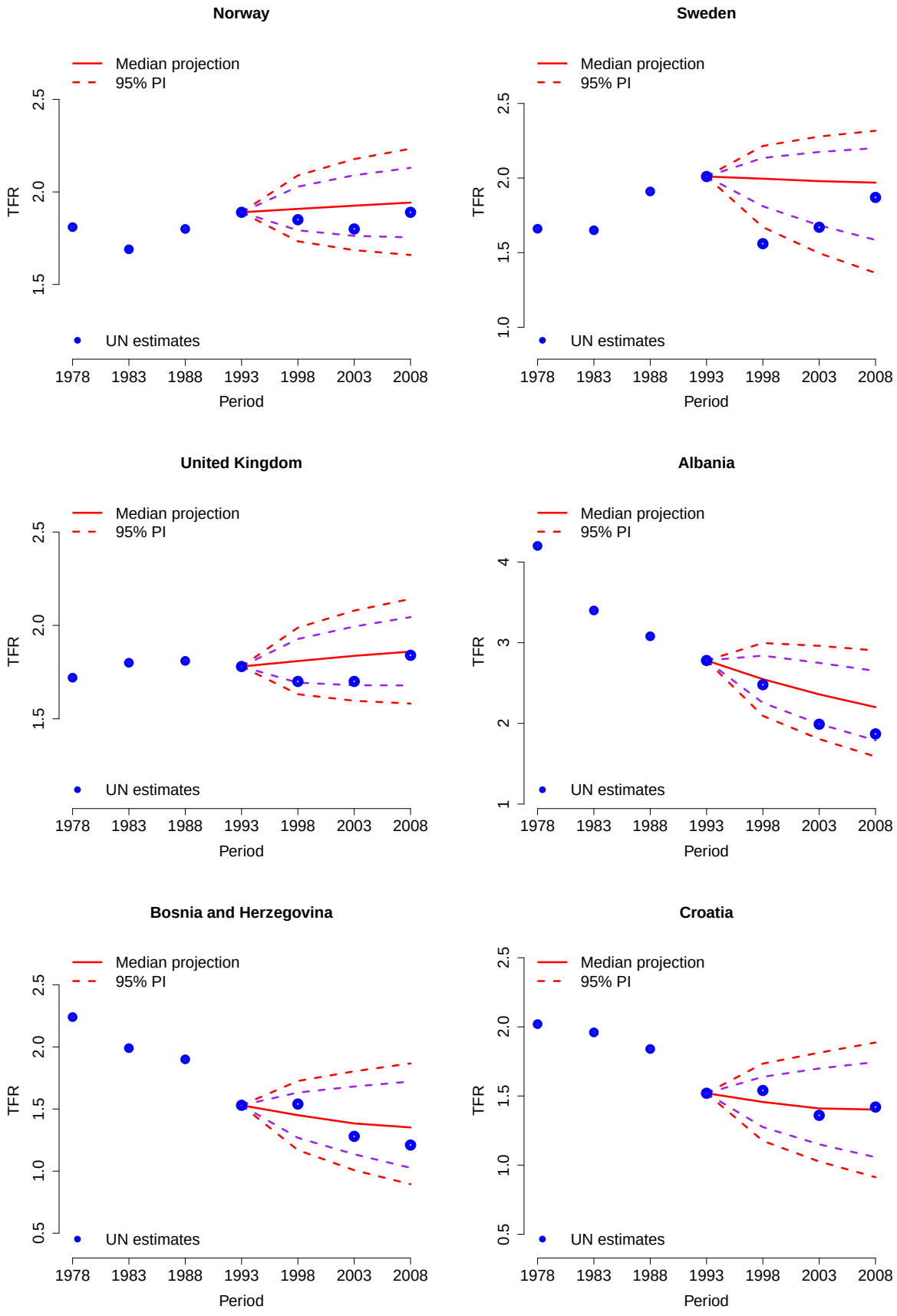

Figure 140: Out-of-sample in 1995

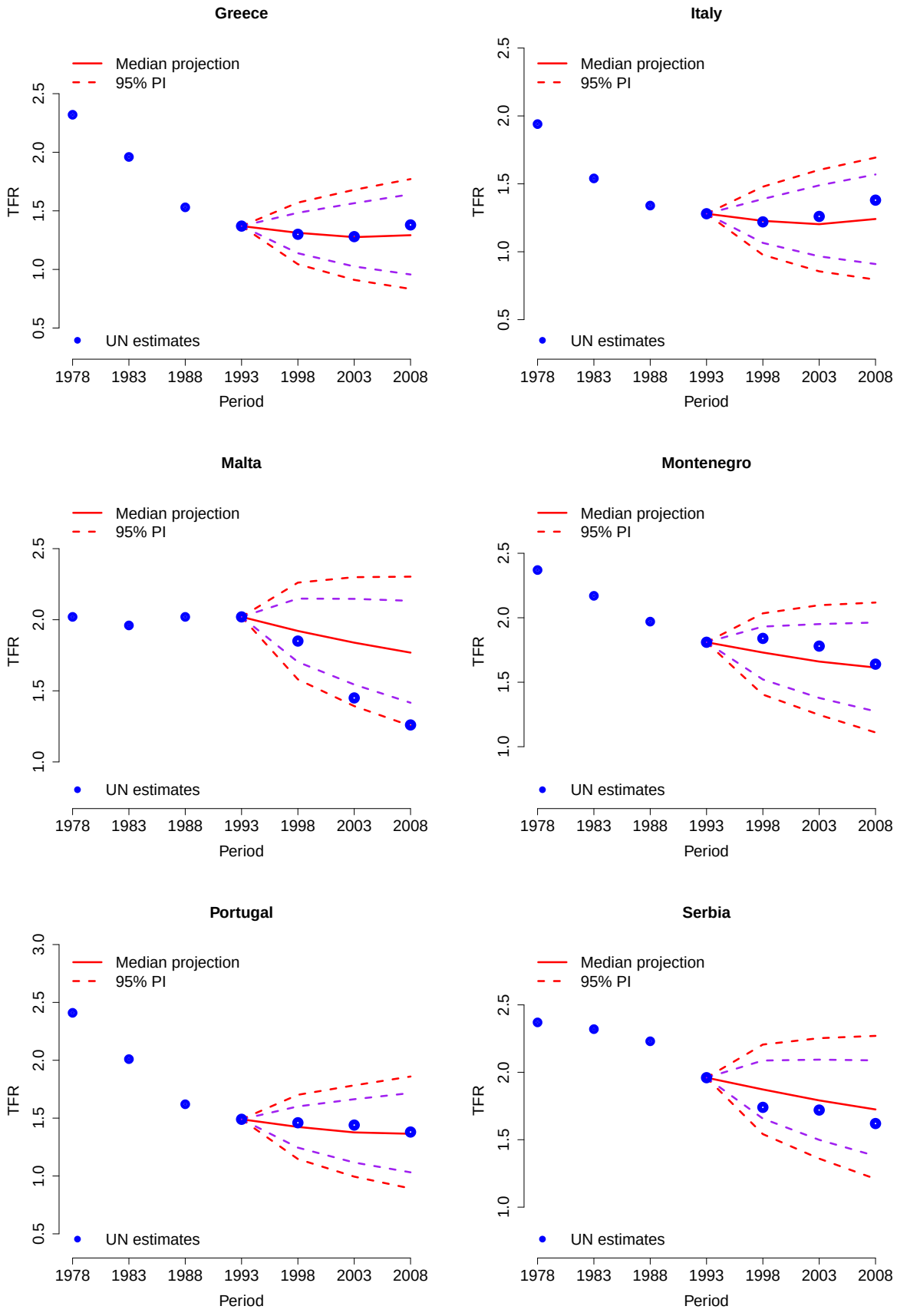

Figure 141: Out-of-sample in 1995

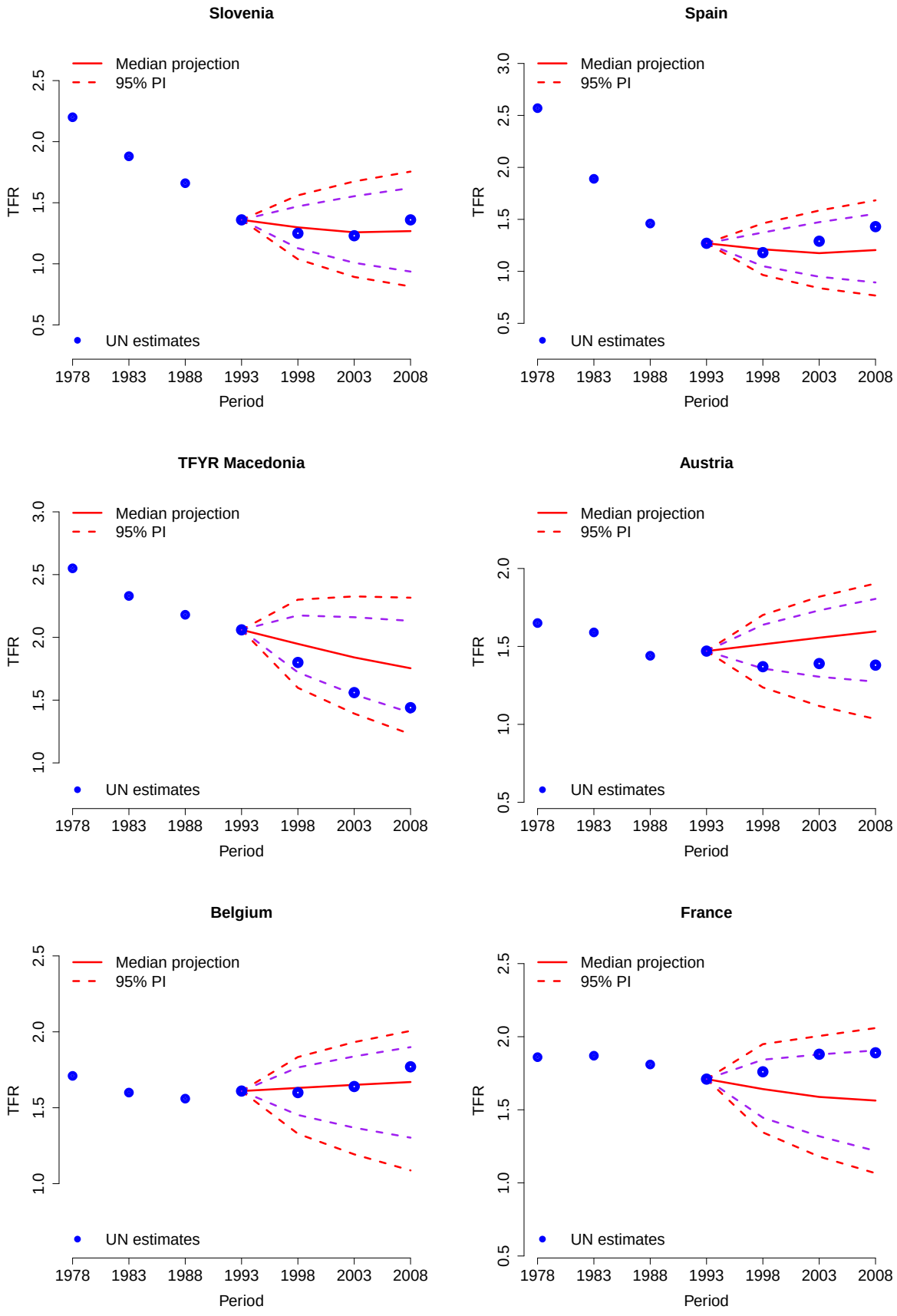

Figure 142: Out-of-sample in 1995

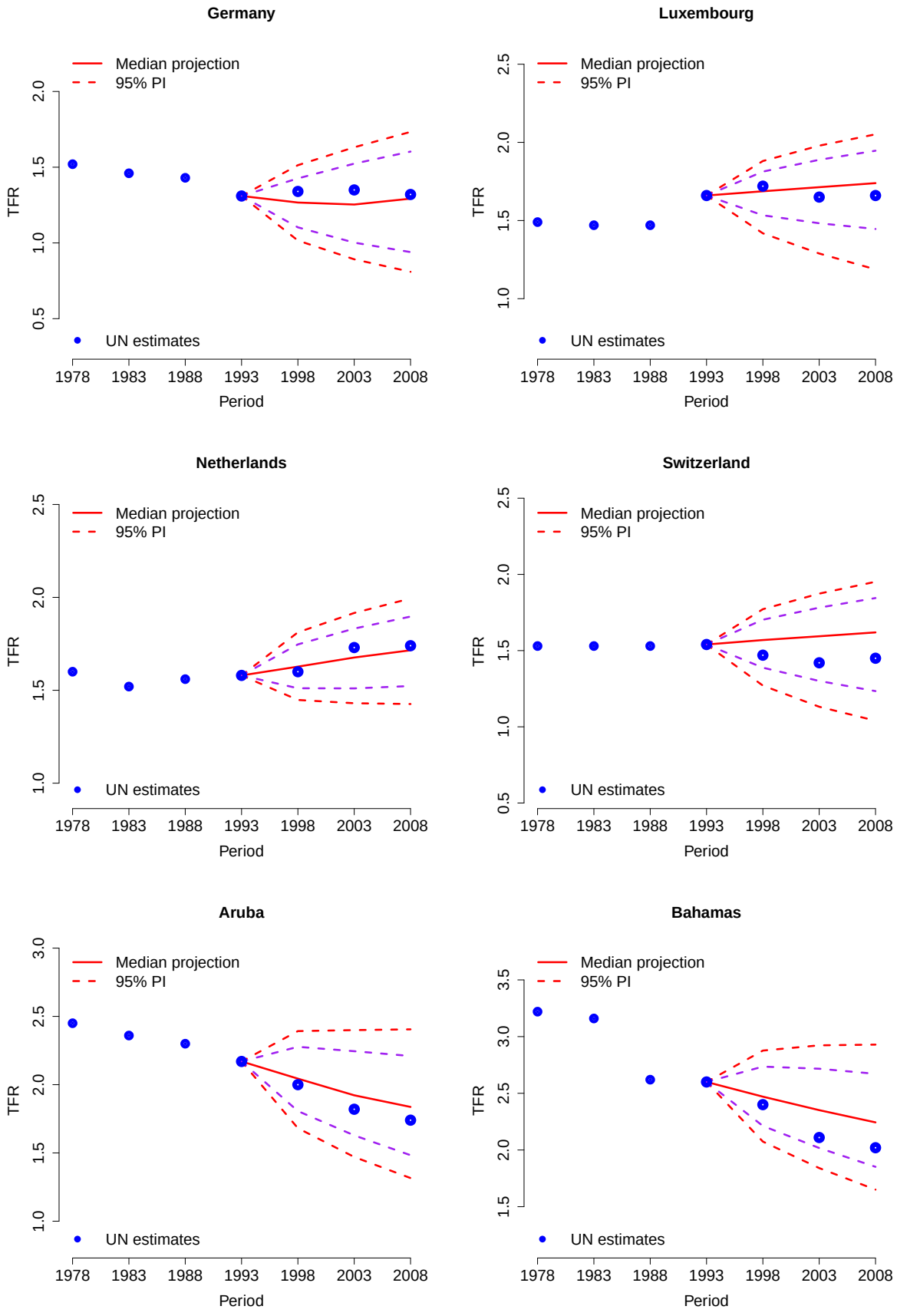

Figure 143: Out-of-sample in 1995

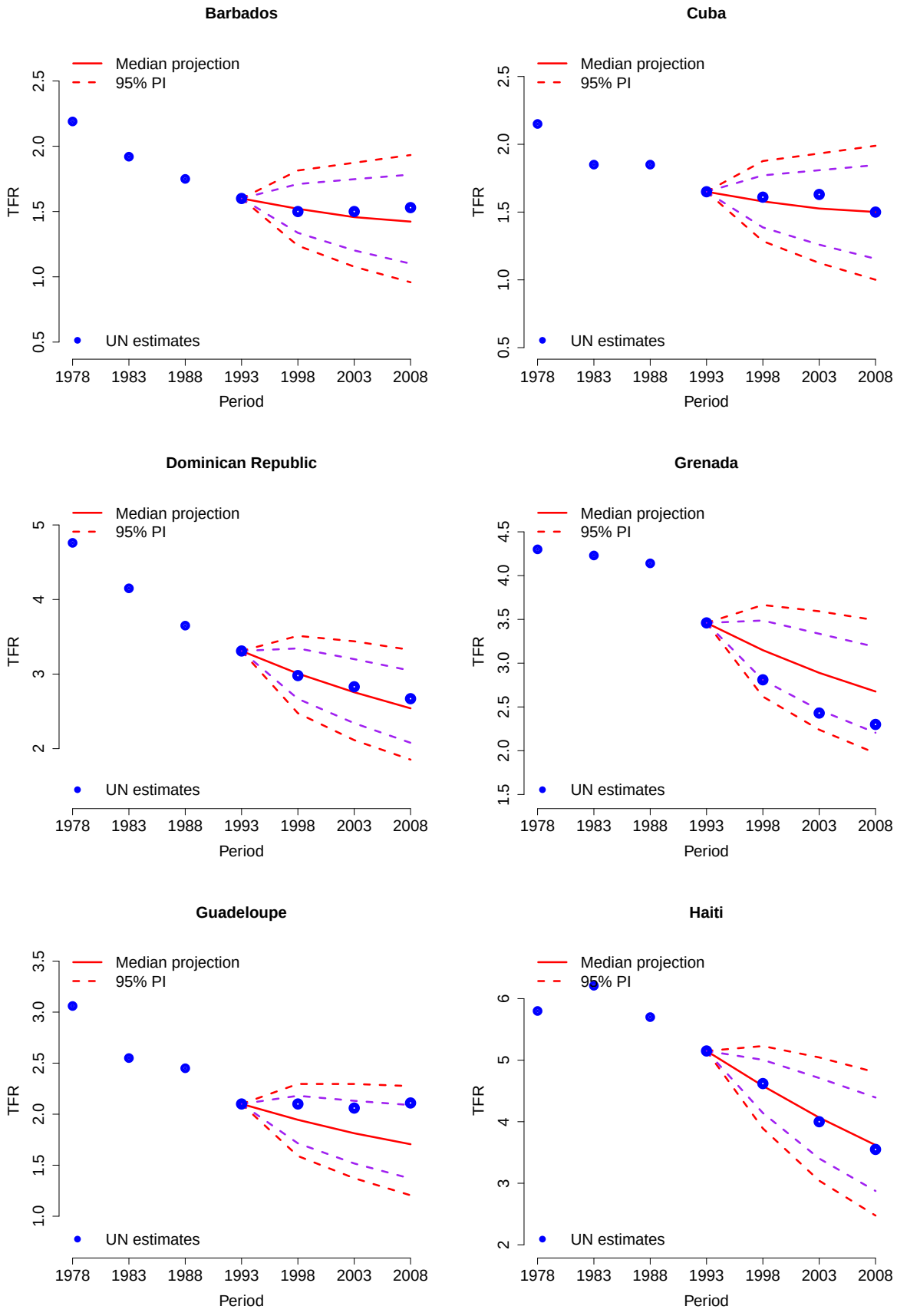

Figure 144: Out-of-sample in 1995

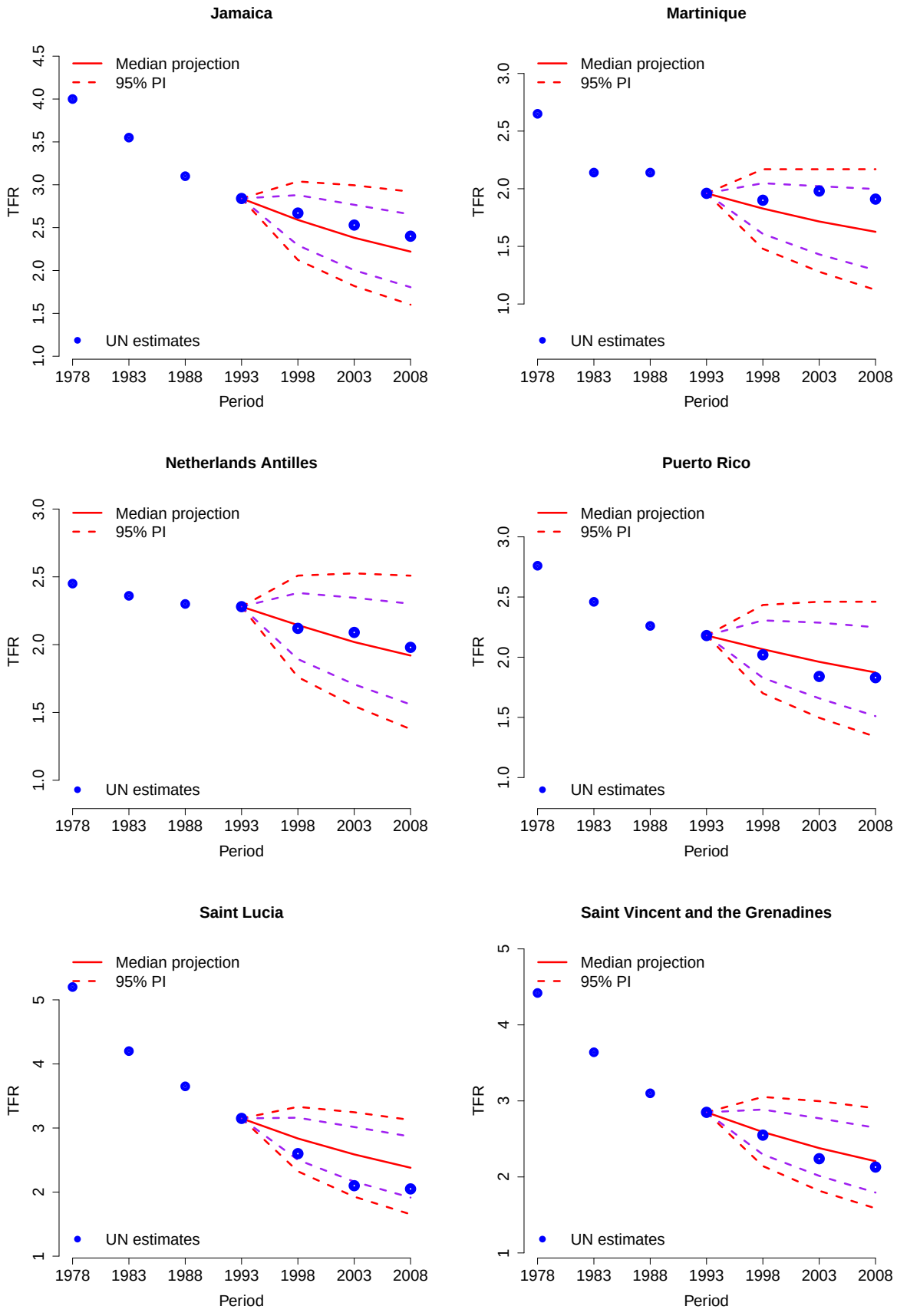

Figure 145: Out-of-sample in 1995

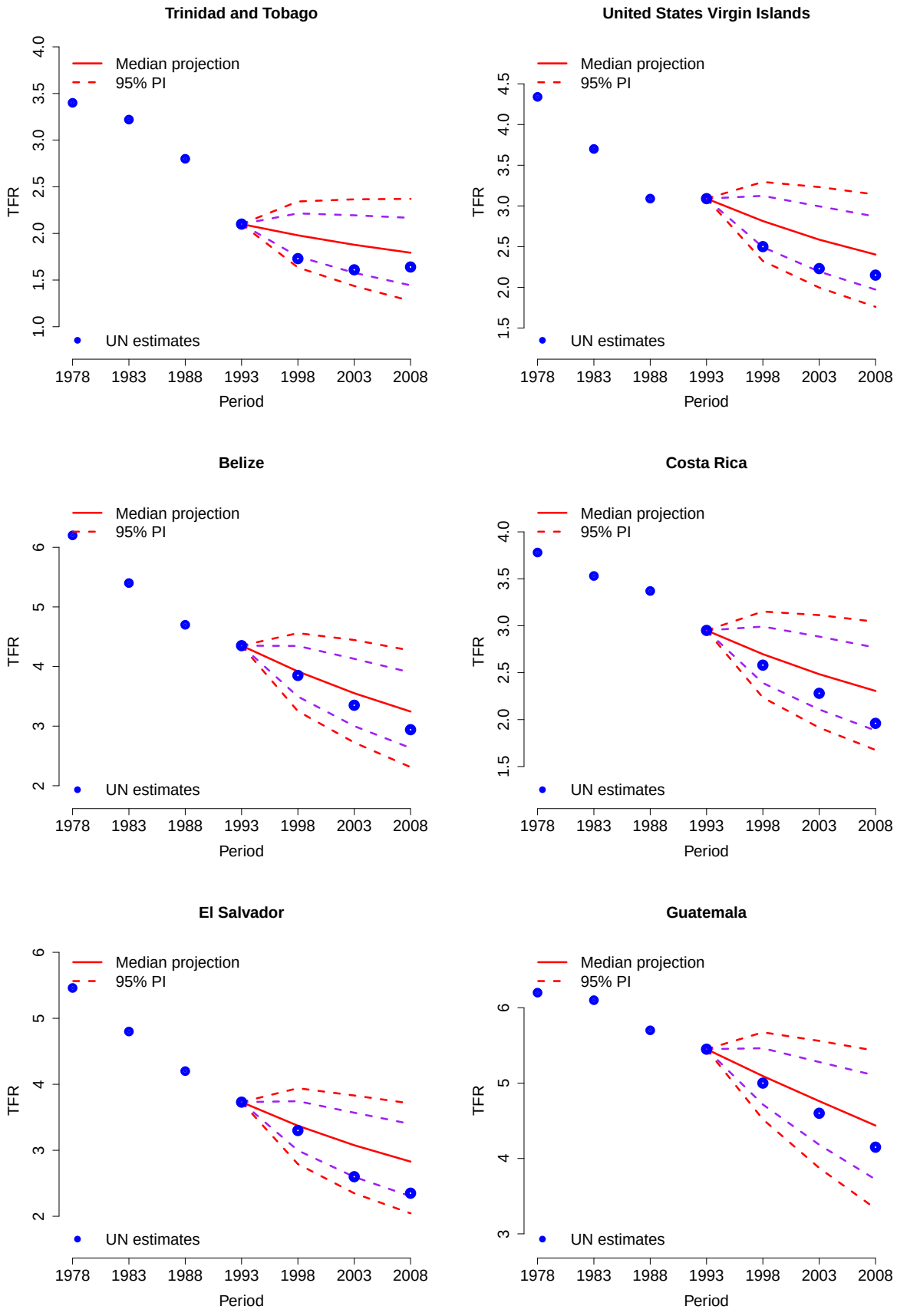

Figure 146: Out-of-sample in 1995

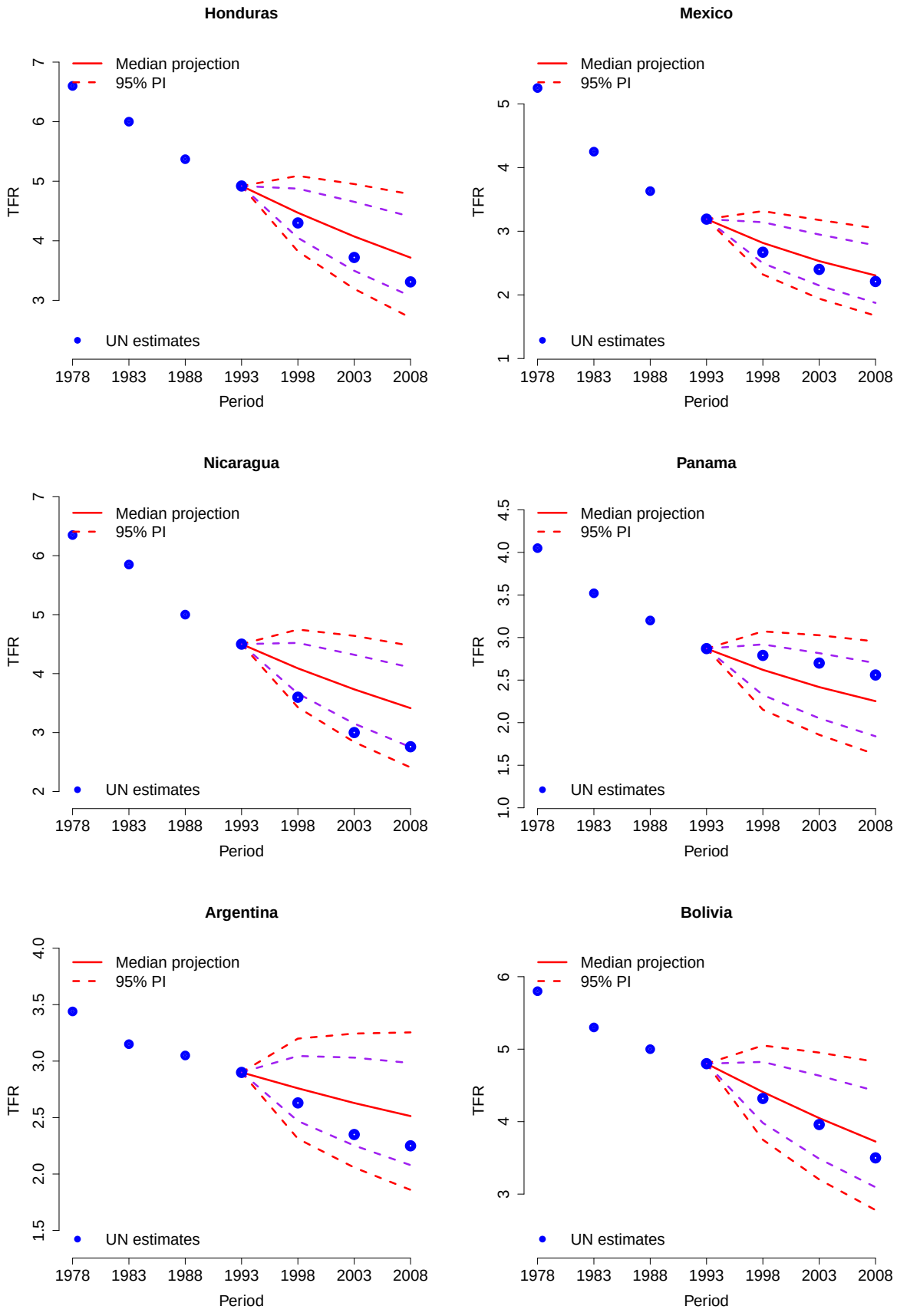

Figure 147: Out-of-sample in 1995

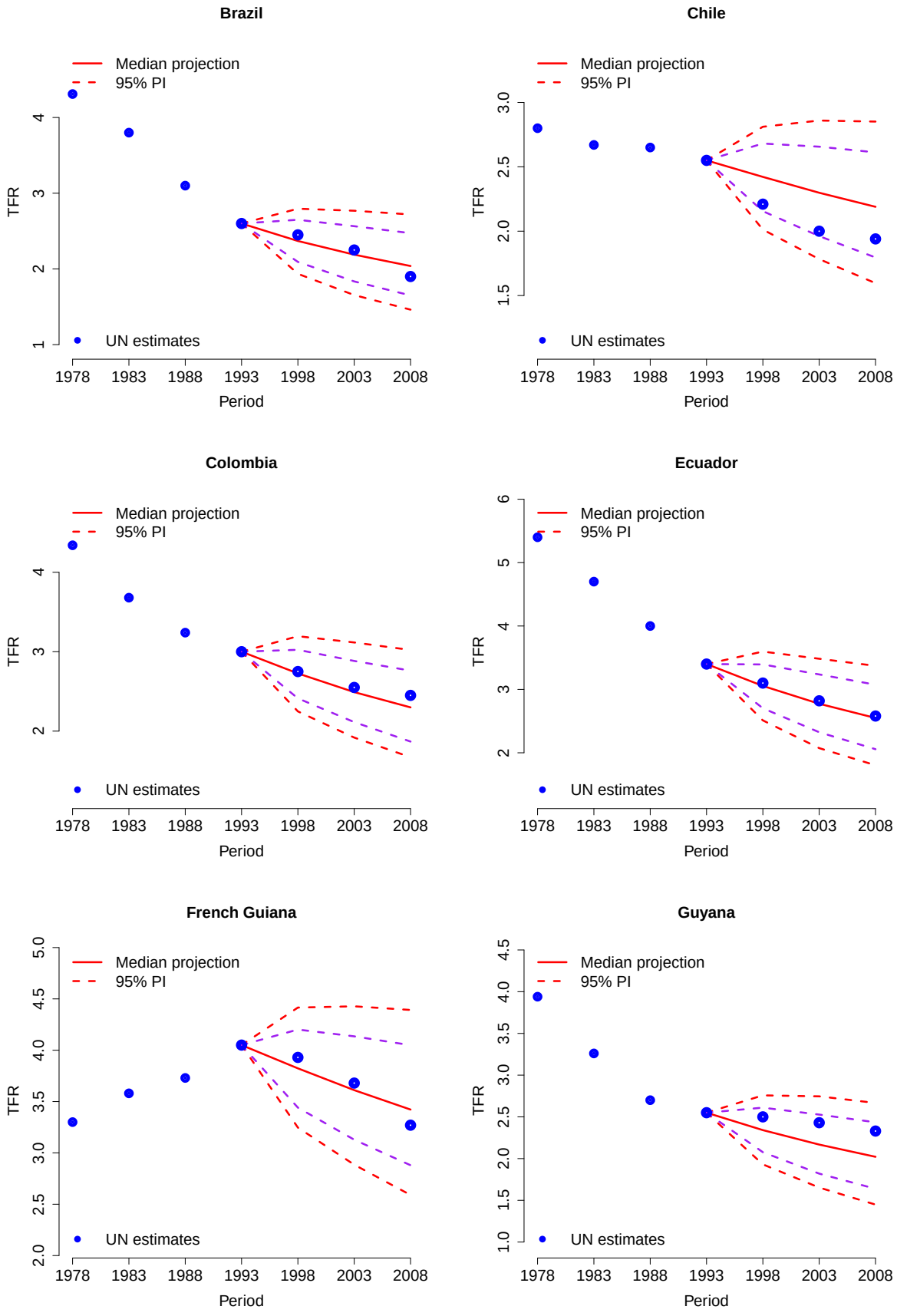

Figure 148: Out-of-sample in 1995

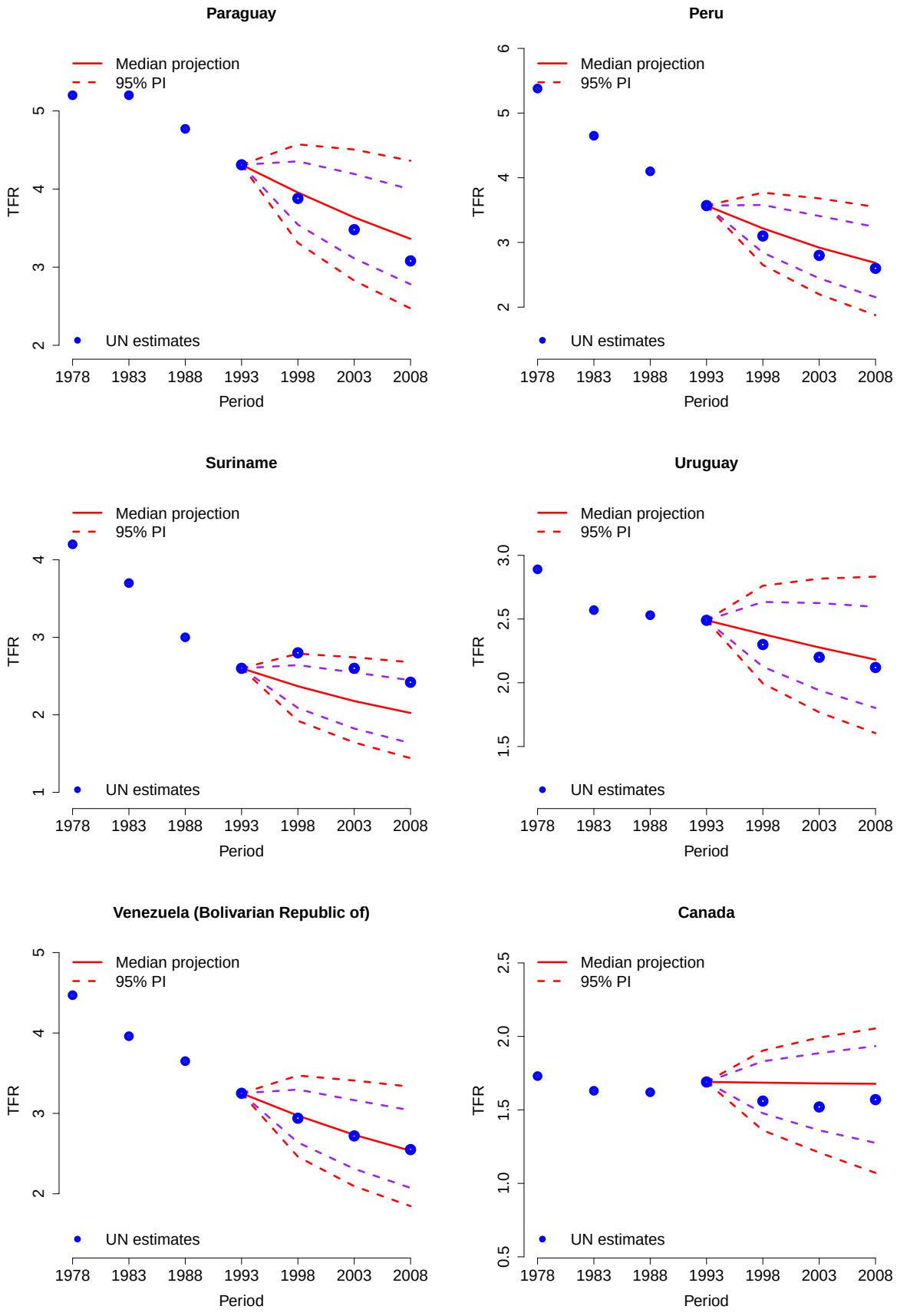

Figure 149: Out-of-sample in 1995

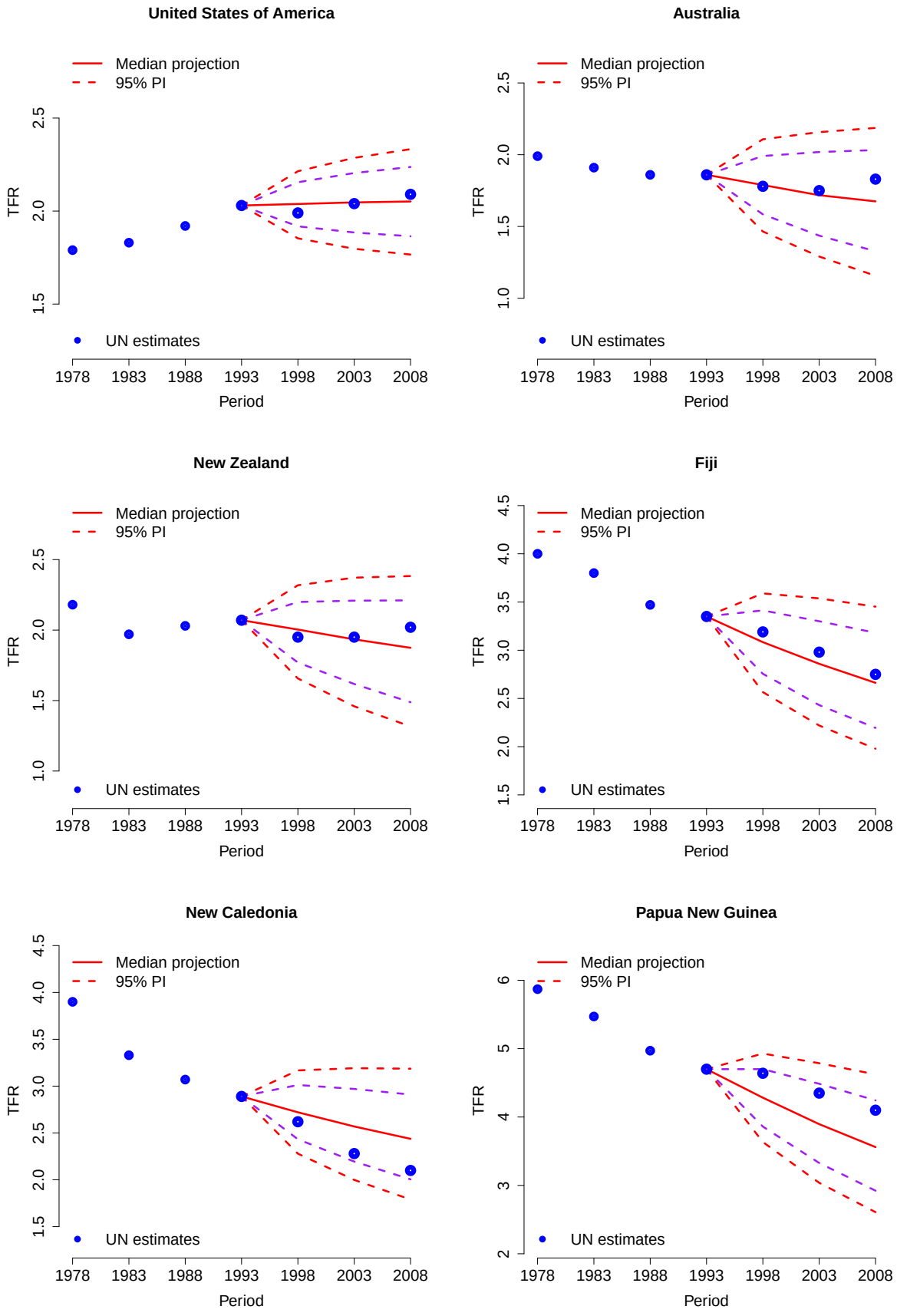

Figure 150: Out-of-sample in 1995

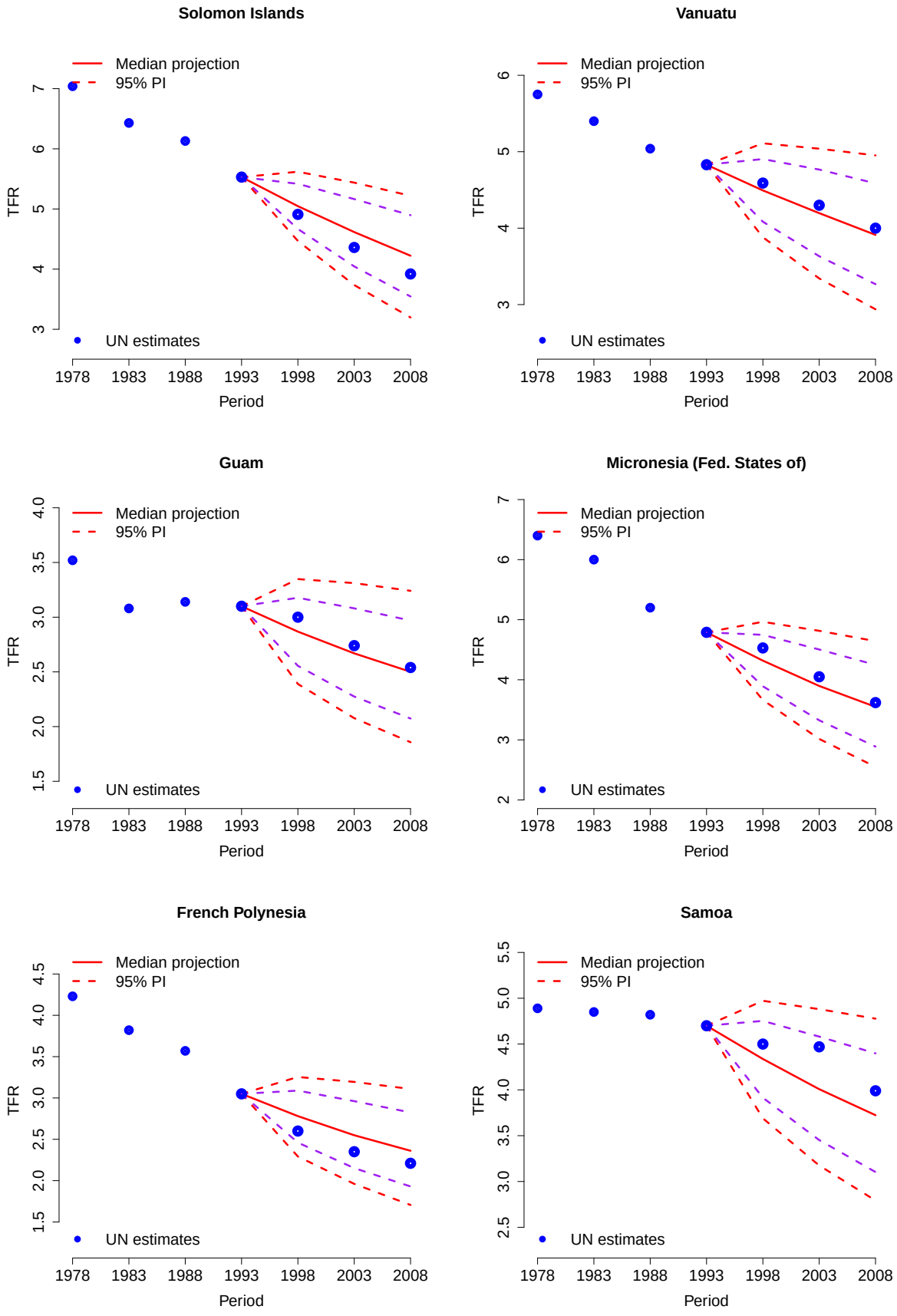

Figure 151: Out-of-sample in 1995

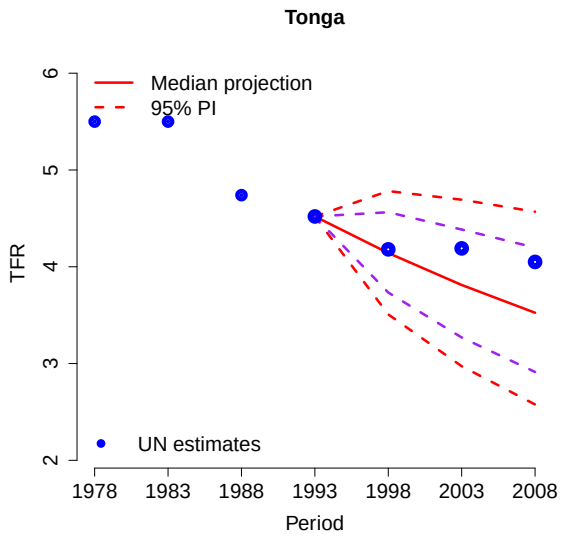

Figure 152: Out-of-sample in 1995

References

Alho, J. (2008). Aggregation across countries in stochastic population forecasts. *International Journal of Forecasting 24*, 243–253.

Alkema, L. (2008). *Uncertainty Assessments of Demographic Estimates and Projections*. Ph. D. thesis, University of Washington.

Alkema, L., A. E. Raftery, P. Gerland, S. J. Clark, and F. Pelletier (2008, April). Assessing uncertainty in fertility estimates and projections. In *Proceedings of the 2008 Annual Meeting of the Population Association of America*, New Orleans, La., USA. http://paa2008.princeton.edu/abstractViewer.aspx?submissionId=80115.

Alkema, L., A. E. Raftery, P. Gerland, S. J. Clark, and F. Pelletier (2009, September). Probabilistic projections of the total fertility rate. In *Proceedings of the 2009 Annual Meeting of the International Union for the Scientic Study of Population*, Marrakech, Morocco. http://iussp2009.princeton.edu/abstractViewer.aspx?submissionId=93084.

Bongaarts, J. and R. Bulatao (2000). *Beyond Six Billion: Forecasting the World's Population*. National Research Council (U.S.), Washington, D.C.: National Academy Press.

Bongaarts, J. and G. Feeney (1998). On the quantum and tempo of fertility. *Population and Development Review 24*, 271–292.

Chunn, J. L., A. E. Raftery, and P. Gerland (2009, May). Bayesian probabilistic projections of mortality. In *Proceedings of the 2009 Annual Meeting of the Population Association of America*, Detroit, Mich., USA. http://paa2009.princeton.edu/abstractViewer.aspx?submissionId=90851.

Cohen, J. (1986). Population forecasts and confidence intervals for Sweden: A comparison of model-based and empirical approaches. *Demography 23*, 105–126.

Gelfand, A. and A. F. M. Smith (1990). Sampling-based approaches to calculating marginal densities. *Journal of the American Statistical Association 85*, 398–409.

Gelman, A., F. Bois, and J. Jiang (1996). Physiological pharmacokinetic analysis using population modeling and informative prior distributions. *Journal of the American Statistical Association 91*, 1400–1412.

Gelman, A., J. B. Carlin, H. S. Stern, and D. B. Rubin (2004). Bayesian Data Analysis, Second Edition. *Boca Raton: Chapman & Hall/CRC Chapter 5*.

Ihaka, R. and R. Gentleman (1996). R: A language for data analysis and graphics. *Journal of Computational and Graphical Statistics 5*, 299–314.

Keilman, N. and D. Q. Pham (2004). Empirical errors and predicted errors in fertility, mortality and migration forecasts in the european economic area. Discussion Paper 386, Statistics Norway, Oslo. Available at http://www.ssb.no/publikasjoner/DP/pdf/dp386.pdf.

Keyfitz, N. (1981). The limits of population forecasting. *Population and Development Review 7*, 579–593.

Lee, R. and S. Tuljapurkar (1994). Stochastic population projections for the United States: Beyond high, medium and low. *Journal of the American Statistical Association 89*, 1175–1189.

Lutz, W., W. C. Sanderson, and S. Scherbov (2001). The end of world population growth. *Nature 412*, 543–545.

Meyer, P. (1994). Bi-Logistic Growth. *Technological Forecasting and Social Change 47*, 89–102.

Neal, R. M. (2003). Slice sampling. *The Annals of Statistics 31, No. 3*, 705–767.

Stoto, M. (1983). The accuracy of population forecasts. *Journal of the American Statistical Association 78*, 13–20.

United Nations, Department of Economic and Social Affairs, Population Division (2006). *World Population Prospects. The 2004 Revision, Vol. III, Chapter VI. Methodology of the United Nations population estimates and projections*, pp. 100–104. http://www.un.org/esa/population/publications/WPP2004/WPP2004 Volume3.htm.

United Nations, Department of Economic and Social Affairs, Population Division (2006). *World Population Prospects. The 2006 Revision, Vol. III, Analytical report.* United Nations publication, http://www.un.org/esa/population/publications/wpp2006/wpp2006.htm.

United Nations, Department of Economic and Social Affairs, Population Division (2009, forthcoming). *World Population Prospects. The 2008 Revision.* CD-ROM Edition - Extended Dataset in Excel and ASCII formats, United Nations publication, http://www.un.org/esa/population/publications/wpp2008/.